

Multi-annual carbon flux at an intensively cultivated  
lowland peatland in East Anglia, UK

Thesis submitted for the degree of  
Doctor of Philosophy  
at the University of Leicester

by

Alexander Michael Joseph Cumming BSc  
School of Geography, Geology and the Environment  
University of Leicester

2018

## Abstract

Multi-annual carbon flux at an intensively cultivated lowland peatland in East Anglia, UK.

Alex Cumming

Peatlands are an important store of carbon (C), accounting for an estimated third of global soil C despite only covering 3% of the land surface. Drainage of these soils for intensive cultivation has already led to considerable peat wastage, largely due to mineralisation of stored C, with associated carbon dioxide (CO<sub>2</sub>) emissions. This thesis provides the first multi-annual measurements of CO<sub>2</sub> flux for a lowland deep peat soil in East Anglia, UK. Measurements of CO<sub>2</sub> exchange between an intensively cultivated field and the atmosphere were made for 3.5 years using the eddy covariance (EC) methodology. During this time two lettuce, a leek and a celery crop were cultivated, with intervening periods of fallow. Drivers of CO<sub>2</sub> exchange were investigated. Soil temperature was identified as a key driver of CO<sub>2</sub> flux during fallow periods while gross primary productivity (GPP), limited by high temperature and vapour pressure deficit, was the key driver of NEE during crop periods. There was some evidence that under a shallower WTD and higher SWC, temperature response was limited and net CO<sub>2</sub> flux was reduced. The annual C-CO<sub>2</sub> flux was  $675.75 \pm 101.45$ ,  $806.38 \pm 88.75$  and  $797.18 \pm 84.6$  g C-CO<sub>2</sub> m<sup>-2</sup> yr<sup>-1</sup>, for 2013, 2014 and 2015 respectively, averaged to  $759.77 \pm 91.6$  g C-CO<sub>2</sub> m<sup>-2</sup> yr<sup>-1</sup>. The import and export of C associated with crop management (planting and harvesting) resulted in a net gain of 20-30 g C m<sup>-2</sup> for lettuce crops, however for crops with greater yields a net loss was estimated at 20-100 g C m<sup>-2</sup>. The first UK quantification of C flux, measured at field boundaries, due to wind erosion from peatland agriculture indicated a loss of 90 to 490 g C m<sup>-2</sup> yr<sup>-1</sup>.

C loss mitigation strategies should aim to reduce periods of bare soil and raise the water table whilst still enabling ongoing agricultural management. Better understanding of the consequences of mitigation strategies for C balance and agricultural productivity are required.

## **Acknowledgements**

There are a lot of people that helped to make this thesis possible, I will endeavour to thank them all here and apologise to anyone I forget.

I would like to start by thanking Natural Environment Research Council (NERC) for funding for the initial purchase of field equipment and research (Urgency grant no. NE/K001590/1), and for their co-funding of the studentship that supported this thesis in combination with the Department of Geography, University of Leicester (UoL) (Studentship no. NE/L501839).

For their motivation, patience and all the comments on the drafts my supervision team of Dr. Jörg Kaduk, Prof. Susan Page and Prof. Heiko Balzter are thanked. Pursuing this study (and completing it) was largely made possible thanks to the belief, enthusiasm and encouragement of Prof. Susan Page, who is a great role model, supervisor and boss!

Additionally, a great deal of appreciation must go to Dr Ross Morrison. Without his friendship, knowledge, guidance, and good humour, provided free of obligation, I would have struggled to complete this work.

G's Fresh, J. G. Shropshire & sons, are thanked for their permission to conduct the study on their farm, and particularly to Martin Hammond (General Manager, Rosedene Farm) for his continued support and helpfulness as a valuable source of additional information. Conducting the fieldwork was made far more enjoyable thanks to the company often provided by the following people: Simon Benson, Keturah Smithson, Valentin Louis, Wayne Murphy, Hao Wang and Gong Pan, who are thanked for their contributions to carrying, entertaining, and tolerating of my driving.

I am grateful to the Centre for Landscape and Climate Research (CLCR) and School of Geography, Geology and the Environment (SGGE) for fostering a professional and friendly working environment, and to those who have co-habited this fun working space in particular: James, Pedro, Valentin, Tom, Peshawa, Issa, NK, Ciaran, Virginia and Veebha.

Thanks also go to the SGGE professional services team that includes: Bill Hickin, Gemma Black, Adam Cox, Kerry Allen, Lisa Barber, Simon Benson, Gary Hancox,

Vanessa Greasley, Ann Williams, Donna Beasley, and Gail Andrews, without whose progress would have slowed considerably. Having previously been a member of this team I have a great appreciation for the work they do. In this same vein the school postgraduate research staff, Charlotte Langley, and Dr. Gavin Brown softened the strains of concluding this PhD. Notably, amongst a great SGGE faculty, I would like to single out Dr. Mick Whelan and Dr. Nick Tate for their candid comments and guidance through the PhD process.

Additional facilities and support were made available to me by the Centre for Ecology and Hydrology, Wallingford and Dr Ross Morrison for conducting calibration of the Li7500 infra-red gas analyser (IRGA), and the Open University through Dr Mike Peacock and Patrick Rafferty for use of their total organic carbon (TOC) analyser.

The data collected in this thesis contributed to a larger study of a network of fifteen lowland peatland sites across England and Wales (DEFRA SP1210) and are published as part of that report (Evans, 2017). Interacting with researchers on this project greatly helped the understanding and development of my thesis. Furthermore, those met along the way at conferences, summer schools and training courses are all thanked for sharing their research.

I have also been fortunate to be involved with several great research projects not directly related to my thesis that have enabled me to see some truly inspirational locations across the globe. Dr Leanne Milner, Wayne Murphy and Dr Rachel Carr, are all thanked for these amazing opportunities that helped to motivate my own research.

Outside of academia I am fortunate to have been able to pursue my passion for sports during my PhD. In doing so, I have not only achieved many personal goals but more importantly made some great friends who have all taken an interest in my studies and helped me to de-stress, in particular: Salman, Nora, Jason, Seb, Anish, George, Yoshi, Simon, Lily, Mari, Catrin, JJ, Luis, Dave, Matt, Paul, Ben and Mark.

I must also thank Margaret Green and her family for taking me in when the rabbits and I needed a home, and my closest friends Mike and Spence for helping to maintain my mental health during the completion of this thesis.

Last but by no means least, my partner Elena, parents Lynne and David, sisters Lessa and Jenny, brothers John, Nathan and Constantin, nephew Stefan, nieces Lyra and Liliana, extended family, all the supportive friends and housemates along the way, thanks for your belief and reassurances, you are too innumerable to list, and are better thanked in person.

I dedicate this thesis to my godchildren, Stefan, Lyra and Liliana.

## **Table of Contents**

Abstract.....	ii
Acknowledgements.....	iii
Table of Contents.....	vi
List of Tables .....	xi
List of Figures.....	xiii
List of Abbreviations .....	xvi
<b>Chapter 1: Introduction and literature review .....</b>	<b>1</b>
1.1 Background.....	2
1.2 Thesis outline.....	6
1.3 Literature review.....	8
1.3.1 Carbon cycle.....	8
1.3.2 Peatlands .....	10
1.3.3 Peatlands & carbon .....	12
1.3.4 Drainage for agriculture.....	16
1.3.5 Climate change .....	21
1.3.6 Lowland peatlands in the UK and peat wastage measurements .....	23
1.4 Research questions and objectives.....	28
1.4.1 Research Questions.....	28
1.5 Chapter summary.....	30
<b>Chapter 2: Materials and Methods .....</b>	<b>31</b>
2.1 Site information .....	32
2.1.1 Regional Climate .....	32
2.1.2 Rosedene Farm .....	33

2.1.3 Study field.....	37
2.2 Measuring fluxes.....	44
2.2.1 Eddy covariance theory .....	44
2.2.2 Measurement system.....	46
2.2.3 Eddy Pro processing .....	50
2.2.4 Quality control .....	52
2.2.5 Summary of gaps .....	57
2.2.6 Gap filling .....	58
2.2.7 Partitioning.....	62
2.2.8 Uncertainty.....	62
2.2.9 Energy balance closure (EBC).....	63
2.3 Lateral C flux .....	66
2.3.1 Import ( $C_i$ ) .....	67
2.3.2 Export ( $C_e$ ).....	67
2.4 Aeolian horizontal mass flux methodology .....	68
2.5 Chapter summary.....	69
<b>Chapter 3: Drivers of CO<sub>2</sub> fluxes at an intensively cultivated drained lowland deep peat soil .....</b>	<b>70</b>
3.1 Analysis method .....	71
3.1.1 Modelling nocturnal TER .....	71
3.1.2 Modelling light response of NEE .....	72
3.2 Environmental conditions .....	74
3.2.1 Radiation.....	74
3.2.2 Temperature .....	76
3.2.3 Precipitation and water management.....	78
3.3 TER.....	80

3.3.1 Data availability .....	80
3.3.2 Model performance .....	80
3.3.3 Residuals .....	85
3.3.4 WTD and SWC as primary drivers .....	87
3.3.5 Comparison of short-term rising and falling water table .....	88
3.4 Light use .....	91
3.4.1 Radiation and temperature .....	91
3.4.2 Whole crop light response .....	93
3.4.3 Peak light response .....	94
3.5 Discussion .....	100
3.5.1 Drivers of NEE .....	100
3.6 Chapter summary .....	106

**Chapter 4: Multi-annual CO<sub>2</sub> flux over 3.5 years at an intensively cultivated drained lowland deep peat soil .....** 107

4.1 EBC .....	109
4.2 NEE .....	113
4.2.1 Daily NEE (GPP and TER) .....	113
4.2.2 Diurnal NEE .....	118
4.2.3 Crop and fallow periods .....	122
4.2.4 Annual .....	123
4.3 Lateral C balance .....	126
4.3.1 Import (C <sub>i</sub> ) .....	126
4.3.2 Yield (C <sub>e</sub> ) .....	126
4.3.3 Carbon balance .....	127
4.4 Discussion .....	129
4.4.1 EBC .....	129

4.4.2 NEE.....	131
4.4.3 NECB: import and yield .....	143
4.5 Chapter summary .....	145
<b>Chapter 5: Wind-blown C flux across an intensively cultivated drained lowland deep peat soil .....</b>	<b>146</b>
5.1 Methodology .....	147
5.1.1 Study site.....	147
5.1.2 Samplers.....	151
5.1.3 Environmental conditions .....	157
5.2 Data analysis .....	159
5.2.1 Environmental conditions .....	159
5.2.2 Vertical distribution of horizontal mass flux (HMF, q).....	161
5.2.3 Horizontal mass transport (HMT, Q).....	166
5.2.4 Organic matter and carbon content .....	168
5.3 Discussion.....	172
5.3.1 HMF.....	172
5.3.2 HMT.....	173
5.3.3 Soil cover .....	175
5.3.4 Deposition, where is the peat going? .....	176
5.3.5 Footprint calculation and speculative field scale annual C loss .....	177
5.4 Chapter Summary .....	179
<b>Chapter 6: Conclusions .....</b>	<b>180</b>
6.1 Overview of chapter findings .....	181
6.2 Implications and mitigation .....	186
6.2.1 Implications .....	186

6.2.2 Mitigation.....	187
6.3 Limitations/future research direction.....	190
6.3.1 EC methodology limitation.....	190
6.3.2 Wind erosion.....	192
6.3.3 General.....	193
6.4 Final summary .....	195
Appendix.....	197
Bibliography .....	201

## List of Tables

<b>Table 2.1:</b> Summary of relevant site management events during the data collection period .....	36
<b>Table 2.2:</b> Summary of EP6.1 processing steps to calculate fluxes from raw data .....	51
<b>Table 2.3:</b> Summary of research on carbon content of crops .....	66
<b>Table 3.1:</b> Calculated dates for number of frost days and the thermal growing season dates from Tair measured at 1.55 m height above the ground.....	78
<b>Table 3.2:</b> Fitted variables for temperature response model and means of Tsoil, WTD and SWC for each period.....	82
<b>Table 3.3:</b> Statistics from linear regression and spearman's rank correlations for relationships of WTD, SWC and Tsoil with NEE during a water table raising and lowering .....	89
<b>Table 3.4:</b> Fitted variables for each complete crop period and the peak two weeks of light use efficiency of each crop .....	96
<b>Table 3.5:</b> Non-parametric Spearman's rank correlation coefficients .....	98
<b>Table 4.1:</b> Ordinary linear regression OLR coefficients and energy balance ratio (EBR) values .....	111
<b>Table 4.2:</b> Maximum, minimum and average daily fluxes of NEE, TER and GPP ....	116
<b>Table 4.3:</b> Crop, fallow and annual sums of GPP and TER .....	123
<b>Table 4.4:</b> Crop, fallow and annual sums of NEE with additional lateral C.....	126
<b>Table 4.5:</b> Measured fluxes for cropland on peat .....	128
<b>Table 4.6:</b> Annual NEE ( $\text{g C-CO}_2 \text{ m}^{-2} \text{ yr}^{-1}$ ) details reported by literature on temperate and boreal peatlands managed for growing vegetable, cereal and some grass crops ...	136
<b>Table 4.7:</b> Annual NEE ( $\text{C-CO}_2 \text{ m}^{-2} \text{ yr}^{-1}$ ) details reported by IPCC (2014) wetland supplement references for fluxes from agricultural boreal and temperate peat soils ...	138
<b>Table 4.8:</b> Annual NEE ( $\text{g C-CO}_2 \text{ m}^{-2} \text{ yr}^{-1}$ ) details reported available literature on temperate and boreal peatlands managed for growing bioenergy crops.....	142

<b>Table 5.1:</b> Summary of sampling efficiencies reported in the literature for BSNE samplers .....	152
<b>Table 5.2:</b> Field activity dates .....	158
<b>Table 5.3:</b> Statistics for HMF's of sediment for the two BSNE arrays .....	163
<b>Table 5.4:</b> Annual sums of integrated mass fluxes with estimated C content .....	168
<b>Table 5.5:</b> Percentage organic matter content of wind-blown sediment samples that were collected at array A and B .....	171
<b>Table 5.6:</b> Literature summary of sediment yields from agricultural soils .....	174
<b>Table A2.1:</b> Chronological table of known site management events .....	197
<b>Table A2.2:</b> Calibration coefficients for the Li7500 IRGA .....	199
<b>Table A2.3:</b> Summary of number of half-hourly flux data values flagged by quality control .....	199

## List of Figures

<b>Figure 1.1:</b> Diagram of the C cycle with major pools and major flows between them ...	8
<b>Figure 1.2:</b> A general schematic for defining wetland types based on wetness and pH/nutrient status .....	10
<b>Figure 1.3:</b> Conceptual model of C cycle processes and flow paths for a fen peat soil with some typical fen vegetation .....	13
<b>Figure 1.4:</b> Conceptual model of C cycle processes and flow paths for a drained intensively cultivated deep peat soil .....	18
<b>Figure 1.5:</b> Global decadal average temperature difference from the average of all years .....	22
<b>Figure 2.1:</b> Monthly and annual averaged climate data for 1960-2010 from Cambridge NIAB station .....	32
<b>Figure 2.2:</b> Maps of Rosedene Farm location.....	34
<b>Figure 2.3:</b> Annotated aerial photograph of the field site.....	35
<b>Figure 2.4:</b> Photos of stages of site vegetation cover development during the lettuce crop year of 2014 .....	39
<b>Figure 2.5:</b> Photos of stages of site vegetation cover development during the leek crop year of 2013 .....	41
<b>Figure 2.6:</b> Photos of stages of site vegetation cover development during the celery crop year of 2015 .....	43
<b>Figure 2.7:</b> Conceptual diagram of an EC tower and the eddies it samples .....	44
<b>Figure 2.8:</b> EC instrumentation photos.....	47
<b>Figure 2.9:</b> Monthly wind-rose plots .....	54
<b>Figure 2.10:</b> Annual wind-rose plots .....	55
<b>Figure 2.11:</b> Quality controlled data.....	57
<b>Figure 2.12:</b> Thirty minute resolution Rn data .....	60
<b>Figure 2.13:</b> Flow diagram of gap filling methodology .....	61
<b>Figure 3.1:</b> Daily meteorological conditions and fluxes.....	75

<b>Figure 3.2:</b> Daily average temperature difference for soil and air (T <sub>soil</sub> -T <sub>air</sub> ).....	76
<b>Figure 3.3:</b> Accumulative degree days plot for each of the four crop growing periods from 2012 to 2015.....	77
<b>Figure 3.4:</b> Modelling nocturnal TER from T <sub>soil</sub> values as a driver of nocturnal NEE 81	
<b>Figure 3.5:</b> Mean nocturnal TER driver assessment for each crop and fallow period ..	83
<b>Figure 3.6:</b> Basal respiration (R <sub>10</sub> ) as a dependant of <b>a:</b> mean water table depth (WTD) and <b>b:</b> soil water content (SWC), for each of the measurement periods .....	85
<b>Figure 3.7:</b> Residuals of T <sub>soil</sub> modelled TER and observed NEE against daytime NEE for the same days of all available values for the <b>a:</b> crop and <b>b:</b> fallow periods. ....	87
<b>Figure 3.8:</b> Observed nocturnal mean NEE (TER) as a function of <b>a:</b> WTD and <b>b:</b> SWC.....	88
<b>Figure 3.9:</b> Raising and lowering of water table as a control of NEE .....	90
<b>Figure 3.10:</b> Monthly diurnal pattern of mean half hourly values for six environmental variables for each year of the complete measurement period.....	92
<b>Figure 3.11:</b> Light use efficiency of average 30 min values of NEE and PPFD for the complete growing period of each crop .....	94
<b>Figure 3.12:</b> Light use efficiency of average 30 min values of NEE and PPFD for the two week peak quantum yield of each crop.....	97
<b>Figure 4.1:</b> Energy balance closure plots.....	110
<b>Figure 4.2:</b> Daily EBC plot, using net radiation (R <sub>n</sub> ), soil heat flux (G), latent heat (LE) and sensible heat (H), all in W m <sup>-2</sup> .....	112
<b>Figure 4.3:</b> Daily NEE, GPP and TER. Black bars are daily NEE, green points are GPP and red points TER .....	114
<b>Figure 4.4:</b> Average monthly diurnal variability for six environmental variables for each year of the complete measurement period.....	121
<b>Figure 4.5:</b> Cumulative gap filled NEE g C-CO <sub>2</sub> m <sup>-2</sup> .....	124
<b>Figure 5.1:</b> Annotated aerial photograph of the field site .....	147
<b>Figure 5.2:</b> Average canopy heights for each field.....	149
<b>Figure 5.3:</b> Soil cover conditions during fallow periods .....	150

<b>Figure 5.4:</b> Ditch weed and riparian vegetation condition between fields A and B facing south east.....	151
<b>Figure 5.5:</b> Photographs of BSNE sampler arrays.....	153
<b>Figure 5.6:</b> Comparison of integration of linear spline and exponential fit techniques .....	156
<b>Figure 5.7:</b> Averages, minimums and maximums of environmental variables for periods of sediment flux accumulation.....	159
<b>Figure 5.8:</b> Wind rose plots describing the 30 min average wind velocities and directions.....	160
<b>Figure 5.9:</b> Horizontal mass flux per day from each BSNE height in array A for each time period averaged over the number of days of collection.....	162
<b>Figure 5.10:</b> Horizontal mass flux from each BSNE height in array B for each time period averaged over the number of days of collection.....	164
<b>Figure 5.11:</b> Contribution of each BSNE HMF to total collected flux plotted by collection date .....	166
<b>Figure 5.12:</b> Horizontal mass transport (HMT), $Q$ (linear spline integrated $q$ , $g\ m^{-2}$ ) for each period of dust collection at each location .....	167
<b>Figure 5.13:</b> Average organic matter content of dried sediment samples collected in BSNE samplers for each collector height at array A and B.....	170
<b>Figure 5.14</b> Photos of nettles lining the ditches with trapped dust. ....	177
<b>Figure A4.1:</b> Monthly NEE for all years (22 <sup>nd</sup> June 2012 – 31 <sup>st</sup> December 2015) .....	200

## List of Abbreviations

$^{137}\text{Cs}$	caesium-137
2D	Two-dimensional
a.m.s.l.	Above mean sea level
am	ante meridiem
AR	Arable
ART	Agroscope Reckenholz-Tanikon (research station ART)
BG	Barley/grass mix
BSNE	Big Spring Number Eight
C	Carbon
CAM	Crassulacean Acid Metabolism
CCM	Corn-cob-mix maize
C-CO <sub>2</sub>	Carbon in CO <sub>2</sub>
C <sub>e</sub>	Laterally exported carbon (C removed in crop harvest)
CEH	Centre for Ecology and Hydrology
CH <sub>4</sub>	Methane
C <sub>i</sub>	Laterally imported carbon (C in seeds and peat plug medium)
CL	Cereals
CLCR	Centre for Landscape and Climate Research
cm	Centimetre(s)
CO <sub>2</sub>	Carbon dioxide
CO <sub>2</sub> e	Equivalent value of carbon dioxide
COAG	Committee on Agriculture
d	Day
DEFRA	Department for Environment, Food and Rural Affairs
DOC	Dissolved Organic Carbon
E	East
e.g.	for example
E <sub>0</sub>	Activation energy (K)
EBC	Energy Balance Closure
EBR	Energy Balance Ratio

EC	Eddy Covariance
EU	European Union
f	fertilised
FAO	Food and Agriculture Organisation of the United Nations
g	Gram(s)
G	Soil heat flux ( $\text{W m}^{-2}$ )
GDD	Growing degree days (units)
GHG	Greenhouse gas
GL	Grassland
GM	Moist grassland
GMT	Greenwich Mean Time
GPP	Gross Primary Productivity
GPP <sub>opt</sub>	GPP at optimum light ( $2000 \mu\text{mol m}^{-2} \text{s}^{-1}$ )
GW	Wet grassland
GWP	Global Warming Potential
H	Sensible heat flux ( $\text{W m}^{-2}$ )
H <sub>2</sub> O	Water vapour
ha	Hectare(s)
HMF	Horizontal mass flux
HMT	Horizontal mass transport
hPa	Hectopascal
Hz	Hertz
IDB	Internal Drainage Board
IPCC	Intergovernmental Panel on Climate Change
IRGA	Infra-red gas analyser
J	Joule(s)
K	Kelvin
kg	Kilogram(s)
kJ	kilojoule
km	Kilometre(s)
kPa	Kilopascal
LE	Latent heat flux ( $\text{W m}^{-2}$ )
LUT	Look up tables

m	Metre(s)
M	Million
MAD	Median of absolute deviation
MC	Mineral content measurement technique
MDC	Mean diurnal course
mg	Milligram(s)
min	Minute(s)
mm	Millimetre(s)
Mt	Megatonne(s)
N	North
n	Number of samples
N <sub>2</sub> O	Nitrous oxide
NBP	Net biome production
NECB	Net ecosystem C balance
NEE	Net ecosystem exchange
NERC	Natural Environment Research Council
nf	non-fertilised
NIAB	Cambridge National Institute of Agricultural Botany
no.	Number of
NPP	Net primary production
OLR	Ordinary linear regression
p or p-value	Calculated probability
Pa	Pascal
PAR	Photosynthetically active radiation
Pg	Petagram(s)
PG	Permanent grassland
pH	Power of Hydrogen
pm	Post meridiem
POC	Particulate Organic Carbon
PPFD	photosynthetic photon flux density ( $\mu\text{mol m}^{-2} \text{s}^{-1}$ )
ppm	Parts per million
PR	Perennial ryegrass
PV	Photovoltaic

PVC	Polyvinyl chloride
QC	Quality control
R	Fitted respiration value for modelling light response ( $\mu\text{mol m}^{-2} \text{s}^{-1}$ )
$R_{10}$	Basal respiration ( $R_{\text{ref}}$ ) at 10 °C
$r^2$	Coefficient of determination
Ra	Autotrophic respiration
RAR	Rotational arable crops
RC	Row crops
RCG	Reed canary grass
Rg	Global radiation ( $\text{W m}^{-2}$ )
Rh	Heterotrophic respiration
Rn	Net radiation ( $\text{W m}^{-2}$ )
$R_{\text{ref}}$	Basal respiration at a reference temperature ( $\mu\text{mol m}^{-2} \text{s}^{-1}$ )
$r_s$	Spearman's correlation coefficient, rho
s	Mixing ratio of the scalar to dry air
S	Heat storage ( $\text{W m}^{-2}$ )
s	Second(s)
s.d.	Standard deviation
s.e.	Standard error
SB	Spring barley
SC	Static chamber
SE	South East
SGGE	School of Geography, Geology and the Environment
SHF	Soil heat flux ( $\text{W m}^{-2}$ )
SOC	Soil organic carbon
Sub	Subsidence
SW	Summer wheat
SWC	Soil water content ( $\text{m}^3 \text{m}^{-3}$ , dimensionless) $\text{m}^3 \text{m}^{-3}$
t	Tonne(s)
$T_0$	Temperature constant ( °C)
Tair	Air temperature ( °C)
TER	Terrestrial ecosystem respiration
$T_{\text{ref}}$	Reference temperature ( °C)

$T_{\text{soil}}$	Soil temperature ( °C)
$u$	Horizontal wind speed (m s <sup>-1</sup> )
$u^*$	Friction velocity (m s <sup>-1</sup> )
UG	Unutilised grassland
UK	United Kingdom
UoL	University of Leicester
V	Volt(s)
VPD	Vapour pressure deficit (Pa)
W	Watt(s)
WEELS	Wind Erosion on European Light Soils
WTD	Ground water table depth (below the field surface, m)
$x$	scalar variable
$x'$	instantaneous fluctuation from mean
yr	Julian calendar year
$z$	Height from the soil surface (m)
$z_m$	Measurement height (m)
$\alpha$	Peak quantum yield
$F$	Vertical flux
$c$	Mixing ratio
$w$	Vertical velocity (m s <sup>-1</sup> )
%	Percent
$Q_e$	Exponential integrated HMT between two heights
$Q_l$	Linearly integrated HMT between two heights
$\bar{x}$	Mean value
$z_b$	Bottom height of integration (m)
$z_t$	Top height of integration (m)
$\rho_a$	Density of dry air
°	Degree
°C	Degree Celsius
µm	Micrometre
µmol	Micromole

## **Chapter 1: Introduction and literature review**

This chapter introduces the context for this thesis, beginning with a background on peatlands, their importance within the terrestrial biome as a global carbon (C) store and the state of understand on how agricultural management and climate are influencing peatland/atmosphere interactions. In doing so, it addresses previous research conducted on these interactions and attempts at measuring the peatland C flux, which provides the basis for identifying gaps in knowledge that were identified based on observations made during field visits and gaps in literature. The identified gaps then form the basis for the research questions investigated and objectives undertaken in the subsequent research chapters of this thesis.

## 1.1 Background

Popular public research tells us that seven portions of fruit and vegetables a day will reduce the risk of cardiovascular disease. With this, and the UK population reported by the Office for National Statistics (2017) to be increasing at a rate of half a million people per year in mind, it is plausible to infer a corresponding increase in demand for Britain's domestic agricultural produce. Undoubtedly there will be both positive and negative consequences for the economy by means of the import and export of cultivated agricultural goods in Britain at a time when trade agreements are uncertain. But what is the C cost of producing crops on the United Kingdom's (UK) highest quality arable land?

At a global scale, peatlands, often also referred to as mires, organic soils and histosols, are estimated to represent a third of the terrestrial C store despite only covering 3% of the land surface (Gorham, 1991) (about 4 M km<sup>2</sup>, which equates to 16 times the land surface area of the UK). Roughly 50% of natural global peatlands are estimated to have been converted for agricultural use (Joosten and Clarke, 2002). In Britain only 1% of peatlands are now estimated to be in a natural state, with 25% of the remaining deep deposits being used for agriculture, both arable and pastoral (Natural England, 2010).

Land use change for agriculture requires drainage of peatlands. Over roughly the last 400 years large areas of the lowland fens of East Anglia have been drained to achieve a lowered water table for this purpose. Lowering of the water table exposes peat organic matter to oxygen, expediting rapid microbial decomposition and the release of C from long-term storage that was historically 'locked' into these C rich soils (Charman, 2002, Holman, 2009). Prolonged exposure of C dense peat soils to oxygen as a result of continued agricultural management, results in peat wastage through sustained losses of the greenhouse gas (GHG) carbon dioxide (CO<sub>2</sub>) to the atmosphere as well as surface lowering (subsidence).

Under the Climate Change Act (2008) a target of mitigating national GHG emissions (from a 1990 baseline) by 80% before 2050, roughly 160 Mt CO<sub>2</sub>e yr<sup>-1</sup>, has been set as part of the UK global commitment to the Kyoto Protocol and Paris Agreement (Committee on Climate Change, 2016). Despite progress by all signatories in reducing emissions by 10% for the first commitment period of 2008 to 2012, total global GHG emissions continue to grow.

Of the GHGs, CO<sub>2</sub> is the greatest contributor (74%) to anthropogenic GHG emissions that since the industrial revolution have led to global average temperature increase (IPCC, 2013b). To limit the warming of global average temperature to well below a 2 °C increase over pre-industrial levels, CO<sub>2</sub> emissions must be mitigated (Committee on Climate Change, 2016).

As part of the European Union (EU)-15 the UK has ratified the Paris agreement and is further committed to continue reduction of its greenhouse gas (GHG) emissions from all sectors. Emissions of CO<sub>2</sub> dominate the UK's national GHG contribution accounting for 81% of the total reported in 2016 (DEFRA, 2017). Agriculture currently is reported to contribute roughly 10% of the annual UK GHG budget, although the majority of this is accounted for by methane (CH<sub>4</sub>) mostly produced by ruminants, and nitrous oxide (N<sub>2</sub>O) largely from fertiliser application (DEFRA, 2017). While agriculture is only reported to account for 1% of total CO<sub>2</sub> emissions, little detailed information is available on this contribution.

Despite reductions in national emissions, the agricultural sector is reported to have failed to make progress. New targets are set out in the UK Clean Growth Strategy (2017) but new policies to reduce agricultural emissions are still needed (Committee on Climate Change, 2018). To meet national targets of GHG emission mitigation, it is essential that knowledge gaps around agricultural emissions are addressed, particularly from C-rich organic soils. The Department for Environment, Food and Rural Affairs (DEFRA) has begun a plan to develop a peatland strategy to assess current C and GHG budgets from cultivated lowland peat soils (including those under agricultural use) in an effort to establish emission factors and mitigation strategies (Committee on Climate Change, 2017, DEFRA, 2017).

An emissions factor of  $7.9 \pm 1.45 \text{ t C-CO}_2 \text{ ha}^{-1} \text{ yr}^{-1}$  for temperate drained cropland on organic soils is provided by the IPCC wetland supplement (IPCC, 2014). The Wetland supplement is a product of measurements from 39 sites across 11 published studies. Of these, the contributing data were largely obtained in Nordic countries with a cooler climate, and measured CO<sub>2</sub> exchange of cereal crops and root vegetables (e.g. Elsgaard et al., 2012, Maljanen et al., 2010, Kasimir-Klemetsson et al., 1997). More intensively cultivated salad crops on UK peat soil are recognised as contributing to anthropogenic CO<sub>2</sub> emissions through land use and land use change, but there is limited available data

(e.g. Morrison et al., 2013, Taft et al., 2017). Furthermore, there are no known available studies that provide multi-annual measurements of CO<sub>2</sub> for this land use which means that uncertainties remain concerning long-term trends and sensitivity of fluxes to year-to-year variation in management (crop type/rotations) and climate (Byrne et al., 2004, Tiemeyer et al., 2016).

Over the last decade the UK has produced 55-60% of its total supply of salad and vegetable crops (DEFRA, 2017), and as demand for food has increased the requirement for sustainable intensification and agricultural expansion has also increased. The continued exploitation of lowland peat soils results in continued peat wastage. Furthermore, cultivation of drained lowland peat soil gives rise to conditions under which the peat is vulnerable to wind erosion accelerating peat wastage (Pollard and Millar, 1968, Hutchinson, 1980, Funk and Reuter, 2006). The flux of C across lowland peat landscapes under agricultural use via aeolian mechanisms has not been measured. Despite partitioning of fields with shelter belts, transport of peat by the wind is visually evident in the fens, and should be quantified and explored to fully understand the net C balance.

At both national and global levels, sustainable management of organic soil is recognised as a priority for food security and reflected in the Food and Agriculture Organisation of the United Nations (FAO) Committee on Agriculture (COAG) declaration of 2015's status as 'International year of soils'. Furthermore, the sequestration capacity of soils, such as peatlands, has been highlighted by the Intergovernmental Panel on Climate Change (IPCC) as a potential area for anthropogenic GHG mitigation. Given the importance of the UK's cultivated lowland peatlands as both an economic and an environmental resource, there is a clear need for accurate understanding of the nature of the store of C and fluxes under a range of management practices.

Better understanding and accurate accounting of fluxes of CO<sub>2</sub> to the atmosphere from intensively cultivated agricultural peat soil in the UK over multi-annual timescales and at different spatial scales is of key importance for informing policy and mitigation strategies of agricultural land managers, the UK government, and the international climate change community.

Within this scientific and policy context, this thesis aims to contribute to filling some of the gaps in knowledge pertaining to the C balance of intensive agriculture on drained lowland peat soil.

## 1.2 Thesis outline

**Chapter 1:** (Introduction and literature review) provides theoretical background to the C cycle and the role of peatlands within that biogeochemical cycle. It also gives background to the drivers of C movement in peatlands with particular reference to temperate lowland fens and the impacts of land use change on them. An overview of existing literature on C exchange from cultivated fens is presented before addressing the research questions and accompanying objectives.

**Chapter 2:** (Methodology) describes the field site including a history of the land use and some climate history for the region. It then goes on to provide a detailed management history for the period of study, that includes site activities and descriptions of the crops cultivated. The chapter also explains the theory of the Eddy Covariance (EC) method that is implemented to measure fluxes of CO<sub>2</sub> and energy at the field site, including the data handling, quality control and gap filling.

**Chapter 3:** (Drivers of CO<sub>2</sub> fluxes at an intensively cultivated drained lowland deep peat soil) Investigates the driving variables behind CO<sub>2</sub> flux for 3.5 years of EC flux data. Nocturnal NEE is modelled to explore its sensitivity to soil temperature, and the limitation of its temperature response to environmental variables, primarily, water table depth and soil water content. Additionally, I look at the daytime response of CO<sub>2</sub> flux to photosynthetically active radiation and limitations of this light response to environmental variables for three crops.

**Chapter 4:** (Multi-annual CO<sub>2</sub> flux over 3.5 years at an intensively cultivated drained lowland deep peat soil) Gives an assessment of daily, crop and fallow, and annual CO<sub>2</sub> fluxes. It describes the annual patterns in meteorology and the magnitude of fluxes of CO<sub>2</sub>, before going on to investigate the explanatory variables for the seasonal variations in CO<sub>2</sub> fluxes.

**Chapter 5:** (Wind-blown C flux across an intensively cultivated drained lowland deep peat soil) evaluates the wind erosion data. It quantifies the wind-blown (aeolian) fraction of C being transported as dust across and potentially out of agriculturally managed peatlands; it explores the drivers and controls on dust movement in this environment for the potential mitigation of that loss.

**Chapter 6:** (Conclusion) To avoid repetition, rather than summarise findings at the end of each data chapter (3, 4 and 5), the summary of key results from each of these are presented here. These summaries provide the framework for the subsequent discussion of proposed mitigation measures. A discussion of limitations of the study undertaken and proposed pathways for future research then complete this chapter and thesis.

### 1.3 Literature review

This section provides the relevant scientific context to the research undertaken in this thesis and highlights gaps in knowledge within current literature which consequently led to the proposed research questions that are addressed by the following chapters.

#### 1.3.1 Carbon cycle

As ‘carbon-based’ life forms, C availability and cycling is a vital part of the Earth system from a human perspective. The biogeochemical C cycle can be represented as a set of stores and fluxes between those stores (Figure 1.1). The main stores of C are the atmosphere, ocean, earth surface (soils/vegetation; terrestrial) and sediment. These stores have complex interactions that couple them together and allow for the cycling of C.

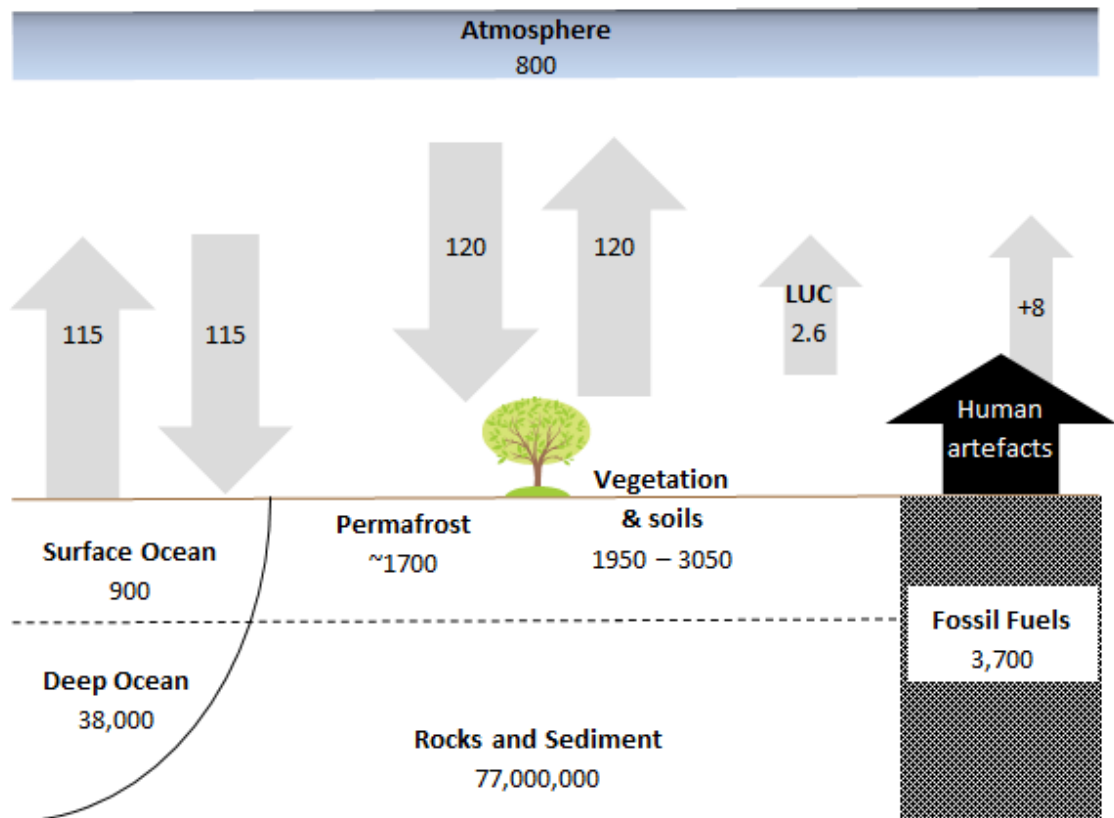


**Figure 1.1:** Diagram of the C cycle with major pools and major flows between them, all values in Pg C, all exchanges are Pg C for 1980 (Post et al., 1990). Adapted from Churkina (2013) and other data provided as per references in text (Post et al., 1990, Tarnocai et al., 2009).

Fossil fuels (gas, coal, oil) that, when burned, release CO<sub>2</sub> to the atmosphere constitute a tiny fraction of the sediment store which otherwise contains the majority (99%) of sedimentary C (Reeburgh, 1997). This store usually sequesters and cycles C on a

geological timescale of millions of years, so the use of fossil fuels has a dramatic impact on its natural cycling, but very little impact on stored C. The second largest store is in the oceans which retain C in dissolved organic/inorganic and particulate organic forms (Post et al., 1990).

The atmosphere is the smallest store of C (roughly 840 Pg C; IPCC, 2013a) but it is the most dynamic as it has the shortest residency period of C, and can be said to act as a 'conduit' between the ocean and terrestrial systems (Post et al., 1990). The terrestrial store of soils and vegetation is estimated to be in the range 1950–3050 Pg C (Batjes, 1996, in IPCC, 2013a). Although soils and vegetation contain much less C than oceans and sediments they are part of a more dynamic exchange with the atmosphere. Vegetation is estimated to contribute to a third of the terrestrial C store, the majority of the C being in soils (Post et al., 1990, Reeburgh, 1997). The terrestrial store has the potential to retain C for periods of 10's to 1000's of years. Further to this, terrestrial C stores are heavily impacted by anthropogenic activities such as deforestation and land use change (Batjes, 1996).

Estimates of the magnitude of the soil and vegetation C stores are constantly being reviewed. A further lack of consistency in measurement technique further hinders these estimates resulting in difficulty in unifying study findings to get accurate and consistent reports. A good example can be seen in the work of Tarnocai et al. (2009) who in re-assessing the contribution made by the northern circumpolar permafrost region to the total global C store determined that this region contained more than eight times the C of previous (nearly 30 year old) studies. Tarnocai's new estimate doubled the value of the total terrestrial C store.

As with estimates of storage, estimates of exchange of C (shown in Figure 1.1) between the terrestrial and atmospheric stores are also regularly re-assessed. New technology and further studies have led to improved quantification of the terrestrial stores and the flux processes which are crucial to understanding the global cycling of C and feedbacks between different pools. Peatlands are estimated to contribute to a third of the terrestrial C store and, as such, justifiably require consideration.

### 1.3.2 Peatlands

#### *General*

Peat is sedentarily accumulated, often less decomposable, plant and animal remains that build up under waterlogged conditions (Charman, 2002, Rydin and Jeglum, 2013). Peatlands, sometimes referred to as peat soils, organic soils or histosols, are commonly defined as areas of peat covered terrain in excess of 30 cm in depth (Gorham, 1991, Charman, 2002, Rydin and Jeglum, 2013, Couwenberg, 2011). There is no standardised classification system for the terminology of peatlands but generally speaking they can be defined by the presence, source and hydrochemistry of their water which then controls other defining factors such as vegetation, and nutrient regime. Figure 1.2 is a diagrammatic representation of wetland terms that demonstrates the importance of water in distinguishing between peatland types.

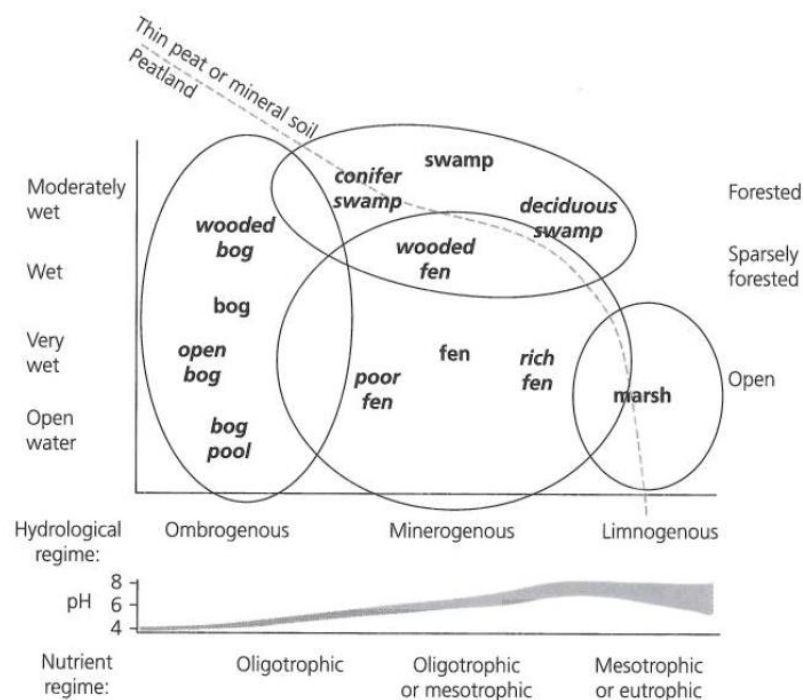


**Figure 1.2:** A general schematic for defining wetland types based on wetness and pH/nutrient status (from Rydin and Jeglum (2013))

It is possible to broadly classify bogs as ombrogenous/ombrotrophic systems that receive all of their water and nutrients from the atmosphere, and fens as minerogenous/minerotrophic systems that receive additional inputs, e.g. from groundwater and overland flow (Figure 1.2) (Charman, 2002). Figure 1.2 further

illustrates that the restriction in the source of water in bogs leads to their low pH, yet fens experience a range of nutrient quality and pH due to the variety of potential water sources. However, both types of peatland can support a diversity of vegetation types. Hydrology therefore is the control that leads to disparity in nutrient content and pH between peatlands, with bogs being acidic and nutrient poor whilst fens demonstrate a range of nutrient and, usually, higher pH levels.

Peatland profiles have been described, predominantly in bogs, as having two layers, the acrotelm and catotelm (Ingram, 1978). The catotelm is where peat accumulates and is permanently waterlogged. The acrotelm is the upper layer of the peat which is regularly supplied with organic material to decompose, within which the water level fluctuates from above the surface down to the catotelm and is therefore described as the oxic layer (Clymo et al., 1998).

When organic material, such as plant detritus, is deposited on most soils it will decompose under the action of heterotrophic micro-organisms (e.g. bacteria, fungi). The presence and rate of action of these microbial communities is controlled largely by availability of oxygen, temperature, presence of moisture and soil condition. As diffusion of oxygen in water is much less than in air, the presence of a water table that is at or near the ground surface in a peatland environment throughout the year, reduces the presence and capacity of aerobic bacteria, which require oxygen, to breakdown litter (Clymo, 1984). Anaerobic bacteria in the soil may continue to breakdown organic matter in the absence of oxygen, however they are less efficient and a reduced rate of decay will be out paced by the accumulation of plant litter. So it follows that the rates of decay and production of litter control the rate of accumulation of peat (Clymo, 1965). Both of these processes are dependent on climatic controls (particularly precipitation amount/seasonality and temperature), and therefore changes in climate may result in changes in the rate of peat accumulation and even degradation.

The majority of the world's peatlands are located in the boreal and temperate biomes of the northern hemisphere where high precipitation and low evaporation are coupled with areas of poor drainage (Strack, 2008). Peatlands are also found in tropical regions with high precipitation and humidity (Rieley et al., 2008). The extent of peatlands and the quantity of C they store is still undergoing investigation (Page et al., 2011b, Morelle, 2014). A good example of this is the recent publication by Dargie et al. (2017) who

measured extensive peat deposits beneath swamp forests of the Cuvette Centrale depression in the central Congo Basin and found their extent to be five times greater than the previous maximum estimate for the whole Congo Basin, which increased the global estimate of tropical peatland C by 36%.

Peat soils in the UK have been accumulating since the end of the last period of glaciation (roughly 10,000 years ago). UK peat is estimated as contributing to over half ( $5.1 \times 10^9$  t) of the UK soil C store  $9.8 \pm 2.4 \times 10^9$  t (Dawson and Smith, 2007, Ostle et al., 2009, Milne and Brown, 1997). The majority of UK peat C,  $4.5 \times 10^9$  t, is in Scotland (Milne and Brown, 1997, Smith et al., 2007), leaving  $639 \times 10^6$  t for England and Wales. Natural England (2010) estimated that peatlands presently constitute 11% of England's land surface area,  $14,185 \text{ km}^2$  (Natural England, 2010), with deep peats (having a peat depth greater than 0.4 m) constituting just under half,  $6,799 \text{ km}^2$ , of this estimate. Upland blanket bogs in the Pennines, North York Moors and the South West of England make up  $3,910 \text{ km}^2$  of this estimate. While lowland fenlands of Somerset levels, Lancashire Mosslands, Lincolnshire, The Broads and fens of East Anglia constitute  $2,880 \text{ km}^2$  but are estimated to contain 57% of the total English C store ( $\sim 330$  Mt C; Natural England, 2010). In the last 400 years the fens have been under the influence of substantial land management practices that have led to reductions in the C store with only a reported 1% of these peatlands remaining in a semi-natural state (Natural England, 2010).

### 1.3.3 Peatlands & carbon

As per the definition of peatlands, they form from organic material that accumulates over long time periods under certain climactic and geomorphological conditions. All organic material contains C and therefore peatlands can be considered to sequester C. Peatlands vary in their C content but as a general rule it is around 50% of their mean dry organic matter content (Chambers et al., 2011, Rydin and Jeglum, 2013).

Peatlands globally are estimated to contain roughly 500 Pg of terrestrial soil C (Post et al., 1990, Clymo et al., 1998, Strack, 2008), which is more than half of the amount that is presently stored in the atmosphere ( $\sim 800$  Pg, IPCC, 2013a), and roughly a third of global soil C, despite only covering 3% of the land surface area (Gorham, 1991). Providing peatlands are accumulating organic matter in excess of decomposition of the material they can be said to be a sink of C.

Peatland-atmosphere interactions are an important part of the terrestrial role within the C biogeochemical cycle. Exchanges between them have the potential to increase and decrease atmospheric concentration of GHG's, such as CO<sub>2</sub>, CH<sub>4</sub> and N<sub>2</sub>O, which have different degrees of global warming potentials (GWP). Global warming potential (GWP) is a measure of the radiative effect of one substance over another for a specific time period; these are commonly compared to CO<sub>2</sub> over 100 years (IPCC, 2013a). A natural peatland is interesting from a radiative forcing viewpoint because it both sequesters CO<sub>2</sub> which reduces radiative forcing, but also emits CH<sub>4</sub> which has a greater (28 times greater over 100 years, without climate feedbacks) GWP than CO<sub>2</sub> which increases radiative warming. Long-term studies of peatlands have revealed some sites fluctuate between being a net source or a sink of C depending on the year and site conditions (Strack, 2008). Over longer periods of time (centuries to millennia) natural peatlands are a C sink based on the balance between the quantity of CO<sub>2</sub> they sequester despite the CH<sub>4</sub> they emit (Frolking et al., 2011, Ciais et al., 2013).

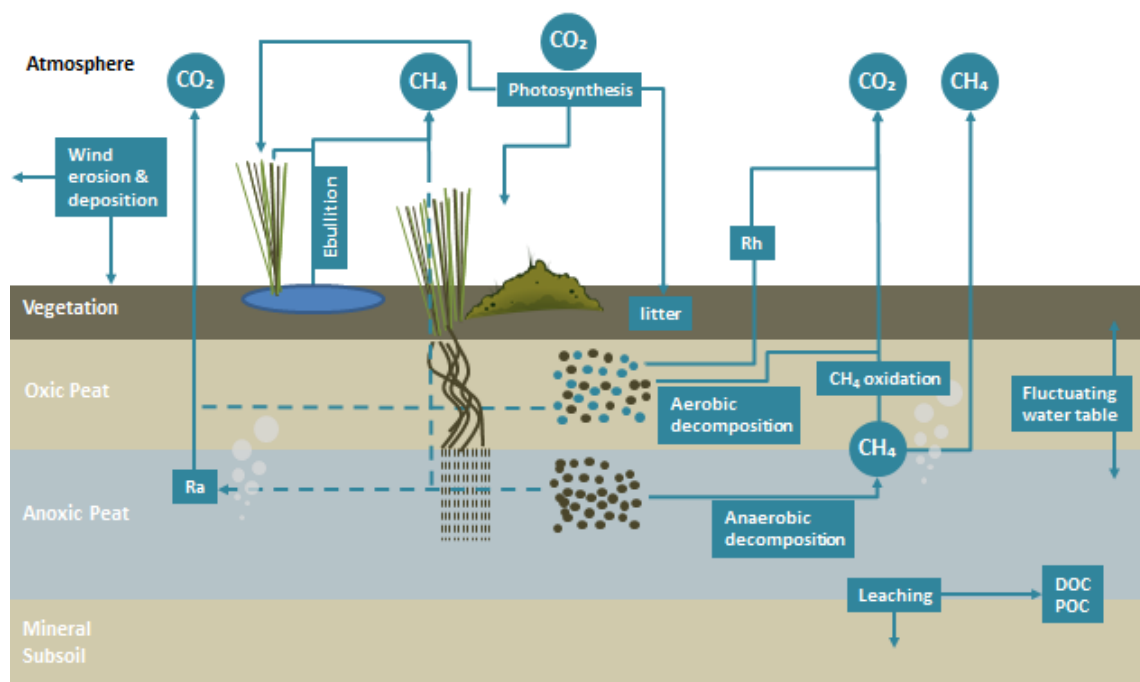


**Figure 1.3:** Conceptual model of C cycle processes and flow paths for a fen peat soil with some typical fen vegetation. Brown dots represent micro-organisms that function anaerobically and blue dots micro-organisms functioning aerobically.

### *Net ecosystem exchange*

It is well established that CO<sub>2</sub>, CH<sub>4</sub> and N<sub>2</sub>O are the ‘main’ GHG’s with CO<sub>2</sub> being the most abundant in the atmosphere (IPCC, 2013b). Peatland vegetation takes up CO<sub>2</sub> from the atmosphere for use in photosynthesis, which is used to build plant biomass (Figure 1.3 and 1.4). The vegetation converts CO<sub>2</sub>, photosynthetic radiation and water into carbohydrates, oxygen and water during photosynthesis. The uptake of CO<sub>2</sub> by vegetation is referred to as Gross Primary Productivity (GPP). During photosynthesis the inorganic C in the form of CO<sub>2</sub> is ‘fixed’ to an organic form. Uptake of CO<sub>2</sub> from the atmosphere in photosynthesis is crucial in reducing atmospheric CO<sub>2</sub> concentrations. The rate of uptake is controlled by vegetation type, availability of CO<sub>2</sub>, photosynthetic radiation, temperature, water and nutrients supplied by the soil (Page et al., 2011a).

During photosynthesis 40-50% of the CO<sub>2</sub> uptake is released as autotrophic respiration (Ra) (Figure 1.3 and 1.4) (Schlesinger and Andrews, 2000) where vegetation, in the process of taking up nutrients through its roots to construct biomass, releases CO<sub>2</sub> as a result of plant growth processes requiring the oxidation of sugars. The amount of CO<sub>2</sub> released is not enough to counterbalance the amount of CO<sub>2</sub> absorbed for photosynthesis, thus there is a net positive sequestration which is referred to as net primary production (NPP). C that is stored in vegetation biomass remains there until the plant dies or loses some biomass to the soil, e.g. as litter (Figure 1.3).

Aerobic decomposition undertaken by micro-organisms in the soil leads to further CO<sub>2</sub> emission to the atmosphere which is referred to as heterotrophic respiration (Rh) (Figure 1.3 and 1.4).

An “enzyme latch” mechanism has been identified as a key control of CO<sub>2</sub> flux in peat soils (Freeman et al., 2001, Freeman et al., 2004). The theory being that a high concentration of recalcitrant phenol compounds is present in anoxic peat soil. These phenols can be decomposed by a phenol oxidase enzyme, however this enzyme requires bimolecular oxygen to function, and therefore while the soil is waterlogged this cannot take place. Additionally, without the elimination of the phenol compounds, decomposition of hydrolase compounds by hydrolase enzymes (which can function in anoxic environments) is restricted (Freeman et al., 2001, Pinsonneault et al., 2016).

Once the phenol compounds are broken down the enzyme latch is considered open and decomposition will continue even once water level rises again.

Both auto- and heterotrophic respiration contribute to terrestrial ecosystem respiration (TER) and have been shown to respond to changes in temperature, the availability of organic matter, microbial communities and moisture (Strack et al., 2008, Pinsonneault et al., 2016, Worrall and Burt, 2004, Parmentier et al., 2009, Lafleur et al., 2005). The combination of Ra and Rh here is discussed as TER.

Photosynthesis (GPP) and TER regulate net ecosystem exchange (NEE) of CO<sub>2</sub> between peatlands and the atmosphere, where  $NEE = TER - GPP$ . In this study the atmosphere is used as the flux reference for NEE; meaning that  $NEE < 0$  reflects the ecosystem operating as a sink (loss of CO<sub>2</sub> from the atmosphere) while  $NEE > 0$  reflects emission to the atmosphere (gain of CO<sub>2</sub> by the atmosphere) (Luyssaert et al., 2009). TER and GPP, however, are both quantified as positive integers.

#### *Methane*

While decomposition and CO<sub>2</sub> emission due to Rh are reduced in waterlogged anoxic peat (as explained above), anaerobic methanogenic bacteria are still active (Rydin and Jeglum, 2013). The activity of these methanotrophs leads to a release of CH<sub>4</sub> (the second most abundant C-based GHG (Mitsch et al., 2013) which is transported to the atmosphere via ebullition, vascular pathways and diffusion (Figure 1.3 and 1.4). The production of CH<sub>4</sub> by peatlands is not as well understood but is similarly believed to be controlled by temperature, quality of organic material and water table level (Strack et al., 2004, Moore and Knowles, 1989, Roulet et al., 1992).

#### *Dissolved Organic Carbon and Particulate Organic Carbon*

Further loss of C from peatlands can be accounted for by Dissolved Organic Carbon (DOC) and Particulate Organic Carbon (POC) loss through waterways (Dinsmore et al., 2010, Evans et al., 2006, Worrall et al., 2004, Moore et al., 2013) or POC loss through wind erosion (Warburton, 2003) (Figure 1.3 and 1.4). The destination of these fluxes is less well understood and can result in accumulation elsewhere in the soil system or undergo oxidation and contribute to further peatland GHG contribution to the atmosphere (Worrall et al., 2011, Dinsmore et al., 2010, Evans, 2013).

Peat as a dry material has a low density (Warburton, 2003), and despite the nature of peatlands as waterlogged environments, the surface of peatlands is not always saturated. Reduced vegetation cover and a strong wind are considered to allow for lateral aeolian transport of POC if the carrying capacity of the wind is strong enough to dislodge particles (Funk and Reuter, 2006). Wind-eroded material has the potential to contribute to loss of POC by waterways if the load transported is deposited over water. Few studies exist that quantify this, as research on wind erosion focuses on more readily transportable sandy soils. Only one report by Warburton (2003) was identified that quantified a peat flux of 0.24-0.48 t ha<sup>-1</sup> yr<sup>-1</sup> for an upland bog in the UK, which equated to a loss of 12-24 g C m<sup>-2</sup> yr<sup>-1</sup>. The combination of wind and rain action was attributed as the key mechanism in driving wind erosion for this UK upland peat bog, with more sediment transported during windy rainfall events than during windy dry spells (Warburton, 2003, Foulds and Warburton, 2007a, Foulds and Warburton, 2007b).

#### *NECB*

The combinations of the net flux from all of the above C pathways make up the net ecosystem C balance (NECB). This is rarely reported in full for any one site (Nilsson et al., 2008, Hendriks et al., 2007). Due to the scale of work achievable within the framework of this thesis, here the two largest contributors to net flux of C, which are considered to be NEE and lateral C, are measured. Additionally, given the complete lack of any flux data for wind erosion from lowland deep peat soils, flux by wind erosion is also quantified. Other components of the NECB, such as CH<sub>4</sub>, N<sub>2</sub>O, and DOC were measured as part of a larger project and reported elsewhere (Evans, 2017, Peacock et al., 2017).

#### 1.3.4 Drainage for agriculture

As described, natural peatlands have a water table that is usually at or near the surface which does not make them suitable for most types of commercial crops nor for mechanised access. Therefore, for agricultural practices to be undertaken on peatlands the water table must be lowered, usually by the digging of ditches to improve drainage. Between 14 and 20% of peatlands worldwide have been utilised for agriculture; in fen peatlands, drainage has yielded organic rich, highly fertile soils (Oleszczuk et al., 2008) but peatland drainage for cultivation has also occurred on oligotrophic bog peats (e.g. in South East Asia for plantation development). As mentioned earlier, large areas of

lowland peat in the Fens of eastern England have been reclaimed, drained and managed for their high agricultural productivity since the early medieval period (Charman, 2002) due to the nutrient rich status of the drained soils. A similar picture can be seen across some other parts of Northern Europe, e.g. in Northern Germany and the Netherlands. Soil water balance is a key limiting factor for crop production (Fuhrer, 2007) which means that despite being vital to the integrity of the peatland system, the water is managed with crop production as a priority over landscape preservation. In particular, the Fens of the UK have been utilised for production of intensively managed crops, e.g. salads and vegetables, reportedly growing 37% of all national outdoor grown vegetables in 2006 (Natural England, 2015).

Drainage and further management leading to peat wastage which is a general term that covers several elements of peat loss and subsidence due to drainage, this includes: shrinkage, compression, oxidation, increased wind erosion, removal on crops, and burning of peat (Holman, 2009, Leifeld et al., 2011). As it is more-or-less saturated with water, peat in a natural condition takes up a much greater volume, so when the water level is lowered the initial subsidence by shrinkage and compression is rapid. In addition, mechanical agricultural activity will increase compaction. These are all physical processes – i.e. there is no net loss of C.

Thus anthropogenic disturbances have the potential to alter the C cycle interactions between the atmosphere and peat soils leading to their becoming a net source of the GHG's CO<sub>2</sub> and N<sub>2</sub>O and a small sink of CH<sub>4</sub> (Frolking et al., 2011, Ciais et al., 2013, Mitsch et al., 2013). A conceptual diagram of the C pathways for an intensively cultivated peat soil is presented in Figure 1.4.

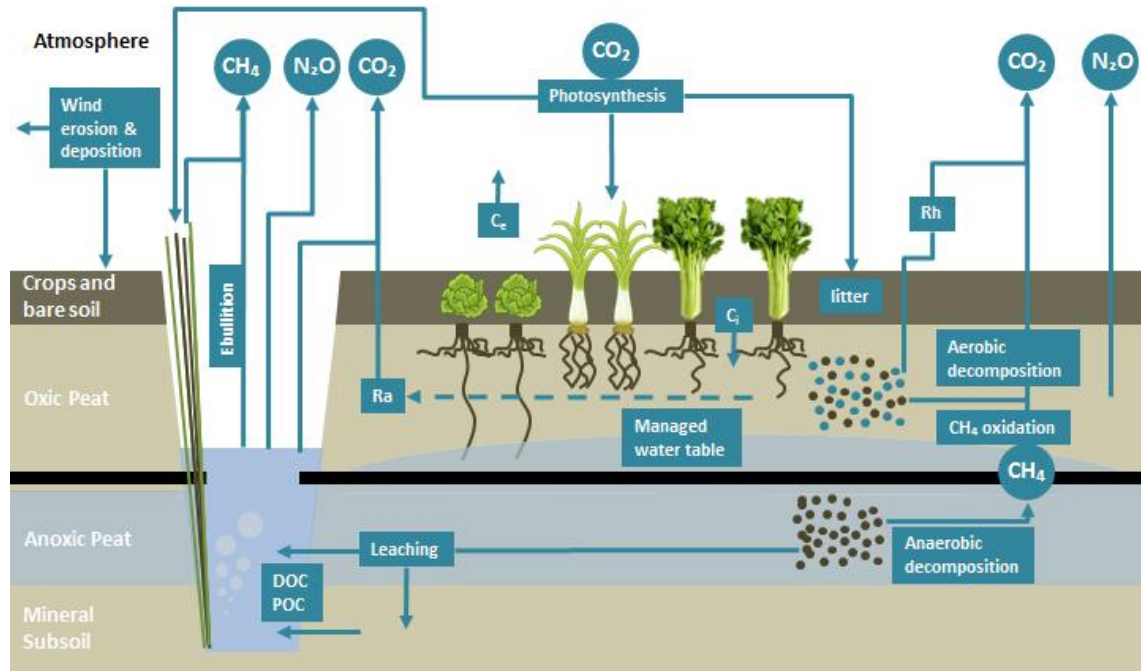


**Figure 1.4:** Conceptual model of C cycle processes and flow paths for a drained intensively cultivated deep peat soil (modelled on the field site in this thesis). The black horizontal bar at the bottom of the oxic peat layer represents pipe drainage system).  $C_i$  is C import, the amount of C added to the field during planting, by plug crops primarily.  $C_e$  is the C exported during harvest.

The focus of this thesis is C flux at an intensively managed deep peat soil via NEE, lateral flux and wind erosion, assessment of the impacts of this land use change on the C cycle are addressed with respect to current understanding of these specific components (despite presenting all pathways in the conceptual diagram, Figure 1.4.)

### *NEE*

Increased and prolonged aeration (oxidation) of the upper peat profile results in an increased rate of decomposition by aerobic micro-organisms that are no longer limited by the saturated nature of the peatland, opening the “enzyme latch”, as discussed above. The increase in aerobic microbial activity substantially alters the peatland NEE balance by increasing  $CO_2$  emissions, although the lower water table results in a reduction in methanogenesis and consequently results in much lower emissions of  $CH_4$  (Mander et al., 2010, Frohling et al., 2011). The result is a net C loss from the peatland and is a constant year-round process that initiates immediately following the implementation of drainage. Agriculturally managed peatlands growing (mostly) cereal crops and grasses have been identified as net annual sources of  $CO_2$  with a positive net C balance (e.g. Eickenscheidt et al., 2015, Tiemeyer et al., 2016, Drösler et al., 2013, Elsgaard et al.,

2012, Poyda et al., 2016, Leiber-Sauheitl et al., 2014, Grønlund et al., 2006, Taft et al., 2017). Those utilised to grow bioenergy crops have yielded reduced net CO<sub>2</sub> loss (e.g. Shurpali et al., 2009, Mander et al., 2012), however once the NPP, accounted for by the harvested crop, was removed from this balance, even these sites were net sources of C.

The IPCC (2014) wetland supplement to IPCC (2006) reports a default emission factor of 7.9 t CO<sub>2</sub>-C ha<sup>-1</sup> yr<sup>-1</sup> for boreal and temperate croplands on drained organic soils, based on findings from 39 sites across 11 published studies. The contributing data were largely obtained in Nordic countries that are unlikely to experience the same magnitude of gas fluxes as would be expected in the UK due to their cooler climate and therefore this necessitates further research to be undertaken on cultivated UK peat soils.

#### *Lateral import and export*

Imported carbon (C<sub>i</sub>) and exported C (C<sub>e</sub>) (Figure 1.4) are annual management-related fluxes of C. Contributions to C<sub>i</sub> include organic fertilisers and planted materials (e.g. seeds and growing media), while C<sub>e</sub> consists of harvested materials. Several studies have been identified where fertiliser has contributed to C gain by a site, and resulted in increased short term CO<sub>2</sub> emission (e.g. Eickenscheidt et al., 2015, Beyer et al., 2015), however no sources have been identified whereby planting mediums of intensive cultivation of salad crops is calculated. Given the, observed (by author), organic rich mediums planted in the fens, accounting for this C<sub>i</sub> to the site could make a substantial contribution to site C balance and therefore warrants quantification.

Quantification of C<sub>e</sub> has been undertaken at a number of agricultural sites as a contribution to C balance at the field scale, although again these have had a focus on cereal crops rather than salad crops. In particular, a cultivated peat soil in Germany where summer wheat was grown with an under sown ryegrass resulted in a C<sub>e</sub> of 650 g C m<sup>-2</sup> for the year (Poyda et al., 2016), which is almost as great as the IPCC emissions factor for NEE contribution just discussed above.

Given that C<sub>e</sub> related to production of salad crops has not been quantified, and harvest contributions to C balance have been shown for other agricultural sites, better understanding of both the imports and exports of these crops should be addressed.

### *Wind erosion - POC*

The impacts of management activity on peatland C budgets have received much attention in relation to losses of soil C in the form of CO<sub>2</sub>, whereas transport of C through aeolian pathways has remained largely unquantified. Wind erosion is expected to increase due to drainage and regular disturbance of peat. It is often accounted for under the umbrella term of peatland wastage but has not been quantified in any peatland C balance studies, despite awareness and qualitative assessments of peak windblown dust (“fen blows”) being made in some of the earlier literature (e.g. Pollard and Millar, 1968, Hutchinson, 1980). Some more recent studies have suggested that loss of C via this pathway is negligible (Dawson et al., 2010) and it has therefore been left unaccounted for in calculations.

Management practices are such that many hectares of drained peatland remain unvegetated for large periods of the year leaving a bare peat surface exposed and vulnerable to erosion and transportation by wind action. Peat has a low density and the exposed nature of peat soil in an agricultural landscape particularly during preparation for cultivation during dry spring months means that it is at high risk of erosion (Warburton, 2003, Pease et al., 2002).

Global scale studies have suggested that erosion of agricultural soil could be responsible for 0.12 Pg C per year being displaced by wind or drained by rivers (Van Oost et al., 2007) and that it is important that this is investigated at smaller landscape scales. This was also the view of the 2014 wetlands supplement to IPCC (2006) which suggested that despite the lack of data it is possible that in areas where land use has led to bare soil being exposed, that airborne erosional POC loss has the potential to be significant (IPCC, 2014). This is identified as a gap in knowledge that should be included in C accounting for peatlands.

Most studies of wind erosion on agricultural soils focus on dry environments (Pease et al., 2002, Zobeck et al., 2003). Despite awareness of this C transport pathway, no studies have been identified that quantify this flux for lowland agricultural peat soils. Those that acknowledge this pathway for agricultural peat soils (Dawson and Smith, 2007, Taft et al., 2017) do not quantify it, but rather reference a value of >3 t ha<sup>-1</sup> yr<sup>-1</sup> reported by Böhner et al. (2003) for mineral agricultural soils in the UK, or 0.46-0.48 t ha<sup>-1</sup> yr<sup>-1</sup> reported by Warburton (2003) for an upland blanket bog in the UK.

Warburton (2003) is one of few wind erosion studies that have been conducted on peatlands to try and account for aeolian flux. Other research on aeolian erosion from loamy sand agricultural soils have estimated a flux between -32 to 37.5 t ha<sup>-1</sup> yr<sup>-1</sup> (Chappell and Warren, 2003). The majority of research on wind erosion has focused on non-organic soil types (Funk and Reuter, 2006) or arid environments (e.g. Webb et al. (2013)), and therefore leave a clear need for assessment of wind erosion of agriculturally managed lowland peat.

Cover crops are regularly planted on agricultural land to consolidate the soil surface and protect seed-planted crops from wind erosion (M. Hammond, Pers. comm.), in addition to shelter provided from high wind velocities by hedgerows. The effectiveness of these wind breaks has not been quantified and while they are considered to reduced transport of POC across peatlands but they have not stopped it, as anyone who has visited the fens in strong April winds can attest. However, the effectiveness of row crops at reducing wind erosion of a cultivated gleysol soil was investigated by Funk and Engel (2015), no other studies have been identified. To better understand and mitigate the erosion of agricultural peat soils by wind-action, quantification of fluxes via this pathway is necessary (Li et al., 2011, Mendez et al., 2011, Panebianco et al., 2010).

### 1.3.5 Climate change

The Earth's climate is acknowledged to be warming (Figure 1.4), and it is largely agreed that this warming is being heavily influenced by increased concentrations of GHGs in the atmosphere, specifically those of anthropogenic origin, arising from the burning of fossil fuels and land use change (IPCC, 2013a). The Intergovernmental Panel for Climate Change (IPCC) describe warming of the climate system as “*unequivocal*” with recent observed changes being unequalled in the time span over which they are occurring (IPCC, 2013b). At present, global annual average CO<sub>2</sub> (the most abundant C bearing GHG) concentration in the atmosphere is just over of 400 ppm, having risen by over 100 ppm since the Industrial Revolution commenced in the 1750's.

It is stated as ‘likely’ in the IPCC (2013a) report that extreme weather events (e.g. floods/droughts) will become more frequent worldwide. This will have an impact on the inter-annual variability of seasonal climate regimes, and consequentially the processes they control. The global climate is intrinsically linked to the C cycle and C cycling is sensitive to climate.

## Climate change and peatlands

Changes in climate that are of most relevance to peatlands involve temperature, precipitation and atmospheric CO<sub>2</sub> concentration as they are of central importance as controls of the biological responses of plants and mineralising bacteria, both aerobic and anaerobic (Newton et al., 2007).

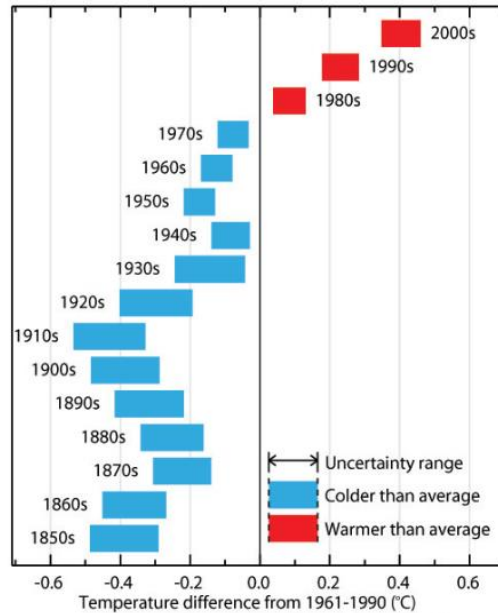


**Figure 1.5:** Global decadal average temperature difference from the average of all years (Source: UK Met Office, 2010)

Temperature and soil moisture are vital controlling influences on rates of peat accumulation and decomposition and even the distribution of peatlands (Zicheng et al., 2010). Temperature controls both photosynthesis and respiration via its influences on vegetation and micro-organisms, making it extremely relevant to peatland studies (Rydin and Jeglum, 2013). It is likely that temperature increase will increase evapotranspiration which reduces the availability of water for photosynthesis.

Kirschbaum (2000) performed field and controlled laboratory soil warming experiments on organic soils to assess temperature sensitivity. He found that TER sensitivity to temperature greatly exceeded that of NPP. As temperature-limited decomposition increases with a warming climate, it is assumed that soils will become a larger source of CO<sub>2</sub> to the atmosphere (Schlesinger and Andrews, 2000). Increased rates of soil organic matter mineralisation, however, have the potential to result in higher nutrient availability to vegetation and higher primary productivity, which could then offset the

loss of C to the atmosphere, although this has only been addressed in one laboratory study of a single radish crop growth on peat soil mesocosms (Musarika et al., 2017).

Atmospheric CO<sub>2</sub> is controlled by complexities of the C cycle and its interactions with climate (Post et al., 1990). An increase in atmospheric CO<sub>2</sub> (as seen since the Industrial Revolution) has been shown to cause a fertilization effect, as there is more abundant CO<sub>2</sub> for absorption by vegetation. In Arctic tundra, Oechel et al. (1994) undertook a controlled experiment to test the fertilisation effect, and found that increasing CO<sub>2</sub> concentration and temperature had the potential to enhance sink activity, and this was attributed to increased mineralisation, related to temperature, leading to enhanced nutrient supply.

The controls of temperature, CO<sub>2</sub> concentration, moisture and nutrient availability on an agricultural peatland are possibly outweighed by management. As crops are only present for the growing season, sometimes only for a two months in that period, there is unlikely to be enough increased GPP from CO<sub>2</sub> fertilisation or from increased nutrient supply from increased temperatures to offset mineralisation losses. Further to this, drought limited GPP as a response to longer periods of dry warm weather and reduced soil moisture contents are unlikely on an intensively managed agricultural peatland as the moisture content of the peat is closely monitored and controlled. To better understand the potential impacts of climate change on NEE of intensively cultivated peat soils, drivers of NEE (and its constituents) require further investigation. Eddy covariance measurements over multiple crop cycles would provide measurements of NEE that could be partitioned into its GPP and TER contributions and allow for identification of the environmental controls of these fluxes, which would improve understanding of the land-atmospheric relationship in this ecosystem and projected impact of forecasted climatic changes.

### 1.3.6 Lowland peatlands in the UK and peat wastage measurements

#### *History*

The fen peatlands of East Anglia and Lincolnshire began their formation 10,000 years ago at the end of the last ice age (Natural England, 2010) and geologically are based largely on easily erodible sedimentary deposits that makes them good aquifers. As glaciers retreated and sea levels rose, forests dominated the landscape of the fens and periodic flooding led to the associated formation of lakes.

The wetlands that developed became a rich source of sustenance and materials that were used for building and burning in settlements. To allow for exploitation of these wetlands as productive agricultural land, extensive areas of the fertile peat soils were reclaimed, drained and partitioned. Large scale drainage of the fens began in the 17<sup>th</sup> century when Cornelius Vermuyden, a Dutch land reclamation engineer, was commissioned by the crown and later again by parliament to increase the drainage by the cutting of new channels. The shortfall of this was that the consequent subsidence and oxidation of exposed peat soils was underestimated and led to extensive seasonal flooding. Pumping was then introduced in order to raise the water from the drainage ditches into the new channels and the rivers (Hutchinson, 1980).

The fens became highly productive farmland supplying the rest of the UK with vegetable, grains and fruits but at the cost of peat soils which continued to decompose and subside. Drainage for agricultural use has continued and at the present time there are only small fragments of undrained fen habitat remaining (Natural England, 2010). Modernised intensified management practices of the 20<sup>th</sup> century further compounded peat wastage, and now large areas of the fens have degraded down to the underlying clay soils and what remains is still largely being farmed. The Agricultural Land Classification (2009) showed that only 21% of agricultural land in England is classified as Grade 1 (excellent) and 2 (very good), and of this the majority is situated in the Fens (Natural England, 2009).

#### *Subsidence measurements*

Subsidence is a reflection of peat wastage and represents the integrated loss of C not just by mineralisation but also, DOC and POC pathways. To calculate a meaningful value of subsidence it is important to have multiple measurement sites to accurately assess the rate of loss. These are time-integrated measures that do not account for peak C loss events but average over the measurement period (Page et al., 2011a).

At the time of initial drainage in the East Anglian Fens, in the 1850s, an attempt was made to quantify the subsidence rate over time by installing a subsidence pole at Holme, Cambridgeshire. Hutchinson (1980) reported a 3.91 m (30.5 mm yr<sup>-1</sup>) lowering of the peat surface over 128 years as measured against the Holme Post as a result of draining of the peatland for agriculture. Notably, over the initial 27 year period, lowering was about 96 mm yr<sup>-1</sup>, before a levelling off to a reduced rate of 11 mm yr<sup>-1</sup> over the last

measurement period of 16 years. In his study, Hutchinson speculated that other locations in the fens that had been drained for much longer periods and more intensively cultivated would have experienced greater peat subsidence. He further ventured that underlying mineralogy and state of decomposition of the peat would control the amount of wastage measured, and concluded by suggesting that keeping a raised water table, as restrictions permit, should decrease the wastage rate. This research is supported by a more recent assessment of subsidence at Methwold Fen, Norfolk (just over 50 km east of Holme) by Dawson et al. (2010) who undertook soil and topographic surveys. They measured an average lowering of between 14 and 11 mm yr<sup>-1</sup> over a 22 year period. They concluded that this reduced rate of wastage partly resulted from moisture in the peat, firstly due to an underlying 'Fen Clay' deposit that, given its impermeable nature allowed for better water table control, and secondly to anthropogenic changes in land and water management practices, such as those suggested by Hutchinson (1980).

Subsidence as a measure of C loss does not allow for identification of the specific disaggregation of its constituents such as peat oxidation and aeolian POC, and as such both estimates of CO<sub>2</sub> fluxes and aeolian POC loss from cultivated temperate fens are scarce (IPCC, 2014).

#### *Chamber technique*

Measurements of gas fluxes are most commonly undertaken using the chamber technique (Page et al., 2011a). The benefits of the chamber technique are that it is spatially very accurate as it measures a controlled volume of air over a set area, so the exact source of flux is well defined. Additionally, chamber measurements allow for partitioning of NEE into TER and GPP via measurements made using dark and opaque chambers. Chambers can be static, whereby air samples are extracted over time and taken to a laboratory to be examined in a mass spectrometer, or dynamic, whereby air is circulated in the chamber and measured in-situ using a portable gas analyser (Denmead, 2008). Flux is determined by linear regression of gas concentration over time and non-linear relationships are rejected.

Due to the necessity of accurately representing seasonal variation, to get a realistic value of seasonal and annual flux, the chamber measurements must be taken as frequently as possible. Replication of measurements over time is required to accurately capture seasonal variation in fluxes and this makes this method labour intensive for little

temporal resolution (Page et al., 2011a), which is a clear drawback of the method that can be improved by use of automated chambers. Additionally upscaling to landscape scale values from these measurements can be difficult unless all land cover types included in the upscaling are covered by the chamber measurement replication and scaled up proportionally (Page et al., 2011a). The advantage of the chamber technique is that it allows for species specific understanding of NEE, and for clearer partitioning of constituents of NEE in comparison to EC.

A study by Taft et al. (2017) report figures of  $3.55 \pm 0.65$  to  $8.43 \pm 0.68$  t C-CO<sub>2</sub> ha<sup>-1</sup> yr<sup>-1</sup> for one year of measurements implementing the static chamber technique at a lowland agricultural site (the same site studied in this thesis) across both bare and cropped soils with a range of soil organic carbon (SOC) contents.

### *EC technique*

The EC technique measures gas flux between the land and the atmosphere as a covariance with vertical velocity in a turbulent air flow (Foken et al., 2012a) (the theory is discussed in more detail in Chapter 2). The instrumentation is deployed in a field location and measures at up to 20 Hz resolution making it better suited to calculate long term fluxes (e.g. seasonal, annual), but can only measure NEE. The instrumentation measures over a much larger footprint than the chamber technique and so can average variation in surface cover more readily; however it functions best over homogenous terrain (Foken et al., 2012a).

The instrumentation generally requires little maintenance; however calibrations of instruments need to be addressed annually. The main disadvantages of the technique are that the instrumentation is expensive to set up, can be technically difficult to set up, and without data telemetry large amounts of data can be lost. Also, due to conditions not always fulfilling the theoretical assumptions of the methodology the data requires considerable post-processing, quality control and gap filling and so should be reported with appropriate uncertainty (Page et al., 2011a). The method allows for averaging fluxes over much larger areas at much higher temporal resolution (20 Hz) than the chamber technique.

The EC technique is used in many studies with a global community for sharing data, FLUXNET, which hosts data from over 500 sites. Many studies are conducted over

cereal crops, grasslands and bioenergy crops in both the boreal and temperate zone on agriculture (e.g. Shurpali et al., 2009, Kandel et al., 2013, Lohila et al., 2004, Nieveen et al., 2005, Kutsch et al., 2010) however none have been identified for intensive cultivation of salad and vegetable crops on temperate drained lowland peat soils.

## 1.4 Research questions and objectives

To address the aim (presented earlier in this chapter) of this thesis to improve gaps in knowledge pertaining to the C balance of intensive agriculture on drained lowland peat soil, and given the literature review four central research questions are presented here, Objectives undertaken to answer each question are additionally provided.

### 1.4.1 Research Questions

1. What are the key drivers of NEE at a lowland peat soil under intensively cultivated land use?
  - a. Maintain an EC tower at Methwold fen, over multiple years and crop cycles. Convert, process, quality control and gap-fill flux data.
  - b. Analyse meteorological and flux data for impacts of agricultural management and drivers of CO<sub>2</sub> exchange on NEE.
  - c. To establish the key drivers of NEE of this managed peat soil.
2. What are the daily, seasonal (crop/fallow) and annual magnitudes of NEE from drained intensively cultivated lowland peat soil, under varying crop management?
  - a. Calculate annual, seasonal and daily fluxes of CO<sub>2</sub>.
  - b. Report the first multi-annual CO<sub>2</sub> fluxes for a drained intensively cultivated peatland in East Anglia using the EC technique.
3. What contribution do planting and harvest of different crops have on the C balance of an intensively cultivated peat soil?
  - a. Calculate lateral flux of C through the planting and harvesting of crops.
  - b. To quantify the contribution that planting and harvesting of different crops has on the annual C balance of lowland peat soil.
4. How much C is transported over intensively cultivated peatlands in East Anglia by aeolian action?
  - a. Install and establish best practice for collecting wind eroded peat samples in this environment using Big Spring Number Eight (BSNE) passive horizontal flux samplers. Maintain the equipment over multiple years and crop cycles to attain data for multi-annual comparison.
  - b. Combine meteorological data from the EC tower with the BSNE data to investigate drivers of horizontal peat flux.

- c. To provide the first quantification of aeolian erosion for peat soil under intensive agricultural management.

Results from this thesis will aim to provide important understanding of the C balance of productive, but degrading, agricultural peat soils under intensive use. Better understanding of the drivers of CO<sub>2</sub> flux, lateral and aeolian fluxes between years and under different crop management will provide a basis for future mitigation strategies.

## **1.5 Chapter summary**

This Chapter has outlined the background to the research to be undertaken. This justifies the research and offers questions that will be addressed by this novel research.

Currently available literature is lacking depth of knowledge on GHG fluxes from lowland peat soils. In particular this literature review has only identified one study that addresses the CO<sub>2</sub> released from intensively cultivated lowland peat soil, and this study is limited temporally and spatially by its measurement technique. Better understanding of the magnitude of and influences on C and C-CO<sub>2</sub> fluxes from intensively cultivated peat soils over multiple years and crops will improve knowledge of this valuable C store and its potential longevity under agricultural land use.

## **Chapter 2: Materials and Methods**

This chapter provides details of the field site of this study and includes information on site management practices and the crops grown. Theoretical underpinnings of the EC instrumentation are addressed, along with details of equipment and data processing for calculating fluxes of CO<sub>2</sub> and energy budgets. Additionally, the methodology followed for calculation of lateral C import (C<sub>i</sub>) and export (C<sub>e</sub>) is explained.

Analysis strategies used in assessing the datasets are discussed in subsequent chapters and the equipment and strategy used to measure and quantify horizontal aeolian C movement across the site are described in Chapter 5.

## 2.1 Site information

### 2.1.1 Regional Climate

The climate of the East Anglian region in which the study site was located is temperate with an annual average temperature between 8.4–11.2 °C, between 380–700 mm of precipitation per year (average < 600 mm), and an average annual thermal growing season in excess of 310 days for the period of 1981–2010 (UK Met Office, 2015).

Average maximum and minimum monthly temperature and average monthly precipitation recorded at the Met Office climate station at Cambridge National Institute of Agricultural Botany (NIAB) are given in Figure 2.1a and b for 1960–2010. The NIAB station records show maximum monthly temperature has never been in excess of 29 °C and minimum temperatures have not been recorded below -6 °C. Additionally, a minimum monthly rainfall has been reported as 0.5 mm and a maximum of 166 mm.

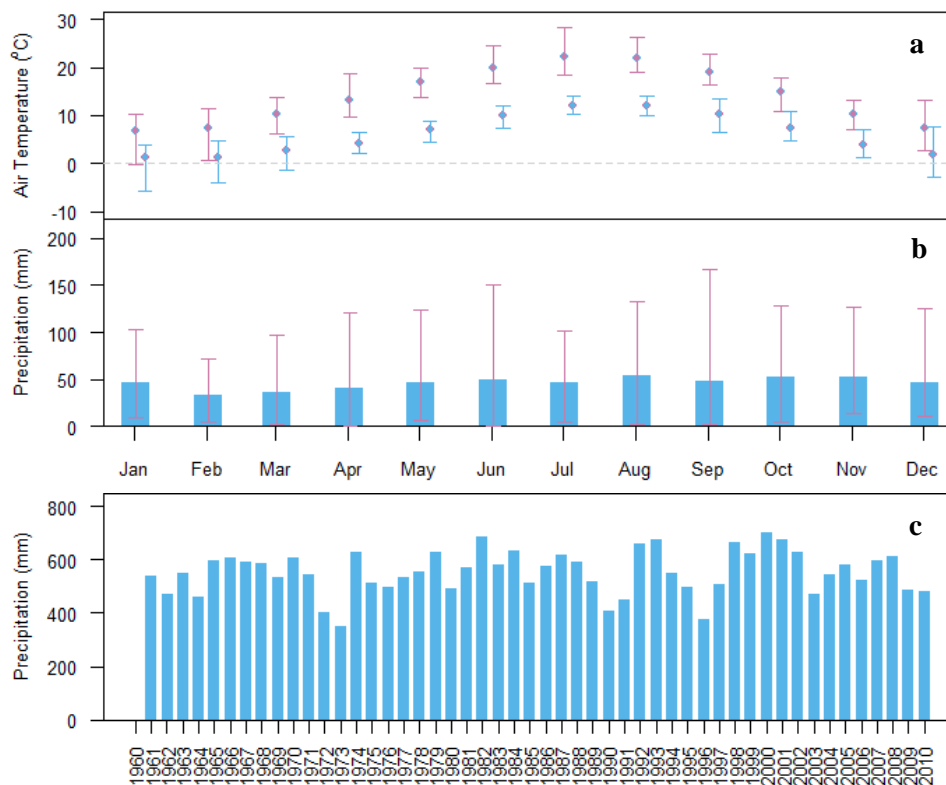


**Figure 2.1:** Monthly and annual averaged climate data for 1960–2010 from Cambridge NIAB station, taken from the (UK Met Office, 2015). **a:** Average maximum (red) and minimum (blue) monthly temperatures. **b:** Average monthly rainfall. Error bars of plots indicate the maximum and minimum record for each monthly average from the 50 year averaging period. **c:** Annual rainfall from the same dataset (1973 and 2009 are incomplete totals).

Maximum and minimum average annual temperature calculated over 1960–1980 and 1980–2010 for the region report an increase of 0.5–1 °C (UK Met Office, 2015). Annual precipitation has increased in its year-to-year variability in more recent years. In 2011 a total annual precipitation of 348 mm was recorded by the Cambridge NIAB station, the lowest value since 1960 (Figure 2.1c). The following year, 2012, 728 mm was recorded, the highest annual sum recorded at this station.

### 2.1.2 Rosedene Farm

The study site is an intensively cultivated agricultural peatland located within Methwold fen in west Norfolk, East Anglia, United Kingdom (UK) (Figure 2.2). The site is in the catchment of the River Wissey which originates in Shipdham in Norfolk, from where it flows west (passing the northern edge of Rosedene Farm) and feeds into the River Great Ouse just west of Southery which then flows north into The Wash (Figure 2.2). Peat depth has not been measured across the site but is reported in other work as being roughly 1–2 m (Dawson et al., 2010, Evans, 2017); the peat overlies a fen clay base (British Geological Survey, BGS). The fen peatland was drained and converted for agricultural use shortly after the Second World War in line with UK wide agricultural expansion in an effort to improve national self-sufficiency, which is why it has deeper peat soils and higher average elevation compared to surrounding farm land that was drained and converted at an earlier date (M. Hammond, Pers. comm.) Despite the later date of conversion, peat wastage as a result of drainage has led to the surface here being below mean sea level. The area is characterised by trapezoidal arable fields separated by hedgerows and ditch systems that are used for agricultural management (described in more detail below). Rosedene farm encompasses over 100 fields totalling 1,400 ha (G's Fresh, 2017) and is owned by G S Shropshire and Sons as a grower member under the umbrella of G's Fresh Ltd.



**Figure 2.2:** Maps of Rosedene Farm location. **Top left:** British National Grid projection of UK with region of bottom left map indicated within. **Bottom left:** British National Grid projection of region within which Rosedene Farm is located, in relation to Thetford Forest and Downham Market (region of right map indicated within). **Right:** Google Earth imagery of Rosedene Farm with field site studied indicated within.

Hedgerows, and in some places tree rows, have been established at field margins to reduce the impact of ‘peat blows’, i.e. the movement of peat that is common during dry and windy periods, particularly during cold dry conditions of spring when the soil has been prepared for cultivation (Pollard and Millar, 1968). Vegetables such as lettuce, celery and Chinese leaf salad crops, potatoes and onions are grown at the farm, and in addition land is regularly rented out for growing radish, leek, red beet, and carrots.

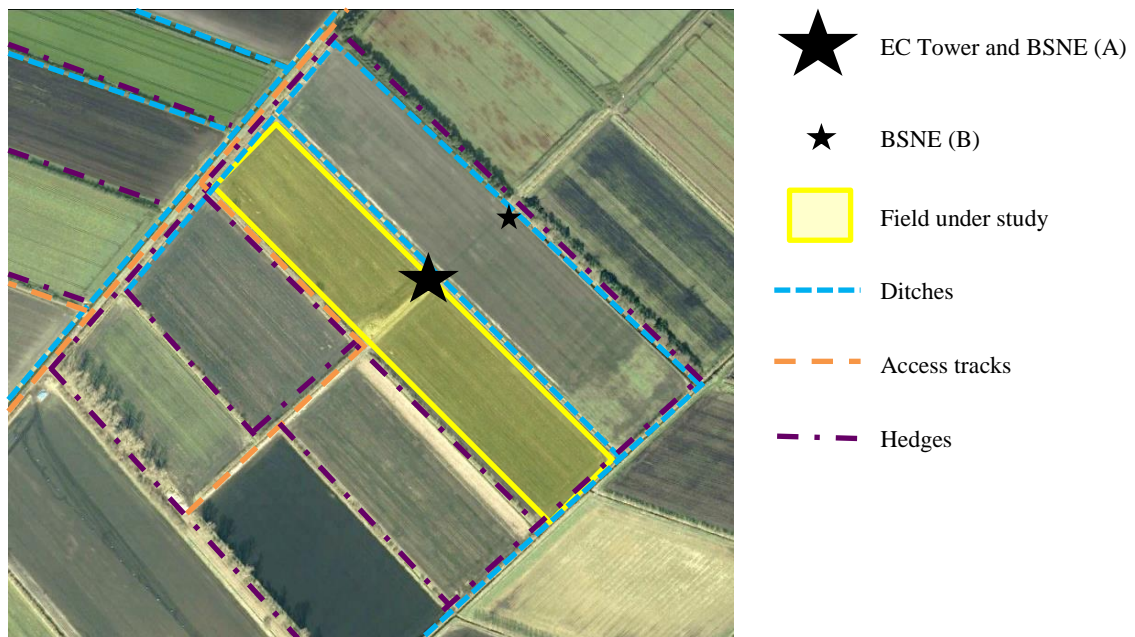


**Figure 2.3:** Annotated aerial photograph of the field site. Google maps (2009).

Water flow is heavily managed at the farm using above ground and sub-irrigation systems in order to ensure crop specific water table level and soil moisture needs are met. Primarily subsurface field drains are used to raise the water table to a crop specific depth during the growing season and to drop this down during fallow months. These drains that take the form of pipes that run in a gridded fashion at 10-15 m intervals along both the length and width of the fields at a depth roughly 1–1.5 m below the peat surface. Water levels in the internal ditches between the fields are controlled by pumping and control gauges, managed by both the farm and the Internal Drainage Board (IDB). The River Wissey is the main source of water and three large site reservoirs are additionally utilised but primarily serve as a back-up in case of drought. Management of the water table has to be adapted to fit with rainfall inputs to avoid saturation of the root zone.

Water table manipulation and natural rainfall at the site can still be further supplemented during the growing season by overhead irrigation dependent on crop requirements, although this activity is limited. Sub-irrigation is preferential as it allows for a reduction in fungicide application whereas overhead irrigation increases humidity and can favour development of diseases (M. Hammond, Pers. comm.).

**Table 2.1:** Summary of relevant site management events during the data collection period. A chronological site management table is provided in Appendix Table A2.1. (Without more farm records it was difficult to pinpoint dates of certain events that definitely happened, they are listed here as missing).

Year	Activity	Date	Details
2012	Ploughing	22/06	Field ploughed to a depth of 0.2–0.3 m with additional 0.1 m sub-soiler tines
	Planting	26–30/06	Iceberg lettuce plugs planted
	Fertiliser applied	-	-
	Weed and disease control	-	-
	Irrigation	13/07	25 mm, per event
	Harvested	12/08	~29 t ha <sup>-1</sup> (average 450 g per head) (M. Hammond, Pers. comm.)
	Disking	20/08	Lettuce residuals turned into topsoil
2013	Ploughing	30/03	Ploughed to a depth of 0.2–0.3 m with additional 0.1 m sub-soiler tines
	Planting	10/12	Crop drilled. 259,455 leek seeds ha <sup>-1</sup> and 50 kg ha <sup>-1</sup> spring barley.
	Fertiliser applied	05/04, 05/07, 01/06, 14/06, 02/07, 05/07, 06/07, 17/07, 30/07, 12/08, 28/08, 12/09	T.S.P. (Triple Superphosphate), MOP (Potash), Manganese DF, Bittersaltz, Nitram, Manganese (N)
	Weed and disease control	30/04, 17/05, 01/06, 08/06, 21/06, 02/07, 06/07, 17/07, 17/07, 30/07, 12/08, 28/08, 12/09	Defy, Stomp Aqua, Anthem, Cleancrop Amigo 2, Master Gly 36 T, Aramo, Afalon, Totril, Starane 2, Dursban Wg, Tepra, Basagran SG, Amistar Top, Hallmark with Zeon Technology, SP057, Tracer, Rudis,
	Irrigation	08/08, 12/09	25 mm, per event
	Harvested	17/10–22/10	21.7 t ha <sup>-1</sup>
2014	Ploughing	22/04	Field ploughed to a depth of 0.2–0.3 m with additional 0.1 m sub-soiler tines
	Planting	29/04–02/05	507,130 Iceberg lettuce plugs planted
	Fertiliser applied	25/04, 01/05, 12/06,	6-6-12, Magnesium sulphate, Manganese sulphate
	Weed and disease control	25/04, 01/05, 12/06	Stomp Aqua, Wing-P, Dual Gold, Invader, Plenum WG, Revus, Gazelle, Bandu (10994)
	Irrigation	01/05, 07/05	25 mm, each event
	Harvested	20–27/06	400,733 heads (average 480 g per head)
	Disking	-	-
	Weeds sprayed	-	-
Other	22–23/10	Ditch weeds cleared	
2015	Ploughing	03/02, 08/05	Field ploughed to a depth of 0.2–0.3 m with additional 0.1 m sub-soiler tines
	Planting	12/05	687,663 celery plugs planted
	Fertiliser applied	26/01, 08/05, 01/06, 15/06, 30/06, 14/07, 25/07	T.S.P., 6-6-12 (NPK application), Manganese sulphate, Magnesium sulphate
	Weed and disease control	21/05, 28/05, 01/06, 08/06, 15/06, 20/06, 30/06, 14/07, 25/07	Cinder, Afalon, Stomp Aqua, Amistar, Plenum WG, Hallmark with Zeon technology, Goltix Flowable, Defy, Plover, Aphox, Tracer, Switch
	Irrigation	18/05, 16/07, 17/07	25 mm, per event
	Harvested	31/07–11/08	639,555 cut plants
	Disking	-	-
	Weeds sprayed	-	-

### 2.1.3 Study field

#### 2.1.3.1 General

The field investigated in this study (52° 31' 52"N 00° 28' 16"E) (Figure 2.2) is roughly 120 m by 600 m (7.2 ha), and peat depth is reported as being roughly 1–2 m (Evans, 2017, Dawson et al., 2010).

Each year of the study saw only one harvested crop grown on the field<sup>a</sup>, lettuce (*Lactuca sativa* var. 37 *apitata* 'Iceberg') in 2012, leek (*Allium ampeloprasum* var. *porrum*) in 2013, the same variety of lettuce again in 2014 and celery (*Apium graveolens* var. *dulce*) in 2015. In 2012, 2014 and 2015 remnants of lettuce and celery crop harvests were ploughed into the top soil of the field; in 2013 the leek remnants were left at the surface. Outside of the cultivation period, the field was left fallow and relatively unmanaged (until preparation for the next crop began, Table 2.1) with only a sparse weed cover. In both 2014 and 2015, a 5 m wide strip of maize was planted along the southwest side of the field as cover for pheasants. Each crop had a consistent height across the field, which peaked at 0.2, 0.8, 0.25 and 0.72 m for lettuce, leek, lettuce and celery, respectively from 2012–2016.

Regrowth of weeds was observed across the field during both cultivation and fallow periods. Nettles (*Urtica dioica*) and Common Chickweed (*Stellaria media*) were predominant during fallow periods, but during the growing season and cultivation periods weeds such as Fat Hen (*Chenopodium album*) and Redshank (*Persicaria maculosa*) were also present and, along with Nettles (*Urtica dioica*), grew taller than the crop at times before being cut back or treated with herbicides (see Table 2.1 for site activity and herbicide application details).

#### 2.1.3.2 Pesticides and fertilisers

A variety of chemicals are used on the farm to prepare the soil for crops, support crop development, prevent weed competition, and further halt weed growth during the fallow. Details of chemicals used by farm managers are recorded in traceability reports, for the field studied here these were provided by the farm manager (for 2013–2015) and some details are given in Table 2.1. Despite their potential to impact on the CO<sub>2</sub> balance

---

<sup>a</sup> Some fields at the farm are used for multiple crops in one growing season, whereby a crop is planted in early spring and protected with fleecing from frosts, then a second crop is developed in the late summer.

of the site, no action has been taken to measure this as it was beyond the scope of the author and available facilities to quantify.

### *2.1.3.3 Crops*

#### Lettuce

Lettuce seeds are germinated in individual peat blocks, roughly 64–125 cm<sup>3</sup>, in greenhouses. Once the seeds have germinated these peat blocks, now lettuce ‘plugs’, are ready for planting (Figure 2.4a and b). The peat used for these plugs is sourced from peat extraction sites primarily in Scotland and Ireland (M Hammond, Pers. comm.). From plugs it only takes two months for a lettuce crop to grow to harvest size and therefore it is possible to plant this crop in early spring, supported by fleecing material that prevents frost damage and then harvest in early summer. This allows for the field to be used for a second crop from mid-summer to early autumn. In 2012 spring was unusually wet and therefore the site and meteorology were not suitable for planting until late June, whereas in 2014 the lettuce crop was planted at the end of April and harvested by the end of June. A second crop was not planted in either year. Irrigation practice for lettuce is to sub-irrigate to maintain a water table at -0.6 to -0.65 m below the surface unless heavy rain is forecast in which case it is allowed to fluctuate down to -0.8 m (M Hammond, Pers. comm.). Top down irrigation is usually applied as 25 mm across the field over a day. Unless the year is unusually wet two applications are made for a lettuce crop. In 2012 only one application was made whilst in 2014 two were applied.

In 2014 a reported 507,130 lettuce plugs were planted, however no record has been provided for 2012. The yield in 2014 was 400,733 (80%) but the yield weights were reported as above average (480 g over 450 g, M Hammond, Pers. comm.). Residual crops and weeds are left on the field following harvest (Figure 2.4c), these were disked into the field topsoil a few weeks after harvest (Table 2.1; Figure 2.4c and d). Weeds grew in autumn months and were additionally treated with selective chemicals before winter (Figure 2.4e and f).



**Figure 2.4:** Photos of stages of site vegetation cover development during the lettuce crop year of 2014. A lettuce plug freshly planted (a), well established lettuce crop a few weeks from harvest (b), field a week after lettuce harvest, crop residues have already begun to decompose and weeds are dominant site vegetation (c), a month after harvest weeds and residues were sprayed with herbicides and mixed with topsoil (d), secondary weed cover developed (e), autumn weed regrowth sprayed for winter (f). Photos by author, with the exception of (d) which was provided courtesy of S. Benson.

### Leek

The stages of field management for growing leek crop are shown in the photos in Figure 4.5a–f. Leeks are usually planted as seeds in early spring given their requirement for a long growing season. Germinating leek crops are particularly susceptible to drying out, and as such soil moisture levels must be maintained until the crop has emerged (Red

Tractor, 2010). As such, barley can be under-sown to draw moisture into the upper soil profile and add stability to prevent loss or movement of vulnerable leek seedlings to movement by wind (Figure 2.5a and b). Leeks have a high demand for water throughout their growth, and sub-irrigation is managed such that the water table average depth is similar to that of lettuce (-0.6 to -0.7 m below the surface, M. Hammond, Pers. comm.) Top down irrigation is again similar to the lettuce crop, with leeks receiving two applications of 25 mm (M. Hammond, Pers. comm.)

In 2013 a reported 259,455 leek seeds were planted per hectare with 50 kg ha<sup>-1</sup> of barley in addition. After the barley was euthanized at the end of May the water table was raised from below 80 cm to roughly 50 cm below the surface until mid-September. Leek harvest was reported as 21.7 t ha<sup>-1</sup>. Residual crop from the harvest, which included trimmings, outer leaves, roots and unsuitable leeks, was left on the surface. These crop residues were left on the surface over the winter months (Figure 2.5e and f).



**Figure 2.5:** Photos of stages of site vegetation cover development during the leek crop year of 2013. Early season growth of barley used to support soil during early leek development (a), sprayed barley that is dying, with young leeks starting to sprout in between (b), established leek crop (c), fully developed leek crop days before harvest (d), residues remaining on the field a week after harvest (e), crop residues on site several months after harvest decomposing into the following year (f). Photos by author.

### Celery

Similar to lettuce, celery plants are also germinated in individual, roughly 64–125 cm<sup>3</sup>, peat blocks in greenhouses before planting in peat blocks in the field (Figure 2.6a). They are also planted when conditions are best suited but require a longer development period than lettuce before being harvested. The roots of celery plants are limited, usually stretching just 15–20 cm away from the plant and only 5–8 cm deep, so the top

part of the soil not only has to have enough moisture, it must also contain all the nutrients the plants need. Sub-irrigation requirements for celery are the same as the lettuce and leek crops, however a third application of top irrigation was required due to the longer period required for growth. To prevent the celery from bolting it is often covered with a fleecing, however this was not done on this field.

In 2015 687,663 celery were planted in the field studied. A good crop with limited pest damage led to a 93% yield of 639,555 cut plants. Across this G's site just under 9 million celery plugs were planted in 2015 and with a 90% yield 8 million plants were harvested.

Crop residues were mixed into the topsoil a month after harvest and, as with lettuce crops, an autumnal weed cover established, before being sprayed in early winter (Figure 2.6e, f and g).



**Figure 2.6:** Photos of stages of site vegetation cover development during the celery crop year of 2015. A celery plug freshly planted (a), well established celery crop (b), field a week after celery harvest, crop residues have already begun to decompose and sparse weeds are present (c), a month after harvest weeds and residues have been mixed into the topsoil (d), a secondary weed cover developed in autumn (e), autumn weed regrowth was sprayed for winter (f). Photos by author.

## 2.2 Measuring fluxes

### 2.2.1 Eddy covariance theory

Eddy Covariance (EC) is a micrometeorological method whereby turbulent fluxes of heat, mass and momentum in the surface boundary layer are measured to calculate the vertical exchange between the atmosphere and ecosystem beneath it (Foken et al., 2012a, Baldocchi, 2003). Despite the fairly regular 2D representation of the nature of the turbulence in the atmosphere in Figure 2.7, it is more complex than this. Eddies of air have different densities, gas concentrations, speeds, directions and size. Further to this, all of these factors are constantly changing also due to the given interactions with the underlying ecosystem.



**Figure 2.7:** Conceptual diagram of an EC tower and the eddies it samples. Adapted from Burba (2013).

The essence of the EC methodology is that a vertical flux (Eq. 1) can be represented as a covariance of vertical wind velocity and the concentration of an atmospheric constituent/scalar (such as CO<sub>2</sub> or water vapour (H<sub>2</sub>O) in this thesis):

$$F = \overline{\rho_a w s} \quad \text{Equation 2.1}$$

where  $F$  is the vertical flux,  $\rho_a$  the density of dry air,  $w$  the vertical velocity, and  $s$  the mixing ratio of the scalar to dry air.

As fluxes are roughly constant within the height of the surface boundary layer it makes an ideal place to take measurements to infer fluxes from the surface beneath (Foken et al., 2012a). However, this is not altogether straight forward and some underlying

assumptions are made to account for these complexities. Reynolds decomposition, also known as Reynolds rules of averaging (Reynolds, 1895), (Eq. 2.2) is applied to establish a statistical representation of each turbulent quantity, whereby, fundamentally, any scalar variable ( $x$ ) can be said to be comprised of its mean value ( $\bar{x}$ ), time averaged, and an instantaneous fluctuation from that mean ( $x'$ ):

$$x = \bar{x} + x' \quad \text{Equation 2.2}$$

Application of Reynolds rules to the vertical mass flux density allow the quantification of covariance between fluctuations in vertical velocity and mixing ratio of a scalar (Eq. 2.3) with the understanding that the mean of fluctuating components are forced to zero.

$$F \approx \overline{\rho_a} \cdot \overline{w'c'} \quad \text{Equation 2.3}$$

where  $\rho_a$  is air density and  $c$  is the mixing ratio where  $c = \rho_c/\rho_a$ . Positive covariance is denoted here as a transfer from the ecosystem to the atmosphere and negative covariance the opposite. It is worth noting here that flux calculation (as described above) assumes a measurement of mixing ratio of a scalar, however instrumentation used here does not measure mixing ratio but density of a scalar in a known volume, and therefore must be accounted for later in data processing.

#### *Theoretical assumptions*

Further major assumptions that the EC theory relies on are:

- i. Flux is measured during steady state fully turbulent conditions within the turbulent boundary layer (Foken and Wichura, 1996).
- ii. Footprint of measurements are appropriate for measurement of flux from a homogenous surface of interest that is upwind of the instrumentation (Foken, 2008) .
- iii. Fluxes are not effected by horizontal advection (Leuning, 2005).
- iv. Averages of fluctuations are zero. Air density fluctuation is zero, convergence or divergence of flow is negligible (Baldocchi, 2003).
- v. Instrumentation is capable of detecting high frequency eddies and analysis conducted to include low frequency loss (Horst, 2000).

Conditions for the accurate measurement of flux by the EC method are rarely met in reality (Foken et al., 2012a). Every effort must be made to install and maintain

instrumentation to reduce measurement inadequacy based on the assumptions above. Additionally, to improve the reliability of the flux measurements corrections need to be made during the processing of data and quality control (QC) procedures. The data processing method is described in Table 2.2, and QC follows this, both are presented after a description of the measurement system installed for this study.

### 2.2.2 Measurement system

The instrumentation was installed adjacent to, and half way along, the north-east ditch boundary of the field under measurement (Figure 2.3). The EC system employed comprised of a LI-7500 open path H<sub>2</sub>O/CO<sub>2</sub> infra-red gas analyser (IRGA) (Li-COR Inc., Lincoln, Nebraska, USA) and a CSAT3 sonic anemometer (Campbell Scientific, Ltd. Logan, Utah, USA) (Figure 2.8.b). Maximum fetch stretched to roughly 300 m in both north-west and south-east directions, however the instrumentation was orientated into the prevailing south west wind direction of 225°, which has a fetch which was restricted to 120 m before meeting a roughly 3 m high hedgerow. The measurement height ( $z_m$ ) was set at 1.5 m above the peatland surface in order to minimise data losses due to the limited fetch in the prevailing wind direction. The two instruments had no vertical separation, however the LI-7500 was separated from the CSAT by 0.13 m in a northward direction and 0.04 m in an eastward direction and was installed at an angle to encourage run-off after precipitation events.

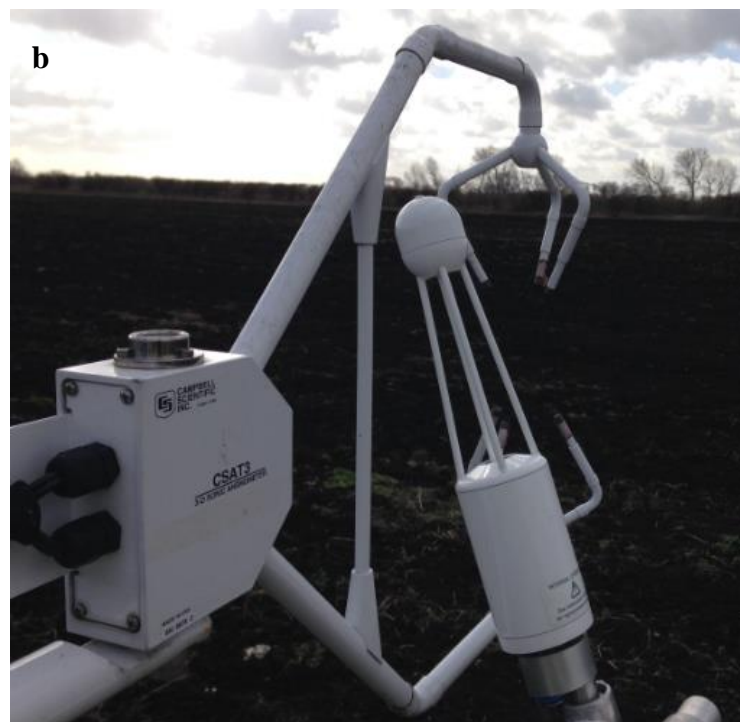


**Figure 2.8:** EC instrumentation photos. **a:** Photo of the EC, power and meteorology instrumentation. **b:** close up of the EC system LI-7500 IRGA and CSAT3 sonic anemometer looking out to the freshly ploughed field. Photos taken by author.

Supporting meteorological data were collected. This included use of an NRLite2 (Kipp & Zonen, Delft, The Netherlands) that measured incoming and outgoing radiation thereby reporting net radiation ( $R_n$ ). In addition a CNR4 radiometer (Kipp & Zonen, Delft, The Netherlands) was installed at the site in winter 2013 and gave more detailed measurements of  $R_n$  that included a breakdown of incoming and outgoing shortwave and longwave radiation and the consequential  $R_n$ . The NRLite2 and CNR4 were installed 1.5 m above the peat surface, 0.5 m apart horizontally, 8 m north-west of the

EC instruments, to minimise the impact of the instrumentation (such as solar panels and tripods) and enclosure footprint on  $R_n$  measurements. The CNR4 was not installed at the site until late in 2013, and the NRLite2 was removed from the site from 4<sup>th</sup> September–7<sup>th</sup> November 2014 and 7<sup>th</sup> January–10<sup>th</sup> June 2015 for use in calibrating radiometers at other field sites managed by the University of Leicester (UoL), but the overlapping datasets allowed for calculation of a complete dataset (discussed below). Photosynthetically active radiation (PAR) was measured using a SKP01 Quantum sensor (Skye Instruments, Llandrindod Wells, UK).

Two arrays of below ground instrumentation were installed 2 m apart beneath the EC instrumentation to measure soil heat flux ( $G$ ). Each array consisted of: two HFP01-SC (Hukseflux, Delft, The Netherlands), a set of TCAV averaging thermocouples (with four thermistors) (Campbell Scientific Ltd., Shepshed, UK) that measured soil temperature ( $T_{soil}$ ), and a time domain reflectometer CS616 (Campbell Scientific Ltd., Shepshed, UK) that recorded volumetric peat moisture content (SWC). In both locations the two HFP01-SC's were installed at 0.08 m depth and 1 m apart, the four thermocouples of the averaging TCAV's were installed as two at 0.02 m depth and 0.06 m below the surface and the other two at the same depths between 0.5 m and 1 m away, while the CS616's were installed horizontally at 0.025 m at the mid-point between the other soil instruments.

Air temperature ( $T_{air}$ ) and relative humidity were measured using an HMP45 (Vaisala, Helsinki, Finland) within a naturally aspirated radiation shield. Precipitation was measured with an ARG100 tipping-bucket rain gauge (Campbell Scientific Ltd., Shepshed, UK) installed 4 m to the south east of the EC instruments (see Figure 2.2a). Two automatic divers (Schlumberger Water Services Ltd., Delft, The Netherlands) were used to measure water table depth below the field surface (WTD) and completed the environmental monitoring equipment in use. These were installed on the 6<sup>th</sup> July 2012 8 m north west and 4 m south east of the EC instruments, suspended at a depth of roughly 0.8 m below the peat surface within perforated polyvinyl chloride (PVC) tubing measuring water table depth via pressure measurements.

Apart from the CNR4 and Schlumberger divers all the instruments were scanned at 20 Hz and their data logged by a CR3000 data logger (Campbell Scientific Ltd., Logan, Utah, USA). Turbulent sensor data were stored at 20 Hz whilst supplementary

instrumentation was recorded as half hour averages. The Schlumberger divers had their own self-contained data storage that logged every half hour, while the ARG100 worked on a pulse system that is registered as a calibrated quantity. The CR3000 did not have capacity for an additional CNR4 Net radiometer, therefore a CR1000 data logger (Campbell Scientific Ltd., Logan, Utah, USA) was used from installation (28<sup>th</sup> November 2013) until 14<sup>th</sup> March 2014 when it was exchanged for a CR3000 data logger. All data loggers were kept on Greenwich Mean Time (GMT) throughout measurement and were synced to a laptop when they began to drift.

The tower was powered by 4 x 6 V 330 Ah block gel leisure batteries (Sonnenshine) which were recharged by 6 x 260 W monocrystalline PV panels (Canadian Solar, Ontario, Canada) via an Outback FLEXmax charge regulator (Outback Power Inc., Washington, USA).

The instrumentation was bounded by a low (between 0.3 and 1 m height) barbed wire fence (roughly rectangular, 15 m long and 5 m wide) to delineate the boundary for agricultural machinery on site and to discourage interference with equipment by those working on the field. Furthermore, no crops were planted within 5 m of the enclosure boundary. The IRGA and sonic anemometer were installed above this boundary to reduce its potential impact on wind flow. Similarly the CNR4 and NRLite2 radiometers protruded beyond this boundary to improve their view of crop radiation rather than bare soil or weeds that grew between the crop and enclosure. It was not possible to measure radiation directly over the crop due to ongoing management activity on site.

A common domestic glyphosate based garden herbicide, 'Roundup', was approved by the land manager for the author and technician to use within and around the enclosure. Glyphosate targets proteins used for growth within a plant which eventually starves. In addition weeds were physically removed.

#### *Calibration of IRGA*

The LI-7500 IRGA was calibrated before measurements began on 31<sup>st</sup> May 2012, again on the 17<sup>th</sup> December 2014 and then after the complete measurement period on the 6<sup>th</sup> January 2016. Calibrations were conducted at the Centre for Ecology and Hydrology (CEH), Wallingford with the support of Dr Ross Morrison. The calibration schedule was less frequent than the manufacturers suggest (weekly/monthly) due to limited access to calibration equipment. Calibration of the instrument was undertaken by

running a control gas with a zero concentration of CO<sub>2</sub> and H<sub>2</sub>O through the Li7500 followed by a control gas with known span concentration at controlled temperatures and pressures.

The IRGA reported minimal drift over the complete measurement period. Sensor drift due to the span measurements from June 2012–December 2014 was 1.3% for H<sub>2</sub>O (at 20.20 °C and 101.3 kPa) and 2.5% for CO<sub>2</sub> (at 400 ppm), and for December 2014–January 2016 2.9% for H<sub>2</sub>O (at 20.20 °C and 101.3 kPa) and 0.4% for CO<sub>2</sub> (at 400 ppm). During the calibration process of 2016 the internal chemicals in the Li7500 were renewed and the calibrations were repeated after a few days. A minimal fully systematic linear correction for these drifts was applied due to the paucity of calibrations. Details of calibrations are provided in Appendix Table A2.2.

### 2.2.3 Eddy Pro processing

The 20 Hz raw EC dataset was processed and fluxes calculated using Eddy Pro LI-COR version 6.1.0 (EP6.1), which was the most up to date at the time of data processing, and allowed for user friendly site and instrumentation specific processing.

Calculating fluxes and footprints of the fluxes requires further information relevant to displacement height that was not captured by the measurement system. Details regarding vegetation height and changes to instrumentation height and orientation were therefore provided to EP6.1 via a dynamic metadata file created manually by the author. Vegetation height details were collected on every site visit, which makes the resolution of this data coarse by comparison to the fluxes, but there was not the necessary instrumentation to measure this more frequently.

Eddy Pro software went through a number of steps during processing which are briefly covered here but explained in more detail in Table 2.2. Eddy Pro software corrected the raw data for axis tilt using a double rotation (Wilczak et al., 2001, Kaimal and Finnigan, 1994) and applied a block (Reynolds) averaging (Moncrieff et al., 2005) de-trend method.

**Table 2.2:** Summary of EP6.1 processing steps to calculate fluxes from raw data.

<b>Processing steps</b>	<b>Description of requirement and application method</b>
<b>Axis rotation for tilt correction</b>	Due to misalignment of vertical axis of the sonic anemometer and the changing dimension of the flow. Cross-contamination of fluxes can occur due to this discrepancy in vertical alignment. Double rotation, that is used here, corrects by forcing the horizontal components of the flow to zero, and aligning the mean wind direction to the x-axis of the instrumentation coordinate system (Aubinet et al., 2012b, Kaimal and Finnigan, 1994).
<b>De-trend of turbulent fluctuations</b>	De-trending removes long-term trends from the data that are not caused by turbulence, but while trying to still capture low frequency events (Malhi et al., 2005), several strategies are available. Block averaging was implemented here which obeys the Reynolds decomposition rule, removing the mean of the available time series for each half hour period from each value in the time series.
<b>Time lag compensation</b>	Calculates and removes the lag between measurements made by the gas analyser and the sonic anemometer. Despite the instruments being within 15 cm of each other, this lag was still computed using the circular correlation technique that looks for similar lags between the vertical wind and scalar measured (Aubinet et al., 2012b).
<b>Density fluctuation</b>	As the open path gas analyser measures a molecular density (absolute number of molecules in a known volume), for the purpose of computing a flux this needs to be transformed to a mixing ratio (mass of gas of per mass of air). Measurements of molecular density are subject to fluctuations due to changes in temperature and humidity and therefore these must be corrected for using. This is undertaken here to correct estimations of CO <sub>2</sub> and H <sub>2</sub> O density fluctuations in order to establish accurate CO <sub>2</sub> and latent heat fluxes (Webb et al., 1980, Leuning, 2005, Baldocchi, 2003)
<b>Quality check</b>	This step involves application of steady state and well-developed turbulence condition tests of each flux. Flags are assigned for high “0”, intermediate “1” and poor “2” quality of fluxes for the inspection of the processor (Mauder and Foken, 2004). Poor quality fluxes are removed during later in the quality control process.
<b>Footprint estimation</b>	Calculates the contributing area of each measured flux. Several different methodologies are available for this but here the Kormann and Meixner (2001) method is applied as it calculates specific variables required for the secondary footprint analysis tool (Neftel et al., 2008) used later in the quality control process for estimating the contributions to a flux from specific locations within the total EC tower footprint.
<b>Spectral/cospectral response corrections</b>	Spectral corrections are necessary to account for loss of flux contributions due to instrumentation sampling limitations and data processing choices that include time interval of flux averaging. The Moncrieff et al. (2005) analytic method is applied to account for loss of low frequency spectra generally associated with the finite averaging period applied and the de-trending method applied. While Moncrieff et al. (1997) is suggested for open-path gas analyser systems to address the high frequency spectral loss caused by finite path lengths of the instruments, measurement response times, and location in relation to the surface.
<b>Statistical tests on raw data</b>	Tests for despiking, amplitude resolution, drop-outs, absolute limits, and skewness and kurtosis are used to assess the statistical quality of the raw data. The limits of each test was left as the prescribed default settings as derived from Vickers and Mahrt (1997).
<b>Random uncertainty due to sampling error</b>	The method of Finkelstein and Sims (2001) was used to calculate the random uncertainty due to sampling bias. The integral turbulent time-scale used here stopped when the cross-correlation function attained the value of 0.369, to assure a value was always calculated. This is later used in combination with gap filling uncertainty to calculate an uncertainty for fluxes at a daily resolution.

As explained above, the calculation of a CO<sub>2</sub> flux requires the mixing ratio of a scalar, however the Li7500 IRGA does not measure a mixing ratio but rather a density of a gas in a volume, and therefore corrections need to be made for changes in air density within that sampling volume. As such, the measured CO<sub>2</sub> was compensated for these fluctuations in air density following WPL corrections laid out in Webb et al. (1980) and Leuning (2005). Without this correction fluctuations in water vapour density and temperature would bias measurements of CO<sub>2</sub>. Quality checks were then performed using the steady state and developed turbulence tests (Foken and Wichura, 1996) which allocated quality flags for each half hourly flux that indicated high, moderate and low quality fluxes under the Mauder and Foken (2004) scheme. A crosswind-integrated footprint model was selected to estimate the contributing distances from the measurement point of each 30 minute flux using the Kormann and Meixner (2001) method.

The data then underwent screening following statistical tests outlined in Vickers and Mahrt (1997). These checks included spike removal, amplitude resolution, drop-outs, absolute limits and skewness and kurtosis. Furthermore, limitations of measurements in space and time mean that flux contributions from long and short term eddies can be underestimated, leading to a requirement for spectral/co-spectral corrections to be made. To address this, transfer functions were calculated following Moncrieff et al. (1997) for low pass and Moncrieff et al. (2005) for high pass filtering, and corrections were applied.

The potential for CO<sub>2</sub> storage below the flux measurement height that is evident at sites with permanently established tall canopies was deemed negligible for this site given the low measurement height of the instrumentation.

#### 2.2.4 Quality control

A consistent quality control (QC) of meteorological data is essential for long term measurements of EC data (Foken et al., 2005). Quality control of the half hourly fluxes produced from the above processing was undertaken using the open source statistical and visualisation environment software 'R' version 3.3.3 (The R Foundation, 2017). A summary table of the number of values flagged by each of the following QC analyses is provided in Appendix Table A2.3.

### *Spike removal*

Although high frequency spikes (instantaneous values) were removed during the previous EddyPro 6.1 processing step, the half-hourly NEE, latent heat (LE) and sensible heat (H) fluxes calculated still contained spikes that would impact later gap-filling (Papale et al., 2006). An outlier detection technique using the robust median of absolute deviation about the median (MAD) technique (Sachs, 2004) was used with a conservative  $z$  value of 5.5. Spike detection annually led to a removal of 10–12%, 5% and 3% of half-hourly NEE, LE and H fluxes, respectively.

### *Footprint*

Establishing the extent of the upwind source of turbulent fluxes (footprint) is crucial to understanding the surface exchange that is being measured (Kormann and Meixner, 2001, Leclerc and Thurtell, 1990).

Given the agricultural nature of the site, parcels of land separated by ditches and hedges, and the aim of this research (to focus on a single field parcel), the ART footprint tool (Version 1.0, 13<sup>th</sup> March, 2007) of Neftel et al. (2008) was employed to estimate the contribution of each field parcel to the flux measurement. The source area for this was calculated using the Kormann and Meixner (2001) analytical flux footprint model within the Eddy Pro processing stage.

Only periods where >70% of the flux originated from the field parcel of interest were retained, but it is also acknowledged that some of the contributing fluxes will have originated from surrounding field parcels and that boundaries and ditches may have minimally impacted the measurements depending on wind conditions and atmospheric stability.

Annual mean wind direction for all years was between 190° and 201°, with the majority (60–75%) of half-hourly wind velocities originating between 135° and 315° which was the field of interest for NEE of CO<sub>2</sub> (Figure 2.10). Poorer turbulent mixing that is associated with slower wind velocities (< 1 m s<sup>-1</sup>) was predominantly associated with the fluxes from the field to the north east from the bearings <135° and >315°. The contribution from this area was most pronounced during 2013 due to the prolonged contribution of arctic air masses mentioned above.

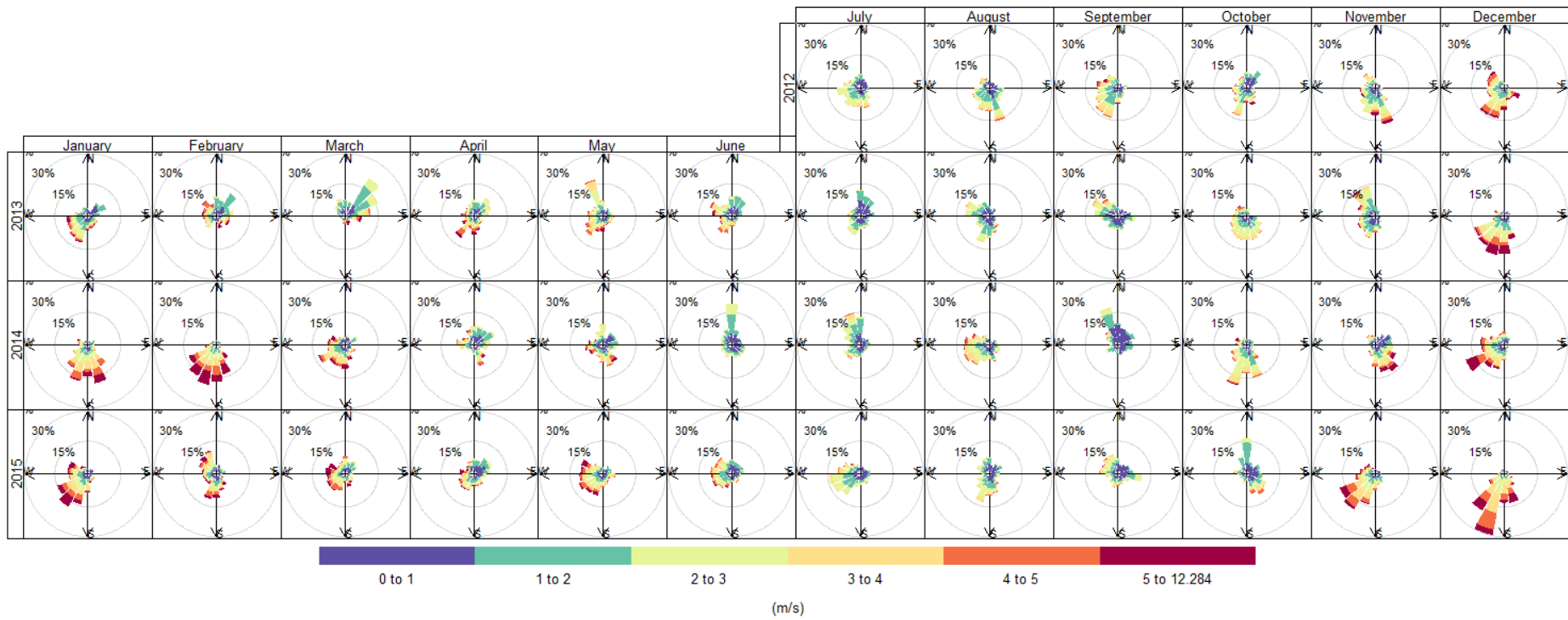


**Figure 2.9:** Monthly wind-rose plots describing the 30 min average wind velocities and directions.

Monthly  $u$  showed a seasonal pattern with daily average horizontal wind speed ( $u$ ) ranging from 1–7  $\text{m s}^{-1}$  in winter months, bounded by 1–5  $\text{m s}^{-1}$  in spring and autumn months but dropping to 1–3  $\text{m s}^{-1}$  in summer months. This trend was least pronounced during 2013 which experienced slower than usual  $u$  during early winter months (January and February), which was followed by an increased influence of maritime arctic air masses in the months of March and April (Figure 2.9).

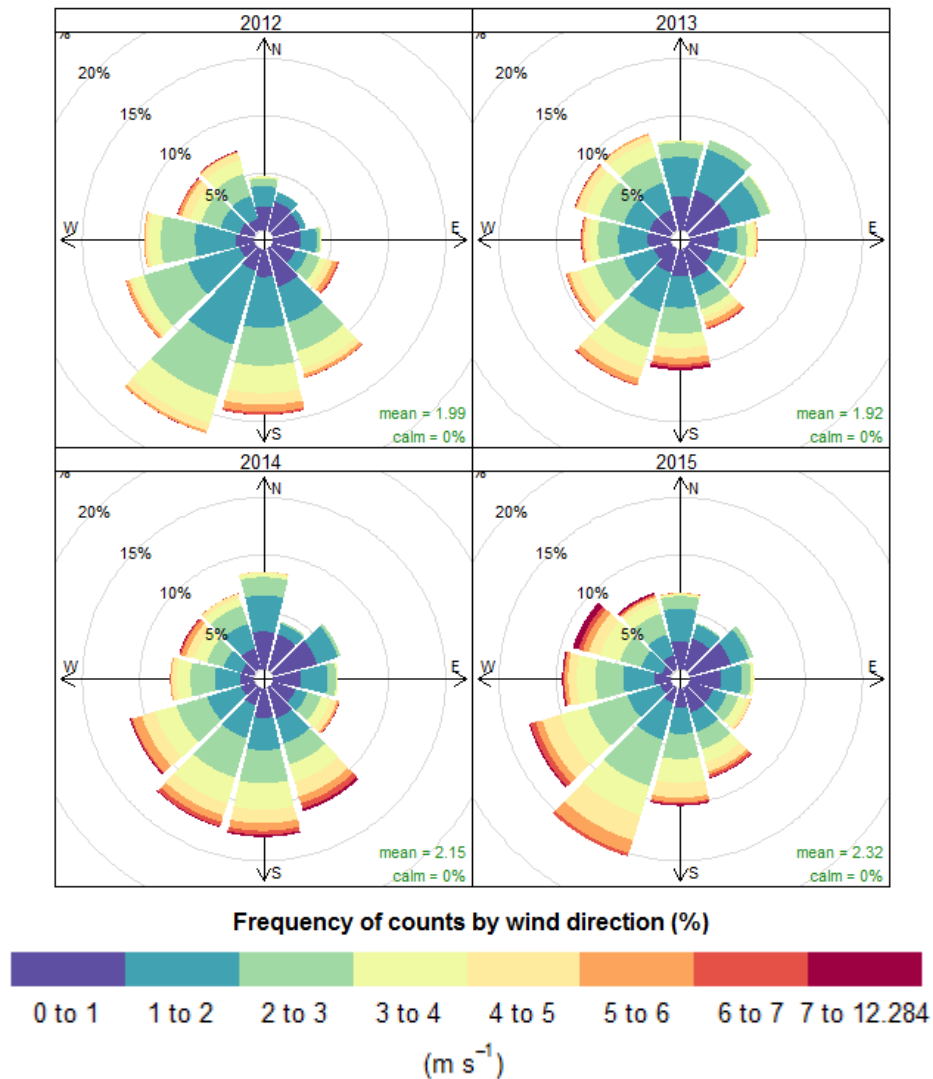


**Figure 2.10:** Annual wind-rose plots describing the contributions percentage contribution of the 30 min average  $u$  from all bearings for each year of the study.

Footprint analysis led to the largest number of half-hourly fluxes flagged for removal; 23, 35, 30 and 29% in 2012, 13, 14 and 15 respectively.

### *Friction velocity ( $u^*$ ) threshold*

Friction velocity ( $u^*$ ) characterises the relationship of shear and turbulence and is calculated here using the momentum fluxes:

$$u^* = (\overline{u'w'^2} + \overline{v'w'^2})^{1/4} \quad \text{Equation 2.4}$$

Where  $u$ ,  $v$  and  $w$  represent the  $x$ ,  $y$  and  $z$  axis wind velocity components, respectively, measured by the CSAT sonic anemometer, with the overbar,  $\overline{\quad}$ , representing the mean value and the apostrophe,  $'$ , representing the instantaneous difference from the mean (see Equation 2.2).

Accurate EC calculations can be biased by stable, less turbulent conditions. These are most common overnight and result in underestimation of ecosystem respiration. Whilst these conditions are usually identified during the steady state and developed turbulence checks of Foken and Wichura (1996) (discussed above Methods/Eddy Pro Processing), if the data required for filtering these is missing they can elude detection. Usually seasonal boundaries would be used to increase the precision of  $u^*$  threshold estimates reflecting the changes in vegetation dynamics and the influence of vegetation growth on surface roughness, however, here the crop/fallow management boundaries were utilised. A threshold value of  $u^*$  was therefore calculated that reflected the management periods at the site. Where limited data was available for threshold estimation the annual threshold was calculated and used. The REddyProc 'R' package freely available from the Max Plank Institute for Biogeochemistry was used for calculating the  $u^*$  thresholds.

### *Visual inspection*

Physically plausible fluctuations can overlap with instrumental errors, and physically implausible fluxes can elude flagging therefore it is important to visually inspect the fluxes and supporting meteorology for values that could influence gap-filling and annual summaries of fluxes (Foken et al., 2005, Rebmann et al., 2012).

Before other stages of quality control were undertaken the flux data were plotted and plausible maximum and minimum values were chosen of  $-40$  to  $40 \mu\text{mol CO}_2 \text{ m}^{-2} \text{ s}^{-1}$  for NEE,  $-200$  to  $600 \text{ W m}^{-2}$  for LE, and  $-200$  to  $400 \text{ W m}^{-2}$  for H. Values outside of these ranges were given a quality control flag. This removed less than 2 days of half-hourly NEE flux values in each year and less than a day of half-hourly LE values. In addition negative night-time fluxes of NEE were flagged, as a net uptake of  $\text{CO}_2$  would

reflect night time photosynthesis which is only seen in Crassulacean Acid Metabolism (CAM) plants (Lloyd, 2006).

Final visual inspection of half-hourly fluxes (those without flags) of NEE, LE and H was undertaken a week at a time, for further implausible values. Furthermore, air temperature ( $T_{air}$ ), soil temperature ( $T_{soil}$ ), soil water content (SWC), soil heat flux (SHF), global radiation ( $R_g$ ) and vapour pressure deficit (VPD) were all also inspected in the same way. This revealed that there were few or no values to eliminate so these are not reported.

### 2.2.5 Summary of gaps

Despite the often reported sensitivity of EC systems to dropouts and loss of data due to power issues and malfunctioning equipment, over the 3.5 years of measurements reported here only minimal data loss of 15% was experienced due to these causes. Notable losses were during spring 2014 when a fuse blew due to cable damage on the IRGA, and led to several weeks of lost data, and in 2015 a data storage error led to two more weeks of data being lost in the mid to late summer. A remaining 85% of data was therefore available for quality control after post-processing.

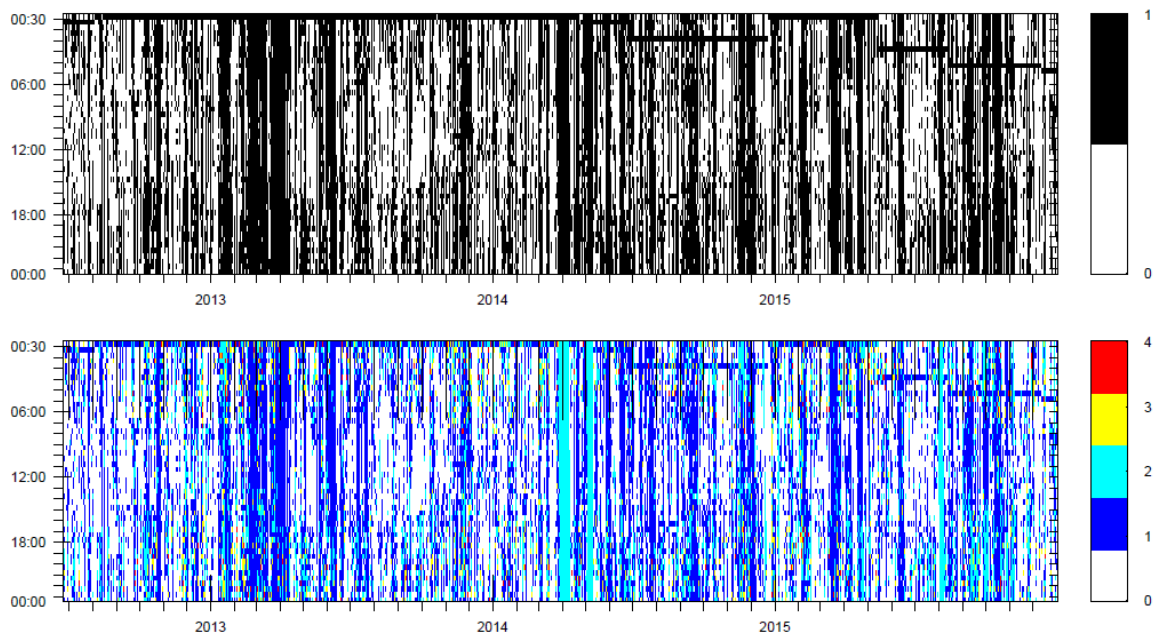


**Figure 2.11:** Quality controlled data: **Upper plot**, 1 (black) are 30 minute values of NEE excluded by quality control, 0 are those that remain. **Lower plot**, Number of QC reasons for excluding a 30 minute value of NEE, colour represents the number of QC reasons for excluding a half hourly vaue.

Data rejection clearly varies from site to site dependant on the conditions/restrictions present (Figure 2.11). Across 12 sites Papale et al. (2006) experienced a removal range of 25–57% of half hourly fluxes over a year, similarly Falge et al. (2001) reported an average loss of 35% across a range (8.5–65%) of European and American sites, and Rogiers et al. (2005) a loss of 58% largely due to instrument malfunction. Only 15% of CO<sub>2</sub> flux data was lost here due to instrumentation or power failure over the complete measurement period, but after quality control only 45% of the original dataset remained (Figure 2.11). The majority of data exclusion was due to footprint restrictions, which ruled out just under 37% of the possible half hourly fluxes, whilst only 12.4% of all data violated the steady state, developed turbulence and friction velocity tests.

Annually 2013 was the most complete dataset before quality control with 92.9% of data values recorded, however during March and April several weeks of north easterly wind flow led to inadequate data and a final recovery of 41.3% for the year. Only 2014 suffered from a higher paucity of acceptable data, with 40.5% left for analysis. During the cultivation period of 2014, only 27% of data remained after quality control, in part due to the tower being without power for a week before and after the time the crop was planted. This was unfortunate, as most likely this would have been a period of increased C loss as the field had just been ploughed prior to planting.

A diurnal bias was evident in quality control, with a higher removal of values between 2–5 am and 9–11 pm which appears during the summer growing season, but is less evident during the rest of the year (Figure 2.11).

#### 2.2.6 Gap filling

To calculate complete daily, monthly and annual sums of meteorological factors, energy and gas fluxes, gaps in the data from the quality control analysis (above) require filling with realistic values. There are a wide range of approaches for dealing with the gap filling of datasets which include interpolation, mean diurnal variation, look up tables (LUT), linear and non-linear regressions, marginal distribution sampling, data assimilation, Bayesian modelling approaches (probabilistic approach) and artificial neural networks (Moffat et al., 2007, Falge et al., 2001, Kunwor et al., 2017, Reichstein et al., 2005, Dengel et al., 2011, Papale, 2012). Several papers exist in the literature that have sought to establish a best practice as a standardisation within the EC community for reliable inter-site comparisons (Reichstein et al., 2005, Moffat et al., 2007, Falge et

al., 2001). However, gap filling can be influenced by unique conditions of particular sites and therefore an appropriate technique for a forested site may not be applicable for an agricultural site. Here, supplementary overlapping data sets were acquired from nearby meteorological equipment and linear relationships between overlapping datasets established in order to fill gaps in meteorological data, while flux data that passed the quality control process were used to gap fill fluxes following the LUT technique laid out by Reichstein et al. (2005).

### *Meteorology*

Using back-up meteorological data from the same site or a nearby site is regarded as the best primary practice for gap-filling (Papale, 2012). The CNR4 was used as the primary source of Rn data as it measures the four components of net radiation independently (shortwave and longwave incoming and outgoing) which is more accurate than the NRLite2 which measures net incoming and outgoing then reports Rn corrected for  $u$  influence on temperature of the instrument (Blonquist et al., 2009). However as the CNR4 was not installed at the site until late in 2013, to fill this dataset available records were compared to those also available for the NRLite2 Rn (Figure 2.12). A linear relationship was calculated with a slope of 1.1 and an intercept of 1.33 with an R squared value of 0.98 (Figure 2.12) which shows how well the NRLite2 Rn explained the CNR4 Rn data, this linear fit was used to calculate missing CNR4 values of Rn. On the rare occasion that neither instrument had power, further filling was performed using further linear correlation with ancillary data provided by the Centre for Ecology and Hydrology (CEH) who have a CNR1 radiometer (Kipp & Zonen, Delft, The Netherlands) at a site 10 km southwest. A strongly significant linear relationship with a slope of 1.03 and intercept of 9.27 with an  $r^2$  value of 0.91 showed that the CNR4 data was consistently underestimated by the CNR1 data.

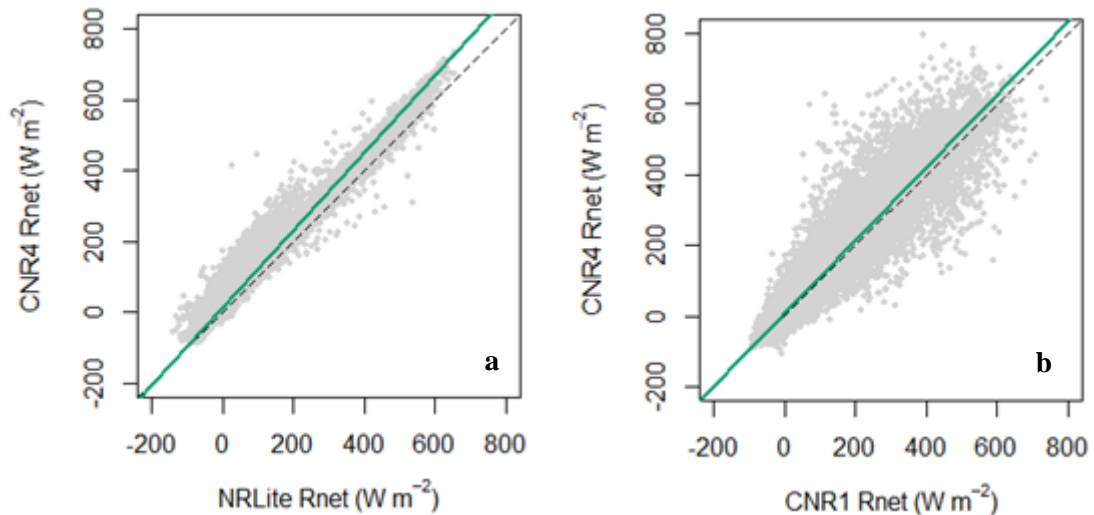


**Figure 2.12:** Thirty minute resolution Rn data. **a:** is relationship of NRLite2 and CNR4, green line is the relationship between the two instruments  $y = 1.1x + 1.33$ . **b:** is relationship between CNR1 at a nearby CEH managed site and CNR4 instruments at Rosedene, this time green line is the relationship between the two instruments  $y = 1.03x + 9.27$ . Dashed black line in both plots represents 1:1 scale.

### *Fluxes*

Energy and gas fluxes were filled following the Reichstein et al. (2005) protocol (Figure 2.13) which utilises the covariance of fluxes with meteorological conditions, and also considers temporally-auto correlated values for filling. The R package ‘REddyProc’, developed by the Max Plank Biogeochemical Institute, used above for analysis of friction velocity, was also used here for gap-filling. Site specific meteorology (Tsoil, Tair, SWC and VPD) were filled using the same methodology. A recent study by Kunwor et al. (2017) demonstrated that moving window with multiple parameter fitting was the best technique for accurate gap-filling<sup>b</sup>.

Look up tables (LUT) were used to identify values of fluxes with similar meteorological conditions (Figure 2.13), global radiation ( $R_g \pm 50 \text{ W m}^{-2}$ ), air temperature ( $T_{air} \pm 2.5 \text{ }^\circ\text{C}$ ) and vapour pressure deficit ( $VPD \pm 5 \text{ hPa}$ ). All three variables were sought within the prescribed range of the values associated with the missing flux for a 7 and then 14 day window. Following this the LUT approach is used again but with only the  $R_g$  variable needing to match. Next, the algorithm calculates average values from the same hour on the same day, then a day before and after and then 2 days either side, which is called the mean diurnal course (MDC). If these approaches fail to fill the gap, then the

<sup>b</sup> using EC data from a pine forest

strategy begins again at the top but with larger window sizes that increase until a value is found. The algorithm also calculates filled values for the data that has not been lost/removed to allow for calculation of uncertainty.

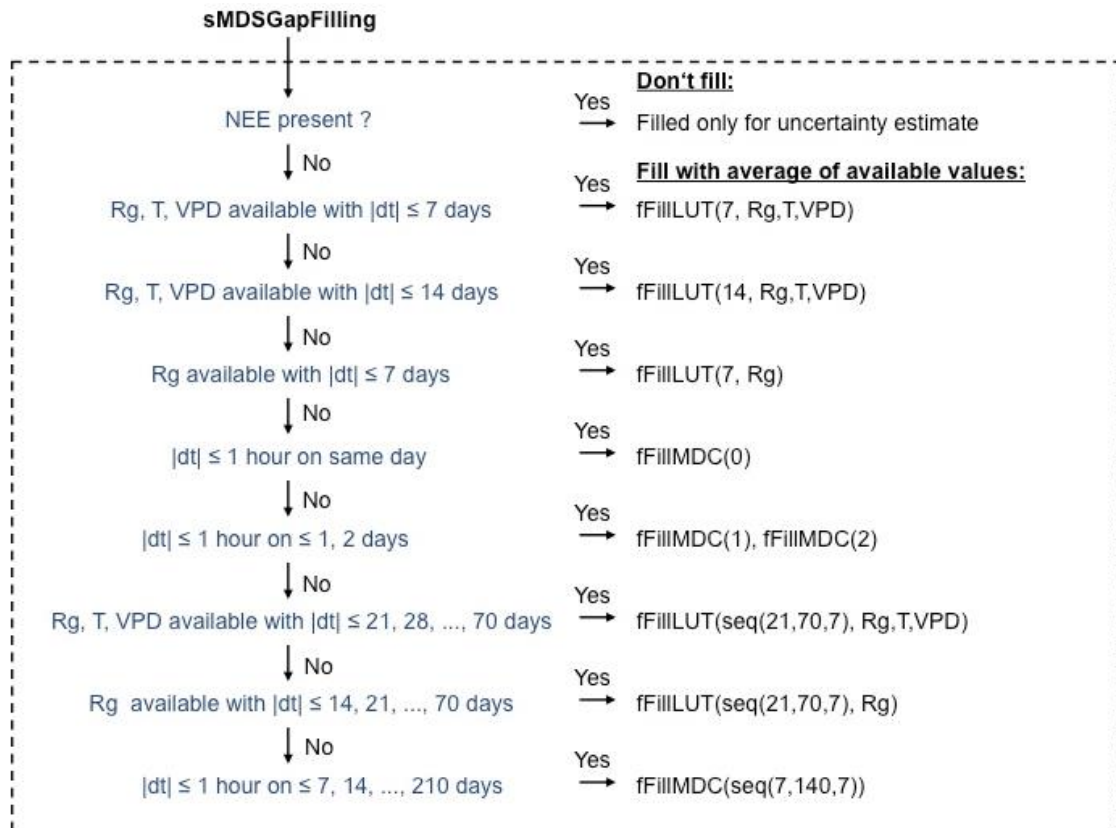


**Figure 2.13:** Flow diagram of gap filling methodology. Adapted from Reichstein et al. (2005) and Max Plank Institute for Biogeochemistry. Temperature can be set as Tsoil or Tair, in this work Tair was used.

As management of the site (ploughing/planting/harvest) can cause abrupt changes in fluxes another methodology was tested to explore if gap filling could be improved by considering crop and fallow periods individually. To do this a new variable was substituted for VPD which defined the boundary and prevented the algorithm from selecting fluxes from the harvested field to fill gaps in fluxes from before harvest, and vice-versa.

Comparing the gap-filled values of the original data allows for a direct comparison of how well the gap filling algorithm using each set of variables fits to the good quality measured fluxes. There was minimal difference between the two gap filling strategies with both filling over 85% of the gaps using the three variables within a LUT window of seven days. The original algorithm, utilising VPD, explained variability with the

original data best with an adjusted  $r^2$  value of 0.845, versus 0.841 of the harvest restricted strategy.

### 2.2.7 Partitioning

NEE was partitioned into TER and GPP, using the commonly implemented respiration model of Lloyd and Taylor (1994) (their Equation 11 and Equation 2.5 here). This method estimates TER using nocturnal NEE and  $T_{air}$  or  $T_{soil}$ . This relationship is extrapolated to day-time to calculate soil respiration. This model was established by Lloyd and Taylor (1994) to give the best unbiased estimate of TER across a variety of ecosystems.

$$TER = R_{ref} * e^{E_0 * \left( \left( \frac{1}{T_{ref} - T_0} \right) - \left( \frac{1}{T_i - T_0} \right) \right)} \quad \text{Equation 2.5}$$

$T_{ref}$  is a reference temperature and  $T_0$  a temperature constant of -46.02 °C.  $T_i$  is the dataset values of nocturnal  $T_{air}$  or  $T_{soil}$  and TER the associated nocturnal NEE values that the equation is fitted to for calculation of the activation energy,  $E_0$ , required for TER and the basal respiration at a reference temperature,  $R_{ref}$ .

For the data presented here, Equation 2.5 was implemented using the REddyProc tool provided by the Max Planck Institute for Biogeochemistry, which calculated  $E_0$  for the complete dataset then used a seven day sliding window that moved in 4 day steps to calculate  $R_{ref}$  allowing for seasonal variation. The ReddyProc tool uses a  $T_{ref}$  of 15 °C. It has been suggested by Wohlfahrt and Galvagno (2017) that  $T_{soil}$  (over  $T_{air}$ ) is the better choice of driving variable of respiration for sites with limited vegetation cover for much of the year (e.g. croplands) due to limited influence of autotrophic respiration, therefore  $T_{soil}$  was selected for use here. The model was then used to extrapolation day-time TER. Half-hourly values of NEE were then subtracted from TER to calculate GPP.

### 2.2.8 Uncertainty

All measurements are subject to some uncertainty (Taylor, 1997). Understanding the nature, source and scale of uncertainty is important for valid comparisons within datasets and to other data sets. Furthermore, with the expectation that these figures will be vital in informing land owners and policy makers on best practice for land use and management it is critical to give confidence in the measurements. EC measurements that pass the quality control process still have an inherent uncertainty associated with

them that reflects the instrument limitations and the underlying theory that sometimes does not accurately reflect nature (Richardson et al., 2012).

Design of the system and quality control process was done to reduce the possible sources of error suggested by Businger (1986). However, it was recognised that sampling error cannot be excluded. Sampling errors relate to the sampling time period and the auto and cross correlation of fluxes within them. Given the homogeneous nature of the managed arable site studied here, the sampling errors are expected to be less than those associated with fluxes from more heterogeneous surfaces (Finkelstein and Sims, 2001). As these fluxes are used to fill missing gaps, there is an additional propagation of uncertainty associated with each 30 minute flux that is gap filled (Richardson et al., 2012).

Uncertainties of half-hourly fluxes were therefore calculated using a combination of random uncertainty based on the calculation of variance of the covariance of the flux calculations following the Finkelstein and Sims (2001) methodology during the processing of the raw 20 Hz data, to account for sampling error, and the standard deviation calculated during gap-filling based on the values used to calculate the filled value. This standard deviation was calculated using the REddyProc tool provided by the Max Planck Institute for Biogeochemistry that implements the standardised method of Reichstein et al. (2005). Sum of squares was then used to calculate a plausible range of uncertainty on a daily timestep.

#### 2.2.9 Energy balance closure (EBC)

Energy balance closure draws on the first law of thermodynamics and requires the sum of the heat flux to equal all other measured energy sinks and sources (Wilson et al., 2002, Leuning et al., 2012). It is commonly accepted as an important reflection of the reliability of EC measurements of gas fluxes being measured at a site (Aubinet et al., 2000, Wilson et al., 2002, Foken et al., 2012a).

Quality controlled, but not gap filled, thirty-minute LE and H heat fluxes calculated during post-processing by Eddy Pro 6.1.0 from raw LI7550 measurements of water vapour, temperature and vertical wind speed were used. Whilst, available energy was calculated as the sum of measured net radiation ( $R_n$ ), soil heat flux ( $G$ ) and heat storage ( $S$ ) which also underwent quality control.

$$LE + H = R_n - G - S \quad \text{Equation 2.6}$$

$R_n$  was measured by the radiometers at the site. Canopy energy storage, given the temporary and short nature of the vegetation combined with the practicality of measuring amongst a managed crop was not calculated and therefore could provide imbalance during the presence of crop on the field. Soil heat flux was calculated following the example of Campbell Scientific (2016) using data from the soil instrumentation described above and values of  $263 \text{ kg m}^{-3}$  for bulk density (established from surface samples taken from the site during fallow months, s.d = 0.03, n = 6). Additionally  $1920 \text{ J kg}^{-1} \text{ K}^{-1}$  and  $4180 \text{ J kg}^{-1} \text{ K}^{-1}$  were used for the specific heat capacity of dry peat soil and water respectively as per Oke (1978).

In this study I use two methods to assess EBC. The first uses ordinary least squares to derive linear regression coefficients (slope and intercept) for the dependence of the energy fluxes on the available energy (equation 2.6), as in Wilson et al. (2002), despite this implying that there is no random error in available energy measurements. The closer the slope value to 1 and the intercept to 0 the better the explanation of the energy fluxes by the available energy.

In practice half-hourly fluxes of LE and H estimated using the EC technique rarely equates to the sum of the available energy (Hendricks Franssen et al., 2010, Leuning et al., 2012). This imbalance is usually reflected in a 10–30% underestimation of turbulent surface fluxes of LE and H to the available energy (Lloyd and Taylor, 1994, Wilson et al., 2002, Leuning et al., 2012). There are several proposed sources for a lack of closure: sampling error due to separation of source areas for fluxes and available energy measurements; systematic issues with instrumentation; energy stores and sinks that are not measured; low and high pass fluxes that elude measurement by EC; and loss of energy from the environment by advection (Wilson et al., 2002, Foken et al., 2012a) particularly during poorly developed turbulence at night (Aubinet et al., 2012a).

To address storage of heat and systematic phase shifting of fluxes, mean daily values of heat flux and available energy were calculated, following the strategy of Leuning et al. (2012), for days with more than 70% available values. Additionally the impact of  $u^*$  on day and night-time EBC is investigated.

The study site of this research has a homogenous surface for most of the year due to management practices (laser levelling and uniformity of vegetable cultivation) and so can be expected to provide a better environment than most sites for closure of the energy budget. As with all EC sites however, it was not possible to avoid separation of source areas of measurements. Additionally, due here to the mechanised nature of management activities at the site, it was not possible to install radiometers directly over the crop canopy that was dominant in contributing to energy fluxes, which resulted in a large portion of the radiometers field of vision including bare peat or weeds when there was crop present over the majority of the field (despite this the measured albedo reflected crop growth). Furthermore, regular mechanistic disturbance of the upper soil profile that occurred across the field was not reflected in the top soil around the heat flux and storage measuring equipment (installed within 10 cm of the surface) which also could not be installed below the crop.

The second technique employed for this research to investigate the energy balance, is also demonstrated by Wilson et al. (2002), is the energy balance ratio (EBR):

$$EBR = \frac{\sum(LE+H)}{\sum(Rn-G)} \quad \text{Equation 2.7}$$

EBR is calculated to gain an overall evaluation of EBC which overlooks biases in half hour data over longer temporal periods. Similarly to EBC slope, the closer the EBR is to 1 the better the available energy explains the heat flux.

### 2.3 Lateral C flux

While the EC system quantifies the flux of C-CO<sub>2</sub> between the biosphere, in this case the agricultural field of interest, and the atmosphere, it does not capture other pathways of C into and out of the field which are referred to here as lateral fluxes. Fertilisers, seeds and other growing mediums represent a lateral import of C into the field, while harvest represents a significant export of C both in the plant and any attached soil.

Organic fertiliser in the form of peat ‘plugs’ were added to the field during planting of the salad crops, but no additional organic fertilisers were added (to my knowledge). Import of C as seeds is rarely reported in the literature. Crop harvest is usually reported by studies as yield and is dependent on what crop was grown and the conditions under which it grew.

Kutsch et al. (2010) highlight the importance of accounting for the lateral C fluxes in croplands. A range of C content estimates have been reported in the literature for a variety of crops (Table 2.3) and where studies have not calculated this a value of 0.4 g g<sup>-1</sup> is most commonly referenced (Hadley and Causton, 1984). Koerber et al. (2009) reported the lowest C content of 0.35 g g<sup>-1</sup> as an average of 10 different crops, which included lettuce, whilst another recent study by Jia et al. (2012) calculated values of 0.43 and 0.42 g g<sup>-1</sup> for celery and lettuce plants, respectively.

**Table 2.3:** Summary of research on carbon content of crops.

<b>Study</b>	<b>Material</b>	<b>C content as % of dry weight</b>
<b>Kandel et al. (2013)</b>	Spring barley and Reed canary grass	45%
<b>Jia et al. (2012) (litter not considered)</b>	celery, tung choy, baby bok choy, amaranth, choy sum, bok choy, Garland chrysanthemum and Lettuce	43.2, 41.8, 39.3, 32.8, 35.4, 42.7, 36.9 and 41.5%
<b>Koerber et al. (2009)</b>	Lettuce, broccoli, cabbages, vining peas, wheat, potatoes, sugar beet, purple sprouting broccoli, French beans and Brussels sprouts	Averaged to 35%
<b>Lohila et al. (2004)</b>	Barley and grass	42%
<b>Hadley and Causton (1984)</b>	Barley and Brussels sprouts	40%
<b>Terry and Mortimer (1972)</b>	Sugar beet leaves	42.1%

Given the quantity of plant material removed from this site (~ 30 t ha<sup>-1</sup> yr<sup>-1</sup> for a lettuce crop (M Hammond, Pers. comm.), with a maximum 14% dry weight) this has potential to equate to a dry weight crop removal of 4.2 t ha<sup>-1</sup>. Applying C content values with a

difference of  $0.065 \text{ g g}^{-1}$  would change the per hectare calculation of C removal by  $0.273 \text{ t C ha}^{-1}$ . Therefore to establish a more accurate picture of net biome production (NBP) and NECB at this site, direct calculations of the C imported during planting and exported during harvest were made.

Although NEE is reported here relative to atmospheric gains and losses (negative fluxes being atmospheric losses and positive atmospheric gains) the lateral fluxes in  $\text{g m}^{-2}$  presented here represent gains and losses from the biosphere (the field). However, to compare and combine these C fluxes with NEE, gains of the biosphere are presented as negative values and losses as positive values. This is not suggesting that harvest represents an instant mineralisation of the vegetation harvest (though it is expected that this is the eventual pathway) but that by leaving the field harvested crops contribute to a C loss from the field that can be combined with positive NEE values.

### 2.3.1 Import ( $C_i$ )

Here I quantify the C import associated with planting. The  $64\text{--}125 \text{ cm}^3$  plugs used for lettuce and celery planting largely consist of a block of peat material, the peat for which is obtained largely from peat extraction sites in Ireland and Scotland (M Hammond, Pers. comm.). Five plug plants of each crop type were obtained. These were dried and then put through a standard loss on ignition protocol whereby the samples were chopped up and dried in aluminium trays at  $105 \text{ }^\circ\text{C}$  for 24 hours before being re-weighed, crushed and decanted into crucibles for incineration in a furnace at  $450 \text{ }^\circ\text{C}$  for 5 hours. The C content in grams was established as 50% of the weight difference between the dry sample and the incinerated sample (Chambers et al., 2011). No seed weight was calculated for the leek crop or the barley cover crop, so literature figures were used from Kutsch et al. (2010) and Ceschia et al. (2010).

### 2.3.2 Export ( $C_e$ )

To establish a C output value for crop harvest, samples of harvested plants of all three crops were obtained and dried in an oven at  $60 \text{ }^\circ\text{C}$  for 48–72 hours in order to establish dry weight values (Hadley and Causton (1984) found less than 1% difference for samples freeze dried as opposed to oven dried). Plants were not washed and so any incidental soil that was trapped within leaves was also analysed. A Shimadzu Total Organic Carbon analyser with solid state sample module (TOC-SSSM) (Shimadzu UK Limited, Milton Keynes, UK) was used to measure C content. The TOC-SSSM requires

a homogenous sample of no more than 1 g with up to 30 mg of C present. With an idea of the potential 40% reported figure for C content, roughly 50 mg of ball milled samples were weighed out into ceramic boats that had previously been heated to 900 °C to remove any potential contaminants. The samples were dried again at 100 °C to remove any further moisture and re-weighed so that the moisture was accounted for, before being combusted at 900 °C and measured on the instrument's infrared detector.

#### **2.4 Aeolian horizontal mass flux methodology**

The methodology for the measurement of C loss by wind erosion and the calculation of horizontal mass fluxes is provided in Chapter 5.

## **2.5 Chapter summary**

This chapter has provided both a broad and more focused history of the East Anglian fen region and the study site climate and management history. This included details of site management activity undertaken by farm operators during the study. Details of the theoretical background of the EC measurement technique employed is given in association with a description of the EC and associated meteorological equipment installed. This was followed by a clear explanation of the post-processing, QC procedures and gap-filling techniques used to quantify daily, seasonal and annual NEE of CO<sub>2</sub> in order to address the first two research questions. To evaluate the validity of the fluxes presented in the later chapters, a method for uncertainty calculation is addressed in addition to a EBC assessment to account for available and measured energy as a further reflection on the validity of measured NEE of CO<sub>2</sub>. Furthermore, the laboratory procedures undertaken to calculate of lateral C fluxes via the import and export of crops were detailed.

### **Chapter 3: Drivers of CO<sub>2</sub> fluxes at an intensively cultivated drained lowland deep peat soil**

This chapter addresses research question 1 from Chapter 1.4: What are the key drivers of NEE at a lowland peat soil under intensively cultivated land use? To do this I investigate the drivers of NEE at the field site over the 3.5 years of EC flux data across four crop cycles. NEE is a balance of TER and GPP and whilst they are not completely independent of each other, the NEE analysis here focuses on the controls on these two contributing fluxes.

As explained in Chapter 1, the impact of Tair, Tsoil, WTD, and SWC are important environmental factors impacting the TER of peat soils (Frolking et al., 2011, Strack, 2008). The extent to which these drivers of TER impact and control peat soil NEE, in particular in intensively managed agricultural peat soils, is less well understood. Therefore, in this chapter TER is modelled as a function of Tsoil using nocturnal NEE. This relationship is assessed and residuals of the model fit are assessed with relation to WTD and SWC to indicate whether they limit TER at the study site.

GPP is modelled using a light response model that utilises photosynthetic photon flux density (PPFD) fitted to daytime NEE. The residuals of the model are plotted to identify potential limiting controls on GPP for this intensively managed lowland peat soil.

The environmental conditions for the complete dataset are reported, to demonstrate the variability in site conditions between the measurement years. Then the key drivers of TER are investigated, and the peak light response of each crop is assessed.

The chapter begins by explaining the modelling methods for the temperature and light responses of night and daytime NEE, respectively. It then provides relevant environmental data recorded during the study before presenting the results of the TER and GPP modelling. This is followed by a discussion of the findings with reference to studies conducted on peat soils at other, mostly temperate, locations globally.

### **3.1 Analysis method**

Models used in this chapter to investigate drivers of NEE as contributions to nocturnal TER and GPP are laid out here.

#### **3.1.1 Modelling nocturnal TER**

The exponential temperature response model of Lloyd and Taylor (1994) presented in Chapter 2 (2.2.7, Equation 2.5) is used to partition NEE of CO<sub>2</sub> to investigate the environmental drivers of TER for each of the crop and fallow periods, several assumptions are inherent in doing this. Firstly, it is assumed that during the night, no photosynthesis takes place and therefore contributions to NEE are solely from TER; thus nocturnal NEE is equivalent to nocturnal TER. More importantly, in the context of this investigation, the model inherently fits itself to T<sub>soil</sub> as a driver of TER, and so is predisposed to find a relationship here. As temperature has been shown within the literature (Chapter 1) to be a key control over TER and Arrhenius type equations are most commonly utilised in many previous research papers investigating drivers of TER on peat soils (Lohila et al., 2004, Parmentier et al., 2009, Lafleur et al., 2005), this is concluded to be a suitable method. Additionally, given the common use of this particular equation within the EC community for the partitioning of NEE into TER and GPP (Reichstein et al., 2005, Wohlfahrt and Galvagno, 2017, Wohlfahrt et al., 2005, Falge et al., 2001, Baldocchi et al., 2001)(which is used here; Chapter 4), and ease of its execution, this method was chosen to evaluate drivers of TER.

The fit of the model to the observed NEE is assessed using linear regression to indicate how well T<sub>soil</sub> models TER, and the residuals of the model fit are then employed to investigate any weaknesses in T<sub>soil</sub> modelling due to fluctuations in water table depth (WTD) and soil water content (SWC) which were discussed as potential key drivers of TER in Chapter 1. Residuals of the fit are calculated by deducting the modelled nocturnal TER from the observed nocturnal NEE. This is a similar strategy to that presented by Parmentier et al. (2009) therefore, as in their study, if the modelled TER explains the observed values well and there is no statistically significant relationship between the residuals and the WTD and SWC, then it is assumed that these have little or no influence on the observed NEE. If a relationship is present between the variables and TER residuals then this will be described.

Additionally, the basal respiration ( $R_{ref}$ ) at 10 °C ( $R_{10}$ ) is calculated for each of the crops and their following fallow period and are considered against mean WTD and SWC. Calculation of  $R_{10}$  allows for the removal of seasonal influence on TER.

TER represents the total of both above and below-ground contributions to respiration. It is well recognised that some bias is introduced following the assumption that these both have the same sensitivity to temperature (Brooks and Farquhar, 1985, Wohlfahrt et al., 2005). The fallow periods contributed to 70% of the complete measurement period and had limited vegetation cover, therefore the influence of  $R_a$  was constrained. However, this likely had a notable impact on the partitioning of TER and GPP during the crop periods and is therefore noted as an accepted limitation of this technique.

As described by Lloyd (2006) it is difficult to compare conditions within the soil and their impact on TER given the lag between measurements caused by length of time for diffusion of  $CO_2$  to the soil surface before measurement by EC instrumentation. In particular, tortuosity (the twisted, ‘tortuous’, nature of the pathway taken) within moist peat soil profiles can lead to a longer lag between measurements. To dampen the influence of time lag in this study nocturnal means ( $R_g < 20 \text{ W m}^{-2}$ , centred around midnight) of non-gap filled NEE are used to model the dependence of TER on  $T_{soil}^c$  for each of the consecutive crop and fallow periods. Only those nights for which a minimum threshold of six half-hourly values were available were used (Lafleur et al., 2005).

### 3.1.2 Modelling light response of NEE

The light use efficiency of each crop is investigated here to assess the contribution of gross primary productivity (GPP) to NEE. Due to the intensively managed nature of crop growth (e.g. control over timing of planting, length of growth, application of fertilisers, irrigation, raising of the water table, harvest) the usual factors that limit photosynthesis (water/nutrient availability, temperature, light) are largely controlled. Individual crop capacity to assimilate based on light use is therefore estimated as a driver of NEE. Several methods were identified in the literature for modelling GPP. More complicated photosynthesis models exist (e.g. ORCHIDEE (Parmentier et al., 2009)) that calculate GPP as a function of multiple variables including radiation,

---

<sup>c</sup>  $T_{soil}$  is used rather than  $T_{air}$  as for the majority of the measurement period there was little or no crop or weed cover on the field and therefore autotrophic respiration will not impact the relationship.

temperature, humidity, pressure, precipitation, CO<sub>2</sub> concentration and surface conductance, Simpler models found that utilised optimum response to temperature (Falge et al., 2001), but primarily models based on the Michaelis-Menten equation are more common within the literature (Falge et al., 2001, Lohila et al., 2004, Gilmanov et al., 2007). Here an adaptation of the Michaelis-Menten equation is utilised and residuals of its fit explored in the manner as the Lloyd & Taylor temperature response method above. Application of the Michaelis-Menten model allows the peak rate of assimilation to be considered by level of PAR without the complication of additional environmental conditions. The Michaelis-Menten type rectangular hyperbola adapted from Falge et al. (2001):

$$NEE = - \left( \frac{\alpha * PAR}{\left( 1 - \left( \frac{PAR}{2000} \right) + \left( \frac{\alpha * PAR}{GPP_{opt}} \right) \right)} \right) + R \quad \text{Equation 3.1}$$

Where  $\alpha$  is the rate of light use (quantum yield),  $GPP_{opt}$  the GPP at optimum light (2000  $\mu\text{mol m}^{-2} \text{s}^{-1}$ ) and R the respiration contribution ( $\mu\text{mol CO}_2 \text{ m}^{-2} \text{s}^{-1}$ ). All parameters ( $\alpha$ ,  $GPP_{opt}$  and R) are fitted values based on the available half-hourly NEE and PAR data.

Light response is modelled for each of the crop periods using the non-gap filled half-hourly NEE and photosynthetically active radiation (PAR) values, where both were available. Night time values were included, as their exclusion led to unrealistic parameters being calculated. Given the arbitrary nature of the length of the crop growing periods the model is additionally fitted to two week periods of NEE and PAR to standardise peak uptake for each crop to allow further comparisons between crop types assimilation. The two week window was defined by inspecting all of the available data with a two week moving window that shifted one day at a time until the peak quantum yield ( $\alpha$ ) was identified.

The strength of fit of the modelled NEE to observed NEE was assessed using linear regression, a strong relationship suggesting limited further dependence on other environmental variables. Furthermore, residuals of the modelled and observed NEE were plotted for their dependence on potential limiting variables (Tair, Tsoil, VPD, WTD and SWC). Both linear regression and Spearman's rank were employed to assess the strength and nature of any relationship between the residuals and potential limiting variables (Tair, Tsoil, VPD, WTD and SWC).

## 3.2 Environmental conditions

### 3.2.1 Radiation

Values of daily global radiation ( $R_g$ ) followed a typical seasonal cycle whereby minimum values were recorded during winter months and ranged from  $0.5\text{--}5\text{ kJ m}^{-2}$  which gradually increased to  $2\text{--}18\text{ kJ m}^{-2}$  for days during summer months and reduced back through autumn (Figure 3.1). Maximum daily  $R_g$  was measured during the period of crop growth every year of measurement, peaking at 16.03, 18.34, 15.56 and  $17.2\text{ kJ m}^{-2}$  for 2012-2015 respectively (Figure 3.1a).

Total  $R_g$  during crop growth was relative to the length of the crop period required to grow the crop. As the leek crop spent double the length of time on the field compared to the celery crop and three times that of the lettuce crops it received the most  $R_g$  at  $1716.13\text{ kJ m}^{-2}$ . The celery crop received  $878.02\text{ kJ m}^{-2}$ , whilst of the two lettuce crops the 2014 crop (that grew for 12 more days) only experienced  $50.5\text{ kJ m}^{-2}$  more than the 2012 crop that grew during peak summer  $R_g$  receiving almost  $1\text{ kJ m}^{-2}$  less mean daily  $R_g$ . Out of the four crops celery received the highest mean daily  $R_g$  of  $9.54\text{ kJ m}^{-2}\text{ d}^{-1}$ .

Annual  $R_g$  values for the three full measurement years were 2145, 1934.65 and 2059.73  $\text{kJ m}^{-2}$ , 2013-2015 respectively, and corresponded to the maximum daily  $R_g$ .

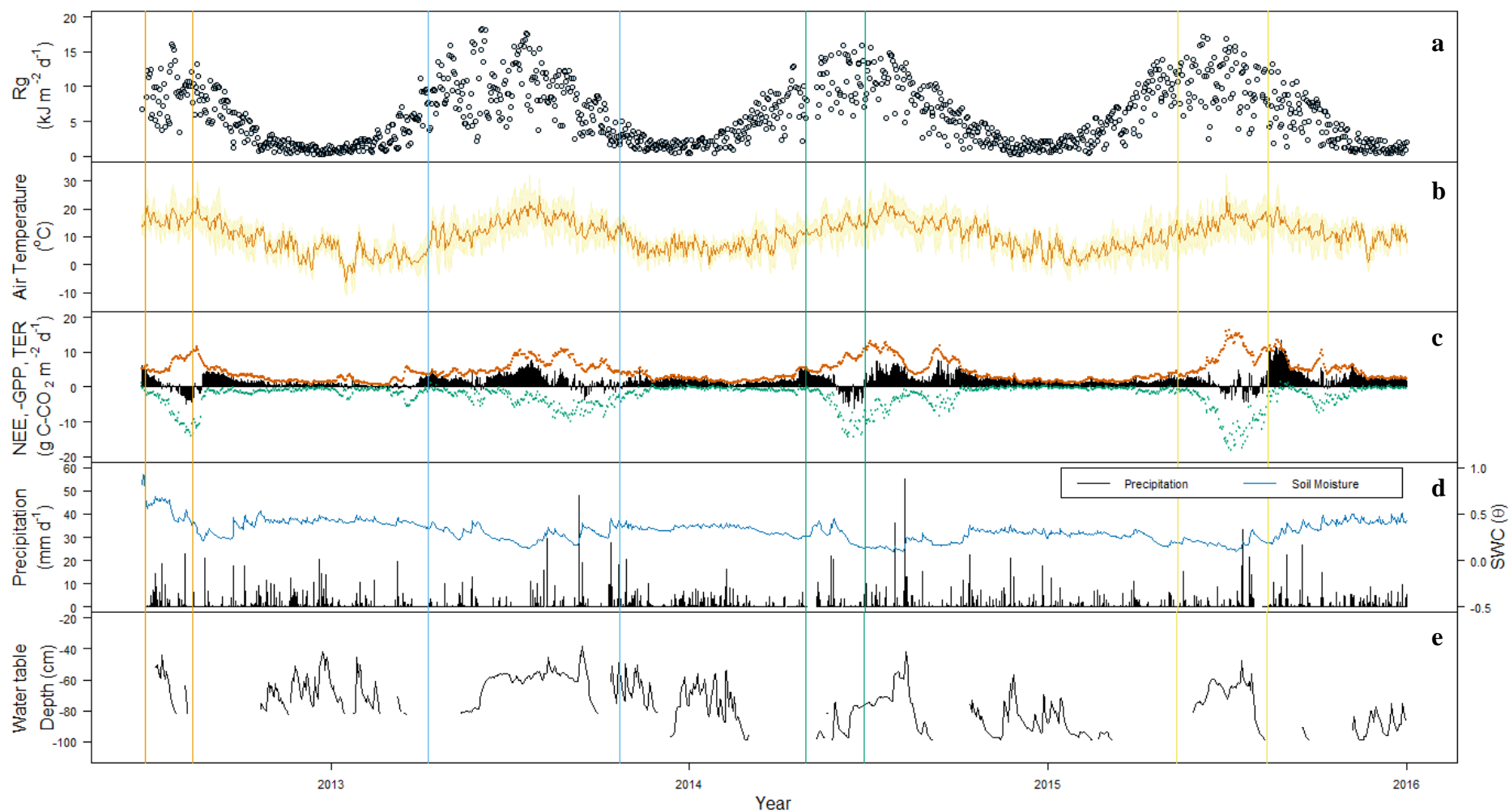


**Figure 3.1:** Daily meteorological conditions and fluxes: **a:** sum of  $R_g$  (global radiation), **b:** mean air temperature, **c:** NEE flux (black bars) with partitioned flux of TER (red dots) and inversely plotted GPP (green dots), **d:** sum of precipitation with mean soil water content (SWC) blue line, and **e:** mean water table depth. Vertical lines represent the planting and harvesting dates of each crop, orange for lettuce (2012), light-blue for leek (2013), green for lettuce (2014), and yellow for celery (2015).

### 3.2.2 Temperature

Air temperatures ( $T_{air}$ ) followed a typical temperate seasonal trend for the region with annual averages of 9.6, 11.2 and 10.4 °C, for 2013-2015 respectively, which were within the range of those reported for the region by the UK Met Office (Chapter 2.1.1; 8.4 to 11.2 °C). Minimum recorded averaged 30-minute  $T_{air}$  was -10.87 °C, recorded in January 2013, and the maximum 32.41 °C was reached in July 2015. The mean monthly air temperature was also within range for monthly UK Met Office records from the National Institute of Agricultural Botany (NIAB) in nearby Cambridge from 1961-2010 (Figure 2.1). Notable differences in  $T_{air}$  between the years of measurement included a colder January to March period in 2013 by 2–5 °C, a warmer winter and spring in 2014 by 3 °C and a warm December in 2014, which was not only 5 °C warmer than the same month in both 2013 and 2014 but also 3 °C warmer than the average maximum 50 year temperature of the NIAB records.

$T_{soil}$  followed the same seasonal trend as  $T_{air}$  but was more accentuated with summer values typically between 1–6 °C warmer than  $T_{air}$  (typically 5–6 °C whilst crops were present on the field) and winter values between 2 °C warmer and 3 °C colder (Figure 3.2).



**Figure 3.2:** Daily average temperature difference for soil and air ( $T_{soil} - T_{air}$ ).

Growing degree days (GDD) were calculated (Equation 3.2) for each crop and reflect the accumulation of heat during crop growth as a reference of plant development rates.

Using a base temperature of 5.5 °C (where plant growth would be expected to cease) and a maximum of 30 °C (where plant assimilation would be expected to saturate).

$$GDD = \frac{T_{air_{max}} + T_{air_{min}}}{2} - T_{air_{base}} \quad \text{Equation 3.2}$$

The two lettuce crops required similar GDD, 527.5 and 545 °C, for 2012 and 2014 respectively which, when planted earlier in the year (in 2014), had 12 extra days to accrue the additional temperature. The leek crop required more than double the amount of GDD (1597 °C) than the lettuce crops and just under double that of the celery crop (826 °C) (Figure 3.3). The similarity in degree day requirements of the lettuce crops despite the difference in the number of days the crop was on the field highlights the difficulty in comparing the drivers of GPP, and therefore why light use efficiency of each crop is used.

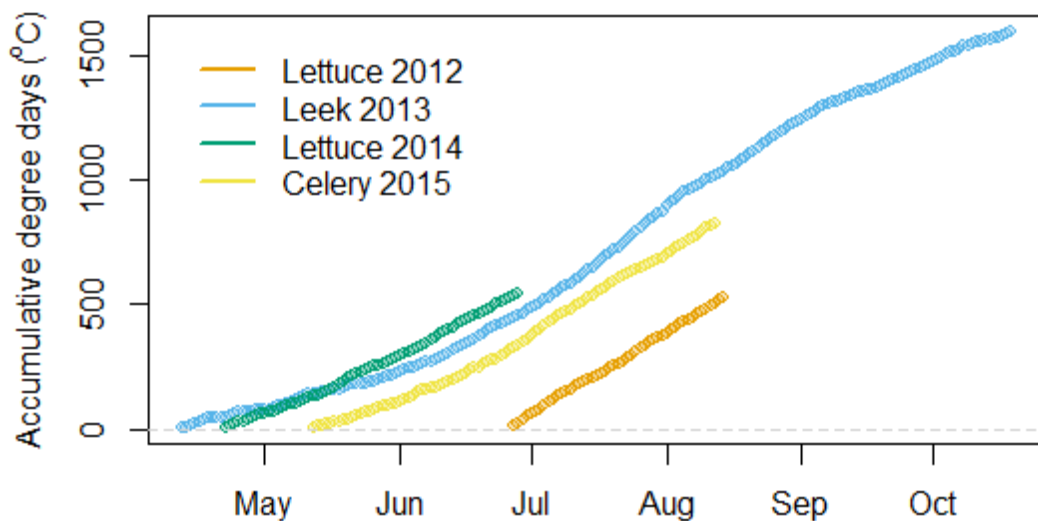


**Figure 3.3:** Accumulative degree days plot for each of the four crop growing periods from 2012 to 2015.

The thermal growing season is defined as starting on the first of five consecutive days of average daily  $T_{air}$  more than 5 °C and ending on the first of five consecutive days that  $T_{air}$  is less than 5 °C. It is reported to be over 310 days annually for the East Anglian region (see Chapter 2.1.1). Mean daily  $T_{air}$  measured at the field site dropped below the 5 °C threshold for calculating the thermal growing season on only 201 days of the entire measurement period (1288 days). The thermal growing season ranged from 266 to 359 days annually (Table 3.1), with the lower value reflecting sustained cooler temperatures in early 2013.

**Table 3.1:** Calculated dates for number of frost days and the thermal growing season dates from Tair measured at 1.55 m height above the ground. Air frost calculated as Tair < 5 °C, and soil frost as minimum daily Tair < 0 °C.

Year	Air frost	Soil frost	Thermal growing season		
	(no. days)	(no. days)	Start	End	no. days
2012	22	12	-	28/11/2012	-
2013	95	62	09/04/2013	31/12/2013	266
2014	38	26	01/01/2014	25/12/2014	359
2015	46	36	06/03/2015	31/12/2015	300

### 3.2.3 Precipitation and water management

The amount of precipitation recorded at the site for each complete year that measurements were made was 647, 744 and 640 mm (2013-2015 respectively).

The complete annual sums for 2013-2015 are all above the average annual sum of 560 mm recorded for the 1961-2010 period at the Met Office Cambridge NIAB station but only the 744 mm of 2014 was outside the range of values from that 50 year period (Chapter 2.1.1). The records from the NIAB station for the same three years were 50 to 150 mm lower.

Comparison of the monthly data showed that summer and autumn months had the largest disparity (2-4 times more/less) from year-to-year with July experiencing as little as 40 mm in 2013 but 90 and 120 mm in 2014 and 2015 respectively, September as little as 20 mm in 2014 but 50 and 90 mm in 2013 and 2015 respectively, and October measured 50 mm in 2015 but 125 and 90 mm in 2013 and 2014 respectively. These months coincide with irrigation dates reported by the farm manager (Table 2.1). Furthermore, a comparison with monthly NIAB station records showed the greatest disparity in precipitation was recorded for months when irrigation took place. It is evident from these comparisons that irrigation of the crops are measured by the rain gauge bolstering monthly and annual totals.

WTD at the study site was heavily influenced by management practices given its important role in influencing crop development. As WTD was regulated by the farm operators (Chapter 2) this led to an unusual, but fairly regular, annual pattern whereby it was maintained at a lower base level for fallow and higher base level for crop periods,

then fluctuated above these depths in response to precipitation and over-head irrigation (Figure 3.1e).

Available measured data for daily WTD ranged from a shallow depth of -0.38 m (relative to the surface) during 2013 to a deeper measurement depth<sup>d</sup> of -0.99 m. The deeper depth was exceeded for most of the autumn and spring months (Figure 3.1e). Figure 3.1e shows that the daily WTD was raised to between -0.6 to -0.7 m during the annual crop growing periods.

The lettuce crop periods of 2012 and 2014 experienced the most variable WTD that reflected the shorter period of crop growth, with over-head irrigation and precipitation leading to fluctuations between -0.45 and -0.95 m. Whilst in 2012 the base level WTD was then lowered following harvest, in 2014 the WTD was not raised until much later in the crop period and was then maintained at -0.7 m after lettuce harvest for the benefit of the neighbouring field where onion (*Allium cepa*) was being grown which, like its relative leek, requires a maintained high water table well into autumn. The longest period of raised WTD was from 15<sup>th</sup> June–20<sup>th</sup> September 2013 (97 days) for the leek crop and the average WTD for each of the crops was -0.62, -0.59, -0.95 and -0.68 m, with the lower WTD of 2014 reflecting the driest crop conditions.

Following harvest water was drained or pumped<sup>e</sup> from the ditches surrounding the field which led to a lowering of the base WTD level for the fallow months during which time input from increased precipitation led to typical variability in WTD (Figure 3.1d and e).

Daily volumetric soil water content (SWC) in the top 0.05 m of soil similarly increased in response to these above-ground inputs (e.g. precipitation and irrigation) and decreased with increases in R<sub>g</sub>, T<sub>air</sub>, and sustained negative NEE. Values fluctuated between 0.09 and 0.68 m<sup>3</sup> m<sup>-3</sup> (Figure 3.1d).

---

<sup>d</sup> Despite being informed that the water table was maintained above a -1 m depth the barometric instruments, set at a 1 m depth, were regularly exposed above the water table resulting in a loss of data.

<sup>e</sup> Water was seen to be pumped from one closed ditch system to another for later season crop planting in neighbouring field units, to avoid having to use water from the River Wissey or on site reservoirs.

### 3.3 TER

#### 3.3.1 Data availability

For the complete measurement period there were 645 nights suitable for analysis out of a possible 1308. For the lettuce 2012, leek 2013 and celery 2015 crops there were 27, 97 and 36 available nights respectively. Data loss due to battery failure and substantial removal of fluxes due to footprint restrictions (Chapter 2.2.5) led to an availability of only 22 nights of NEE fluxes during the lettuce crop period of 2014. Of these, 14 had less than six contributing half-hourly flux values and so were additionally removed. This meant that for the lettuce crop period of 2014 there were only eight available nocturnal mean values (Figure 3.5; Table 3.2). These nights were well spread across the first month of crop growth but did not include any nights from the last two weeks before harvest when  $R_g$  and  $T_{soil}$  were at their highest, WTD at its shallowest and SWC was low (Figure 3.1a, b, d and e). The nocturnal values for the 2014 lettuce crop were comparable with those measured during the 2012 lettuce crop, and followed a similar trend in SWC values. However, this comparison (and any comparison to the 2014 lettuce crop nocturnal NEE) is clearly constrained due to the limited number of available values.

The fallow periods had the largest number of available nights for modelling (83-164, Table 3.2), due to their larger timeframes. The average number of available half-hourly fluxes for calculation of nocturnal means (after removal of nights with less than six contributing values) was higher during fallow periods, ranging from 18-20 (Table 3.2). The average numbers of available half-hourly means for nights during the crop periods were 11–14. This difference reflects the seasonal variation in hours of day and night.

#### 3.3.2 Model performance

For all of the nocturnal values available for analysis the modelled TER had an almost 1:1 relationship with observed values and the ordinary linear regression (OLR) had a coefficient of determination ( $r^2$ ) of 0.7 (Table 3.2) which showed that variability in observed NEE was well explained by the modelled TER (Figure 3.4a).

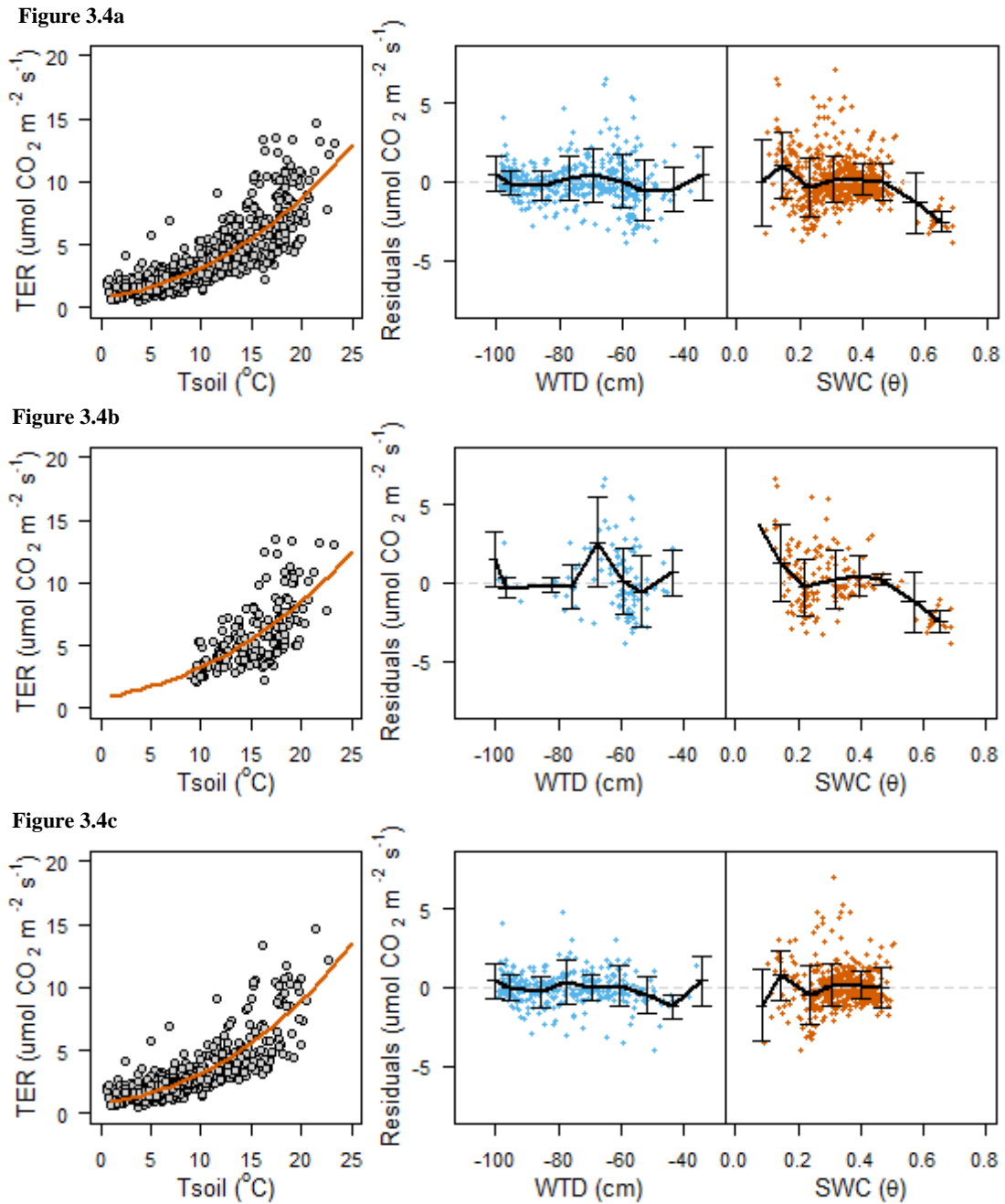


**Figure 3.4:** Modelling nocturnal TER from Tsoil values as a driver of nocturnal NEE (parameters  $R_{10}$ ,  $E_0$  and  $r^2$  are provided in Table 3.2). **a:** All nights from the complete measurement period. **b:** The nights from the crop periods only. **c:** The nights from the fallow periods only. The left most plot is the nocturnal TER plotted as a function of mean Tsoil, with the modelled fit plotted over the top. The residuals of the modelled TER and observed NEE are plotted on the right as responses to WTD (left, blue dots) and SWC (right, vermilion dots). Residuals were binned by WTD and SWC classes for each plot to identify trends. A class width of 0.08 m was used for WTD and  $0.08 \text{ m}^3 \text{ m}^{-3}$  for SWC.

Figures 3.4b and c present the data from the entire cropping period and the complete fallow periods, respectively, while Figure 3.5 presents each period individually. Variability in nocturnal TER is better modelled by Tsoil response during the combined

fallow periods (Figure 3.4c and Table 3.2) particularly at colder temperatures (<8 °C). During the combined crop periods (Figure 3.4b and Table 3.2) which had no nights of average temperature below 8 °C, variation in nocturnal NEE had an  $r^2$  of 0.43. Above 12 °C Tsoil response of TER also had greater variability for all periods (Figure 3.4a, b and c).

**Table 3.2:** Fitted variables for temperature response model and means of Tsoil, WTD and SWC for each period.  $r^2$  values of how well modelled TER explains the variability of observed  $NEE_n$  with significance of the linear fits ‘.’ 0.1, ‘\*’ 0.05, ‘\*\*\*’ 0.01 and ‘\*\*\*\*’ 0.001. SE is the standard error of the fitted value.

Period	$R_{10}$ $\mu\text{mol CO}_2 \text{ m}^{-2} \text{ s}^{-1}$ (SE)	$E_0$ K (SE)	Tsoil °C	WTD m	SWC $\text{m}^3 \text{ m}^{-3}$	n	Average n per night	$r^2$
<b>Lettuce crop 2012</b>	1.38 (0.47)**	664.39 (158)***	17.03	-0.62	0.57	27	12.59	0.39
<b>Fallow 2012/13</b>	2.60 (0.11)***	448.71 (22.95)***	8.70	-0.65	0.39	126	18.50	0.79
<b>Leek crop 2013</b>	3.70 (0.26)***	287.55 (35.37)***	14.85	-0.59	0.28	97	13.92	0.43
<b>Fallow 2013/14</b>	3.11 (0.14)***	224.42 (32.5)***	6.15	-0.73	0.35	104	19.53	0.31
<b>Lettuce crop 2014</b>	3.61 (0.49)***	214.63 (72.84)	14.64	-0.95	0.35	8	10.50	0.60
<b>Fallow 2014/15</b>	2.87 (0.12)***	397.11 (19.39)***	9.03	-0.84	0.26	164	18.51	0.78
<b>Celery crop 2015</b>	3.05 (0.41)***	464.54 (58.19)***	15.52	-0.68	0.19	36	11.89	0.69
<b>Fallow end of 2015</b>	3.63 (0.18)***	493.06 (33.28)***	10.65	-0.9	0.40	83	20.29	0.74
<b>All crop</b>	3.25 (0.22)***	354.73 (32.48)***	15.36	-63.1	0.31	168	-	0.43
<b>All fallow</b>	3.18 (0.07)***	382.52 (11.81)***	8.6	-77.97	0.34	477	-	0.71
<b>All nights</b>	3.19 (0.07)***	371.51 (11.14)***	10.42	-0.74	0.33	645	15.72	0.7
<b>All 30-min</b>	3.27 (0.02)***	351.2 (3.65)***	9.78	-0.75	0.34	12263	-	0.48

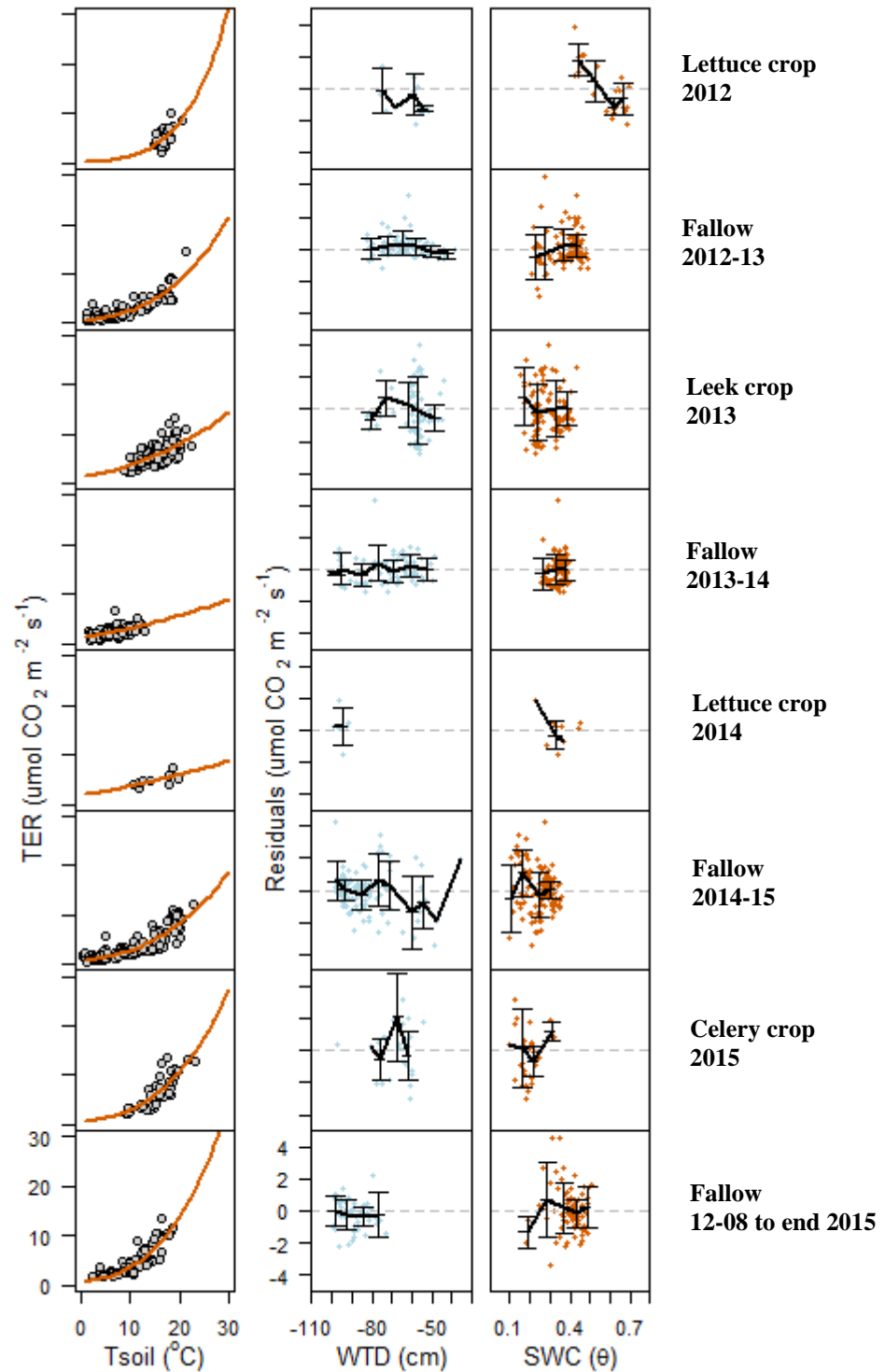


**Figure 3.5:** Mean nocturnal TER driver assessment for each crop and fallow period (parameters  $R_{10}$ ,  $E_0$  and  $r^2$  are provided in Table 3.2). The left most plots are the nocturnal TER plotted as a function of associated mean  $T_{soil}$  values, with the modelled fit in vermilion. The residuals of the modelled TER and observed TER are plotted on the right as responses to WTD (left, blue dots) and SWC (right, vermilion dots). Residuals were binned by WTD and SWC classes for each plot to identify trends, a class width of 0.08 m was used for WTD and  $0.08 \text{ m}^3 \text{ m}^{-3}$  for SWC.

Aside from the first lettuce period of 2012 the crop/fallow periods all experienced similar range of sensitivity to  $T_{\text{soil}}$  with  $R_{10}$  values ranging from  $2.6 \pm 0.11$  to  $3.63 \pm 0.18 \mu\text{mol CO}_2 \text{ m}^{-2} \text{ s}^{-1}$ . The 2012 lettuce crop was the least sensitive period of TER to  $T_{\text{soil}}$  with an  $R_{10}$  of  $1.38 \pm 0.47 \mu\text{mol CO}_2 \text{ m}^{-2} \text{ s}^{-1}$ .

Modelled TER explained 31-79% of variability in observed NEE across all of the crop and fallow periods. With the exception of the fallow period of 2013-14, modelled TER explained 74–79% of the variation of observed nocturnal TER during the fallow periods (Table 3.2). The 2013-2014 fallow period had the lowest average  $T_{\text{soil}}$  of 6 °C and a maximum  $T_{\text{soil}}$  of 13 °C, despite this the  $R_{10}$  was  $3.11 \pm 0.14 \mu\text{mol CO}_2 \text{ m}^{-2} \text{ s}^{-1}$ . Crop residual waste was the dominant field cover (Figure 2.5 e and f) throughout this period and was left above-ground to decompose during cool winter temperatures. The other fallow periods began during summer months and decomposition of crop residuals took place during warmer conditions. Initial residue decomposition appears to take place during comparative temperatures to those measured later in the same period once the residue was ploughed back into the soil. This may have led to the poorer explanation of variability by the model.

For the lettuce period of 2012 and leek period of 2013 modelled TER explained 39 and 43% of the variability in measured NEE suggesting that  $T_{\text{soil}}$  was not as significant a variable in driving TER during these periods.

#### *Fitted variables*

Basal respiration ( $R_{10}$ ) gives an impression of how sensitive the TER is to changes in  $T_{\text{soil}}$ , and  $E_0$  the energy required for TER. The  $R_{10}$  (respiration at 10 °C) for each modelled period of TER was additionally inspected for a potential relationship with mean WTD and SWC for each period.  $R_{10}$  values ranged from  $1.38 \pm 0.47$  to  $3.7 \pm 0.26 \mu\text{mol CO}_2 \text{ m}^{-2} \text{ s}^{-1}$  and  $E_0$  (activation energy) ranged from  $214.63 \pm 72.84$  to  $664.39 \pm 158 \text{ K}$  (Table 3.2). Neither variable demonstrated a bias with respect to crop or fallow period.

The fallow periods appear to show a negative correlation with WTD (Figure 3.6a) but once the crop periods (notably lettuce crop of 2012 and the leek crop) are included the correlation is no longer significant. No significant correlation is found therefore for WTD or SWC with respect to  $R_{10}$  (however the linear fit is plotted as a dashed line in Figure 3.6a and b), and they explained less than 1% of the variability in  $R_{10}$ .

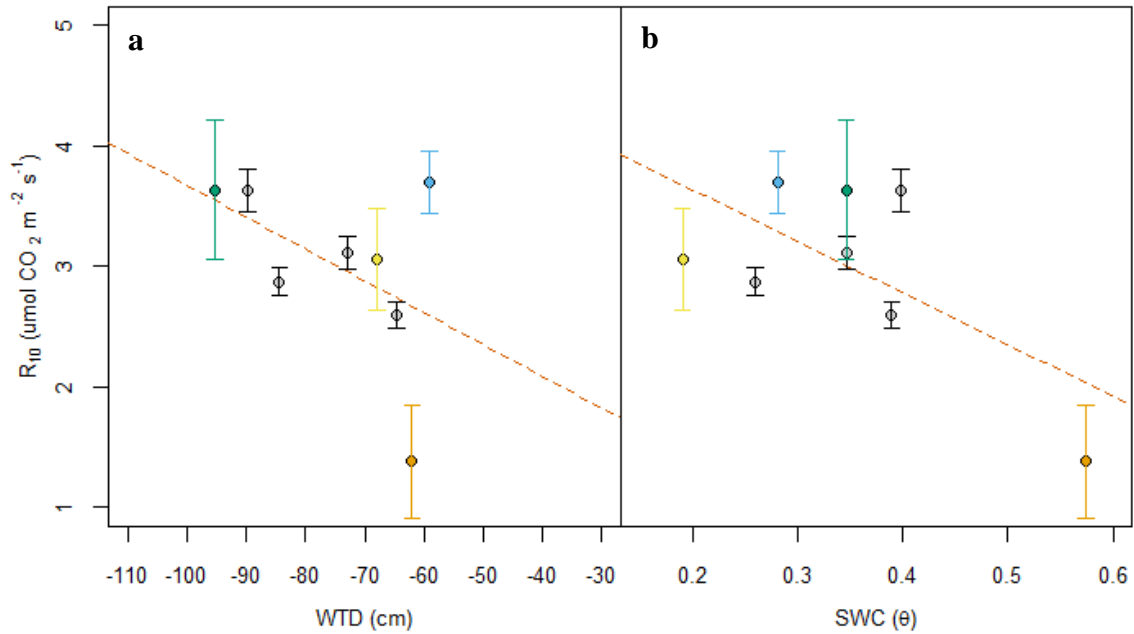


**Figure 3.6:** Basal respiration ( $R_{10}$ ) as a dependant of **a:** mean water table depth (WTD) and **b:** soil water content (SWC), for each of the measurement periods. Colours correspond to crop and fallow periods (as per previous plots), orange for lettuce (2012), light-blue for leek (2013), green for lettuce (2014), yellow for celery (2015), and all of the fallows are grey and black. The dashed vermilion line is the non-significant linear correlation for each dataset.

### 3.3.3 Residuals

#### *Water table depth*

The residuals for the complete measurement period (Figure 3.4a) demonstrated no significant relationship ( $p < 0.05$ ) with binned WTD averages despite a small number of nights where the model underestimate of nocturnal TER was outside the standard deviation for the residuals binned between -0.65 and -0.75 m depth. The same pattern is seen in the model TER fit for the complete crop periods (Figure 3.4b). There is no significant impact of WTD on the residuals.

The residuals from the fallow period model fit (Figure 3.4c) also show no significant relationship to WTD. However when comparing the two residual plots (WTD and SWC), it is clear that there are significant underestimates of TER ( $> 2.5 \mu\text{mol m}^{-2} \text{s}^{-1}$ ) that are present when comparing residuals to SWC but these are omitted due to the limited data availability from the WTD comparison. The gaps in WTD data were typically when WTD was in excess of -0.9 m, suggesting a possible underestimation of the modelled TER at deeper WTD, but without a more complete set of WTD measurements it is difficult to support this. Overall there were 208 extra missing nights

of WTD that could not be plotted against model residuals due to limited data availability.

The individual periods of modelled TER (Figure 3.5) similarly show no significant correlation between residuals and WTD, and only the celery crop period experiences the peak in underestimation of TER between -0.65 and -0.75 m depth described above.

#### *Soil water content*

Similarly to WTD there was no significant relationship ( $p < 0.05$ ) between the residuals and SWC for the complete dataset of nocturnal values, despite an increase in underestimation of TER between 0.2 and 0.35  $\text{m}^3 \text{m}^{-3}$  and an increase in overestimation when SWC was greater than 0.5  $\text{m}^3 \text{m}^{-3}$  (Figure 3.4a). As already noted, for the combined crop periods (Figure 3.4b) Tsoil sensitivity explained nocturnal NEE less well. The residuals of the combined crop periods have a weak negative correlation with SWC,  $r_s = -0.26$ ,  $n = 167$ ,  $p < 0.001$  (analysis performed using Spearman's rank;  $r_s$  is the correlation coefficient for this). Simple linear regression suggests an increase in underestimation by 0.5  $\mu\text{mol m}^{-2} \text{s}^{-1}$  for every decrease of 0.1  $\text{m}^3 \text{m}^{-3}$  of SWC above 0.51  $\text{m}^3 \text{m}^{-3}$ ; and the same rate of increase when SWC is below 0.31  $\text{m}^3 \text{m}^{-3}$ . Therefore, SWC is limiting during crop growth, however the relationship poorly explains the variability in residuals ( $r^2 = 0.16$ ).

The lettuce crop of 2012 (a period for which variability in observed NEE was less well explained by modelled TER) had a moderate negative correlation,  $r_s = -0.59$ ,  $n = 25$ ,  $p < 0.001$ , with SWC which explained 60% of the variability in the residuals. At lower SWC ( $< 0.55 \text{m}^3 \text{m}^{-3}$ ) modelled TER was underestimated and overestimated at higher SWC ( $> 0.55 \text{m}^3 \text{m}^{-3}$ ). No Spearman's rank correlation was found between residuals and SWC for the remaining crop and fallow periods, which means if there is a relationship it was non-monotonic.

#### *Daytime NEE*

The residuals of the Tsoil modelled TER for the crop periods have a significant moderate correlation,  $r_s = -0.56$ ,  $n = 169$ ,  $p < 0.001$ , with daytime NEE (Figure 3.7a). Available daytime NEE was averaged from and modelled nocturnal TER was found to underestimated for nights where daytime NEE experienced its greatest uptake (crop was most productive), suggesting the nocturnal NEE was increased due to crop maintenance and growth respiration in response to increased daytime photosynthesis. A similar

relationship was not present during the fallow periods despite weed growth (Figure 3.7b).

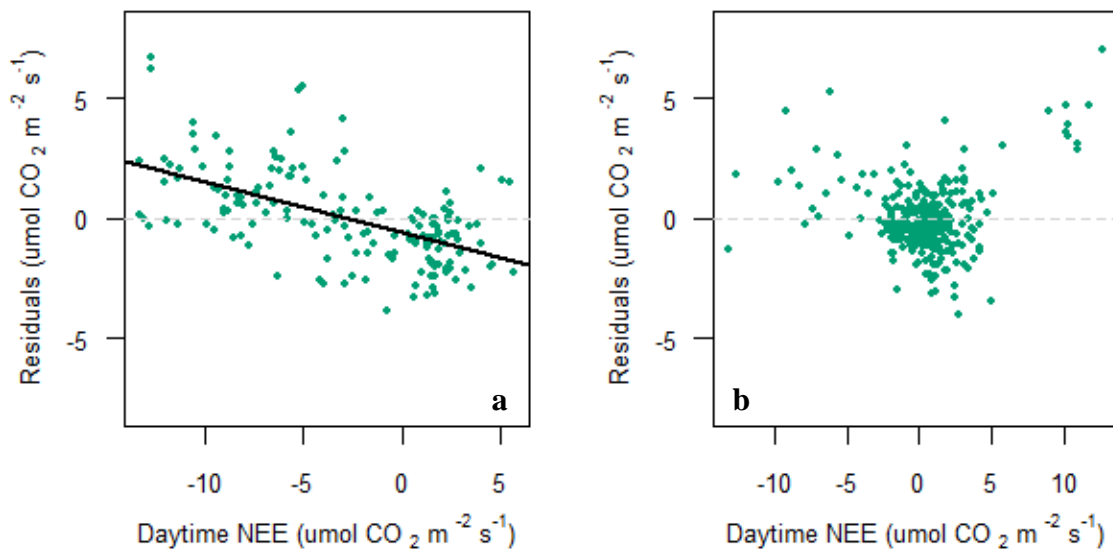


**Figure 3.7:** Residuals of Tsoil modelled TER and observed NEE against daytime NEE for the same days of all available values for the **a:** crop and **b:** fallow periods.

#### 3.3.4 WTD and SWC as primary drivers

Figure 3.8a and b show the entire available dataset of mean nocturnal NEE plotted as a function of WTD and as a function of SWC, respectively. No significant correlation is identified for WTD. An exponential fit of SWC (Figure 3.8b) led to an explanation of 22% of variability, with the variables showing moderate negative correlation,  $r_s=-0.35$ ,  $n=649$ ,  $p<0.001$ . This relationship suggests an increase in observed NEE with reduction in SWC.

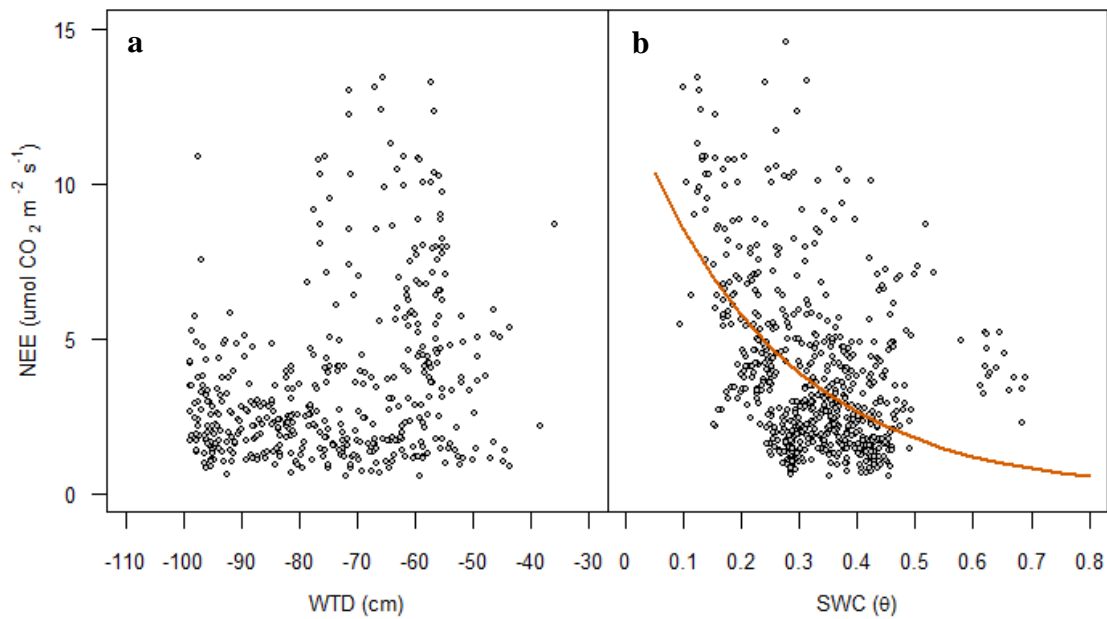


**Figure 3.8:** Observed nocturnal mean NEE (TER) as a function of **a:** WTD and **b:** SWC for all un-gap-filled nights of the complete measurement period. SWC fitted to TER with an exponential relationship:  $TER = \exp(3.84 * SWC - 2.52)$  using the non-linear least squares method.

### 3.3.5 Comparison of short-term rising and falling water table

Despite a lack of evidence in the crop and fallow periods that WTD influences TER, it has been shown by several studies that WTD drives short term TER response in peat soils (Oechel et al., 1998, Lloyd, 2006, Musarika et al., 2017, Poyda et al., 2016). Therefore two periods of WTD change were identified and extracted to identify any short term response of mean nocturnal NEE that was better explained by mean values of WTD or Tsoil.

Annual raising and lowering of the WTD meant that under fairly stable temperature conditions the WTD was changed significantly and artificially, predominantly around the planting and harvest of the crops. No significant relationship is identified here between WTD and NEE for the artificial raising of the water table associated with the planting and harvest of the crops, possibly due to increased contributing factors (e.g. fertilisers, crop growth, soil aeration following ploughing).

During the fallow periods the water table generally fluctuated in relation to precipitation inputs and there were also some large drops in WTD that can likely only be management related. Two significant changes in WTD during the fallow period of

2013-2014 were identified and are assessed here. The first was in December 2013 when the WTD rose from -0.96 to -0.62 m over 15 days (Figure 3.9a). Over this period 41 mm of rain was measured. The second event was during February 2014 when the WTD lowered from -0.5 to -0.99 m over 22 days (Figure 3.9b). This lowering took place regardless of 53 mm of rainfall, more than during the raising period, which largely fell over the first six days, suggesting the lowering of the WTD was a management response to this rainfall.

Visual inspection of mean nocturnal NEE for these periods suggests an inverse relationship to WTD, with NEE lowering from 3.5 to 2  $\mu\text{mol m}^{-2} \text{s}^{-1}$  during the WTD raising event (Figure 3.9a and c). During the lowering event the NEE visually appears to follow a similar trend to Tsoil (Figure 3.9 b and d). The SWC rose from 0.32 to 0.38  $\text{m}^3 \text{m}^{-3}$  during the raising WTD reflecting the contribution of continuous rainfall. During the lowering period SWC began at 0.38  $\text{m}^3 \text{m}^{-3}$  and fluctuated between 0.35 and 0.4  $\text{m}^3 \text{m}^{-3}$  until 16<sup>th</sup> February when it then steadily lowered to 0.33  $\text{m}^3 \text{m}^{-3}$ .

**Table 3.3:** Statistics from linear regression and spearman's rank correlations for relationships of WTD, SWC and Tsoil with NEE during a water table raising and lowering. < 0.001 '\*\*\*', <0.01 '\*\*', <0.05 '\*', <0.1 '.'

Period	Variables	Slope	Intercept	r <sup>2</sup>	r <sub>s</sub>	n
<b>Raising water table</b> (12/12 - 27/12/2013)	NEE v Tsoil	0.18 (0.06)*	1.72 (0.35)***	0.47	0.64**	9
	NEE v WTD	-0.04 (0.01)***	-0.5 (0.53)	0.8	-0.87***	9
	NEE v SWC	-20.64 (7.58)*	10.1 (2.69)**	0.4	-	9
<b>Lowering water table</b> (07/02 - 02/03/2014)	NEE v Tsoil	0.1 (0.05).	0.86 (0.29)**	0.14	0.44*	15
	NEE v WTD	-0.01 (0.01).	0.41 (0.55)	0.13	-0.52**	15
	NEE v SWC	-5.5 (6.08)	3.37 (2.19)	0.01	-	15

The raising WTD has a very strongly negative correlation with NEE (Figure 3.9g, and Table 3.3). Tsoil for the same period has a strong positive correlation to NEE (Figure 3.9e, Table 3.3). A linear regression of these variables yielded poorer explanation of variability in NEE, 47%, by Tsoil while WTD explained 80%. This suggests that the raising WTD here was dominant in causing short term reduction of NEE. The NEE for the lowering water table period only had moderate positive and negative correlations with WTD and Tsoil, respectively (Figure 3.9f and h, and Table 3.3) and variability of linear regression fits were poorly explained suggesting a limited response to these drivers during a lowering (drainage event).

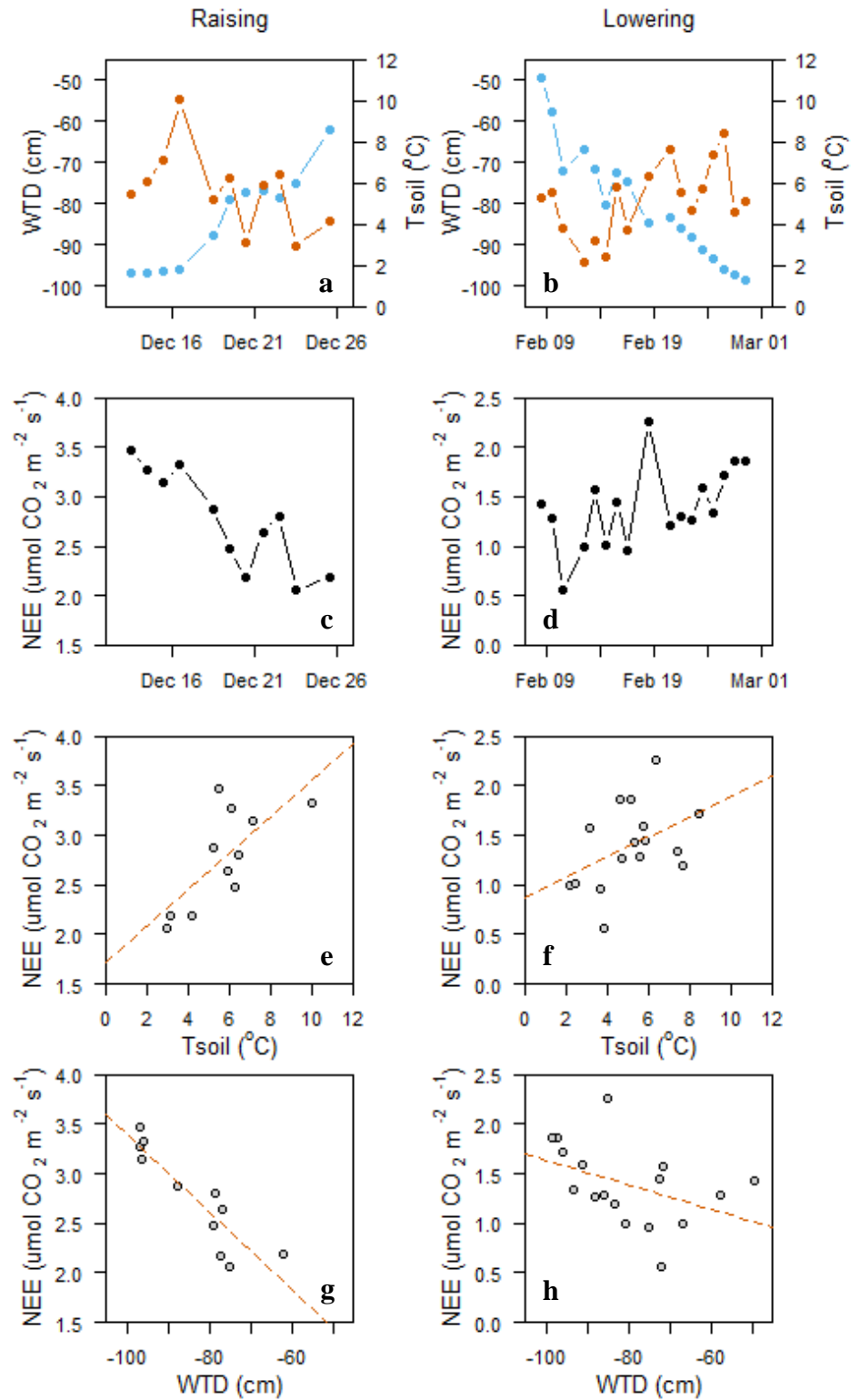


**Figure 3.9:** Raising and lowering of water table as a control of NEE. **a and b:** Mean nocturnal WTD (blue) and Tsoil (vermillion) for the raising and lowering events, respectively. **c and d:** Mean nocturnal NEE for the raising and lowering events, respectively. **e and f:** Tsoil as a driver of NEE with fitted simple linear relationships (details given in Table 3.3). **g and h:** WTD as a driver of NEE with fitted simple linear relationships (details given in Table 3.3). NEE axes differ in scale for each set of raising and lowering plots.

### **3.4 Light use**

#### **3.4.1 Radiation and temperature**

Monthly mean diurnal patterns in  $R_g$ ,  $T_{air}$  and  $T_{soil}$  followed similar patterns between years.

Figure 3.10 shows that there were two notable variations between years for  $T_{air}$ , the first was March of 2013 which was on average 3-4 °C cooler all day which corresponded to a decrease in  $R_g$ ; the second was December 2015 which was on average 4-5 °C warmer all day but did not correspond to  $R_g$  which was within the trend measured for December in other years.  $T_{soil}$  showed increased variability between years, which likely reflects the changes in vegetation cover and impacts of management. Variations measured in  $T_{air}$  are additionally seen in  $T_{soil}$  but less pronounced (Figure 3.10). The colder  $T_{air}$  of March is evident in April and May 2013 also, and in July and August of the same year there was a warmer mean diurnal pattern than other years. The increase in  $T_{soil}$  is probably due to the limited canopy cover of the developing leek crop during the months of peak  $R_g$  (Figure 3.10). The lower diurnal  $T_{soil}$  in April of 2013 potentially corresponds to the growth of the barley cover crop, as  $R_g$  and  $T_{air}$  were not much different to other years and energy fluxes of LE and H do not vary significantly year-to-year in April (Figure 4.4).

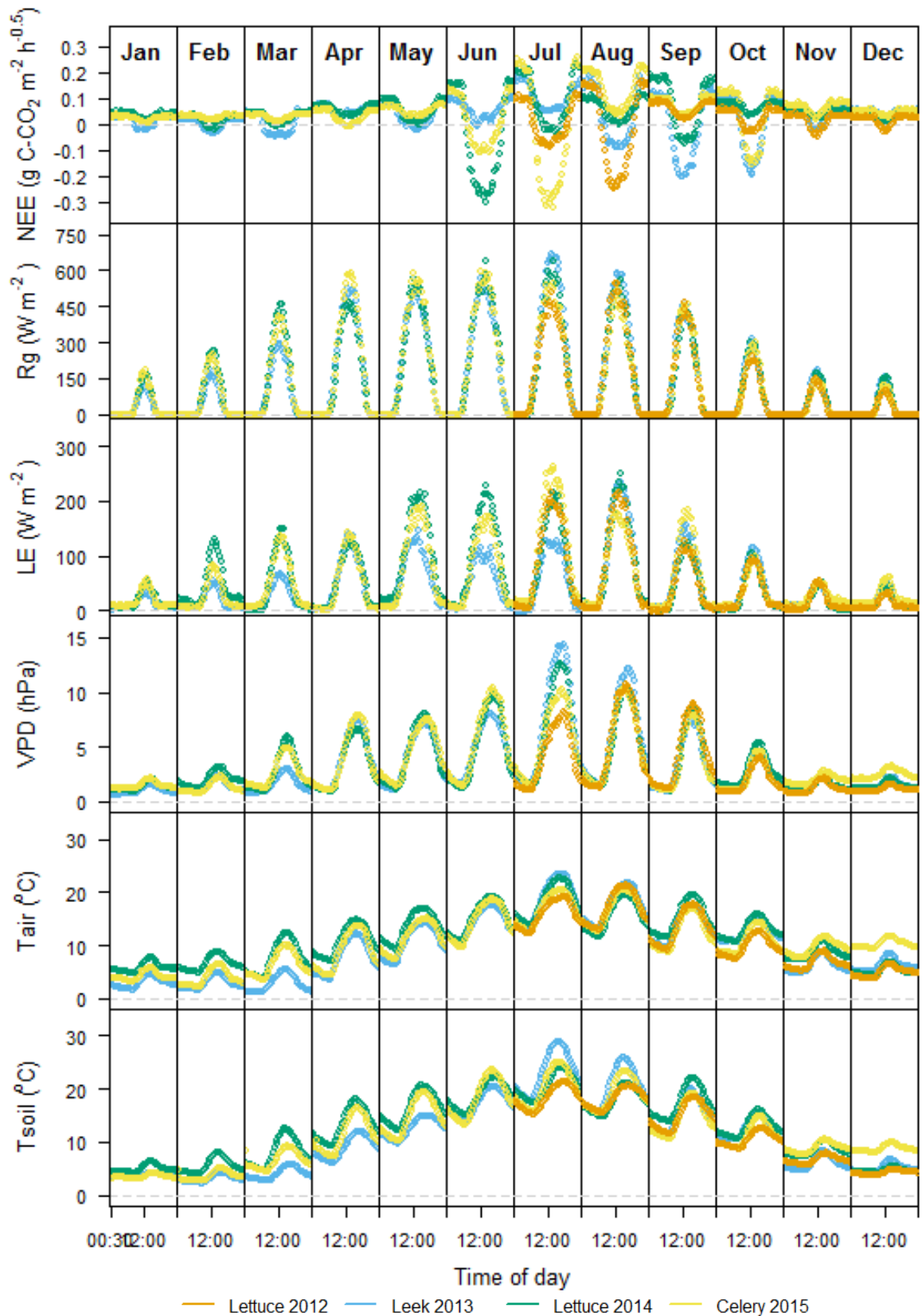


**Figure 3.10:** Monthly diurnal pattern of mean half hourly values for six environmental variables for each year of the complete measurement period (22nd June 2012–31st December 2015). NEE, Rg, LE, VPD, Tair and Tsoil. (Daylight savings is not applied so all times are in GMT).

### 3.4.2 Whole crop light response

Figure 3.11 shows the light response for each of the complete crop periods and demonstrates the variation of light use from crop establishment through to senescence and harvest. The three plug crops displayed two trends in light use with early crop establishment characterised by low values of net CO<sub>2</sub> uptake for the full range of PPFD. Then once the crop was more developed higher net CO<sub>2</sub> uptake was measured for similar light intensity. Therefore, crop development led to poor modelling of light response (Figure 3.11). The leek crop had a longer period of development than the plug crops which was further complicated by the use of a cover crop. Variability in the observed NEE therefore was not well accounted for by the light response modelled NEE (38–55%) for the entire crop periods (Figure 3.11 and Table 3.4).

Peak  $\alpha$  ( $0.05 \pm 0.01 \mu\text{mol CO}_2 \mu\text{mol photons}^{-1}$ ) of the four complete periods was measured for the leek crop (Table 3.4) this is likely due to its longer period of sustained assimilation, whilst the plug crops had shorter periods of sustained peak assimilation. The two lettuce crop periods understandably had similar  $\alpha$  ( $0.03 \pm 0.01$  and  $0.03 \pm 0.01 \mu\text{mol CO}_2 \mu\text{mol photons}^{-1}$ , respectively),  $\text{GPP}_{\text{opt}}$  ( $15.19 \pm 1.08$  and  $15.22 \pm 1.38 \mu\text{mol m}^{-2} \text{s}^{-1}$ ) and R terms ( $5.26 \pm 0.48$  and  $5.61 \pm 0.96 \mu\text{mol CO}_2 \text{m}^{-2} \text{s}^{-1}$ ) (Table 3.4). The limited data availability for the 2014 lettuce crop led to notably higher error estimations. The celery crop period had the highest  $\text{GPP}_{\text{opt}}$  ( $18.02 \pm 0.82 \mu\text{mol m}^{-2} \text{s}^{-1}$ ) and a higher R ( $7.61 \pm 0.45 \mu\text{mol m}^{-2} \text{s}^{-1}$ ) indicating that it had a higher threshold for utilising PAR.

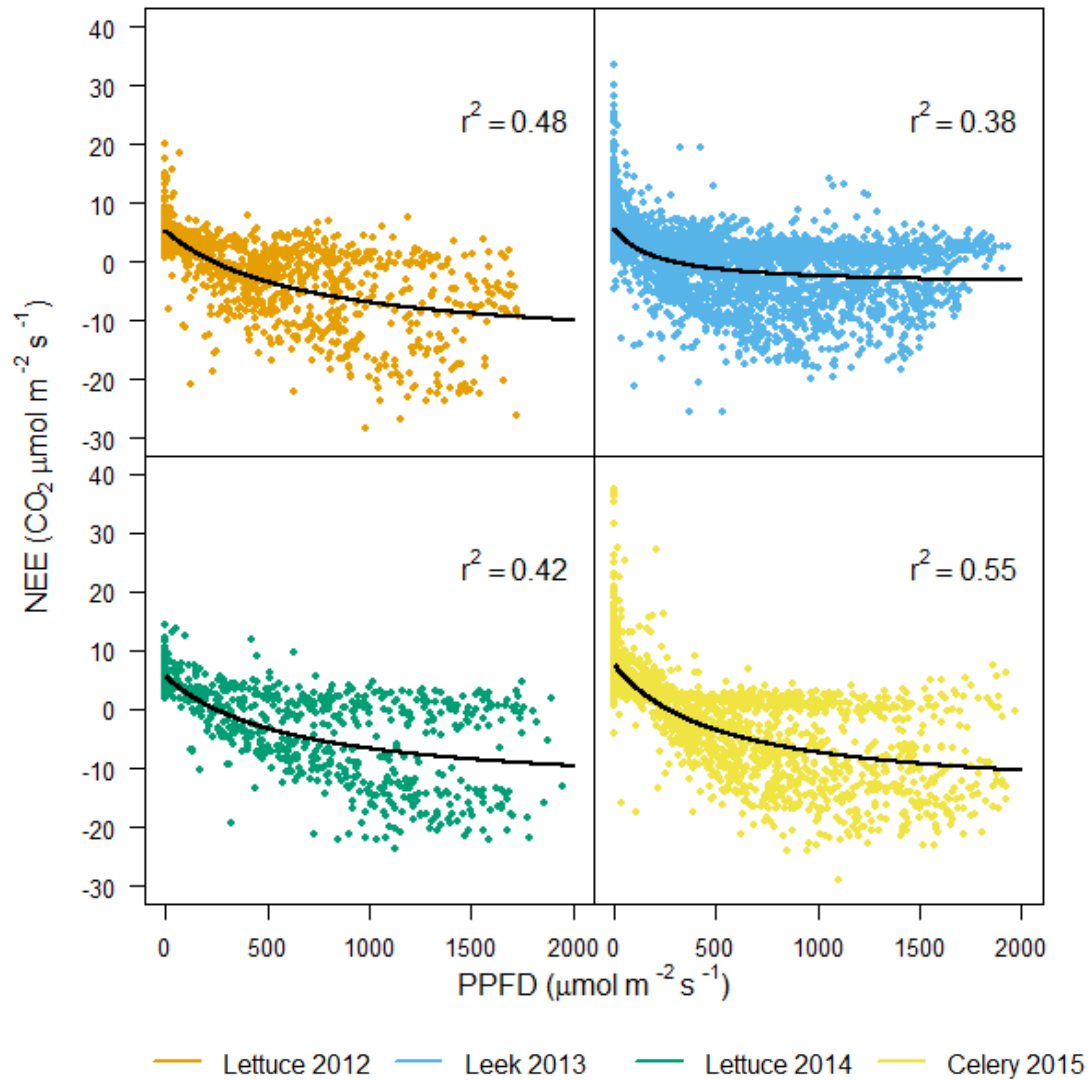


**Figure 3.11:** Light use efficiency of average 30 min values of NEE and PPFD for the complete growing period of each crop (from first planting day to final harvest day, see Table 2.1). Model terms are provided in Table 3.4.

### 3.4.3 Peak light response

For all crops the peak two week  $\alpha$  was plotted and corresponded to the peak average diurnal uptake for that year (Figure 3.10 and Table 3.4). For the two lettuce crops the two weeks started towards the end of the growing period when the crop was about to be harvested. For celery, this was a month before harvest when  $R_g$ ,  $T_{air}$  and  $T_{soil}$  were at their monthly diurnal peaks (Figure 3.10 and Table 3.4). Despite peak  $R_g$  and temperatures during July and August in 2014 the peak light  $\alpha$  of the leek crop was during September.

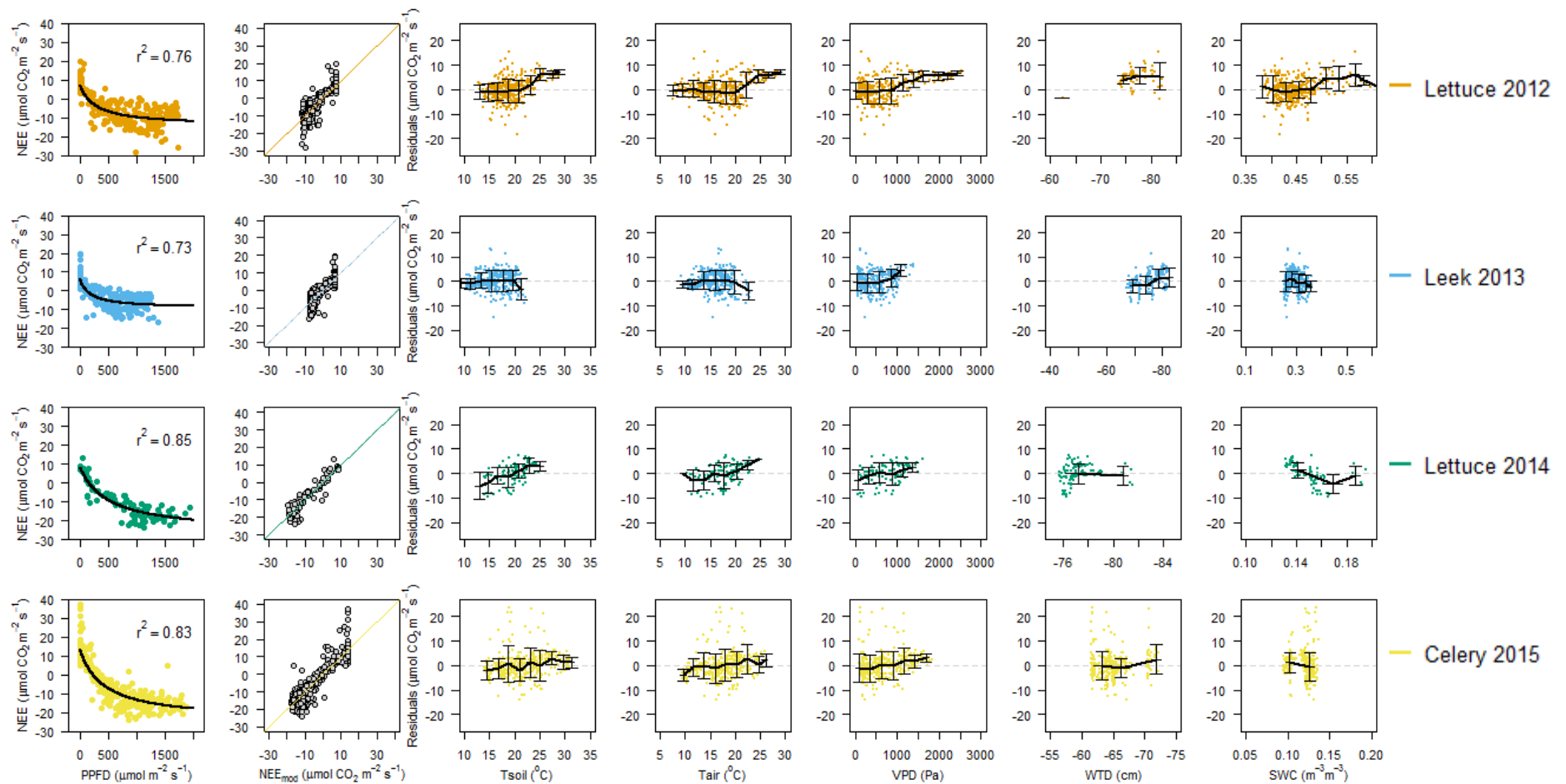
The light response model fitted better to the NEE of the peak two week periods of  $\alpha$  for each crop (Figure 3.12) than it did to the values for the entire crop period (Figure 3.11), but this relationship similarly deteriorated with greater variability in NEE as PPFD increased. The variability in daytime NEE values was best explained by the model fit of the lettuce crop period of 2014 ( $r^2=0.85$ ) which has the fewest available measurements (Table 3.4 and Figure 3.12). The modelled NEE still accounted for 77, 73 and 83% of the variability in observed NEE for the other periods, 2012, 2013 and 2015 respectively. Nocturnal TER led to greater variability and overestimation of observed NEE at low-light for the 2012, 2013 and 2015 crops.

Figure 3.12 shows the peak two week light response for each crop, with  $\alpha$  ranging from  $0.07 \pm 0.03$  to  $0.09 \pm 0.02 \mu\text{mol CO}_2 \mu\text{mol photons}^{-1}$ . Despite similar  $\alpha$  values, the fitted values of  $\text{GPP}_{\text{opt}}$  for these peak periods all differed significantly (Table 3.4). The leek crop peak  $\text{GPP}_{\text{opt}}$  was the lowest with  $14.4 \pm 1.01$  and the celery crop was double that with  $31.74 \pm 1.57 \mu\text{mol CO}_2 \text{m}^{-2} \text{s}^{-1}$ . The two lettuce crops differed by roughly 8-10  $\mu\text{mol CO}_2 \text{m}^{-2} \text{s}^{-1}$  with the 2012 crop  $\text{GPP}_{\text{opt}}$  similar to that of the leek crop and the 2014 crop similar to that of the celery crop which could well be due to the difference in time of year that these two lettuce crops were grown.

The R term followed the same pattern as the  $\text{GPP}_{\text{opt}}$  with values ranging from  $6.33 \pm 0.59 \mu\text{mol CO}_2 \text{m}^{-2} \text{s}^{-1}$  for the leek crop and  $13.64 \pm 1 \mu\text{mol CO}_2 \text{m}^{-2} \text{s}^{-1}$  for the celery.

**Table 3.4:** Fitted variables for each complete crop period and the peak two weeks of light use efficiency of each crop. A is the quantum yield,  $GPP_{opt}$  is GPP at the optimum light level ( $2000 \mu\text{mol m}^{-2} \text{s}^{-1}$ ), and R the respiration.  $r^2$  is how well the modelled values explain variability in the observed values (coefficient of determination). n—is the number of available values during each fitted period. The standard error of the fitted variable is provided in parenthesis (s.e.).

Crop/Weed	All					Peak						
	$\alpha$	$GPP_{opt}$	R	n	$r^2$	Start date	Finish date	$\alpha$	$GPP_{opt}$	R	n	$r^2$
<b>Lettuce 2012</b>	0.03 (0.01)	15.19 (1.08)	5.26 (0.48)	1347	0.49	23/07/2012	06/08/2012	0.08 (0.02)	19.32 (1.16)	7.52 (0.73)	417	0.76
<b>Leek 2013</b>	0.05 (0.01)	8.84 (0.37)	5.70 (0.22)	4672	0.38	21/09/2013	04/10/2013	0.09 (0.03)	14.4 (1.04)	6.33 (0.59)	372	0.73
<b>Lettuce 2014</b>	0.03 (0.011)	15.22 (1.38)	5.61 (0.96)	799	0.42	13/06/2014	26/06/2014	0.07 (0.03)	27.86 (2.44)	8.16 (2.29)	113	0.85
<b>Celery 2015</b>	0.04 (0.01)	18.02 (0.82)	7.61 (0.45)	2242	0.55	03/07/2015	16/07/2015	0.09 (0.02)	31.74 (1.57)	13.64 (1)	384	0.83
<b>September 2014 weeds</b>	0.07 (0.03)	13.93 (1.26)	7.93 (0.7)	365	0.64	-	-	-	-	-	-	-
<b>October 2015 weeds</b>	0.08 (0.02)	18.95 (1.48)	6.47 (0.49)	351	0.8	-	-	-	-	-	-	-



**Figure 3.12:** Light use efficiency of average 30 min values of NEE and PPFDF for the two week peak quantum yield of each crop. Model terms are provided in Table 3.4. Modelled NEE for available values of PPFDF are plotted and the residuals explored for driving effects of soil and air temperature, vapour pressure deficit, water table depth and volumetric soil water content. Residual values were binned based on bin widths of 2  $^{\circ}\text{C}$  for air and soil temperatures, 250 Pa for VPD, 5 cm for WTD and 0.025  $\text{m}^3 \text{ m}^{-3}$  for SWC. Axis scale for WTD and SWC varies between crop, whilst soil and air temperature and VPD scales remain the same across each year.

### *Residuals and limits of light use*

Modelled daytime NEE for each peak two week crop period explained 73-86% of the variability in observed daytime NEE, suggesting a strong fit of the model (Figure 3.12). The residuals of these relationships are presented in Figure 3.12 against potential environmental driving variables and were binned to see trends more clearly. Positive residuals infer that the light use model is overestimating net CO<sub>2</sub> uptake and therefore GPP, conversely, negative residual values result from an underestimation of net CO<sub>2</sub> uptake and GPP. Correlation coefficients for the plots in Figure 3.12, and their significances, are provided in Table 3.5.

**Table 3.5:** Non-parametric Spearman’s rank correlation coefficients ( $r_s - \rho$ ) and their significance (p-value) < 0.001 ‘\*\*\*’, <0.01 ‘\*\*’, <0.05 ‘\*’, <0.1 ‘.’. Environmental variables as drivers of residuals of observed and modelled daytime NEE for peak two weeks of light use.

	Lettuce 2012	Leek 2013	Lettuce 2014	Celery 2015
Tsoil/Residuals	0.33***	0.15**	0.52***	0.31***
Tair/Residuals	0.25***	0.11*	0.41***	0.29***
VPD/Residuals	0.30***	0.17**	0.40***	0.33***
WTD/Residuals	0.33**	0.38***	0.34***	0.11*
SWC/Residuals	0.08 .	-0.09 .	-0.76***	-0.32***

For all three of the plug crops temperature and VPD have a significant but weak positive correlation with residuals. When Tair was greater than ~22 °C and VPD in excess of 1000 Pa the model overestimated CO<sub>2</sub> uptake, which represents a limitation of photosynthesis. This limitation is a response to the increased pressure of VPD, which increases with temperature, leading to a stomatal closure response to prevent excessive water loss by transpiration. The moderate positive correlation in Table 3.5 suggests that the 2014 lettuce crop was the most affected by stomatal closure during peak light use.

The 2014 lettuce crop residuals had significant strong negative correlation with the SWC despite SWC values only ranging from 0.13 to 0.19 m<sup>3</sup> m<sup>-3</sup>, which suggest that at lower available SWC (<0.15 m<sup>3</sup> m<sup>-3</sup>) in the upper soil surface CO<sub>2</sub> uptake was overestimated. A similarly confined range of values (0.09 to 0.14 m<sup>3</sup> m<sup>-3</sup>) for SWC was measured during the celery crop peak but was only weakly negatively correlated. During the peak lettuce crop period of 2012 the SWC experienced a much greater range of (more saturated) values than the 2014 crop (0.38 to 0.6 m<sup>3</sup> m<sup>-3</sup>) which has an

overestimation of CO<sub>2</sub> uptake when SWC is in excess of 0.5 m<sup>3</sup> m<sup>-3</sup>. The lettuce 2014 period had the fewest available values, however it had significant relationships with all of the variables and was best modelled by light response (Table 3.4 and 3.5).

### *Weeds*

Significant diurnal uptake of CO<sub>2</sub> was evident outside of crop growing periods, during September of 2014 and October of 2015 (Figure 3.1 and 3.10). These corresponded with a secondary weed cover that developed on the field in these two years. Light use was modelled for these two months to compare weed assimilation with that of the crops.

The two significant weed development periods had an  $\alpha$  value at the lower end of those reported for peak crop light use,  $0.07 \pm 0.03$  and  $0.08 \pm 0.02$   $\mu\text{mol CO}_2 \mu\text{mol photons}^{-1}$  for September 2014 and October 2015, respectively (Table 3.4).  $\text{GPP}_{\text{opt}}$  was  $13.93 \pm 1.26$  and  $18.95 \pm 1.48$   $\mu\text{mol m}^{-2} \text{s}^{-1}$  which again were towards the lower end of those calculated for lettuce in 2012 and leek in 2013. Both weed periods were well modelled by light response and had significant weak and moderate positive temperature correlations with daytime NEE residuals, but no significant correlations with VPD, WTD or SWC.

### 3.5 Discussion

#### 3.5.1 Drivers of NEE

Sensitivity of TER to Tsoil explained 70% of the variability in observed nocturnal NEE for the intensively managed agricultural fen peat soil under investigation in this study, and had a basal respiration of  $3.19 \pm 0.07 \mu\text{mol CO}_2 \text{ m}^{-2} \text{ s}^{-1}$ . Temperature (use of Tair/Tsoil depends on sites) sensitivity has been identified in previous research on drained peat soils as the key or primary driver of CO<sub>2</sub> exchange with the atmosphere (Kirschbaum, 1995, Nieveen et al., 2005, Lafleur et al., 2005, Parmentier et al., 2009, Shurpali et al., 2009, Elsgaard et al., 2012, Taft et al., 2017). Notably, Taft et al. (2017) found that Tsoil was the “best” predictor of CO<sub>2</sub> emission for the same agricultural peat soil in East Anglia that was studied here.

Variability in observed NEE here was best explained by the Tsoil sensitivity of the modelled TER during the fallow periods, 71%, with no significance between residuals of the modelled TER and WTD or SWC. However, for the combined crop periods only 43% of the variability was explained, suggesting a less significant Tsoil sensitivity of TER (Figure 3.4b, c and Table 3.2), while SWC had a weak negative correlation with the residuals. Peat soils drained for use as cropland in three regions (defined as North, East and West) of Denmark (Elsgaard et al., 2012) reported a range of 29–61% for this relationship. The variation between these sites is attributed to differences in environmental conditions at each location and crop type, whereby potato crops had a poor explanation of variability in temperature response and barley and grasses much better. Crop type here showed similar variability from 31–69% of variability in observed NEE explained by the temperature response model, no pattern in crop type could be established here.

Tsoil sensitivity of TER has been demonstrated for a site drained for pasture to explain as much as 93% of variability in nocturnal TER at a temperate peat bog (Nieveen et al., 2005). Nieveen et al. (2005) binned their 30 minute nocturnal data into 1 °C temperature classes, which improved the variability explained by the temperature response model, however the same method did not result in improved fitting of the model when applied to the data in this thesis likely due to the significant shifts in soil surface conditions under management, compared to the pasture managed site. Similarly, Parmentier et al. (2009) demonstrated that for a semi-natural grassland on temperate

peat soil (that was previously agriculturally managed) in the Netherlands, that NEE of CO<sub>2</sub> is heavily dependent on T<sub>soil</sub> with modelled respiration explaining 66% of variability in observed NEE, with no additional residual bias influenced by WTD, as was the case for all years presented here.

Water table has been established as a key parameter controlling peat formation in natural peatlands. It is also well known that drainage of peatlands results in increased oxidation and mineralisation. However, it is less well understood how CO<sub>2</sub> fluxes are affected by a fluctuating water table in a managed drained peat soil (Tiemeyer et al., 2016). The ongoing assumption is that the higher the WTD the less oxidation and therefore the less C loss as CO<sub>2</sub>, but higher potential for CH<sub>4</sub> losses. Studies by Oechel et al. (1998), Lloyd (2006), Musarika et al. (2017), Poyda et al. (2016), Taft et al. (2017), Leifeld et al. (2011) have all reported WTD to be a key driving force behind CO<sub>2</sub> emissions from managed peat soils.

Although there was a lack of WTD correlation to modelled TER residuals in the data presented here there was a large increase in underestimation of modelled TER when WTD was between -0.55 and -0.7 m. A comparison of all observed nocturnal NEE values as a function of WTD (Figure 3.8a) also highlighted this anomaly. Poyda et al. (2016) found a significant negative correlation between WTD and annual NEE of four lowland peat soils under different land uses in northern Germany. Unutilised and wet grasslands were shown to have a shallower mean annual WTD (>-0.3 m) and lower annual net CO<sub>2</sub> losses, while moist grasslands and an arable site (growing spring barley in the first year then spring wheat and grasses in the second) had deeper mean WTD (< -0.3 m) and greater net CO<sub>2</sub> losses. WTD was suggested by Poyda et al. (2016) to increase NEE by 22 g C-CO<sub>2</sub> m<sup>-2</sup> yr<sup>-1</sup> for every 1 cm increase in depth from the surface, across all four land use types. Focusing on just the arable site, the spring barley year reported 2 t C-CO<sub>2</sub> m<sup>-2</sup> yr<sup>-1</sup> less emission than the spring wheat crop that followed, which could be attributed to the increased rainfall received for the spring barley crop of 150 mm over the year, a 0.2 m shallower mean WTD, or simply the difference in crop types at the German site. In my study when WTD rose from -0.96 to -0.62 m (Figure 3.9) over a 15 day period as a result of increased rainfall (Figure 3.9) this resulted in a short-term reduction in CO<sub>2</sub> loss which had a significant strong positive correlation suggesting that a rain fed rise in WTD was a greater influence on NEE during this

period over decreasing  $T_{\text{soil}}$ . But no increase in loss due to increased depth was evident and likely reflects the ability of peat of this site to retain moisture and thus inhibit increased loss.

A controlled environment study undertaken by Musarika et al. (2017) on peat soil cores, extracted from the same farm investigated here, manipulated WTD to -0.3 and -0.5 m for both bare soil cores and cores growing radish (*Raphanus sativus*). They measured a reduced TER for both bare peat soil cores and radish growing cores with a WTD of -0.3 m, compared to those with a WTD of -0.5 m. The two lettuce crop periods in this thesis allowed for a field based comparison of two crops but under different environmental conditions and limited availability of the 2016 crop data. Results of the  $T_{\text{soil}}$  model of TER suggest that the 2014 lettuce crop had a deeper mean WTD of -0.95 m, greater  $R_{10}$  of  $3.61 \pm 0.49 \mu\text{mol CO}_2 \text{ m}^{-2} \text{ s}^{-1}$  and required less  $E_0$   $214.63 \pm 72.84 \text{ K}$  than the 2012 crop with a shallower WTD of -0.62 m, reduced  $R_{10}$  of  $1.38 \pm 0.47 \mu\text{mol CO}_2 \text{ m}^{-2} \text{ s}^{-1}$  and increased  $E_0$  requirement of  $664.39 \pm 158 \text{ K}$ , demonstrating a lower sensitivity to  $T_{\text{soil}}$ . This corroborates the findings of Musarika et al. (2017) that a lower mean depth of WTD for the same crop in different years will result in reduced net  $\text{CO}_2$  loss, although findings are based on a limited number of available nights (8) for the 2014 crop. The 2012 lettuce also had a higher average SWC of  $0.59 \text{ m}^3 \text{ m}^{-3}$  compared to  $0.3 \text{ m}^3 \text{ m}^{-3}$  in 2014 (measured at a depth of -0.05 m), which explained some of the night-to-night variation seen in the observed NEE of 2012 (Figure 3.5). SWC was measured but not reported by Musarika et al. (2017), but if the core WTDs were controlled from the bottom up, it is possible that the SWC would not have increased as it would if it were rain fed. SWC retention at depths of WTD above -0.5 m have been shown to impact TER (Nieveen et al., 2005, Lloyd, 2006, Parmentier et al., 2009), and so could alter the significance of these findings if they varied between cores.

SWC here had a significant but weak negative correlation to the residuals, suggesting that during the crop periods  $\text{CO}_2$  loss increased at low SWC values and was reduced at higher SWC. Additionally, NEE as a function of SWC for all available nights (Figure 3.8b) found an increase in NEE with decreasing SWC and vice versa. A clearer relationship was identified by Lloyd (2006) for the restored grassland of Tadham Moor in the Somerset levels, UK (previously farmed soil) where, as the WTD deepened from above the surface to -0.7 m, SWC was retained at more than  $0.5 \text{ m}^3 \text{ m}^{-3}$  by the peat soil which buffered the  $T_{\text{soil}}$  sensitivity of TER (measured at a depth of 0.1 m), making

WTD the key driver of nocturnal TER. Lloyd (2006) additionally identified a negative correlation of  $R_{10}$  as a function of WTD, whereby a deepening of WTD by 0.1 m results in an increased  $R_{10}$  of  $0.5 \mu\text{mol CO}_2 \text{ m}^{-2} \text{ s}^{-1}$ . Figure 3.6a shows a similar but not significant trend for the data in this study. As the water level here was never shallower than 0.38 m, unlike at Tadham Moor, the upper soil profile (which additionally was regularly disturbed and vegetation free) was never as saturated enough to retain significant moisture and for a similar response to be measured, which was highlighted by the 22 day period of managed WTD lowering where retention of SWC was not seen in this study (Figure 3.9). Instead SWC fluctuated with rainfall before lowering in combination with WTD lowering and temperature increase.

A comparison of nocturnally averaged values here also demonstrated that SWC was not a function of WTD. Ultimately, the lettuce crop of 2012 was the only period in this study when SWC was found to be a limiting factor of TER (Figure 3.5; Table 3.2). However, these were the highest recorded values of SWC for the whole dataset, and were recorded during the two months immediately following installation of the instrumentation. It is unknown whether the data reflect an adjustment of the instrumentation or soil conditions (recently ploughed).

The strong relationship of NEE with  $T_{\text{soil}}$  and lack of clear dependence or influence of WTD and SWC identified at this cultivated lowland peat, was similarly demonstrated by Parmentier et al. (2009) who studied a peat excavation site in the Netherlands that was converted to a managed wetland. They attributed the lack of dependence on WTD to the relatively smaller variation in SWC (compared to that of Lloyd (2006) at Tadham Moor), which over a drop from -0.2 to -0.45 m in WTD retained a significant volume of water (only reduced from  $0.9$  to  $0.7 \text{ m}^3 \text{ m}^{-3}$ ). Similarly, Nieveen et al. (2005) identify a significant retention of SWC at  $0.65 \text{ m}^3 \text{ m}^{-3}$  until WTD dropped below -0.5 m for a grazed peatland in New Zealand, where once WTD dropped below this depth SWC (measured at 0.05 m) also reduced significantly. However, for the Mer Bleue temperate peat bog in Canada Lafleur et al. (2005) measured better retention of SWC at depths of -0.5 m compared to SWC retention measured at -0.28 m which reduced to  $0.2 \text{ m}^3 \text{ m}^{-3}$  before stabilising, for a more similar range of WTD (-0.30 to -0.75 m) to that measured here. These papers suggest that a deeper WTD results in a larger range of SWC which was certainly the finding of the measurements made at this cultivated peat soil.

However, these potential drivers were not identified as greater controls on TER than  $T_{soil}$ .

Limited  $T_{soil}$  response during crop growing periods here were shown to respond to the  $R_a$  contribution to TER and identified as having a significant relationship with residuals of modelled nocturnal TER (Figure 3.7). This contribution is characterised here using the daytime NEE which is dominated by GPP during crop periods, and daytime  $CO_2$  uptake is shown to increase nocturnal TER (Figure 3.7).  $CO_2$  uptake was greatest for days of  $T_{soil}$  between 15 and 25 °C, this was the same range over which the temperature response of TER was least well explained during the crop periods (Figure 3.8). Similarly, root respiration was calculated to be contributing 35-45% of TER during summer months of a mesocosm study on drained fen peat soil by Silvola et al. (1996). Taft et al. (2017), using the closed chamber technique, reported that microbial activity accounted for 58-96% of TER annually (at the same study site used here) across a range of soil organic carbon content (SOC). The most similar SOC to the field studied here using the EC technique reported a microbial contribution of 92% to TER over a full year across a range of locations and crops (Taft et al., 2017). This suggests that although the impact of  $R_a$  on TER was notable during the crop periods, over a complete year it is minimal compared to the  $R_h$  contribution. Management of the site studied here meant that the field surface experienced periods with bare soil making a sole contribution of  $R_h$  to TER, and a period with a fully developed crop contributing additional  $R_a$ , both under similar  $T_{soil}$  conditions which complicated the  $T_{soil}$  response during crop periods. The  $R_a$  influence on nocturnal NEE means that crop type and environmental controls on GPP also influence nocturnal TER during crop periods.

The daytime NEE data presented here were modelled well as a function of PPFD with residuals of the relationship of peak light use notably limited by high temperature and VPD that caused stomatal closure, which particularly impacted peak crop growth of the lettuce crops. Shurpali et al. (2009) conducted a study of a boreal organic soil in Finland that was utilised for growth of the bioenergy crop reed canary grass (RCG; *Phalaris arundinacea*). They identified a relationship between GPP and TER whereby GPP accounted for as much as 70% of variability in TER during drier conditions. This is a much greater influence of crop growth on TER than measured here. They attribute this to the decreased SWC, shallow rooting of RCG (95% of roots in top 0.15 m of soil) and higher VPD during the daytime in dry years. As a response to water limitations they

suggest that the RCG closes its stomata to reduce transpiration which consequently reduces CO<sub>2</sub> uptake by the crop. In my study, the modelled daytime light use of the celery crop had the greatest GPP<sub>max</sub> suggesting that it would have the greatest Ra contribution to nocturnal TER and was not limited by VPD. This appears to be the case as the increased underestimation of TER for the crop periods (Figure 3.4b) by the model was noted as being most evident during the celery crop period (Figure 3.5).

### **3.6 Chapter summary**

This data chapter has presented the results of investigating the drivers of NEE at an intensively cultivated temperate lowland deep peat soil. An empirical Arrhenius (temperature response) model was used to investigate the sensitivity of  $T_{\text{soil}}$  as a key driving environmental variable influencing nocturnal NEE (TER) of four crops (lettuce, leek, lettuce and celery) and their subsequent fallow periods at an intensively farmed peat soil in East Anglia, UK over 3.5 years. Residuals of the observed and modelled TER were investigated with respect to the influence of WTD, SWC and  $R_a$  as additional driving variables. In order to further assess the influence of WTD and SWC on nocturnal NEE, modelled basal respiration rates at 10 °C were investigated for their correlation with these variables. The short term (two week) responses of NEE to individual WTD raising and dropping events during a fallow period were assessed. Finally, light response of NEE was modelled using a Michaelis-Menten type model for complete crop periods and peak two week light response periods and the residuals of the peak periods were reported.

## **Chapter 4: Multi-annual CO<sub>2</sub> flux over 3.5 years at an intensively cultivated drained lowland deep peat soil**

This chapter addresses research questions 2 and 3 from Chapter 1.4:

1. What are the daily, seasonal (crop/fallow) and annual magnitudes of NEE from drained intensively cultivated lowland peat soil, under varying crop management?
2. What contribution do planting and harvest of different crops have on the C balance of an intensively cultivated peat soil?

The first multi-annual NEE of CO<sub>2</sub> measured by the EC technique for an intensively managed agricultural peatland is reported and the full 3.5 years of EC data over four consecutive crop cycles of lettuce, leek, lettuce and celery are presented and each crop is compared.

The reliability of the dataset is addressed through an assessment of the energy balance closure (EBC) and the uncertainty of the NEE fluxes which is calculated based on flux calculation and gap-filling restrictions described in Chapter 2. Energy balance closure is assessed using the two techniques, described in Chapter 2.2.9. The first calculates linear regression coefficients of the relationship between turbulent heat fluxes of energy and available energy, and the second calculates a ratio of summed energy over different temporal scales. These techniques are applied to all available quality controlled (but not gap filled) data on three temporal scales: each consecutive crop and fallow episode - delineated by the first day of planting and the last day of harvesting for each crop, annually - based on a calendar year (1<sup>st</sup> Jan – 31<sup>st</sup> Dec), and the complete data period, from 22<sup>nd</sup> Jun 2012 – 31<sup>st</sup> Dec 2015.

Net ecosystem exchange is reported on daily, crop and fallow period, and annual timescales. Additional annual calculations are made for the import and export of C with organic materials due to planting and harvesting of each crop as a step towards calculation of a fuller NECB. These values are compared within the context of the literature averaged to calculate the emissions factor figure of  $790 \pm 150 \text{ g C-CO}_2 \text{ m}^{-2} \text{ yr}^{-1}$  for drained temperate cropland on peat soil provided by the IPCC wetland supplement (IPCC, 2014), and other relevant literature published since.

All fluxes of NEE are presented in  $\text{g C-CO}_2 \text{ m}^{-2}$ . Values in the literature have been converted for consistency;  $100 \text{ g C-CO}_2 \text{ m}^{-2}$  is equivalent to  $1 \text{ t C-CO}_2 \text{ ha}^{-1}$  or  $366.44 \text{ g CO}_2 \text{ m}^{-2}$ .

#### **4.1 EBC**

Over the complete 3.5 years reported in this study, the EBC was 89% (Figure 4.1a). For the fallow and cultivation periods EBC values were 86 and 89%, respectively (Figure 4.1b and c) and with values for each year (2012 to 2015) of 91, 89, 88, and 87% respectively. These high closure values were similarly reflected in the calculated energy balance ratio (EBR) values of 0.93, 0.87, 0.9 and 0.9 for the same years (Table 4.1). However, over the complete dataset heat energy fluxes were underestimated or the available energy was overestimated; this was more pronounced at higher energy levels ( $>200 \text{ W m}^{-2}$ , Figure 4.1a, b and c). Available energy was a good explanatory variable of 94, 93 and 93% of energy fluxes for the full years of measurements, 2013-2015. The half a year of energy flux in 2012 was less well explained by the measured energy (90%) despite having a better EBC slope and EBR (Table 4.1).

Despite the combined crop periods having a slope value closer to 1 than that for the fallow periods, the intercept value was  $4 \text{ W m}^{-2}$  compared to the ideal value of  $0 \text{ W m}^{-2}$  recorded for the complete set of fallow measurements. No significant pattern of EBC slope and intercept or EBR relating to crop and fallow periods was identified. Generally, slope and intercept values reflected an underestimation of energy fluxes when available energy was high, and a slight overestimation at lower available energy (particularly during the fallow periods).

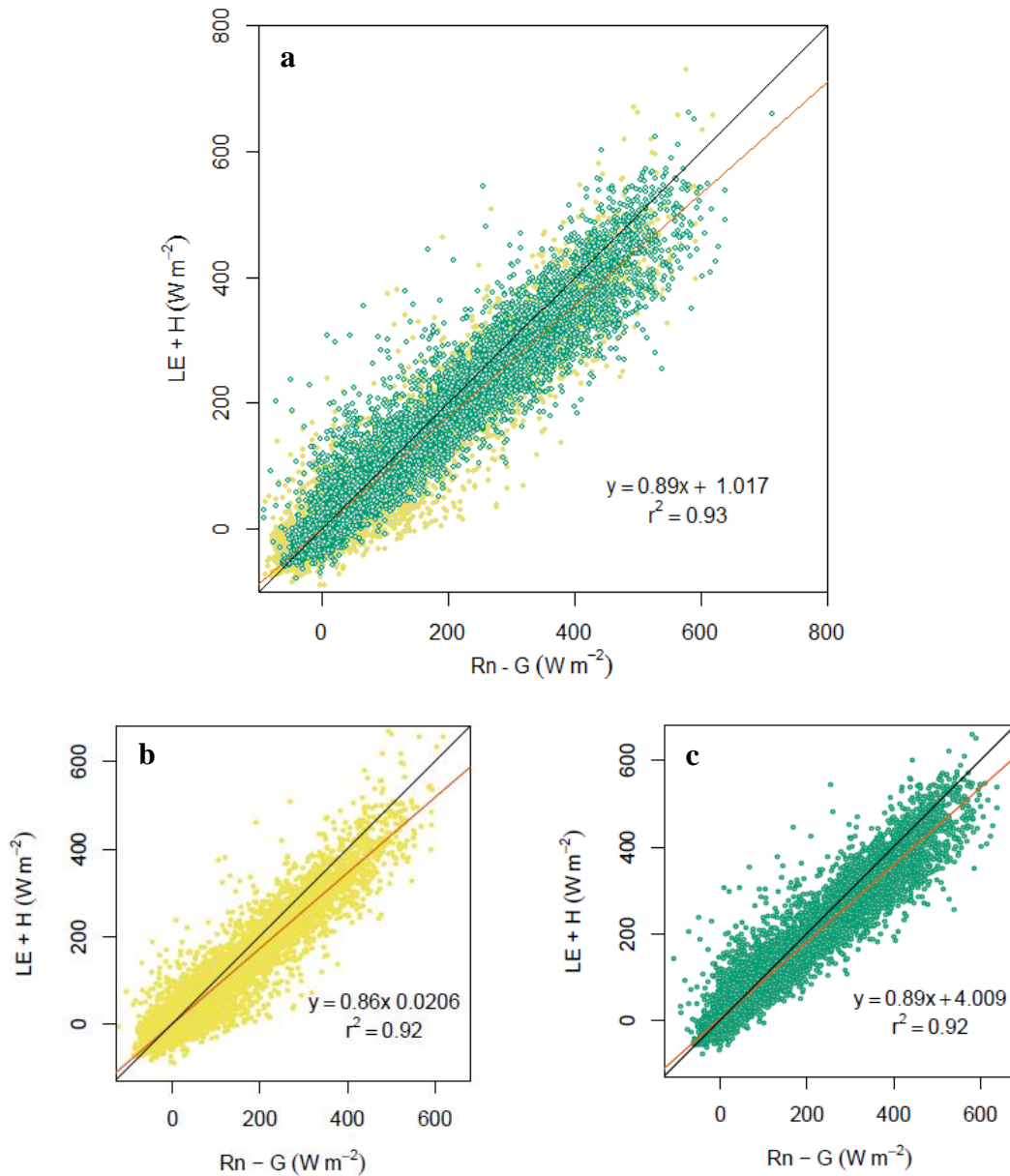


**Figure 4.1:** Energy balance closure plots. Quality controlled half-hourly values of net radiation (Rn), soil heat flux (G), latent heat (LE) and sensible heat (H), all in  $\text{W m}^{-2}$ . **a.** All available data. **b.** Fallow periods. **c.** Crop growth periods. Yellow points are for fallow periods, and green are those for the crop periods.

Nocturnal EBC was the least well closed with a slope of 0.47 and an intercept of -10.43 for all available half-hourly values (Table 4.1); however, this produced the best figure for EBR. The nocturnal energy balance was further investigated for the influence of poor turbulent exchange on fluxes by comparing the influence of  $u^*$  on nocturnal EBC slope, despite a  $u^*$  filter having been applied during quality control of fluxes (Chapter 2.2.4).

Friction velocity values were partitioned into five subgroups across the full range of available values from 0.01 to 1.88 m s<sup>-1</sup>, with a median of 0.25 m s<sup>-1</sup>. For all available daytime half-hourly energy fluxes, the EBC slope reduced to 0.6-0.77 for 0.01 m s<sup>-1</sup> <  $u^*$  < 0.2 m s<sup>-1</sup>, and 0.84-0.9 for all values with a  $u^*$  > 0.2 m s<sup>-1</sup>. However, nocturnal slope values were reduced to 0.17-0.39 for 0.01 m s<sup>-1</sup> <  $u^*$  < 0.2 m s<sup>-1</sup>, and 0.62 to 0.75 for  $u^*$  > 0.2 m s<sup>-1</sup>. This increase in imbalance presented by the reduction in slope at low  $u^*$  reflects poor turbulent mixing, particularly during the night, and a potential for the drainage or advection of fluxes during the night despite the homogenous nature of the site. Due to the uniformity of the site studied here, loss due to drainage and advection would be expected to be minimal and any lack of closure to be resolved by integrating the flux over a diurnal cycle.

**Table 4.1:** Ordinary linear regression OLR coefficients and energy balance ratio (EBR) values (as no soil instruments were installed until the 26<sup>th</sup> June 2012, it was not possible to calculate EBC for the first period).

Date (Period)	Slope	Intercept	R <sup>2</sup>	EBR	n
22 – 26/06/12 (1)	-	-	-	-	0
26/06 – 13/08/12 (2)	0.91	13.55	0.86	1.01	1310
13/08/12 – 12/04/13 (3)	0.87	-2.62	0.91	0.82	4487
12/04 – 19/10/13 (4)	0.89	1.31	0.93	0.90	4428
19/10/13 – 22/04/14 (5)	0.92	-2.66	0.93	0.82	3803
22/04 – 28/06/14 (6)	0.86	9.75	0.89	0.91	881
28/06/14 – 12/05/15 (7)	0.85	3.59	0.92	0.89	6579
12/05 – 12/08/15 (8)	0.89	1.90	0.93	0.90	2231
12/08/15 – 01/01/16 (9)	0.94	0.31	0.94	0.95	2996
2012	0.91	1.07	0.90	0.93	4736
2013	0.89	-1.91	0.94	0.87	6998
2014	0.88	1.80	0.93	0.90	6965
2015	0.87	2.39	0.93	0.90	8015
22/06/12 – 01/01/16 (Day)	0.87	5.43	0.90	0.91	15462
22/06/12 – 01/01/16 (Night)	0.47	-10.43	0.36	1.00	11253
All Fallow (Periods 1, 3, 5, 7, 9)	0.86	0.02	0.92	0.87	17865
All Crop (Periods 2, 4, 6, 8)	0.89	4.01	0.92	0.92	8850
ALL	0.89	1.02	0.93	0.90	26715

Daily values of available and measured energy fluxes were therefore integrated for days with a threshold of 70% available half-hourly terms (Figure 4.2). Evaluating daily values commonly leads to an improvement in EBC, as it reduces errors associated with storage terms (Leuning et al., 2012, Wilson et al., 2002). Slope of the linear regression for daily fluxes improved the closure for the combined crop and fallow periods to 0.92 and 0.94 respectively, whilst the intercept term reduced and became negative for the combined fallow ( $-1.66 \text{ W m}^{-2}$ ) and increased slightly for the crop periods, but still remained close to zero ( $0.29 \text{ W m}^{-2}$ ). Closure for the complete dataset was 0.94, whilst the intercept term (as with the intercept term for the crop period) became negative, at  $-1.53 \text{ W m}^{-2}$ . This reflects a decrease in the underestimation of energy flux at higher levels of available energy.

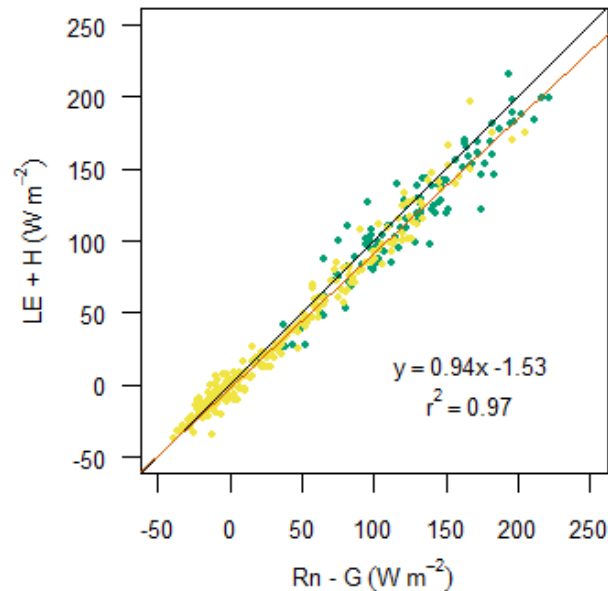


**Figure 4.2:** Daily EBC plot, using net radiation (Rn), soil heat flux (G), latent heat (LE) and sensible heat (H), all in  $\text{W m}^{-2}$ . Only days with 70% of the half hourly values available were used ( $n_{\text{all}} = 349$ ,  $n_{\text{crop}} = 114$ ,  $n_{\text{fallow}} = 235$ ). Yellow points are days during the fallow periods, and green are those during the crop periods.

## 4.2 NEE

### 4.2.1 Daily NEE (GPP and TER)

The patterns of daily NEE, GPP and TER within years and between years are reported in relation to Figure 4.3. First the daily fluxes are considered in terms of their pattern and contribution to each crop and fallow period, followed by a comparison of the contribution of the crop and fallow periods to each year and an account of the annual flux.

#### *Crop periods*

The three crops planted as plugs, lettuce (2012 and 2014) and celery (2015), had a similar pattern of daily NEE, but were grown over 48, 66 and 91 days respectively. After ploughing and for 2-3 weeks after planting, the site acted as a consistent net average source of between 3-5 g C-CO<sub>2</sub> m<sup>-2</sup> d<sup>-1</sup> (Figure 4.3) due to increased aeration of the upper soil profile. As there was no established crop present on the field at these times, the partitioned GPP values represent the imperfect temperature based partitioning of NEE and the TER is expected to be fully heterotrophic in nature. The source of this C-CO<sub>2</sub> is therefore the decomposition of organic material from either the previous year's crop litter and weeds or the parent peat. In 2012 this resulted in the greatest daily loss of C-CO<sub>2</sub> recorded that year.

Once the plugs were planted the magnitude of net daily CO<sub>2</sub> losses reduced as GPP increased to outweigh TER which also increased due to the addition of autotrophic respiration and warming T<sub>soil</sub>. With GPP continuing to increase at a greater rate than TER all three crops became daily net sinks of CO<sub>2</sub> for 2-3 weeks (Figure 4.3) experiencing maximum daily net uptake values of CO<sub>2</sub> during the crop growing phases of  $-4.87 \pm 0.32$ ,  $-6.27 \pm 0.4$  and  $-4.24 \pm 0.46$  g C-CO<sub>2</sub> m<sup>-2</sup> d<sup>-1</sup> for 2012, 2014 and 2015, respectively (Table 4.2). Maximum CO<sub>2</sub> uptake coincided with days of high GPP values of 14.21, 14.52 and 18.08 g C-CO<sub>2</sub> m<sup>-2</sup> d<sup>-1</sup>, for 2012, 2014 and 2015 respectively, when TER was slightly reduced from its maximum values of 10.01, 10.97 and 16.4 g C-CO<sub>2</sub> m<sup>-2</sup> d<sup>-1</sup> for the same periods.

The lettuce crop of 2012 was harvested during peak GPP and net uptake, whilst the lettuce of 2014 and the celery of 2015 had both begun to see reduced GPP values and consequential reduction in net daily uptake, before they were harvested. During the later periods of crop growth, and particularly for the celery crop (Figure 4.3), the site

returned to being a net daily source following persistent precipitation and reduced  $R_g$ . These days of net loss were also marked by a reduction in GPP but a maintained level of TER. Altogether the site was a net daily sink of  $\text{CO}_2$  for 20, 26 and 31 days for each of the plug crops, in 2012, 2014 and 2015, respectively.

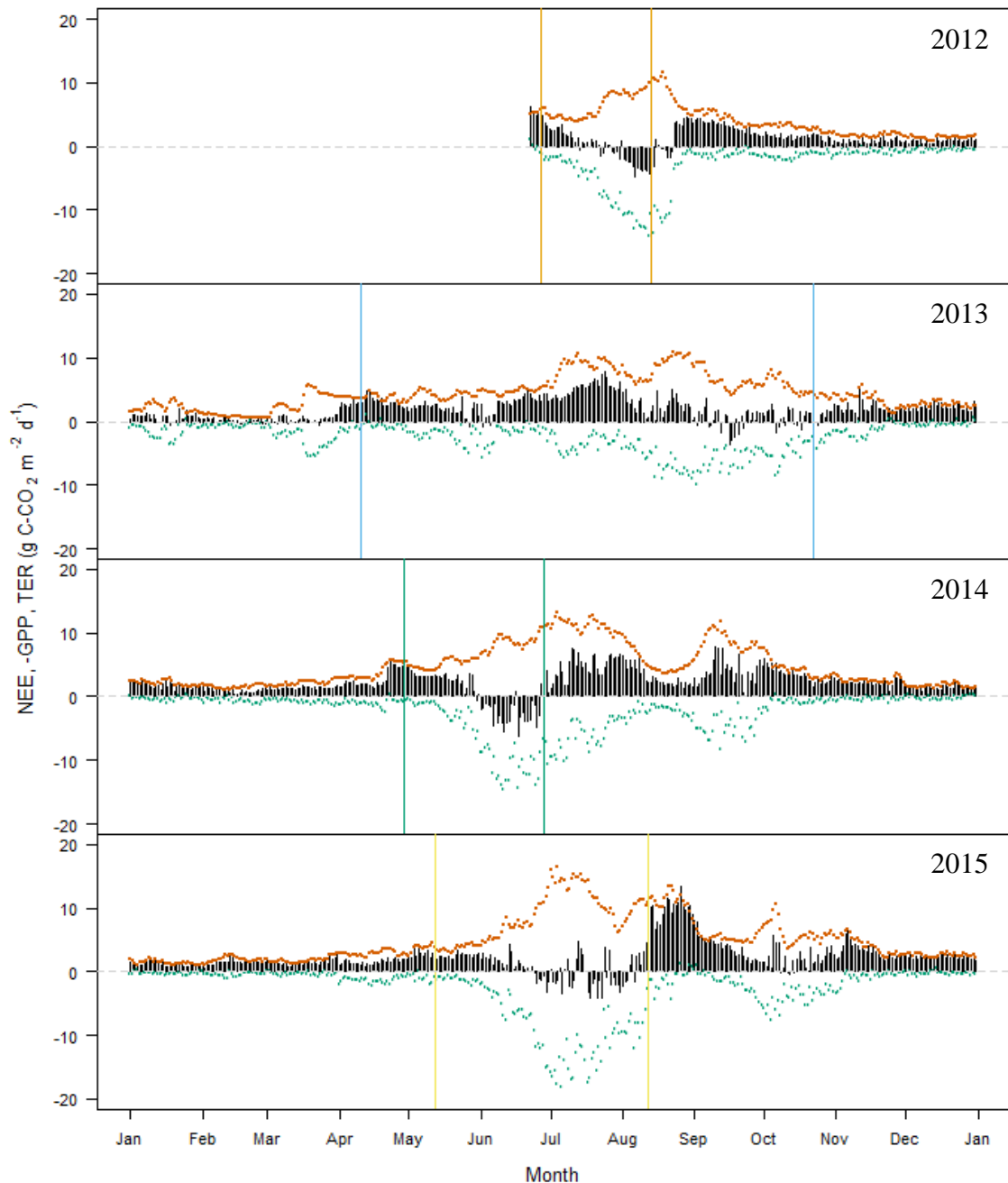


**Figure 4.3:** Daily NEE, GPP and TER. Black bars are daily NEE, green points are GPP and red points TER. Vertical lines represent first day of planting and last day of harvest for each crop. Colours correspond to crop: orange - 2012 lettuce crop, light blue - 2013 leek, dark green - 2014 lettuce, and yellow - 2015 celery. GPP is plotted as a negative for ease of plot interpretation.

By contrast with the plug crops, the 2013 direct-sown leek crop was managed over a much longer portion of the thermal growing season (189 days, more than double that of the celery crop) but showed only a comparable 19 days when it operated as a net daily sink. The leek was drilled with a cover crop of barley which led to a steady increase in GPP and a resultant gentle reduction in net daily losses of CO<sub>2</sub> after planting in early spring (Figure 4.3).

Before the field could become a net daily sink in spring 2013 it was sprayed with selective chemicals (see Table 2.1 and S2.1) to prevent further growth of the barley and allow for the leek to grow through without competition. The response of the system to this management treatment was a reduction in daily GPP and continued behaviour as a net daily source of CO<sub>2</sub>, until the leek crop became more established. During this early leek development phase, TER increased at a faster rate than the growing GPP, additionally GPP became more limited during July leading to the largest net daily loss of CO<sub>2</sub> recorded for 2013 at  $7.82 \pm 0.31 \text{ g C-CO}_2 \text{ m}^{-2} \text{ d}^{-1}$ .

July 2013 marked the maximum average daily recorded values of R<sub>g</sub>, T<sub>air</sub> and T<sub>soil</sub> for that year and the complete dataset (Figure 4.4b, e and f). It is evident in Figures 4.4c and 4.4d that the average diurnal LE and H reduced and increased, respectively, during July 2013 whilst GPP had been increasing during late June (Figure 4.3) which likely indicates a reduction or limitation of the leek crop to photosynthesise in response to peak radiation and temperature, demonstrating that the increase in emission was not only due to higher temperatures causing increased microbial activity and loss of CO<sub>2</sub> but was also exacerbated by a reduction in photosynthesis (and therefore CO<sub>2</sub> uptake). An additional likely contributing factor to the higher C-CO<sub>2</sub> loss was the availability of labile plant residues on the peat surface from the recent herbicide treatment of the barley cover crop.

Development of the leek crop eventually led to increased GPP, and combined with a drop in TER, this resulted in several days of net uptake of CO<sub>2</sub> during September and October for which the maximum uptake was  $-3.73 \pm 0.43 \text{ g C-CO}_2 \text{ m}^{-2} \text{ d}^{-1}$  (Table 4.2). On average the site was a net daily source of CO<sub>2</sub> during all crop growing periods experiencing a loss of  $0.06 - 0.7 \text{ g C-CO}_2 \text{ m}^{-2} \text{ d}^{-1}$  (Table 4.2) for the plug crops whilst the leek crop averaged  $2.42 \text{ g C-CO}_2 \text{ m}^{-2} \text{ d}^{-1}$  which was comparable to the average for the fallow periods ( $2.18 \text{ g C-CO}_2 \text{ m}^{-2} \text{ d}^{-1}$ ; Table 4.2). Average GPP and TER were

similar for each plug crop, whilst average TER was almost double the GPP, 6.11 to 3.7 g C-CO<sub>2</sub> m<sup>-2</sup> d<sup>-1</sup>, respectively, for the leek crop period, and was more than double the average TER for the fallow days of 2013.

**Table 4.2:** Maximum, minimum and average daily fluxes of NEE, TER and GPP in g C-CO<sub>2</sub> m<sup>-2</sup> d<sup>-1</sup>. Quality controlled and gap filled data is used. Negative minimum values of NEE reflect maximum uptake of CO<sub>2</sub>, and maximum positive values a loss to the atmosphere; ± is the associated uncertainty for the maximum and minimum daily values. TER and GPP were calculated using partitioned gap-filled NEE using the Lloyd & Taylor (1994) equation, and should all be positive. Negative values result from physically implausible minimum GPP values which have been omitted as an artefact of partitioning.

Year		GPP		TER		NEE	
		Crop	Fallow	Crop	Fallow	Crop (±)	Fallow (±)
2012	Max	14.21	13.58	10.01	11.56	4.81 (0.12)	6.24 (0.23)
	Mean	6.24	1.80	6.30	3.33	0.06	1.64
	Min	1.04	0.06	3.91	0.87	-4.87 (0.32)	-3.03 (0.32)
2013	Max	9.97	5.59	10.97	5.71	7.82 (0.31)	5.22 (0.62)
	Mean	3.70	1.42	6.11	2.63	2.42	1.20
	Min	-	-	2.70	0.56	-3.73 (0.43)	-0.63 (0.16)
2014	Max	14.51	10.72	10.81	13.09	4.69 (0.16)	7.89 (0.72)
	Mean	6.22	1.82	6.61	4.39	0.39	2.57
	Min	0.27	-	4.08	1.08	-6.27 (0.4)	0.11 (0.23)
2015	Max	18.08	7.54	16.40	13.51	4.87 (0.68)	13.33 (0.36)
	Mean	7.85	1.16	8.55	3.85	0.70	2.69
	Min	0.61	-	2.99	1.02	-4.24 (0.46)	-0.41 (0.26)

### *Fallow*

The site was a net daily source for 96% of the fallow period days, with the magnitude of this flux ranging from 0.03 ± 0.23 to 13.33 ± 0.36 g C-CO<sub>2</sub> m<sup>-2</sup> d<sup>-1</sup> (Table 4.2) with a mean of 2.3 g C-CO<sub>2</sub> m<sup>-2</sup> d<sup>-1</sup>. Maximum daily losses of 5 and 7 g C-CO<sub>2</sub> m<sup>-2</sup> d<sup>-1</sup> followed the harvest of each of the lettuce plug crops (2012 and 2014 respectively) when the field switched from a net daily sink to a significant net daily source of CO<sub>2</sub>. The difference in the magnitude of these net daily losses of CO<sub>2</sub> for the same crop type are attributable to the warmer (3-4 °C) daily T<sub>air</sub> and T<sub>soil</sub> (Figure 4.4e and f) and drier (~0.13 m<sup>3</sup> m<sup>-3</sup>) SWC of 2014 (Figure 3.3) which facilitated greater respiration.

Notably, the maximum daily NEE value recorded across the full dataset, of  $13.33 \pm 0.36$  g C-CO<sub>2</sub> m<sup>-2</sup> d<sup>-1</sup>, was also recorded shortly after the harvest of a crop. This value, double that of the values measured following harvest in other years, reflects the significant heterotrophic respiration that occurs during decomposition of the celery crop residue remaining on the field during the warm late summer.

After the initial peaks in daily net loss of C-CO<sub>2</sub> in the weeks following harvest of the plug crops, the site reduced to be a net daily source of <5 g C-CO<sub>2</sub> m<sup>-2</sup> d<sup>-1</sup> within a month and a half. In all three of these years the site developed a secondary vegetation cover of weeds (described in Chapter 2.1.3.1). Weed growth particularly dominated daily fluxes in the late summer and early autumn of 2014 and 2015, leading to a reduction in emissions following the post-harvest losses of C-CO<sub>2</sub> and leading to several days of weak net uptake in 2015. Weed growth was treated with targeted chemicals (Table 2.1) in the late autumn of both 2014 and 2015. The subsequent die-back of weeds resulted in further net daily losses of CO<sub>2</sub> to the atmosphere evident in September – October 2014 and November 2015. Aside from the herbicide treatment, daily NEE responded to increases in T<sub>soil</sub> and SWC (as shown in Chapter 3).

In contrast, at the time of the leek harvest in the autumn of 2013 the site was already a weak net daily source of C-CO<sub>2</sub> invariably experiencing days of minimal net uptake. Following leek harvest, the site was a maximum net daily source of  $5.22 \pm 0.62$  g C-CO<sub>2</sub> m<sup>-2</sup> d<sup>-1</sup> which was comparable to values recorded in the same months (late-November/early-December) in the plug crop years but not to the same magnitude with respect to post-harvest emissions. Despite the presence of considerable crop residues, the cooler T<sub>soil</sub> (~10 °C) and wetter conditions in November 2013 compared to the months following each of the plug crop harvests (August 2012, July 2014 and August 2015), led to reduced decomposition and resultant C-CO<sub>2</sub> loss.

During the cold early months of each year, January to April, the site was a weak net source of 0 – 3.6 g C-CO<sub>2</sub> m<sup>-2</sup> d<sup>-1</sup> until preparations for planting started (i.e. the site was ploughed), which led to an instant increase in daily net loss of CO<sub>2</sub> (discussed above). In 2013 a lower average daily T<sub>soil</sub> of 3.4 °C was recorded for January through to planting of the leek crop (compared to 7.8 and 6.9 °C in 2014 and 2015, respectively) which led to reduced soil respiration such that the site was a weaker daily source of C-

CO<sub>2</sub> with an average of 0.65 g C-CO<sub>2</sub> m<sup>-2</sup> d<sup>-1</sup>, as opposed to 1.66 and 1.50 g C-CO<sub>2</sub> m<sup>-2</sup> d<sup>-1</sup> for the same periods in 2014 and 2015 respectively.

### *Summary*

For each year of available data, minimum daily NEE (maximum CO<sub>2</sub> uptake) was measured during crop growth, and whilst the majority of net uptake days (over two-thirds) were during the crop growing periods the fallow periods also experienced 35 days of net uptake (out of 886 fallow days). These days of uptake during the fallow periods were predominantly the result of assimilation by weeds causing an increase in GPP and therefore a reduction in NEE and had a median of -0.24 g C-CO<sub>2</sub> m<sup>-2</sup> d<sup>-1</sup>, but a mean uptake of -0.45 g C-CO<sub>2</sub> m<sup>-2</sup> d<sup>-1</sup>. A few peak values, < -1 g C-CO<sub>2</sub> m<sup>-2</sup> d<sup>-1</sup>, recorded following the lettuce crop harvest in 2012 were attributable to unharvested crops rather than weeds. Crops were more productive primary producers on the field over the year than the weed cover which was present in late summer and early autumn.

Conversely the maximum daily NEE (maximum CO<sub>2</sub> loss) values of 6.24 ± 0.23, 7.89 ± 0.72 and 13.33 ± 0.36 g C-CO<sub>2</sub> m<sup>-2</sup> d<sup>-1</sup> were measured during the fallow periods for each of the plug crops just before planting in 2012 and soon after harvest in 2014 and 2015, respectively, while the 2013 maximum of 7.82 ± 0.31 g C-CO<sub>2</sub> m<sup>-2</sup> d<sup>-1</sup> was measured during the establishment phase of the leek crop after planting.

### 4.2.2 Diurnal NEE

Figure 4.4a illustrates the mean monthly diurnal variation in NEE, and allows for further comparison of the different management cycles across each year. Diurnal variability was evident throughout the complete measurement period and was amplified during the thermal growing season (March to November), most notably during the growth of crops and weeds.

The site was a minimal net source of CO<sub>2</sub> overnight during colder months and a greater source during warmer months. During daylight hours assimilation, or a limitation of respiration, meant the site was a net sink for 6-12 hours around the solar maximum, which was most pronounced once crops had established. When crops were at peak growth the largest diurnal variation was measured; during August in 2012, September in 2013, June in 2014 and July in 2015 which reflects the difference in timing of management practices for each crop (Figure 4.4a, and more clearly Appendix 4.1).

Understandably, the extent of CO<sub>2</sub> uptake dramatically reduced in the month following harvest of each crop causing the average diurnal NEE to show no average half hours as a net sink, particularly following the harvest of the 2014 lettuce crop and the 2015 celery crop. All plug crop years (2012, 2014 and 2015) saw a return of net uptake around the solar maximum once weeds had developed on the field.

Minimum daily NEE and maximum values for R<sub>g</sub>, LE, H were recorded at mid-day/early afternoon, while T<sub>air</sub> and T<sub>soil</sub> peaks lagged these. The diurnal amplitude was flatter during the winter and spring months and at its most pronounced between the months of June – and October. Additionally, values were less smooth about diurnal maximums during the crop dominant summer months. Chapter 3 has already demonstrated that all the crops responded well to PPFD but, particularly the plug crops, were limited by temperature and vapour pressure deficit. Therefore, these fluctuations likely highlight the limitation of plant assimilation and heterotrophic respiration in response to maximum values of radiation and temperature.

#### *Light limitations*

Reduced uptake during peak light hours was most notable for the 2013 leek crop. In June and July of 2013, following a reduction from peak loss overnight, the site fell short of becoming an average net sink for peak mid-day half hours, suggesting that the young leek crop had a low (~400 W m<sup>-2</sup>) threshold for light saturation (Figure 4.4a). These same months additionally recorded reduced LE and increased H for half hour periods with R<sub>g</sub> values greater than ~400 W m<sup>-2</sup> when compared with the same months in other years (Figure 4.4b). Higher light saturation thresholds (~500 W m<sup>-2</sup>) of photosynthesis limited early celery growth in June 2015 and lettuce development in May 2014. No diurnal limitation at a monthly resolution was evident for the first lettuce crop during its development in July 2012, however the average mid-day R<sub>g</sub> did not exceed 500 W m<sup>-2</sup>.

#### *Temperature limitations*

Maximum half hourly values of average diurnal T<sub>air</sub> and T<sub>soil</sub> lagged peak R<sub>g</sub> by 1-3 hours, affording an opportunity to differentiate the limitations on NEE of temperature from radiation. The 2012 lettuce displayed a limited CO<sub>2</sub> uptake in the early afternoon during July and August when T<sub>air</sub> was at its diurnal maximum (Figure 4.4e); LE reflected this pattern with a slight reduction in energy being used for vaporisation in

early afternoon, suggesting a closing of stomata leading to a combined reduction in both uptake of CO<sub>2</sub> and loss of H<sub>2</sub>O (Figure 4.4c).

In addition to radiation limitations observed in the developing leek crop in July 2013, in the early afternoon NEE increased as peak average T<sub>air</sub> for the dataset was registered. This suggests a further limitation in photosynthetic assimilation that did not limit soil respiration. The more developed leek crop appeared to have a lower temperature (~5-10 °C cooler) threshold in September and October of 2013 which also saw a reduction in early afternoon uptake of CO<sub>2</sub> (Figure 4.4a) that followed the trend in maximum average T<sub>air</sub> for those months. The 2014 lettuce crop did not show this same temperature limitation during its peak month of development, June, experiencing a peak T<sub>air</sub> value only a few degrees cooler (Figure 4.4e).

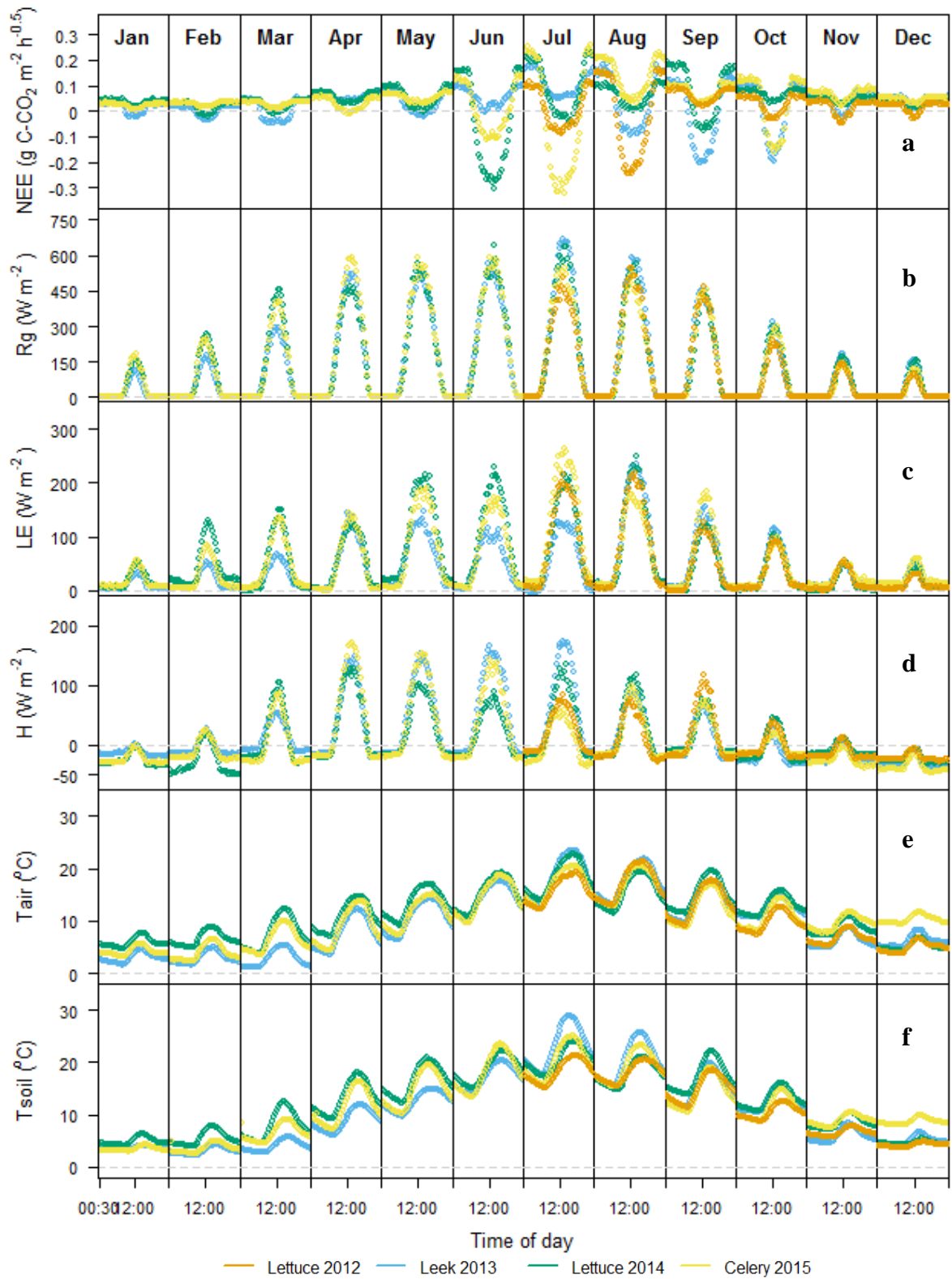


**Figure 4.4:** Average monthly diurnal variability for six environmental variables for each year of the complete measurement period (22nd June 2012 – 31st December 2015). a- net ecosystem exchange (NEE), b- global radiation (Rg), c- latent heat flux (LE), d- sensible heat flux (H), e- air temperature (T<sub>air</sub>), f- soil temperature (T<sub>soil</sub>). Orange for lettuce (2012), blue for leek (2013), green for lettuce (2014), and yellow for celery (2015).

#### 4.2.3 Crop and fallow periods

Time integrated NEE (with uncertainties) and partitioned fluxes were calculated for crop and fallow periods within each year, from the start of January through to the end of December (Table 4.3). For all crop and fallow periods the site was a net source of C-CO<sub>2</sub>. The shorter growing periods of the plug crops were only minimal net sources of  $2.93 \pm 15.59$ ,  $23.41 \pm 18.46$  and  $64.62 \pm 33.77$  g C-CO<sub>2</sub> m<sup>-2</sup>, for 2012, 2014 and 2015 respectively, whilst over the 2-3 times longer growth period of the leek crop the site was a net source of  $468.74 \pm 63.14$  g C-CO<sub>2</sub> m<sup>-2</sup>, which was double the value of  $207.01 \pm 38.31$  g C-CO<sub>2</sub> m<sup>-2</sup> measured during the six months of fallow field conditions during 2013.

For both the lettuce crop of 2014 and the celery crop of 2015 the NEE values for the crop and fallow periods were within the uncertainty calculations of each other, despite the 25 day longer growing period of celery. Partitioning of the NEE (described in Chapter 2.2.7) again led to similar net values of GPP and TER for these two crops over a full annual cycle. However, the GPP contribution of the celery crop was calculated as almost double that of the 2014 lettuce, duly reflecting the 32 day longer growing period of celery and its greater mass (Table 4.4). The fallow period of 2014 recorded a greater GPP due to the greater residual crop and weeds left on the field following lettuce harvest, compared to the more thorough harvest of celery in 2015. The two lettuce crops had comparable GPP and TER during crop growth, however their fallows were not comparable.

The leek growing period recorded a greater TER of  $1185.89$  g C-CO<sub>2</sub> m<sup>-2</sup> yr<sup>-1</sup> than the 2014 lettuce and 2015 celery which was comparable considering the greater number of days for integration. However, GPP for the same period was not as comparably large, but it must be taken into account that the leek was grown from seed. Total GPP and TER for 2013 were still comparable with the plug crops.

**Table 4.3:** Crop, fallow and annual sums of GPP and TER. Based on time integrated partitioned 30 minute NEE fluxes.

Year (no. days Crop/Fallow)	GPP (g C-CO <sub>2</sub> m <sup>-2</sup> )			TER (g C-CO <sub>2</sub> m <sup>-2</sup> )			NEE (g C-CO <sub>2</sub> m <sup>-2</sup> )		
	Crop	Fallow	Total	Crop	Fallow	Total	Crop (± SE)	Fallow (± SE)	Total (± SE)
<b>2012 (48/145)</b>	299.61	252.32	551.93	302.54	489.02	791.57	2.93 (15.59)	236.70 (27.77)	239.64 (43.36)
<b>2013 (194/171)</b>	717.15	242.09	959.25	1185.89	449.11	1635	468.74 (63.14)	207.01 (38.31)	675.75 (101.45)
<b>2014 (60/305)</b>	372.95	554.22	927.17	396.36	1337.18	1733.6	23.41 (18.46)	782.96 (70.29)	806.38 (88.75)
<b>2015 (92/273)</b>	721.87	316.09	1037.96	786.49	1048.65	1835.14	64.62 (33.77)	732.56 (50.83)	797.18 (84.60)

#### 4.2.4 Annual

As data collection began halfway through 2012 the data for the first half of the year would require modelling as a gap that size would be too big to fill using the methods followed in the rest of this thesis. Additionally, the January to June of 2012 was unusual, meteorologically speaking, in that an uncommonly dry winter was followed by the wettest spring and summer on record. As such it was deemed imprudent to attempt to model this flux as values were likely outside of the range of those captured during the rest of the data collection, although given the data presented here for 2014 and 2015, the higher soil moisture content and cooler drier weather of the winter and spring of 2012, combined with a crop cover during the peak summer months would have been expected to result in a lower annual source of CO<sub>2</sub> to the atmosphere (Shurpali et al., 2009) by comparison to the full year of lettuce crop measurements presented here (2014). Therefore the 2012 data set is excluded from the annual comparisons.

There is a clear similarity in the trends of daily fluxes of the plug crop NEE of CO<sub>2</sub> which is evident in Figure 4.3, and is similarly shown in the cumulative plot of Figure 4.5, for 2014 and 2015. Figure 4.5 shows more clearly the similarity between these two years. Despite January and February of 2014 experiencing slightly higher mean diurnal temperatures (Figure 4.4e and f) they follow an almost identical net daily loss trend. During the months of April to September both the lettuce and the celery crops had at least a month of sequestration where daily uptake outweighed net loss, and which was more significant in 2015. However in both years the site returned to being a net source following harvest of each crop and the magnitude of the net loss in 2015 (values reported above in Table 4.2 and Figure 4.3) counterbalanced the increased sequestration

seen compared to 2014. In the final months of each year the site was a consistent source of C-CO<sub>2</sub> comparable to that of the early months of the year leading to an almost identical annual integrated NEE of  $797.18 \pm 84.60$  and  $806.38 \pm 88.75$  g C-CO<sub>2</sub> m<sup>-2</sup> yr<sup>-1</sup>, for 2014 and 2015 respectively.

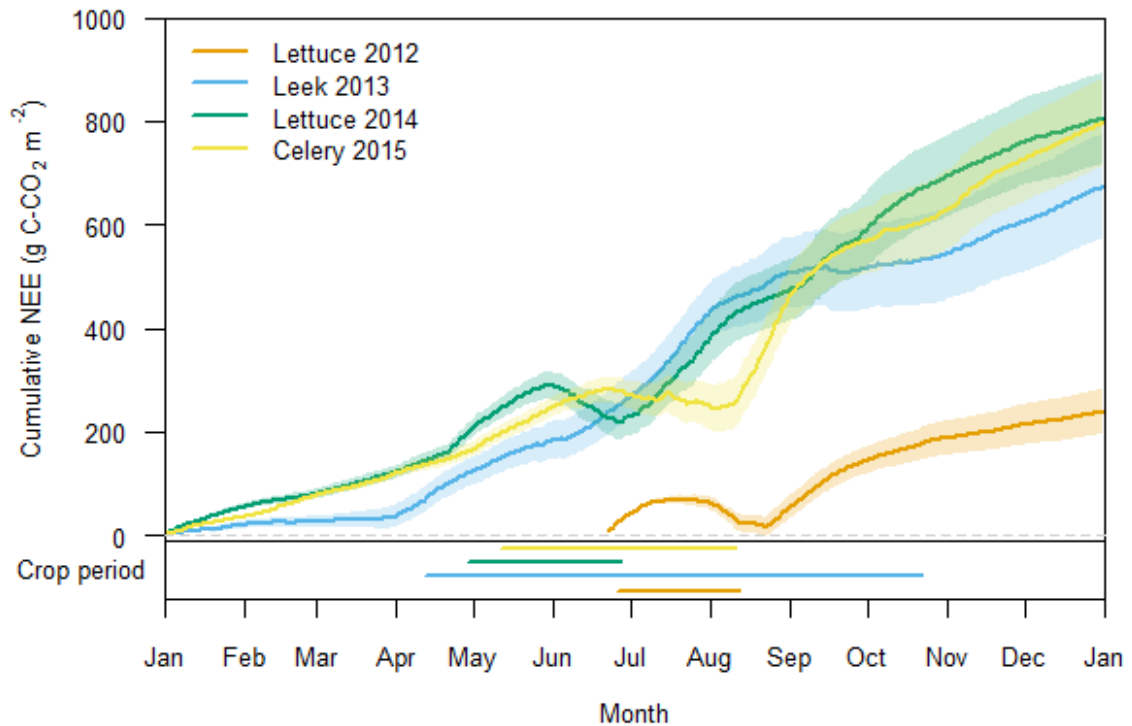


**Figure 4.5:** Cumulative gap filled NEE g C-CO<sub>2</sub> m<sup>-2</sup> with uncertainty (shaded band). Positive accumulation reflects a transfer of C-CO<sub>2</sub> from the biosphere to the atmosphere through auto-heterotrophic respiration. A reduction in accumulation reflects uptake by the biosphere through photosynthesis. Horizontal shading represents periods where there is a crop present on the field. The shading colour refers to the same colour of year, as per the key.

In 2013 the colder conditions in the early months of the year (discussed above) led to lower than usual accumulation of net C-CO<sub>2</sub> loss, until management activity began in April. Contrary to the plug crop years, the leek crop never became a consistent net sink of C-CO<sub>2</sub>, although it did become near neutral during the more productive months of September and October (Figure 4.5). Despite a lack of consistent sequestration the annual integrated NEE of  $675.75 \pm 101.45$  g C-CO<sub>2</sub> m<sup>-2</sup> yr<sup>-1</sup> for the leek crop was within the uncertainty of the plug crops and therefore this crop was not significantly more or less productive over a calendar year (Table 4.4). Additionally, the site did not become as significant a source of CO<sub>2</sub> following harvest as was seen during plug crop years, this

reflects the slower decomposition during colder conditions that likely displaced associated CO<sub>2</sub> release from leek residue decomposition into the early months of 2014. Generally speaking, uncertainty values were greater when longer periods of fluxes were missing following quality control of the data. The greater uncertainty associated with the 2013 NEE was chiefly a result of a long spell of dominant north-easterly winds bringing fluxes to the instrumentation from a field under different management practice. This was largely during spring months and this data had to be discarded during quality control (Chapter 2.2.5; Figures 2.9, 2.10 and 2.11). These conditions were difficult to gap fill due to the paucity of available data to use for this purpose, which increased the uncertainty in the calculation.

### 4.3 Lateral C balance

#### 4.3.1 Import ( $C_i$ )

As described in Chapter 2.1.3.3, the lettuce and celery crops were planted as peat plugs. Loss on ignition analysis of samples of plugs yielded an average figure of  $7.2 \pm 0.21$  g C (n=5) for lettuce plugs, and  $5.79 \pm 0.24$  g C (n=5) for celery plugs. Additionally, information on the number of plugs planted was provided by the farm manager, which enabled a calculation of the amount of C added to the site during each planting cycle. On average, plugs accounted for additions of  $64.44 \pm 1.88$ ,  $50.71 \pm 1.48$  and  $55.27 \pm 2.29$  g C  $m^{-2}$  for the 2012, 2014 and 2015 crops respectively (Table 4.4).

Leek seeds were reportedly planted at a density of  $25.95$  seeds  $m^{-2}$ , with an additional  $5$  g  $m^{-2}$  of barley seeds (M. Hammond, Pers. comm.) leading to an estimated combined C addition to the site of  $2.16$  g C  $m^{-2}$  in 2013.

**Table 4.4:** Crop, fallow and annual sums of NEE with additional lateral C. †based on figure from Kutsch et al. (2010) and Ceschia et al. (2010). ‡ based on a sample of 5 plugs. All NEE figures are g C-CO<sub>2</sub>  $m^{-2}$ , whilst  $C_i$  and  $C_e$  are g C  $m^{-2}$  based on loss on ignition calculations. NECB is the combined C balance of NEE and import and export calculations.

Year (no. days of C/F)	NEE (g C-CO <sub>2</sub> $m^{-2}$ $\pm$ uncertainty)			C balance (g C $m^{-2}$ $\pm$ SE)			
	Crop ( $\pm$ )	Fallow ( $\pm$ )	Total ( $\pm$ )	$C_i$	$C_e$	$C_e - C_i$	NECB
<b>2012 (48/145)</b>	2.93 (15.59)	236.70 (27.77)	239.64 (43.36)	64.44 (1.88)‡	34.68 (6.94)	-29.76 (8.82)	209.87 (50.3)
<b>2013 (194/171)</b>	468.74 (63.14)	207.01 (38.31)	675.75 (101.45)	2.16†	109.85 (25.83)	107.69 (25.83)	783.44 (127.28)
<b>2014 (60/305)</b>	23.41 (18.46)	782.96 (70.29)	806.38 (88.75)	50.71 (1.48)‡	31.95 (6.39)	-18.76 (7.87)	787.61 (96.62)
<b>2015 (92/273)</b>	64.62 (33.77)	732.56 (50.83)	797.18 (84.60)	55.27 (2.29)‡	74.44 (2.44)	19.17 (4.73)	816.35 (89.33)

#### 4.3.2 Yield ( $C_e$ )

Records of harvested crops provided by the farm manager gave yields of  $2.9$  kg  $m^{-2}$  for lettuce in 2012,  $2.17$  kg  $m^{-2}$  for leek in 2013,  $400,733$  ( $\sim 2.67$  kg  $m^{-2}$ ) individual lettuce in 2014 and  $639,555$  ( $\sim 2.67$  kg  $m^{-2}$ ) individual celery plants in 2015 ( $\sim 4$  kg  $m^{-2}$ ).

Farm records reported a higher lettuce yield in 2012 compared to 2014 despite a higher per head weight in 2014 (480 g compared to a usual figure of 450 g, M. Dymowski and M. Hammond, Pers. comm.). The reduced yield of 2014 was partly due to a greater portion of bare soil on the field as fewer lettuce per unit area were cultivated. Celery had a similar average harvested plant weight (450 g) and planting density as the lettuce

crop, however lettuce heads had a greater moisture content reflected in an average dry weight of 3% of the original, whilst celery was 6%.

Leek was grown at a greater density than the plug crops, but it had a lower average plant weight (228 g) and less than 70% of the number of planted crops (per square meter) were estimated to have been harvested, resulting in the lowest yield per square meter measured for these crops. In contrast to the plug crops, leek had a lower moisture content and therefore a greater dry weight that accounted for 7% of the original weight.

Analysis of each crop for C content (as described in Chapter 2.3) gave values of 39.86, 41.46 and 33.66% as the percentage of dry weight for the lettuce, leek and celery crops, respectively. The 2013 leek crop, therefore, despite having the lowest per square meter yield, had the highest  $C_e$  value of  $109.85 \pm 25.83 \text{ g C m}^{-2}$  (Table 4.4), celery was the greatest plug crop exporter of C at  $74.44 \pm 2.44 \text{ g C m}^{-2}$ , whilst the two lettuce crops did not differ significantly reporting  $34.68 \pm 0.94$  and  $31.95 \pm 6.39 \text{ g C m}^{-2}$  for 2012 and 2014, respectively. The variability in error of export for each crop likely reflects the minimal number of plant samples available for analysis each year.

#### 4.3.3 Carbon balance

For both lettuce crops, a greater quantity of C was estimated to have been imported compared to the exported quantity by harvest, resulting in a net gain by the ecosystem of roughly  $29.76 \pm 8.82$  and  $18.76 \pm 7.87 \text{ g C m}^{-2}$  for 2012 and 2014 respectively (Table 4.4). Despite importing a similar quantity of C to the lettuce crops, the quantity of C exported in celery led to a further contribution to C loss from the ecosystem of  $19.17 \pm 4.73 \text{ g C m}^{-2}$ . The leek crop, with the least C imported and the most C exported, made the greatest contributory ecosystem loss of  $107.69 \pm 25.83 \text{ g C m}^{-2}$ .

When considering an NECB comprised of NEE,  $C_i$  and  $C_e$  (Table 4.4), all of the years measured here found the site to be a net source at  $783.44 \pm 127.28$ ,  $787.61 \pm 96.62$  and  $816.35 \pm 89.33 \text{ g C m}^{-2} \text{ yr}^{-1}$  for 2013 – 2015, respectively. It is acknowledged, however, that the NECB values reported here do not take account of other pathways of C loss/gain, such as other GHG fluxes ( $\text{CH}_4$ ) into and out of the field or surrounding ditches, wind-blown flux, and dissolved/particulate organic/inorganic aquatic fluxes. Measurements of some of these pathways (ditch and field  $\text{CH}_4$  and aquatic C fluxes) were made at the site as part of a larger-scale study and the values have been published

elsewhere (Peacock et al., 2017, Evans, 2017; Table 4.5), whilst wind-blown flux is addressed later in this thesis (Chapter 5).

**Table 4.5:** Measured fluxes for cropland on peat. Information taken from Table 6.4 in DEFRA SP1210 report (Evans, 2017). Units have been converted from original values to the same units used here.

<b>Pathways</b>	<b>Flux (g C-CO<sub>2</sub>/CH<sub>4</sub> m<sup>-2</sup> yr<sup>-1</sup>)</b>
CO <sub>2</sub> (land)	694 (647 to 758)
DOC	14 (5 to 32)
CH <sub>4</sub> (land)	-0.11 (-0.29 to 0.1)
CH <sub>4</sub> (ditch)	1.7 (0.1 to 3.3)

## 4.4 Discussion

### 4.4.1 EBC

The unclosed annual energy balance of this site at 87-89%, using half-hourly values for the complete years, was at the higher end of reported values of 70-97% for a range of European sites (Foken, 2008, Wilson et al., 2002, Hendricks Franssen et al., 2010, Leuning et al., 2012, Schrier-Uijl et al., 2014). A homogenous surface and low vegetation cover (e.g. grasslands, crops) were characteristic of sites, like this one, with better closure. Typically it has been found that available energy fluxes are overestimated and energy fluxes are underestimated at EC sites (Wilson et al., 2002) which was also the case with this dataset. Wilson et al. (2002) in a study of 50 European and American flux towers reported that only nine experienced a slope of 80% or better following linear regression analysis, whilst a closure of 85% was found for the permanently wet grassland on peat soil of Tadhham Moor in the Somerset Levels, UK and, although the imbalance was not investigated in detail, it was attributed to systematic error of turbulent or  $R_n$  measurements (Harding and Lloyd, 2008). The majority of the energy, at both Tadhham Moor and at this site, was utilised in LE of vaporisation despite the difference in land use.

Poorer nocturnal closure compared to daytime closure is a difference identified at other sites as well as in this dataset. Increased nocturnal imbalance can be attributed to advection fluxes that are often associated with poor  $u^*$  (Wilson et al., 2002, Hendricks Franssen et al., 2010). It has also been shown that absolute differences in balance may well be greater during daylight but a larger relative imbalance is evident during nocturnal periods (Wilson et al., 2002, Hendricks Franssen et al., 2010, Harding and Lloyd, 2008).

The nocturnal EBC closure of 0.47 and intercept of  $-10.43 \text{ W m}^{-2}$  (Table 4.1) reported here was a little better than the mean calculated by Wilson et al. (2002) of 0.35 and  $-5.5 \text{ W m}^{-2}$  for slope and intercept respectively but was within the range of reported values.

The annual EBC slope values improvement from 0.87 – 0.89 to 0.9-0.96 when thirty minute values of the energy balance terms were integrated over a daily time step, this was similarly demonstrated in other EC datasets. For the public FLUXNET La Thuile dataset of a range of global measurement sites in Leuning et al. (2012) daily time-

integration yielded a median slope of 0.9 for 439 site years as opposed to 0.75 for 594 site years of half hourly data.

As the cultivation period of each crop was close to or included the summer equinox the nocturnal energy fluxes for these periods contributed to between a fifth and a third of the values used, whilst during the fallow periods available data was more evenly distributed between day and night. Despite the increased reliance on less balanced nocturnal measurements no significant distinction could be made between the closure of the crop and fallow periods based on nocturnal contributions.

Lack of closure of the energy balance is a well-documented issue (Foken et al., 2012b, Wilson et al., 2002, Leuning et al., 2012). The implications of this imbalance are that it may reflect an error in flux estimates (Wilson et al., 2002). Whether or not the CO<sub>2</sub> flux is independent of the imbalance depends on the root cause of the imbalance.

Assuming the fundamental eddy covariance assumptions have been met (which were addressed during installation and data processing), and the radiation measurement instrumentation error is small, the remaining potential causes of imbalance have been suggested to include: spatial error in contributing terms; incorrect accounting of storage terms; vertical flux divergence and advective fluxes usually related to measurement height and heterogeneous terrain or vegetation; low frequency eddies uncaptured by averaging (Oncley et al., 2007, Foken et al., 2012b, Leuning et al., 2012).

With regard to spatial error, whilst turbulent energy fluxes originated from crop covered soil it was not possible to measure soil conditions directly under each crop or to measure radiation directly overhead, due to ongoing management activities at the site that would have interfered with the instruments. Soil conditions (e.g. temperature, porosity, moisture content) at the origin of turbulent heat fluxes were controlled by management activities that included ploughing, planting, harvesting and compaction by machinery, while the conditions where the monitoring instruments were located at the field margin were left undisturbed after installation. It is likely that the imbalance would be greater during crop periods than fallow if differences in agricultural management were a dominant cause, but this is not seen in the EBC presented here. It is likely, therefore, that differences in crop and soil conditions make a minor contribution to the imbalance.

Imbalance due to storage terms could be caused by known difficulties encountered in quantifying soil heat flux in peat soils using heat flux plates (Harding and Lloyd, 2008). However, this term is understood to be small, and too small to have solely caused the imbalance measured here (Leuning et al., 2012). Given the homogenous nature of the local area, advective fluxes of turbulent energy would also make only a minimal contribution. Similarly, given the low measurement height of the instruments (1.5 m), low frequency eddy loss and possible vertical flux divergence should also both be non-significant at this site.

Possible additional contributors to the remaining imbalance that have not already been mentioned include: storage of energy in glucose production during photosynthesis, canopy storage and irrigation. These would likely cause greater imbalance during crop periods but, as has already been stated, trends associated with these potential causes of imbalance could not be identified and therefore their influence on EBC could not be quantified.

Despite an intense quantification of the energy balance terms at a flooded cotton field in California, Oncley et al. (2007) found several contributing factors for imbalance at their study site (notably as a result of vertical flux divergence) but were unable to completely explain the average imbalance of 10%. They did, however, identify the error as being at least partly caused by non-local effects. No additional cause of imbalance was firmly identified in this thesis, but the suspicion of the author lies with the heterogeneity between measurement locations of the different terms of EBC calculation.

In summary, it is generally advised not to correct gas fluxes for the imbalance of the related energy closure (Foken et al., 2012b, Foken et al., 2011), but to accept that they likely represent an underestimation of positive NEE. In the case of my study site, the imbalance is an acceptably small underestimation that is within the measure of uncertainty which was 10 – 15% of the annual NEE.

#### 4.4.2 NEE

##### 4.4.2.1 Daily

Peak daily uptake values,  $-4.87 \pm 0.32$ ,  $-3.73 \pm 0.43$ ,  $-6.27 \pm 0.4$  and  $-4.24 \pm 0.46$  g C-CO<sub>2</sub> m<sup>-2</sup> d<sup>-1</sup>, measured during the crop growing periods (2012-15 respectively), were comparable to values of  $-5.35$  and  $-4.09$  g C m<sup>-2</sup> d<sup>-1</sup> for barley crop and grasses, respectively (76% of *P. pratense* and 24% of *F. pratensis*) grown on a southern Finnish

peat soil (0.8-1 m deep) measured by Lohila et al. (2004) using the EC technique. The barley crop was grown over 4 months and was a net sink for 39 days of that period, whereas in this study no crop experienced more than 31 days as a net sink and the crops were grown over 2-6 months. Lohila et al. (2004) showed that the shorter growing period of a barley crop experienced greater peak daily uptake of CO<sub>2</sub> than grasses grown over a longer period, which was similar to the plug crops grown here in comparison to the leek. It is perhaps surprising that despite the higher planting density of the barley crops that they were not a greater sink of CO<sub>2</sub> on a daily basis than the crops grown at this site.

A more recent study by Poyda et al. (2016) measured CO<sub>2</sub> exchange of a lowland peatland under agricultural management in northern Germany using the chamber technique over two years, and two crops, a spring barley in the first year followed by a summer wheat under-sown with grass in the second. The maximum daily uptake reported was -5 to -7 g C-CO<sub>2</sub> m<sup>-2</sup> d<sup>-1</sup> for the spring barley crop, greater than the values reported here for salad crops in eastern England and spring barley in southern Finland (Lohila et al., 2004), whilst the summer wheat under-sown with grass had a much greater estimated daily uptake of -10 g C-CO<sub>2</sub> m<sup>-2</sup> d<sup>-1</sup> reflecting the greater assimilation capacity of the wheat crop. The lower peak daily uptake of barley crop in Finland compared to Germany reflects the difference in boreal to temperate climate, while the greater uptake with respect to the salad crops measured in here likely reflects a greater assimilation rate of a cereal crop.

Multiple years of lettuce crops here yielded different peak daily NEE  $-4.87 \pm 0.32$  and  $-6.27 \pm 0.4$  g C-CO<sub>2</sub> m<sup>-2</sup> d<sup>-1</sup>. Similarly, Shurpali et al. (2009) measured peak daily NEE uptake values of -4.5 and -5.5 g C-CO<sub>2</sub> m<sup>-2</sup> d<sup>-1</sup> for a perennial bioenergy crop reed canary grass (RCG) (*Phalaris arundinacea* L.) during 2005 and 2006 on a peat soil in eastern Finland. Values for the same crop in 2004 and 2007 peaked at -9.6 and -7.5 g C-CO<sub>2</sub> m<sup>-2</sup> d<sup>-1</sup>, respectively, which are much higher than the peak values for the crops studied here but similar to those recorded for wheat with an undersown grass in Germany. Shurpali et al. (2009) attributed the variability in maximum daily values of CO<sub>2</sub> uptake for the same crop in the same location over multiple years to correspondingly wetter and drier conditions, with drier conditions judged to have limited assimilation of CO<sub>2</sub> and increased soil respiration. In contrast, the opposite was

true of the two lettuce crops studied here, as the crop received more precipitation in 2012 (133.7 mm) than in 2014 (102 mm) (with both amounts including above ground irrigation) and had a greater average SWC, yet the 2014 crop experienced higher daily net CO<sub>2</sub> uptake (Table 4.2). Despite the greater maximum daily uptake of the 2014 lettuce crop over the course of the complete crop period (planting to harvest) it was a greater net source of CO<sub>2</sub> (Table 4.3).

Reversals are evident in the data presented here, whereby during a prolonged period of 3-4 weeks of consistent daily net CO<sub>2</sub> uptake, GPP reduced and the site became a net daily source of CO<sub>2</sub>; most notably during the 2015 celery crop period when during the period 12<sup>th</sup> – 15<sup>th</sup> July the site, which had been a net sink of ~2 g C-CO<sub>2</sub> m<sup>-2</sup> d<sup>-1</sup>, became a net source of 2-5 g C-CO<sub>2</sub> m<sup>-2</sup> d<sup>-1</sup> (Figure 4.3) as PPFD values halved. Lohila et al. (2004) reported similar events during a prolonged period of 3-4 weeks of consistent daily net CO<sub>2</sub> uptake by a barley crop where their site became a net daily source of CO<sub>2</sub>, which correlated with reductions in the mean midday (1000-1600) PPFD associated with overcast and rainy conditions corroborating the findings here.

Management activities, which included ploughing, harvest and herbicide spraying of weeds, resulted in sustained periods of net loss of CO<sub>2</sub> from the site. For each year peak net daily CO<sub>2</sub> emissions were  $6.24 \pm 0.23$ ,  $7.82 \pm 0.31$ ,  $7.89 \pm 0.72$  and  $13.33 \pm 0.36$  g C-CO<sub>2</sub> m<sup>-2</sup> d<sup>-1</sup> for 2012-2015 respectively, which are higher than comparable values reported for spring barley and RCG grown on Finnish peat soil, at 2 to 4.5 g C-CO<sub>2</sub> m<sup>-2</sup> d<sup>-1</sup> (Lohila et al., 2004, Shurpali et al., 2009), but are on the same scale as the ~11 g C-CO<sub>2</sub> m<sup>-2</sup> d<sup>-1</sup> reported for spring barley on a temperate German peat soil (Poyda et al., 2016). Poyda et al. (2016) reported a much greater net daily loss of ~20 g C-CO<sub>2</sub> m<sup>-2</sup> d<sup>-1</sup> that followed the harvest of a summer wheat crop and which also coincided with the highest mean daily temperatures recorded during their study (>20 °C). In this study, the exposed post-harvest crop residues of the 2015 celery crop led to 12 days of more than 10 g C-CO<sub>2</sub> m<sup>-2</sup> d<sup>-1</sup> in late August and the maximum daily NEE value of  $13.33 \pm 0.36$  g C-CO<sub>2</sub> m<sup>-2</sup> d<sup>-1</sup> for the entire celery crop study period despite a decrease in both Tair and Tsoil during this period. Incorporation of harvest residuals at the end of August 2015 into the topsoil corresponded with the start of a gradual reduction in daily NEE which closely correlated with a continued steady reduction in Tsoil, which suggests that the

incorporation of crop residues led to a decrease in daily NEE, which then responded to Tsoil.

A reduced post-harvest daily CO<sub>2</sub> loss was measured in August 2014 following the lettuce crop harvest, and this correlated to a steady reduction in Tsoil but was more likely a result of herbicide treatment of the weeds in the field rather than incorporation of the residuals into the topsoil. Harvest has been shown to result in an instant drop in GPP and an increase in TER at a number of other peat soil sites used for production of wheat, oats and grasses (Poyda et al., 2016, Eickenscheidt et al., 2015, Lohila et al., 2004). In these studies, the decomposition of harvest residuals combined with increased exposure of the upper soil profile resulted in increased CO<sub>2</sub> emissions.

The 2013 maximum daily NEE reflected crop assimilation limitations as a result of young crop development whereby the crop struggled to photosynthesise under high Rg and Tair, which did not limit TER. No similar examples of this effect have been identified from studies at similar cropland sites on peat soils, however other limited assimilation such as senescence has been shown to cause significant daily CO<sub>2</sub> loss from peat soils growing barley and RCG crops prior to harvest (Poyda et al., 2016, Shurpali et al., 2009, Lohila et al., 2004) as GPP reduces whilst significant TER (largely from soil respiration) continues until environmental conditions become limiting for TER. Despite a similar quantity of harvest residue (personal observation) in late October and November 2013, decomposition of leek residues did not impact daily NEE as significantly as plug crop harvests. This likely represents a threshold for controls on residue decomposition (i.e. temperature, SWC, lability of crop material) which was not quantified. The leek residue remained on the field until the site was ploughed in early 2014 in preparation for the next crop, and therefore likely contributed to TER during 2014.

#### *4.4.2.2 Annual*

Salad crops on peat soil

Annual NEE reported here was  $675.75 \pm 101.45$ ,  $806.38 \pm 88.75$  and  $797.18 \pm 84.6$  g C-CO<sub>2</sub> m<sup>-2</sup> yr<sup>-1</sup>, for 2013 – 2015 respectively, averaged to  $759.77 \pm 91.6$  g C-CO<sub>2</sub> m<sup>-2</sup> yr<sup>-1</sup>. A recent study in the same region of East Anglia using closed static chambers by Taft et al. (2017) reported an annual flux of  $772 \pm 63$  g C-CO<sub>2</sub> m<sup>-2</sup> yr<sup>-1</sup> as an average of six horticultural crops over three fields with peat soils across a range of values for soil

organic C (SOC) content (Table 4.6). This figure fits well with the EC measurements made by this study for salad and bulb horticultural crops on one field, despite the reduced sampling frequency and spatial resolution of static chamber measurements. The annual sum presented by Taft et al. (2017) was calculated from June 2011 to June 2012 and therefore crossed two management regimes on most of the fields studied; encompassing at least one complete crop cycle in 2011 and ending during the development of a second crop in 2012. Integration of the NEE in this chapter from June to June reduces the average annual site NEE by over 100 g C-CO<sub>2</sub> m<sup>-2</sup> d<sup>-1</sup> largely due to the effect of the value for NEE during 2012-2013 ( $381.67 \pm 77.12$  g C-CO<sub>2</sub> m<sup>-2</sup> yr<sup>-1</sup>) which is lower largely as a result of reduced CO<sub>2</sub> emissions recorded during the cooler conditions of late 2012 and early 2013. Whilst the uncertainty of the average annual loss fits within the original average annual sum presented here, it demonstrates the need for caution when comparing varying time-integrated sums reported in the literature and the importance of consistency in reporting annual sums either by management regimes or by singular calendar years.

Furthermore, Taft et al. (2017) report a figure of  $709 \pm 68$  g C-CO<sub>2</sub> m<sup>-2</sup> yr<sup>-1</sup> for bare soils on the same fields over the same period suggesting that the majority (58-96%) of TER resulted from microbial activity, i.e. from heterotrophic soil respiration. The inference from this is that regardless of the crop planted, continued intensive management at the site will cause a continued loss of at least this quantity of C-CO<sub>2</sub> on an annual basis.

**Table 4.6:** Annual NEE (g C-CO<sub>2</sub> m<sup>-2</sup> yr<sup>-1</sup>) details reported by literature on temperate and boreal peatlands managed for growing vegetable, cereal and some grass crops. Literature not reported in (IPCC, 2014)

Paper	Location	Site details	Vegetation	Annual NEE (g C-CO <sub>2</sub> m <sup>-2</sup> yr <sup>-1</sup> )
<b>This study</b>	East Anglia, UK. 52°31'N, 00°28'E, -5 m a.m.s.l.	Intensively managed. EC.	Leek, Lettuce, Celery	675.75 ± 101.45 806.38 ± 88.75 797.18 ± 84.6
<b>Taft et al. (2017)</b>	East Anglia, UK. 52°31'N, 00°28'E, -5 m a.m.s.l.	Intensively managed. Static chamber technique with gas chromatography.	Celery, red beet (cover crop of barley), romaine lettuce, iceberg lettuce, radish, potato.	Crops 523 ± 74 (SOC 30%) 772 ± 63 (SOC 70%) Bare peat 355 ± 65 (SOC 30%) 709 ± 68 (SOC 70%)
<b>Poyda et al. (2016)</b>	Schleswig- Holstein, Germany 54°21' N, 9°24' E	Drained for agriculture. Three grasslands (unutilised (UG); wet (GW); moist (GM)) and one arable (AR). Chambers, gas chromatography	AR growing spring barley (SB) and summer wheat (SW) with under sown perennial ryegrass (PR)	900 ± 150 (SB) 1120 ± 230 (SW) 280 ± 250 (UG) 800 ± 70 (GW) 1170 ± 120 (GM)
<b>Eickenscheidt et al. (2015)</b> (included in Tiemeyer et al. (2016))	Freisinger Moos, Germany. 48°21'N, 11°41'E 450 m a.m.s.l.	Four arable sites, two with medium and two with high C content. Dynamic chamber method using a portable LICOR infrared gas analyser.	Maize and oats.	-6 ± 546 to 1139 ± 394 (maize) 815 ± 200 to 1707 ± 619 (oat)
<b>Beyer et al. (2015)</b> (included in Tiemeyer et al. (2016))	Dümmer, North West Germany. 52.30°N, 8.20°E	Drained for agriculture since start of the 20 <sup>th</sup> Century. Dynamic chamber technique.	Two sites one cultivated with corn-cob-mix maize (CCM) and the other a grassland (GL)	-276 ± 249 to 252 ± 156 (CCM) 142 ± 144 to 565 ± 133 (GL) Averages -61 (s.e. 104) (CCM) 311 (s.e. 81) (GL)
<b>Beyer and Höper (2015)</b>	Nordhümmlinger Moore, Lower Saxony, Germany 53°N, 7.32°E, 5 m a.m.s.l	Three sites on a bog formerly used for peat extraction, rewetted in the 1980's, and one site used for agriculture before extraction then rewetted in 2000s. Dynamic chamber technique with portable gas analyser	Sphagnum cultivation	-201 ± 126.8 to 29.7 ± 112.7 (rewetted) -118 ± 48.1 to -78.6 ± 39.8 (average: - 98.7 ± 20.1) (Shpagnum)
<b>Kutsch et al. (2010)</b>	Denmark	Drained bog. Measured by EC.	Grain crops	-273

## IPCC literature

No further literature was identified reporting CO<sub>2</sub> fluxes of salad crops grown on drained peat soil. The emission factor of  $790 \pm 150$  g C-CO<sub>2</sub> m<sup>-2</sup> yr<sup>-1</sup> reported by the IPCC (2014)<sup>f</sup> is derived from a range of studies (Table 4.7). These are largely studies of cereal and a limited number of root vegetable crops (individual contributions of these are not given, only averages) on both boreal and temperate drained peat soils using a range of methodologies that include EC, chambers and subsidence estimates (Table 4.7). The reduced planting density, shorter growing periods and warmer temperate climate of East Anglia would be expected to result in a greater CO<sub>2</sub> loss compared to those included in the IPCC (2014) report, however the annual figures for this site fit within the 95% confidence interval of the emission factor provided.

The root vegetable contribution to the IPCC (2014) NEE figure derived from chamber measurement studies of potato and carrot crops<sup>g</sup> have a range of 600 to 860 g C-CO<sub>2</sub> m<sup>-2</sup> yr<sup>-1</sup> (Table 4.7) (Elsgaard et al., 2012, Maljanen et al., 2010, Grønlund et al., 2008) which is similar to that of the salad crops measured here despite root crops having a larger biomass but similar growing periods. The maximum value reported for root crops was 1910 g C-CO<sub>2</sub> m<sup>-2</sup> yr<sup>-1</sup> (Kasimir-Klemetsson et al., 1997) which was estimated via peat soil subsidence, whereby oxidative loss was estimated using meteorological records.

---

<sup>f</sup> The figure reported by IPCC (2014) includes only one UK site which is the first three months of data from this study as reported by Morrison et al., (2013).

<sup>g</sup> Some papers only provided site averages for several crop on one field or several crops across several sites. Only those that are discernible as having sole root vegetable contribution are referred to here.

**Table 4.7:** Annual NEE (C-CO<sub>2</sub> m<sup>-2</sup> yr<sup>-1</sup>) details reported by IPCC (2014) wetland supplement references for fluxes from agricultural boreal and temperate peat soils. Excluding Morrison et al. (2013).

Paper	Location	Site details	Vegetation	Annual NEE
<b>Drösler et al. (2013)</b>	Germany	Lowland arable peat sites. Measured using chambers.	Maize and cereals.	922.37 (min 387.51, max 1364.46) includes equivalents)
<b>Kasimir-Klemedtsson et al. (1997)</b>	Finland, Sweden and Netherlands	Review of reported values for peat soils. Measured via subsidence (70% Oxidation) Oxidative loss from climatic data	GL, cereals (CL) and row crops (RC, potatoes and carrots)	300 (GL) 545 (CL) 1910 (RC)
<b>Elsgaard et al. (2012) (parallel study with Petersen et al. (2012) who measured N<sub>2</sub>O and CH<sub>4</sub> contributions)</b>	West, East and North Denmark. 55°56'N, 8°26'E, 56°23'N, 10°24'E, 57°14'N, 9°51'E	3 permanent grasslands (PG) and 5 rotational arable sites (RAR). Dynamic chamber technique.	Barley, barley/grass (BG), and potato	510 ± 90 (PG) 860 ± 200 (RAR) 1360 ± 360 (BG) 390 ± 540 (G)
<b>Maljanen et al. (2010), Includes: (Shurpali et al., 2009, Kasimir-Klemedtsson et al., 1997, Lohila et al., 2004)</b>	Nordic sites. 57°20' - 67°17' N, 13°30' - 30°58' E	Summary paper of agriculturally managed peat soils from seven studies in Nordic countries. Static and dynamic chambers	Grasses, barley, potato, carrot.	1790 (Mean) 3040 (Max) 290 (Min)
<b>Grønlund et al. (2008)</b>	Five counties of Norway.	11 sites largely southern. Changes in mineral content (MC), subsidence (Sub) and static chambers (SC)	Sub and MC: 30 years mostly grass, but also, potatoes, vegetables and barley. SC: One year grass and ryegrass	600 (SC) 800 (Sub) 860 (MC)
<b>Leifeld et al. (2011)</b>	'Grosses Moos' Witzwil, Switzerland, 46°59'N, 7°03'E 430 m a.m.s.l.	Four sites, measured by subsidence. P33- (GL) Staatswald - PG Spring – Crop rotation Lindenhof – Crop rotation.	Crop rotation sites grew wheat, root crops and GL	190 (P13) 500 (GL) 380 (Spring) 300 (Lindenhof)
<b>Lohila et al. (2004)</b>	Southern Finland. 60°53'N, 23°30'E	EC	SB GL	210.4 ± 28.38 (SB) 79.14 ± 24.83 (GL)

Estimates for cereal crops grown on temperate and boreal peat soils in IPCC (2014) ranged from  $-276$  to  $1364$  g C-CO<sub>2</sub> m<sup>-2</sup> yr<sup>-1</sup> (Table 4.7) (Beyer et al., 2015, Drösler et al., 2013, Elsgaard et al., 2012, Maljanen et al., 2010, Lohila et al., 2004, Kasimir-Klemedtsson et al., 1997). These mostly comprised of spring barley crops with a few maize crops grown for silage or corn-on-cob. The higher end of annual losses of CO<sub>2</sub> included Elsgaard et al. (2012) who reported an NEE of  $1270 \pm 450$  g C-CO<sub>2</sub> m<sup>-2</sup> yr<sup>-1</sup> as an average of four years of barley crop under-sown with grass in Denmark, which is within the uncertainty of the more recently published figure of  $900 \pm 150$  g C-CO<sub>2</sub> m<sup>-2</sup> yr<sup>-1</sup> reported by Poyda et al. (2016) for a spring barley crop grown in northern Germany (Table 4.6), which itself is within the uncertainty of the average annual NEE calculated here. Poyda et al. (2016) suggest that their figure may be below average due to unusual waterlogging at the site following harvest. Finish boreal sites report much lower net flux of  $210.4 \pm 28.3$  g C-CO<sub>2</sub> m<sup>-2</sup> yr<sup>-1</sup> (Lohila et al., 2004) which is attributed in the literature to the cooler boreal climate of Finland.

However, recent studies by Karki et al. (2015) and Kandel et al. (2013) report net CO<sub>2</sub> uptake of  $-120 \pm 80$  and  $-41 \pm 47$  g C-CO<sub>2</sub> m<sup>-2</sup> yr<sup>-1</sup>, respectively, for another Danish site growing spring barley (Table 4.8). The NEE uptake reflects a similar GPP but greatly diminished TER estimate compared to Poyda et al. (2016) (Table 4.6). Both sites reported similar mean annual WTD (roughly  $-0.4$  m) and Tair ( $7.4$  and  $9.6$  °C, Denmark and Germany respectively), but Kandel et al. (2013) report that no peak in CO<sub>2</sub> loss followed harvest at the Danish site unlike in this study, but that it was possibly missed due to sampling frequency. This likely contributed to some of this reduction in NEE estimate, and highlights the potential variability between sites growing the same crop under relatively similar conditions.

In 2013 colder conditions during spring led to reduced CO<sub>2</sub> loss, contributing to a reduced annual NEE. Similarly, Poyda et al. (2016) suggested that at their site TER processes were stimulated more than GPP by earlier growing season start, so shorter winters potentially increase the risk of C losses. Additionally, Poyda et al. (2016) recorded a greater annual loss of  $1120 \pm 230$  g C-CO<sub>2</sub> m<sup>-2</sup> yr<sup>-1</sup> (Table 4.6) for a summer wheat crop under sown with grass of in northern Germany, largely due to significant TER following multiple harvests and regardless of a high ( $-0.4$  m) WTD, despite assumptions made here that a site growing two crops might be expected to yield a

higher GPP and a reduced NEE. Compared to the large net loss of C reported by this and most other studies, Beyer et al. (2015) report the lowest annual figures of NEE identified in the literature for a crop grown on a drained peat soil. Four years of maize crop grown in southern Germany had an annual NEE of  $-276 \pm 249$  to  $252 \pm 156$  g C-CO<sub>2</sub> m<sup>-2</sup> yr<sup>-1</sup> (Beyer et al., 2015). This reduced loss (and net uptake) was attributed to a greater uptake for plant biomass and a high WTD of -0.28 m, although no within site trend was identified between annual mean WTD and annual NEE, as was the case at my study site (Chapter 3).

### Grasslands

The emissions factors for managed grasslands on temperate peat soil are reported by the IPCC (2014) to range from  $360 \pm 180$  g C-CO<sub>2</sub> m<sup>-2</sup> yr<sup>-1</sup> for shallow drained nutrient rich sites, to  $610 \pm 115$  g C-CO<sub>2</sub> m<sup>-2</sup> yr<sup>-1</sup> for deep drained nutrient rich sites. This suggests that peat soils under cropland, as studied here, are a more significant source of C-CO<sub>2</sub> than grassland. However, a more recent study of German peat soils by Eickenscheidt et al. (2015) found the NEE from arable sites growing maize and oats (Table 4.6) to be -6 to 1707 g C-CO<sub>2</sub> m<sup>-2</sup> yr<sup>-1</sup> but from grasslands sites to be at the higher end of this range at 1354 to 1823 g C-CO<sub>2</sub> m<sup>-2</sup> yr<sup>-1</sup>. Poyda et al. (2016) reported a similar range of annual NEE values for another study of German peat soils, but identified wetter sites with a higher average annual WTD (both grassland and arable) which had reduced NEE. Furthermore, Poyda et al. (2016) calculated an increased loss of 22 g C-CO<sub>2</sub> m<sup>-2</sup> yr<sup>-1</sup> for every 0.01 m increase in the depth of the water table below the peat surface. Although in my study there were no two complete years of the same crop, comparison of the two lettuce crop growing periods gave a 20 g C-CO<sub>2</sub> m<sup>-2</sup> reduction in net CO<sub>2</sub> loss for the 2012 crop which had an average 0.3 m shallower WTD. The limitations of this are that the 2012 crop period was 12 days shorter than in 2014 but accrued a similar number of accumulative degree days (527.5 and 545 °C, Figure 3.3).

Multiple reports find that grasses, spring barley, wheat, and potatoes grown on temperate peat soils are all large sources of CO<sub>2</sub> and conclude that arable cropping of peatlands does not lead to significantly different NEE compared to grasslands (Drösler et al., 2013, Elsgaard et al., 2012, Poyda et al., 2016). The findings here suggest that the annual CO<sub>2</sub> loss from salad crops is also within the same range of values as grasslands.

## Bioenergy

In addition to agricultural land uses for arable crops or grazing, several studies have investigated the potential for growing the bioenergy crop reed canary grass (RCG) on organic soils at sites previously used for either peat extraction or arable agriculture. Studies report large variance in annual NEE values: studies in Finland and Estonia show that sites under RCG are net sinks in the range of  $-8.7$  to  $-315.19$  g C-CO<sub>2</sub> m<sup>-2</sup> yr<sup>-1</sup> (Table 4.8) (Shurpali et al., 2009, Shurpali et al., 2010, Mander et al., 2012), whilst a study site in Denmark reports a net loss of 69 to 230 g C-CO<sub>2</sub> m<sup>-2</sup> yr<sup>-1</sup> (Kandel et al., 2013, Karki et al., 2015).

The difference between the NEE of the RCG crops at the Finnish and Danish sites (Table 4.8) is attributed by Kandel et al. (2013) to higher average temperatures (7.3 °C warmer) and deeper average depth of the water table at their Danish site (>50 cm). Additionally, they report that the RCG crop was harvested in August and the site remained without green cover over the (warmer, comparative to Finland) winter months, leading to increased TER over that period of the year compared to a neighbouring field with a vegetation cover of volunteer grass. Shurpali et al. (2009) report annual planting and harvest to have been undertaken in spring; this will have caused less site and soil disturbance, and limited exposure of the soil during the crop fallow period. These studies suggest that growing bioenergy crops on peat soils as an alternative to the salad crops of this study will lead to a net uptake of C-CO<sub>2</sub>, however fail to take into account the C removed in harvest.

Shurpali et al. (2009) reported RCG to have a high dependence on soil moisture and a high water table was necessary for the crop to be productive and for soil respiration to be reduced. Although in my own study the 2012 lettuce crop showed a small response of the residuals of the TER and T<sub>soil</sub> relationship to SWC, both WTD and SWC were previously shown to have had no significant control on NEE (Chapter 3).

**Table 4.8:** Annual NEE (g C-CO<sub>2</sub> m<sup>-2</sup> yr<sup>-1</sup>) details reported available literature on temperate and boreal peatlands managed for growing bioenergy crops.

Paper	Location	Site details	Vegetation	Annual NEE
<b>Karki et al. (2015)</b> (same site as <b>Kandel et al. (2013)</b> )	Viborg, Denmark, 56°44' N, 9°68' E	Drained fen peat for agriculture. Measured with Chambers (Opaque static)	Reed Canary Grass (RCG) and SB	230 ± 20 (RCG) -120 ± 80 (SB)
<b>Kandel et al. (2013)</b>	Viborg, Denmark, 56°44' N, 9°68' E	Drained fen peat for agriculture. Measured with Chambers (transparent dynamic) & LiCOR Gas Analyser, clear , phased to dark for varying PAR intensity	RCG and SB.	69 ± 36 (RCG) -41 ± 47 (SB)
<b>Mander et al. (2012)</b>	Estonia, 28°34'20"N, 24°23'15"E	Previously a peat extraction site. Static chambers used.	RCG on a fertilised (f) crop and a non- fertilised (nf)	-163.2 (f) -90.6 (nf)
<b>Shurpali et al. (2010)</b>	Eastern Finland, 62°30'N, 30°30'E	Previously a peat extraction site now cultivated. Measured using EC.	RCG	-315.19
<b>Shurpali et al. (2009)</b>	Eastern Finland, 62°30'N, 30°30'E	Previously a peat extraction site now cultivated. Measured using EC.	RCG	-211.4, -8.7, - 51.5, -126.6

In summary, the utilisation of peat soils for the production of bioenergy crops has been shown to result in a reduced loss of C-CO<sub>2</sub> compared to the salad and bulb crops studied here, albeit without taking yield into consideration (see below). Lower levels of site disturbance during the management of RCG crops and a limited fallow period were the most likely causes of this difference.

#### Restored

Intensive agricultural management of peat soil results in a loss of C from the soil C store whether it is for salad, cereal or bioenergy crops. But it has been shown that the restoration of peat soils before the peat is completely depleted can lead to the peatland re-establishing a C sink potential. A restored peatland previously used for agriculture in the Netherlands has been reported as being an annual sink of  $-446 \pm 83$  to  $-232 \pm 57$  (Hendriks et al., 2007). Following the cessation of agricultural use the site was managed as a wetland nature reserve for ten years with a shallow water table that fluctuated

between 0.05 and 0.45 m. Although a considerable loss of CH<sub>4</sub> was reported, the site remained an annual net sink of C.

#### 4.4.3 NECB: import and yield

Here it was found that importing germinated crops in peat plugs led to a field gain of 51 to 64 g C m<sup>-2</sup> however, no comparative data could be found. Kutsch et al. (2010) report a value of 5 g C m<sup>-2</sup> for C<sub>i</sub> of grain crops for a drained Danish peat bog, which is comparable to the 2.16 g C m<sup>-2</sup> reported here for the leek plus barley cover crop, and reflects the difference in planting density of these crops.

Yield is regularly reported in studies of GHG balance for arable crops on peat soils, however no studies could be found for lettuce, leek and celery crops. The majority of the available information focuses on peatlands used for perennial grassland, spring barley, and bioenergy crops.

While I report a yields of 35, 110, 32 and 74 g C m<sup>-2</sup> for the lettuce, leek, lettuce and celery crops respectively, several German and Nordic peatland studies have reported greater yields, and specifically for the cereal crops spring barley, summer wheat (*Triticum aestivum*) and maize with yield values of 126 to 470, 650 and 58 to 457 g C m<sup>-2</sup> yr<sup>-1</sup>, respectively (Eickenscheidt et al., 2015, Drösler et al., 2013, Elsgaard et al., 2012, Lohila et al., 2004, Beyer et al., 2015, Poyda et al., 2016). The high C<sub>e</sub> value of 650 ± 70 g C m<sup>-2</sup> yr<sup>-1</sup> reported for a summer wheat crop was for a German peat soil site (Poyda et al., 2016), with the higher C<sub>e</sub> in part due to an under sown ryegrass (*Lolium perenne*) crop that was also harvested, resulting in a dry matter yield of 1460 ± 160 g m<sup>-2</sup> yr<sup>-1</sup>.

The greatest range of available yields are presented by studies of grassland grown on German, Swiss, Nordic (Finnish, Danish, Swedish, Norwegian), Dutch and Irish peat soils with values from 0 to 593 g C m<sup>-2</sup> yr<sup>-1</sup> (Eickenscheidt et al., 2015, Elsgaard et al., 2012, Lohila et al., 2004, Beyer et al., 2015, Poyda et al., 2016, Tiemeyer et al., 2016, Leiber-Sauheitl et al., 2014, Beetz et al., 2012, Grønlund et al., 2006, Renou-Wilson et al., 2014, Leifeld et al., 2011). The greater yield values are usually a result of multiple annual grass harvests and the lesser values to sites where no grass was removed. The average reported value for C<sub>e</sub> at all these grassland sites is roughly 300 g C m<sup>-2</sup> yr<sup>-1</sup>, which is much greater than the range of values (32 to 110 g C m<sup>-2</sup>) found for the lettuce, leek and celery crop harvests.

Similar  $C_e$  values to those reported here were reported for a drained agricultural Finnish peatland, previously used for extraction, but now growing bioenergy crops. Despite a longer growing period and higher density of crop planting compared to the crops studied here, the RCG yield in Finland was between  $76 - 181 \text{ g C m}^{-2} \text{ yr}^{-1}$  (Shurpali et al., 2009, Shurpali et al., 2010), although this range was low in comparison to a Danish RGC site where  $540 \text{ g C m}^{-2}$  was reported (Karki et al., 2015, Kandel et al., 2013). The greater yield of the RCG crop at the Danish site is attributed to higher PAR, temperature and a longer growing season than experienced in Finland. The difference in yields of the two lettuce crops grown in 2012 and 2014 at this study site is more likely a reflection of cosmetic quality criteria for crop harvest that leads to limited harvest rather than environmental controls. Following all four harvests an unquantified amount of crop waste remained on the field. It is estimated that only 70% of crops in the UK are harvested (IMEchE, 2013) due to their physical characteristics not meeting guidelines set out by major supermarkets.

#### NECB

Harvest of biomass has been shown to be a substantial contributor to the C balance of agricultural sites. Grazing and cuttings offtake from a grassland in Ireland was reported to contribute to more than 50% of the site C loss, reversing the site from a net sink to a net source of C (Renou-Wilson et al., 2014). Whilst the agricultural site studied here was already a large source of C from NEE of  $\text{CO}_2$ ,  $C_e$  was calculated to contribute between a further 4 and 16% of C loss on an annual basis. In the case of the plug crops, however, this was largely (completely, in the case of the lettuce crops) counter balanced by the  $C_i$  associated with the addition of the plug media onto the site. There have been a number of studies of arable peat soils where the site was operating as a net sink of C as  $\text{CO}_2$  but accounting for  $C_e$  led to the site becoming a net source of C to varying degrees (Shurpali et al., 2009, Eickenscheidt et al., 2015, Kutsch et al., 2010, Beyer et al., 2015, Karki et al., 2015, Kandel et al., 2013). In this study the leek crop of 2013 experienced the longest growing period and lowest net C- $\text{CO}_2$  emission,  $675.75 \pm 101.45 \text{ g C-CO}_2 \text{ m}^{-2} \text{ yr}^{-1}$ , which was just within the uncertainty bounds of the 2014 lettuce and 2015 celery crops. The leek crop however had the greatest additional net loss of C due harvest of  $109.85 \text{ g C m}^{-2}$ , which led to the annual NECB for the three years of observations here being well within uncertainty of one another ( $\pm 33 \text{ g C m}^{-2} \text{ yr}^{-1}$ , Table 4.4).

#### **4.5 Chapter summary**

This chapter has presented daily, crop and fallow period, and annual sums of NEE from EC measurements made over 3.5 years. Management activities, which included ploughing, harvesting of the crop and application of selective herbicides, were identified as causing maximum daily losses of C-CO<sub>2</sub> from the biosphere to the atmosphere, whilst maximum daily C-CO<sub>2</sub> uptake was related to each crops' period of peak light use efficiency, usually shortly before harvest.

It was expected that a longer crop growing period would result in a greater CO<sub>2</sub> uptake. The results presented in this chapter found that despite the extra month of growth for a celery crop in 2015 (and the maximum measured daily uptake values) the annual loss equalled that of a lettuce crop grown over two months in 2014. Additionally, a leek crop, grown over six months, recorded the highest loss of C-CO<sub>2</sub> compared to the other shorter crop growth periods despite having almost double the planting density of the plug crops.

## **Chapter 5: Wind-blown C flux across an intensively cultivated drained lowland deep peat soil**

This chapter addresses research question 6: How much C is transported over intensively cultivated peatlands in East Anglia by aeolian action?

The nature of low density peat cultivated for annual crops in a low lying region such as Eastern England is that the peat surface is often exposed and dry during months experiencing high  $u$ , specifically during the spring when the soil is being prepared for planting (Wilson and Cooke, 1980). As a result, “Fen blow” is a commonly experienced phenomenon in this region. These blows, and lesser events, lead to a horizontal mass flux and a potential loss of peat soil and associated C from agricultural fields; this flux has not been quantified. While the wind eroded flux of C is important and a particular focus of this work, it also has a negative impact on agricultural production, since wind-driven soil erosion can damage young crops, thereby reducing yields.

Here the horizontal mass flux (HMF) is quantified. The chapter describes the methodology employed; the use of two arrays of Big Spring Number Eight (BSNE) samplers which were installed at the same intensively managed agricultural study site described in previous chapters. An explanation is provided of the best established practice for the collection of wind-blown peat soil samples in order to measure HMF and to quantify longer term horizontal mass transport (HMT).

The results of wind-erosion monitoring are supplemented by exploring potential driving environmental variables: horizontal wind speed ( $u$ ), soil water content (SWC), friction velocity ( $u^*$ ) and vegetation height using data provided by the EC tower described in Chapter 2.2.2 and with some additional observations.

This chapter reports and analyses the first known quantification of horizontal mass transport (HMT) of C from a cultivated fen peat soil with an accompanying investigation of the drivers of mass transport, conducted over multiple years and crop cycles.

## 5.1 Methodology

### 5.1.1 Study site

Wind erosion was quantified in two locations; the first was co-located with the EC tower, referred to here as array A in field A, and the second 150 m 40° northeast, referred to here as array B in field B (Figure 5.1, A and B respectively). Both locations were bounded on the northeast side by ditches running along a 135-315° transect, whilst the south westerly side (dominant wind direction) faced open fields.

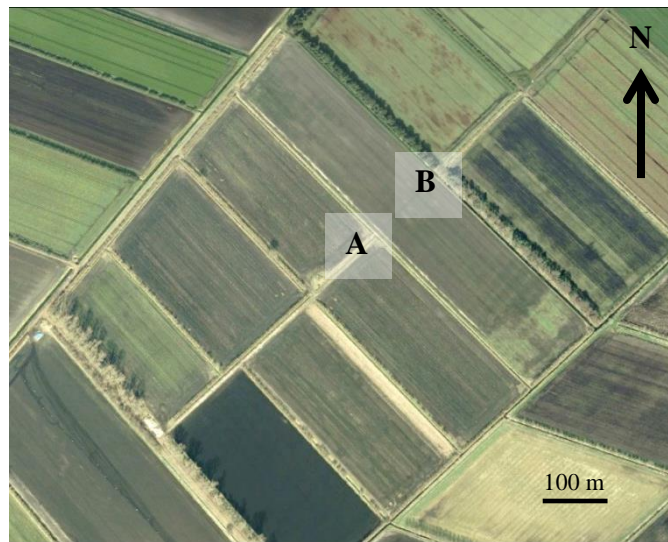


**Figure 5.1:** Annotated aerial photograph of the field site, A – BSNE array A, B – BSNE array B, Google maps (2009)

Regional and Rosedene Farm information is described in Chapter 2.1.3. Given that field A also contains the EC instrumentation, field specific information on management and crops grown on field A have also already been provided in Chapter 2.1.3 along with photos of field surface conditions, notably Figures 2.3, 2.4 and 2.5. However, the data in this chapter goes beyond the end date of the EC observations and so the additional crop information of 2016 for field A is given here with a description of the field cover for all years, along with the same information for field B.

#### 5.1.1.1 Field surface

In May 2016 a romaine (or cos) lettuce (*Lactuca sativa L. var. longifolia*) crop was planted on field A. Figure 5.2a gives the vegetation heights which shows that during the crop periods the canopy height increased gradually after initial crop planting until maximum crop canopy was reached shortly before harvest. The vegetation canopy

across the field was predominantly homogenous<sup>h</sup> during crop growth, peaking at average heights of 0.8 (leek), 0.25 (lettuce) and 0.7 m (celery), in 2013 to 2015 respectively. After each harvest, the crop residuals and weeds made up a low heterogeneous canopy, with height values averaged for the post-harvest period. This vegetation cover was turned into the topsoil within a month of harvest, which resulted in a re-homogenising of the field surface in 2014 and 2015, followed by the development of a secondary weed cover peaking at 0.32 and 0.2 m in 2014 and 2015, respectively (the weeds in 2014 exceeding the maximum crop height for that year). These weeds were sprayed with herbicide but left on the surface as soil cover during the winter months. Due to the later harvest of the leek crop in 2013 the crop remnants were left on the field over winter and no secondary weed cover was established. The romaine lettuce crop of 2016 was not fully developed when measurements ended, but had reached a height of 0.13 m by the end of the dataset (end of May 2016).

Figure 5.2b shows the canopy cover for field B where patches of iceberg lettuce were trialled in 2013, but the field was dominated by weeds that grew to a height of 2 m and were cut in late autumn. In 2014 an onion crop (*Allium cepa L.*) was grown from 10<sup>th</sup> March – 1<sup>st</sup> September following the same strategy as with leek (grown on field A in 2013) whereby barley was sown to stabilise the top soil during the early crop establishment before being sprayed with targeted chemicals before the onion crop grew through. This crop was largely un-harvested due to a widespread disease affecting the majority of the crop (M Hammond, Pers. comm.). The onions were gathered into piles and left to decompose before eventual inclusion into the top layer of soil or removal from the field. Crop height was less than that of leek grown in field A during 2013. For 2015 a barley (*Hordeum vulgare L.*) crop was grown from February to September, which grew to an average height of 0.8 m. All but the bottom 0.1 m of the barley was harvested in September with the bristle remaining on the field through the winter, until ploughing of the field in 2016.

---

<sup>h</sup> Sparse weeds grew taller than the crop canopy, and sections of crops underperformed due to localised issues, e.g. wind-blows damaging crop development.

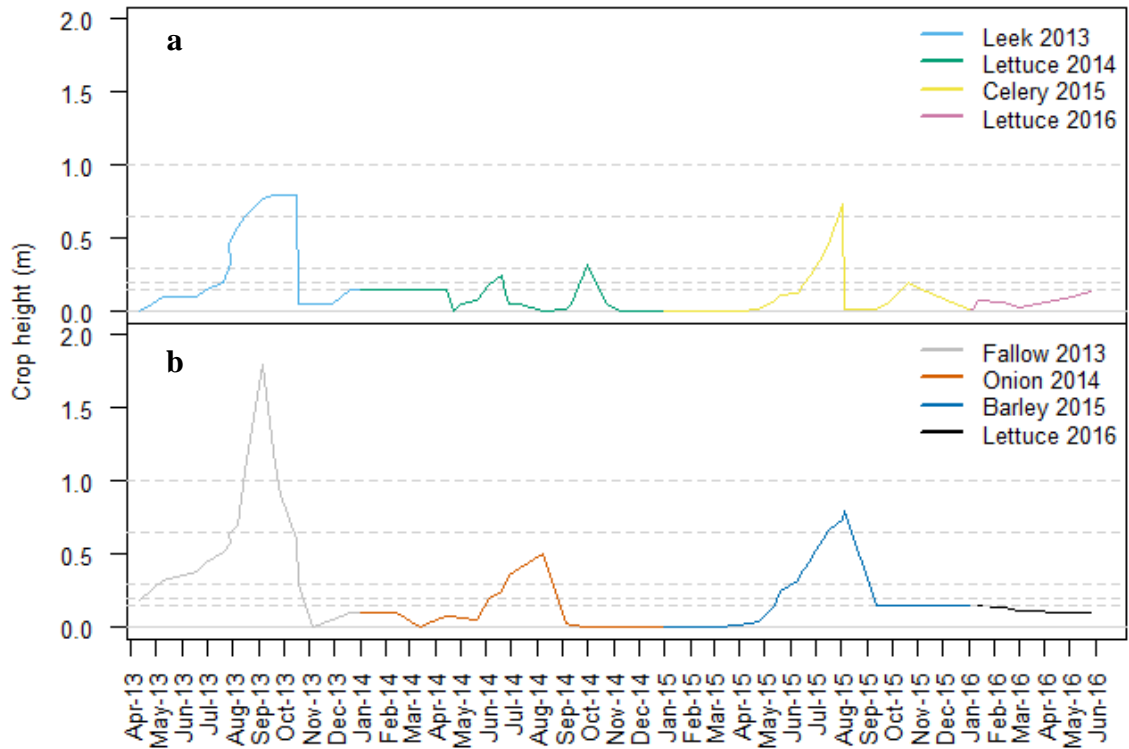


**Figure 5.2:** Average canopy heights for each field. **a:** Field A. **b:** Field B. Canopy height is the average vegetation height in meters measured on the day of field visits for sediment sample collection ( $n > 20$ ) and linearly interpolated between collection dates. Horizontal light-grey dashed lines are the measurement heights of the wind erosion sediment samplers (BSNEs, see below 5.1.2), and the solid grey line delineates 0 m.

The 2016 lettuce crops on each field were only recently planted when the measurement period ended. A staged lettuce crop was grown on field B in 2016, and half of the field (the first, earlier planted, stage) was grown under fleecing for several weeks to avoid damage by frosts.

Areas of non-vegetated surface (bare peat) were evident not just following ploughing and disking (details of which are provided in Table 5.2) but also as 5–10 m buffer strips between the field edge and the crops. Photographs in Figure 5.3 demonstrate the variety of peat soil surface conditions seen in the fields including: cracked dry peat (Figure 5.3a), waterlogged areas (Figure 5.3c) predominantly in compacted machinery tracks, and loose freshly disked surface peat conditions (Figure 5.3b).



**Figure 5.3:** Soil cover conditions during fallow periods. **Top left, a:** Dried and cracked peat, May 2014. **Bottom left, b:** Ploughed, loose topsoil, March 2014. **Right, c:** Standing water in machinery tracks around entrance to field A, October 2014.

#### 5.1.1.2 Ditch vegetation

Ditches bounded both fields A and B. A row of trees roughly 3.5 m tall lined the north east side of the ditch on the north east edge of field B (background Figure 5.4a), and will have prevented substantial aeolian sediment transport by north-easterly winds and therefore limited sediment collection in samplers year round. The ditch between field A and B was lined with weeds and riparian vegetation which underwent annual management (Figure 5.4 a-d), whereby they were cleared early in most winters and grew to 1 - 1.5 m during the growing season. When present, this ditch vegetation acted as a wind break limiting horizontal sediment flux in both south-westerly and north-easterly directions across the ditch and was often observed to trap sediment. The reduced height of this wind-break vegetation between the two fields of interest (Figure 5.4b) prior to the winter and early spring months, when peak  $u$  was measured, will likely have allowed for increased aeolian sediment transport across the ditch.



**Figure 5.4:** Ditch weed and riparian vegetation condition between fields A and B facing south east. **a:** top left: August 2013, with ditch vegetation taller than BSNE's. **b:**, top right: March 2014, ditch was cleared in winter months. **c:**, bottom left: June 2014, riparian vegetation taller than crops and BSNE's, ditch weeds minimal. **d:**, bottom right: September 2015, both fields have been harvested and both ditch weeds and riparian vegetation are high again. All photos were taken by the author.

### 5.1.2 Samplers

Wind-blown soil can be collected using active or passive samplers. Active samplers have a greater capability for trapping finer particles and allowing for a reduction in static pressure by pumping air flow out of the sampler and trapping sediment in a fine

filter. But active samples require a constant power source. By comparison, passive samplers require no power source and require a coarser filter, so are more commonplace in measurements of horizontal mass flux (HMF), but underestimate the fine fraction of HMF as these can be both re-activated by high winds and gusts entering the sampler and transported through the filters (Shao et al., 1993, Mendez et al., 2011).

In this study, Big Spring Number Eight (BSNE, Custom Products, Big Spring, TX, USA) passive dust samplers were used for measuring aeolian dust transport as described by Fryrear (1986) (Figure 5.5). Whilst passive samplers are not as accurate at measuring HMF, BSNE's have been demonstrated to provide a complete representation comparative to more sophisticated samplers (Goossens and Buck, 2012). The BSNE sampler entrapment efficiency has been estimated by previous research as being up to 90% for sand particles (Fryrear et al., 1991, Shao et al., 1993) but only 10%-45% for finer particles of soil (Goossens and Offer, 2000, Shao et al., 1993, Sharratt et al., 2007) (Table 5.1).

**Table 5.1:** Summary of sampling efficiencies reported in the literature for BSNE samplers.

<b>Paper</b>	<b>Sampling efficiency</b>	<b>Soil type</b>	<b>Particle size</b>	<b>Wind speed (m s<sup>-1</sup>)</b>
<b>Warburton (2003)</b>	70-120%	Peat	-	-
<b>Fryrear et al. (1991)</b>	89%	Sand – sieved soil	<250 $\mu$ m	10 - 15
<b>Goossens and Offer (2000)</b>	35-45%	dust	<30 $\mu$ m	1 - 5
<b>Goossens and Offer (2000)</b>	35-45%	dust	<30 $\mu$ m	1 - 5
<b>Shao et al. (1993)</b>	40%	dust	100 - 10 $\mu$ m	8 - 12.5
	90% +/- 5%	sand	1000 $\mu$ m	8 - 12.5
<b>Sharratt et al. (2007)</b>	10%	Silt loam	PM10 (2.5-10 $\mu$ m)	18
	25%	Silt loam	PM10 (2.5-10 $\mu$ m)	5

Whilst Goossens et al. (2000) found the BSNE not to be the most efficient dust collector in a wind tunnel, they did observe the least variation in efficiency with relation to wind speed, whilst other samplers showed considerable changes in efficiency in relation to wind speed. The only study that assessed efficiency for BSNEs on peat soils gave a figure of 70 to 120% (Warburton, 2003). Sampling efficiency is not calculated in this chapter due to difficulties in assessing the particle size of peat samples, but it is

acknowledged that the sampling efficiency could be causing an uncertainty in a similar range.



**Figure 5.5:** Photographs of BSNE sampling arrays, installed at measurement heights of 0.15, 0.2, 0.3, 0.65 and 1 m, photos taken by author.

A variety of assemblage strategies were identified in the available literature from as few as 3 measurement heights to 9, but notably it has been shown that greater sampling density in one vertical location results in improved estimates of HMF (Panebianco et al., 2010). Here, two arrays of samplers were installed to measure horizontal mass flux (HMF) at measurement heights of 0.15, 0.2, 0.3, 0.65 and 1 m (Figure 5.5). A greater density of measurements were made closer to the ground as the major part of mass flux is reported to occur nearer the surface (Panebianco et al., 2010). Single unit samplers were installed at 0.65 m and 1 m above the surface, while a triple sampler was installed below this which allowed for denser measurements at heights of 0.15, 0.2 and 0.3 m above the surface where the majority of peat transport is reported to happen (<0.3 m; Warburton (2003)). The lowest possible measurement elevation for the BSNE is 0.15 m, although Panebianco et al. (2010) showed that estimates of the region between 0-0.15 underestimated HMF, so any calculation of HMF will have to account for this. The 0.65 and 1 m samplers were chosen in an attempt to get a representative profile of lower boundary layer values for HMF on an annual timescale. Calculation of HMF is discussed in the data analysis section below.

### *Sample collection and processing*

Samples were collected roughly once a month, and more frequently in the spring months of April and May in 2014 in an attempt to discern and quantify the impact of ploughing against, and in conjunction with, periods of unsettled atmospheric conditions. Weeds that grew around the samplers (obstructing their rotation) were cleared when necessary during site visits.

Distilled water was used to rinse dust from a collector into a 250 ml polypropylene bottle. The samplers cannot prevent rainfall from entering but excessive rainwater should have been able to flow out of the samplers through the 60 µm mesh side panels (designed for the discharge of wind flowing through the sampler) to limit the removal of previously accumulated dust. As there can be no drainage under the height of the mesh side panels, it was often the case that the samplers contained rain water in addition to wind-blown material. In these situations the rainwater was collected and the sampler rinsed. Fine sediment seen to be stuck to the collector was aggravated with a brush and washed out with the distilled water. Each BSNE collector was rinsed three times with distilled water into the bottles regardless of the amount of precipitation present. Occasionally insects (notably: earwigs (*Dermaptera*), flies (*Diptera*) and small spiders (*Araneae*)) and their nests were found in samplers. While efforts were made to remove these and still collect the samples, this was not always possible and some samples were corrupted and had to be removed from later analysis. Once back in a University of Leicester laboratory the bottles were decanted and rinsed three times into aluminium trays, and where necessary the bottles were also cleaned with a brush to ensure all the sample was removed from the bottle. The samples were then dried in an oven at 105 °C for 24-48 hours before weighing on an analytical balance (OHAUS Adventurer, Parsippany, New Jersey, USA) with a precision of 0.0001 g.

Loss on ignition was undertaken where enough of a sample was collected for results to be significant. These samples were combusted in a furnace at 450 °C for 4.5 hours to determine the organic matter content of the transported material.

Aggravation of the sample during the process of collection from the samplers meant that it would be unreasonable to undertake particle size analysis.

### *Calculating horizontal mass flux (HMF) of peat*

Horizontal mass flux (HMF) is quantified as the mass of soil material retained after passing through an inlet area at a point in a vertical profile and is usually reported as g or kg per m<sup>-2</sup> (Mendez et al., 2011, Panebianco et al., 2010, Fryrear et al., 1991, Warburton, 2003).

$$\text{HMF, } q \text{ (g m}^{-2}\text{)} = \text{Mass, } m \text{ (g)} \times \text{area, } a \text{ (m}^{-2}\text{)} \quad \text{Equation 5.1}$$

As the collection periods of the sediment differed, the HMF is divided by the number of days of collection and reported in g m<sup>-2</sup> d<sup>-1</sup> to make values comparable with previous studies.

### *Interpolating HMF to horizontal mass transport (HMT)*

Horizontal mass transport (HMT) is given as the integration of the amount of soil material passing through an area of horizontal plane between two defined heights.

Values of HMF can be interpolated linearly between collection heights, which is regarded as a powerful, robust and simple way to estimate mass transport (Panebianco et al., 2010). HMT is then given by:

$$\text{HMT, } Q_l \text{ (g m}^{-2}\text{)} = \int_{z_b}^{z_t} q \text{ (g m}^{-2}\text{)} \quad \text{Equation 5.2}$$

Where  $Q_l$  is the horizontal mass transport integrated over a vertical profile between two heights.

Alternatively, exponential functions (such as equation 5.3) have been shown to produce good agreement with measured fluxes (Namikas, 2003, Mendez et al., 2011), for example:

$$Q_e = \int_{z_b}^{z_t} a \cdot \exp^{bz} \quad \text{Equation 5.3}$$

Where  $Q_e$  is the exponential horizontal mass transport integrated over a vertical profile between two heights in g m<sup>-2</sup>,  $a$  and  $b$  are regression coefficients, and  $z$  is height from the soil surface ( $z_t$  top height of integration and  $z_b$  the bottom height of integration). This exponential equation was found to be most stable in its estimates and comparable to linear spline interpolation over limited measurement points in a study by Panebianco et al. (2010).

Both integrated linear spline interpolation and exponential function (Equation 5.3) were applied to calculate HMT for each of the collection periods here and these values are compared in Figure 5.6. Integrated from 0.15 to 1 m height above the peat surface, Figure 5.6 shows that both the exponential and linear spline methods gave similar HMT values especially at low yields ( $<80 \text{ g m}^{-2}$ ) of HMT. As HMT increased, however, either the exponential method led to underestimation or the linear interpolation to an overestimate which led to a difference in peak HMT of  $\sim 100 \text{ g m}^{-2}$ .

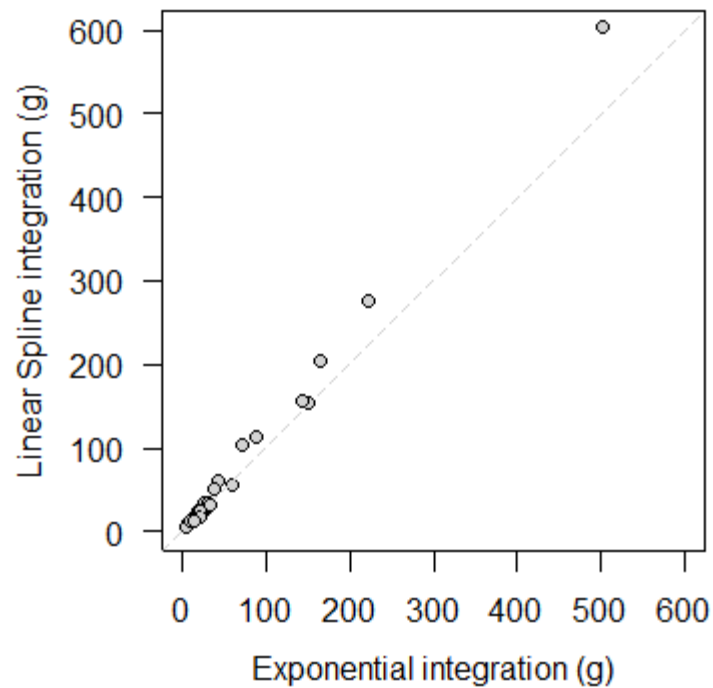


**Figure 5.6:** Comparison of integration of linear spline and exponential fit techniques. Data was taken from array A samples and HMT calculated by linear spline interpolation, Equation 5.2 (y axis) and via fitting to an exponential function, Equation, 5.3 (x axis).

Furthermore when fitting the exponential over the 0–1 m height range the discrepancy between the two fits was more drastic with the exponential function instead calculating significantly greater HMT values than the linear spline method over the same height range. Whilst both fitting techniques assume (reasonably) that transport at 0 m is  $0 \text{ g m}^{-2}$ , Shao (2005) showed that for large sediment particle size and low turbulence vertical HMT can be exponential, and increasing mass can be measured closer to the ground (Panebianco et al., 2010). Whilst the linear spline integration may be correct in its assumption that the mass transport reduces to zero below 0.15 m it is also possible that,

if conditions are suitable, the linear spline method will not measure the peak flux and will lead to an underestimation of  $Q$ .

Panebianco et al. (2010) compared linear spline interpolation and several exponential functions and concluded that at agricultural sites, where mass flux can be irregular, HMT can be poorly represented by regression procedures, leaving linear spline interpolation as a feasible and simple alternative. Therefore, the linear spline method was implemented here.

### 5.1.3 Environmental conditions

Wind erosion results from an imbalance of stress exerted by the wind and climate on soil (erosivity) and the strength of the soil to resist stresses (erodibility) (Funk and Reuter, 2006). The extent of aeolian sediment flux is understood to be controlled by meteorology, soil, and vegetation properties and interactions between them (Panebianco et al., 2010, Dawson and Smith, 2007).

Greater aeolian fluxes are expected in combination with high wind and friction velocities, however, the threshold of velocities required to activate wind erosion depend on the erodibility of exposed soil and an understanding of sediment size which is not measured here (Funk and Reuter, 2006, Dawson and Smith, 2007, Zobeck et al., 2003, Warburton, 2003). The soil type and condition undoubtedly have an impact on soil erodibility, accordingly soil moisture and organic matter content will impact aggregation and therefore increase particle size and increase the required wind speed to mobilise particles. Vegetation cover is generally the best way to decrease erodibility of soil, with a cover of 40% or more preventing wind erosion completely (Funk and Reuter, 2006).

Half-hourly meteorology data of  $u$ , friction velocity ( $u^*$ ) (as defined in Chapter 2.2.3, using momentum fluxes, Equation 2.4) and soil water content (SWC) were taken from the instrumentation described in Chapter 2 as part of the EC system (Chapter 2.2.2) in field A. There was no instrumentation to monitor these variables in field B, and therefore the same dataset was used for field B; the limitations of this approach are acknowledged. Sediment flux measurements began almost a year after EC measurements on 12<sup>th</sup> April 2013 and, to complete three full years of measurements, continued until 25<sup>th</sup> May 2016. The meteorology presented here is therefore for this period within which there were 45 individual periods of dust collection. Half-hourly

meteorological values are considered in terms of their contribution within each period, whereby means of the 30 minute average for each period are given along with the maximum and minimum 30 minute average measurement, as shown in Figure 5.7. An additional record of crop canopy observations made during site visits for both fields is also reported here.

Management activity (i.e. ploughing, harvesting, disking) is expected to exacerbate aeolian soil flux, most notably during dry and windy spring months (Dawson and Smith, 2007). A record of regular site management activities for both fields is given in Table 5.2; additional detail of management in field A was provided by the land owners and is given in Table 2.1 in Chapter 2.1.3.

**Table 5.2:** Field activity dates.

<b>Activity</b>	<b>Field A</b>	<b>Field B</b>
Ploughing	30 <sup>th</sup> March 2013, 22 <sup>nd</sup> March 2014, 3 <sup>rd</sup> February and 8 <sup>th</sup> May 2015 -	- Beginning March 2014 2 <sup>nd</sup> February 2015 -
Planting	10 <sup>th</sup> April 2013, 29 <sup>th</sup> April – 2 <sup>nd</sup> May 2014, 12 <sup>th</sup> May 2015 1 <sup>st</sup> May 2016	- 10 <sup>th</sup> March 2014, 3 <sup>rd</sup> February 2015, 1 <sup>st</sup> May 2016
Harvest	17 <sup>th</sup> - 22 <sup>nd</sup> October 2013, 20 <sup>th</sup> - 27 <sup>th</sup> June 2014, 31 <sup>st</sup> July - 12 <sup>th</sup> August 2015	- 1 <sup>st</sup> September 2014, 11 <sup>th</sup> September 2015
Disking	Leek residuals left End of July 2014 End of August 2015	- Mid-September 2014 Barley stubble left as wind break

## 5.2 Data analysis

### 5.2.1 Environmental conditions

#### *Wind velocity ( $u$ ) and direction*

Over the complete sediment measurement period the average half hourly  $u$  (at 1.55 m height) was  $2.16 \text{ m s}^{-1}$  with maximum velocities of  $9\text{--}12 \text{ m s}^{-1}$  measured predominantly during winter and into the early spring months when they constituted a large percentage of the  $u$  (Figure 5.7 and 5.8). The average half-hourly  $u$ , which ranged from  $1.1$  to  $3.4 \text{ m s}^{-1}$ , was calculated for each of the sediment collection periods and presented in Figure 5.7. The average half hourly wind direction was  $194^\circ$  (south by south-west) for the complete period of sediment collection (April 2013–June 2016).

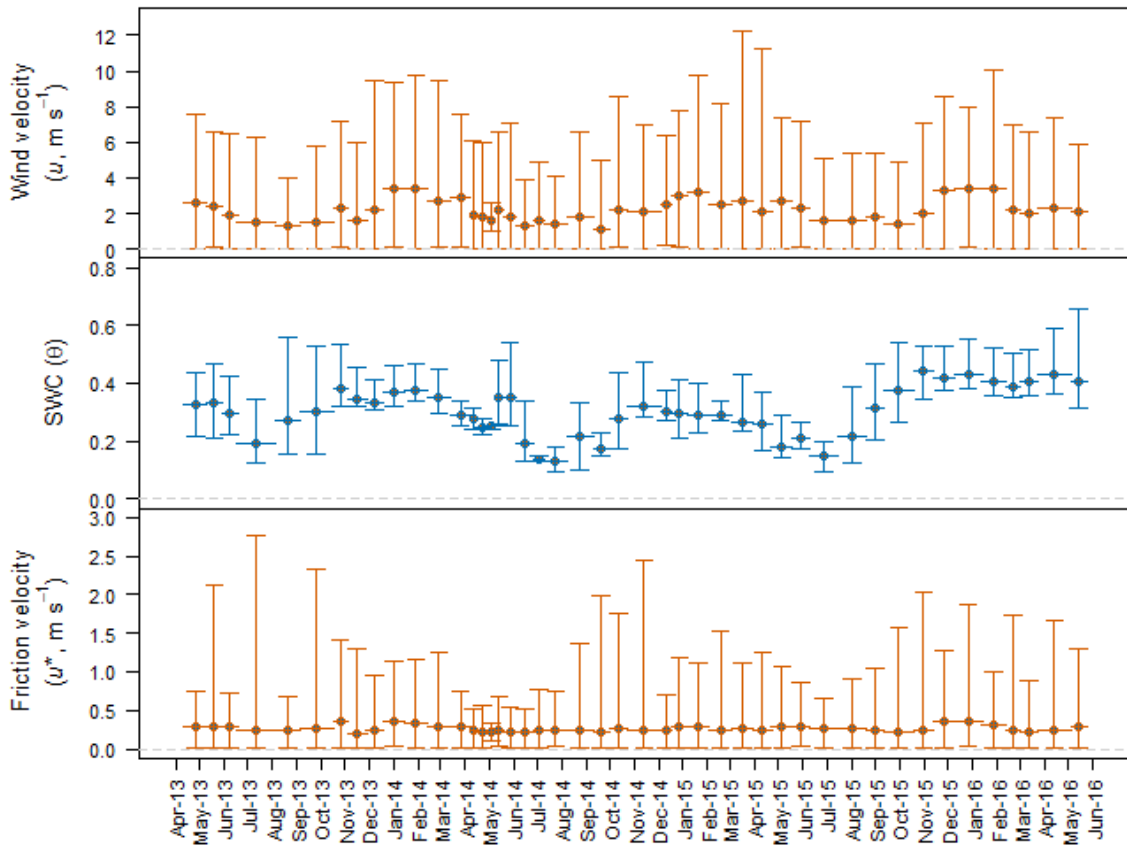


**Figure 5.7:** Averages, minimums and maximums of environmental variables for periods of sediment flux accumulation. **a** – Horizontal wind velocity at 1.55 m height. **b** - soil water content at 0.1 m depth. **c** - friction velocity ( $u^*$ ). All values were taken from the 30 minute resolution data, and the mean (points) are the average 30 minute value for each dust collection period (represented by the horizontal lines through the points, which extend from the start to the end of each measurement period), while the vertical lines extend between the maximum and minimum recorded 30 minute value for each period.

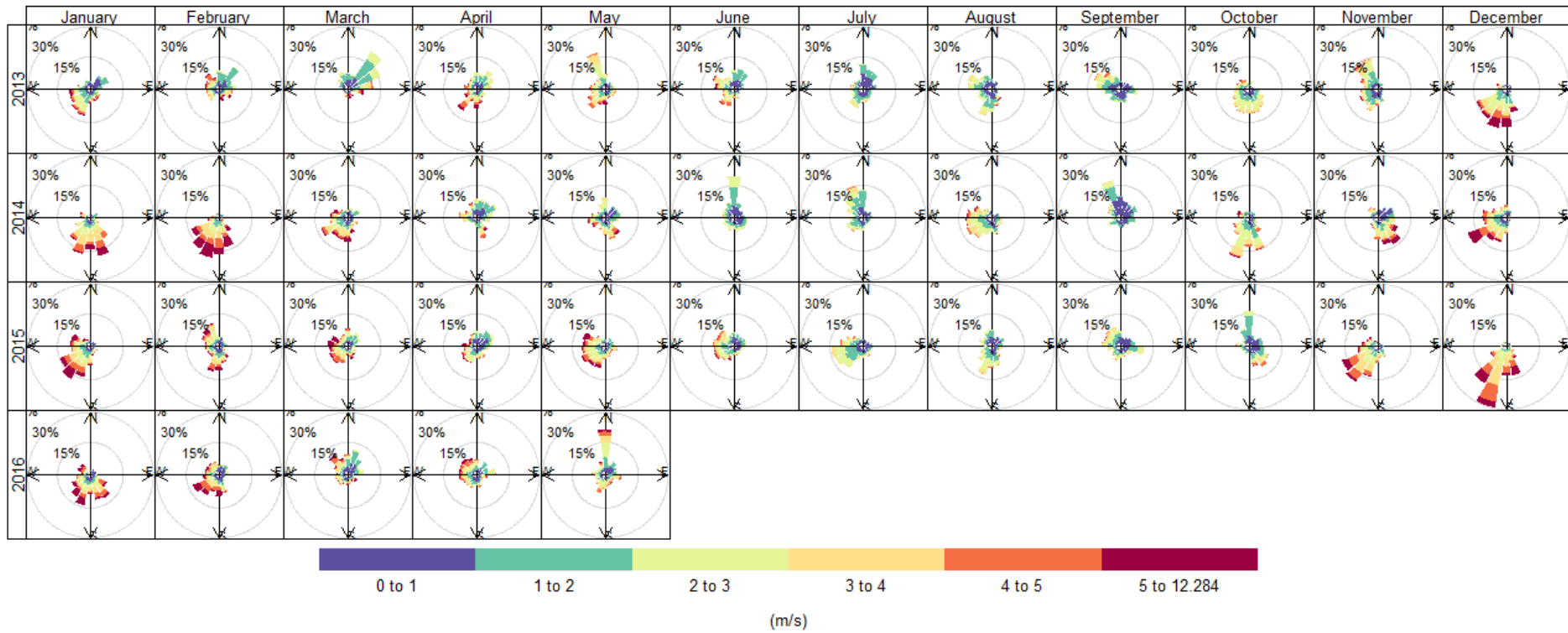


**Figure 5.8:** Wind rose plots describing the 30 min average wind velocities and directions.

Despite several days and weeks of colder conditions in late winter and early spring that were brought on by dominant conditions descending from the north and north-easterly bearing, most notably in March of 2013 and April 2014 (Figure 5.8), the average wind direction for each sediment collection period was between 128 and 245°.

#### *Soil moisture*

Half hourly volumetric soil water content measurements made in the top 0.1 m of the soil profile had an overall range of 0.09 to 0.62 ( $\text{m}^3 \text{m}^{-3}$ ) with a mean of 0.3 ( $\text{m}^3 \text{m}^{-3}$ ). The mean half hourly value was again calculated for each sediment collection period (Figure 5.7) which had a narrower range of mean values from 0.13 to 0.44 ( $\text{m}^3 \text{m}^{-3}$ ). Soil moisture was impacted by management strategy that included the application of above ground irrigation and pesticides, with significant increases in SWC during the crop growing period due to both irrigation and rainfall events. The lowest mean values were calculated during summer collection periods when moisture use by crops was high, despite added irrigation, and loss by evaporation was high. Peaks in the mean values corresponded with winter months, increasing the  $u$  threshold for wind erosion. Spring months of April and May, which have been highlighted for their soil erosion potential, were significantly drier in 2015 than the other three years.

#### *Friction velocity ( $u^*$ )*

Average half hourly  $u^*$  for the 45 periods of sediment collection ranged from 0.19 to 0.36  $\text{m s}^{-1}$ , with above average values ( $>0.27 \text{ m s}^{-1}$ ) and peak maximum values ( $>1.5 \text{ m s}^{-1}$ ) measured during the late autumn and winter periods (that included November, December and January) which coincided with peaks in mean wind velocities (Figure 5.7). The maximum half hourly  $u^*$  of 2.77 was unusually recorded during July of 2013.

#### 5.2.2 Vertical distribution of horizontal mass flux (HMF, $q$ )

Wind-blown peat was present in nearly all samples collected throughout the year with notable peaks in transport during dry months in March, April and May, and almost no peat collected during peak vegetation growth months of June and July and minimal transport during wet autumn and winter months from October through to February, despite the peak annual wind velocities during the latter (Figure 5.7). For every period of collection, HMF was found to rapidly decline with height for both arrays, with the bulk of HMF occurring below 0.3 m (Figure 5.9 and 5.10).

The maximum daily averaged  $q$  values for each measurement height (1, 0.65, 0.3, 0.2 and 0.15 m) in array A were all measured over the same 23 day period from the 31<sup>st</sup> March to the 23<sup>rd</sup> April 2015, at 4.7, 8, 20.7, 163 and 231.5  $\text{g m}^{-2} \text{d}^{-1}$ , respectively, with 231.5  $\text{g m}^{-2} \text{d}^{-1}$  at 0.15 m being the largest amount of material collected by any of the BSNE's (in both array A and B). This period followed ploughing and preceded planting of the celery crop on field A (Table 5.2).

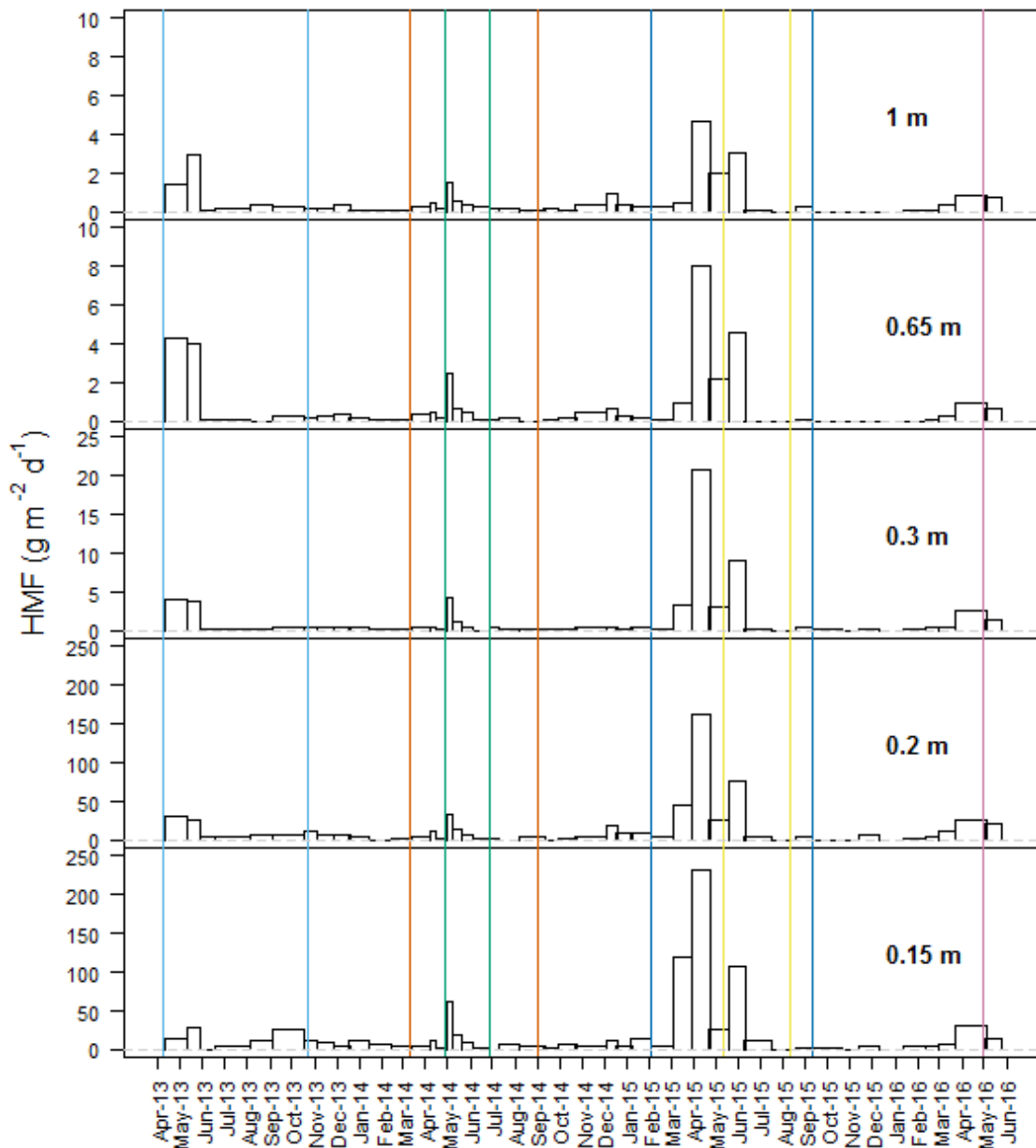


**Figure 5.9:** Horizontal mass flux per day from each BSNE height in array A for each time period averaged over the number of days of collection. Bar width extends from the start to finish of collection on the x-axis. Vertical lines relate to planting and harvest of crops (significant management that could affect mass flux). Field A: Light blue- leek, green – lettuce, yellow – celery, purple – lettuce. Field B: Vermillion 2014 (red) – onion, dark blue 2015 – barley. Note: the scale on the y axis switches from 10 to 25 to 250  $\text{g m}^{-2} \text{d}^{-1}$ .

Out of the 45 periods of collection there were 8 that significantly exceeded the average and quartiles for each measurement height in array A (Table 5.3), and these were all recorded during March, April, May and June each year.

**Table 5.3:** Statistics for HMF's of sediment for the two BSNE arrays.

Height (m)	Average contribution to total flux, A (%)	Average contribution to total flux, B (%)	Mean HMF A ( $\text{g m}^{-2} \text{d}^{-1}$ )	Mean HMF B ( $\text{g m}^{-2} \text{d}^{-1}$ )	Periods where A>B	Periods where A<B	Periods where A=B
1	2	2	0.58	0.64	26	12	7
0.65	2	2.5	0.8	0.81	17	21	7
0.3	3	3	1.45	1.22	23	17	5
0.2	42	47.5	14.74	13.5	18	18	9
0.15	51	45	20.3	16.29	22	18	5

As with array A, the maximum daily averaged HMF (Figure 5.10) for 0.3 m at array B ( $10.26 \text{ g m}^{-2} \text{ d}^{-1}$ ) was recorded between the 31<sup>st</sup> March–23<sup>rd</sup> April 2015, however the lower end of the profile (0.15 and 0.2 m) had maximum daily average HMF's of 126.9 and  $92.6 \text{ g m}^{-2} \text{ d}^{-1}$ , respectively, which were collected between 4<sup>th</sup>–31<sup>st</sup> March 2015 and were likely due to maximum wind velocities (Figure 5.7) from the north west (Figure 5.8) transporting peat sediment parallel to the developing barley row crop.

The upper profile (0.65 and 1 m) measured  $7.59$  and  $6.31 \text{ g m}^{-2} \text{ d}^{-1}$  during the first measurement period from the 12<sup>th</sup> April to the 11<sup>th</sup> May 2013, the corresponding collectors in array A measured more peat than usual during this period but only half as much as those in array B (All the samplers in array A measured half that of array B for this period, Figure 5.9 and 5.10).

Similarly to array A, peaks in daily HMF were measured across all heights for the first two measurement periods in 2013 (12<sup>th</sup> April–11<sup>th</sup> May and 11<sup>th</sup>–30<sup>th</sup> May 2013) and additionally the two periods preceding planting of the celery crop in field A in 2015 (4<sup>th</sup>–31<sup>st</sup> March and 31<sup>st</sup> March–23<sup>rd</sup> April 2015). Interestingly the peaks in fluxes of peat seen in array A after celery planting in 2015 were not measured in array B, again this likely reflects the more developed barley canopy on field B at this time. Whilst increases in daily HMF were measured in array B after planting in field B in 2014 and 2016, these were less significant than those measured in array A following planting.

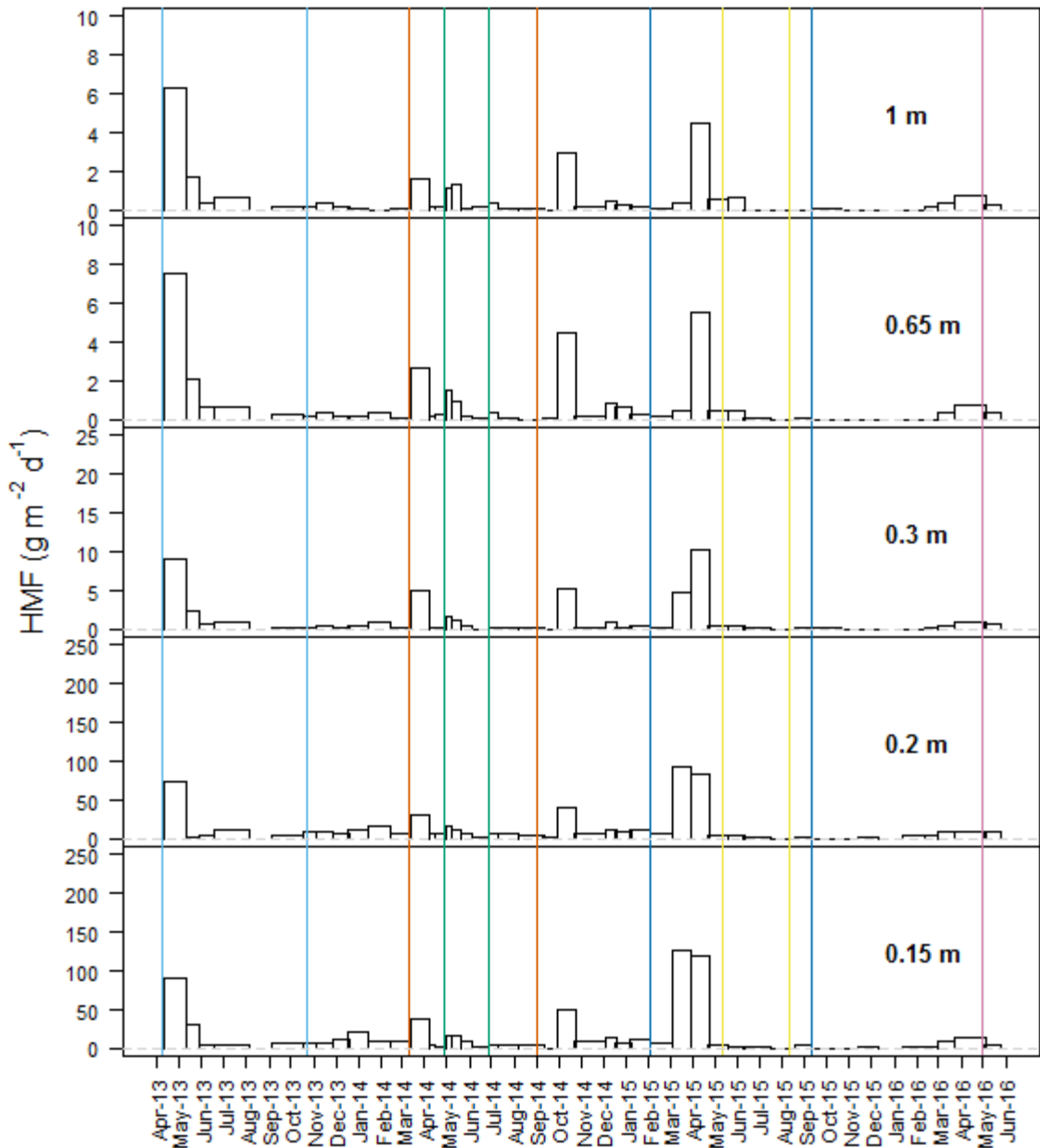


**Figure 5.10:** Horizontal mass flux from each BSNE height in array B for each time period averaged over the number of days of collection. Widths of bars extend from the start to finish of collection on the x-axis. Vertical lines relate to planting and harvest of crops (significant management that could affect mass flux). Field A: Light blue- leek, green – lettuce, yellow – celery, purple – lettuce. Field B: Vermillion 2014 (red) – onion, dark blue 2015 – barley. Note the scale on the y axis switches from 10 to 25 to 250  $\text{g m}^{-2} \text{d}^{-1}$ .

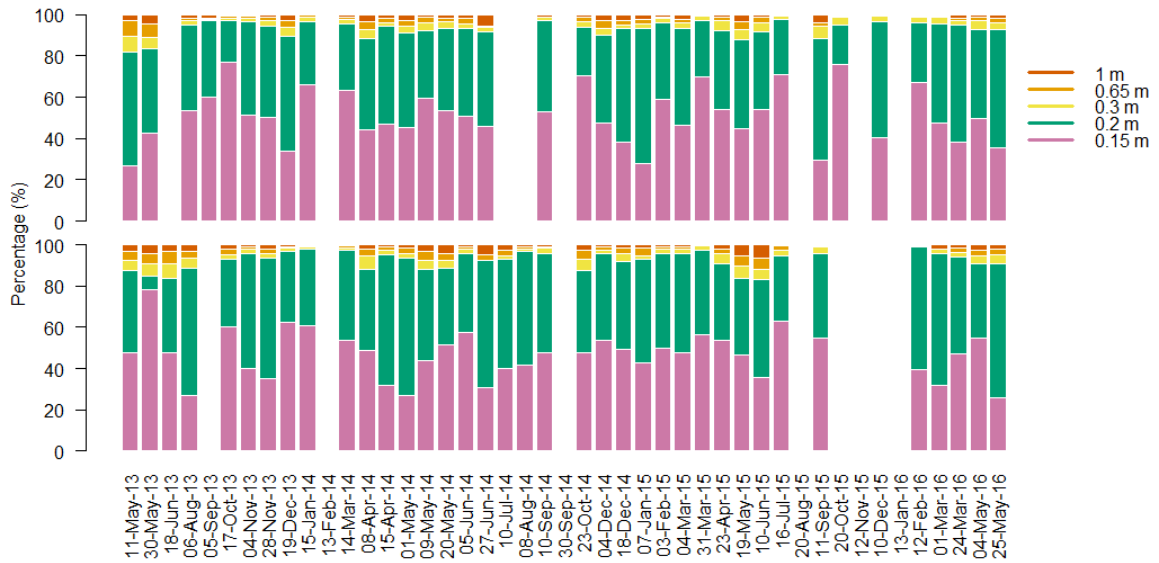
Notably, two periods of increased HMF were measured in array B but not A and occurred in 2014. The first occurred during the period 14<sup>th</sup> March–8<sup>th</sup> April which followed planting of the onion crop in field B whilst field A was yet to be ploughed in preparation for planting. The second was the only peak daily HMF measured outside of spring months, from the 30<sup>th</sup> September–23<sup>rd</sup> October. This period corresponded with

higher wind and friction velocities from the dominant south-westerly wind direction (Figure 5.7 and 5.8) and a lack of vegetation cover on field B as the onion crop had been largely turned into the topsoil, albeit with some mounds of crop left at the surface to decompose. During this same period field A had a significant weed cover that likely prevented reciprocal fluxes there.

A comparison of measurements from each sampling height in array A to the corresponding samples at the same height in array B for the same periods is given in Table 5.3. This reveals that overall array A samplers generally collected more sediment than the corresponding samplers in array B.

For 26 out of the 45 collection periods, the sampler at height of 1 m in array A captured more sediment than its counterpart in array B. The opposite was true for only 12 periods (Table 5.3). At the other measurement heights neither site dominated sediment collection over its counterpart. But only at the collection height of 0.65 m did array B capture more sediment on more occasions than array A.

The same was true of total HMF whereby at the maximum sampling height of 1 m the array A sampler collected more sediment over the complete study, however at all other heights array B samplers collected more sediment. It is possible that the more exposed location of array A allowed for collection of HMF from field B in addition to field A during periods when the wind came from a north-easterly bearing and ditch vegetation was not preventing this transport at this uppermost measurement height.



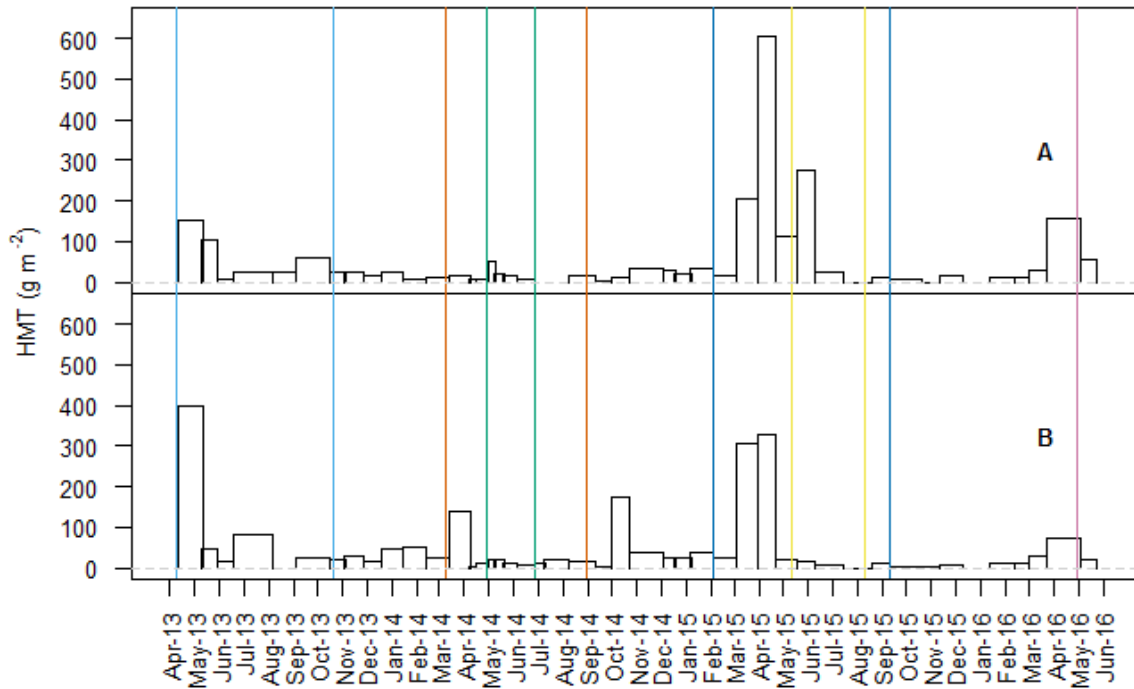
**Figure 5.11:** Contribution of each BSNE HMF to total collected flux plotted by collection date. Top plot is collector A and bottom is collector B. Records were removed where no samples were collected or sampling was corrupted (see above).

Figure 5.11 shows that the percentage contribution of each sampling height to the total daily HMF varied throughout the year. Generally the lower two sampling heights (0.15 and 0.2 m) comprise at least 80% of the total HMF collected for each period, indicating the importance of increased measurements at this elevation. Individually these samplers varied in their contribution between 10 and 80%. The contribution of the other three sampling heights (0.3, 0.65 and 1 m) varied with the quantity of total HMF collected. For periods during the spring months of March, April and May that experienced greater total HMF (Figures 5.8, 5.9 and 5.11), particularly in array B, these more elevated samplers contributed up to a combined 20% of the total HMF, and a minimum of 1% at other times of year. Individually these higher samplers contributed 0–8% of the total HMF.

### 5.2.3 Horizontal mass transport (HMT, Q)

Over the complete measurement period, somewhat more peat was collected in array A samplers than those in array B, at 9.91 and 9.17 g respectively. Following conversion to a consistent scale and integration over 0.15 - 1 m this equated to 2.31 and 2.22 kg m<sup>-2</sup>. Maximum integrated HMT of 605 g m<sup>-2</sup> was measured from 31<sup>st</sup> March–23<sup>rd</sup> April 2015 in array A corresponding to the period of maximum HMF at each sampler height. Only 329.05 g m<sup>-2</sup> was measured in array B for the same period. The maximum HMT in array B of 396.33 was measured from 12<sup>th</sup> April–11<sup>th</sup> May 2013 when the field was left bare,

and corresponded to the period of maximum HMF for the upper two samplers (0.65 and 1 m) rather than the lower samplers. Only 153.55 g m<sup>-2</sup> was collected in array A for the same period (Figure 5.12). Figure 5.12 shows that the HMT followed the same trend as the daily HMFs reported above.



**Figure 5.12:** Horizontal mass transport (HMT),  $Q$  (linear spline integrated  $q$ , g m<sup>-2</sup>) for each period of dust collection at each location. Widths of bars extend from the start to finish of collection on the x-axis and is the integrated HMF for the whole of each period. Vertical lines relate to planting and harvest of crops (significant management that could affect mass transport). Field A: Light blue- leek, green – lettuce, yellow – celery, purple – lettuce. Field B: Vermillion 2014 (red) – onion, dark blue 2015 – barley.

Temporal integrations of the calculated HMT for each year are reported in Table 5.4. Maximum time and height integrated HMT of sediment for both array A and B, was measured in 2015, equating to a flux of 487.67 and 294.32 g C m<sup>-2</sup> respectively. Integrated sums are provided for 2013 and 2016 despite neither year having a complete year of measurements, although the measurements in each year did include the typical peak sediment transport periods seen in 2014 and 2015 (i.e. March, April and May). Despite only five months of collected samples provided for 2016 at array A, a similar quantity of sediment was transported when compared to the complete 2013 year. The incomplete year (nine months) of sample collection in 2013 measured more HMT than the full year in 2014 for both fields (Table 5.4). At array B the shorter five month collection period of 2016 recorded the least HMT (149.44 g m<sup>-2</sup>) of all the years, and

the full year of 2014 still recorded less HMT than that collected in the nine months of 2013.

**Table 5.4:** Annual sums of integrated mass fluxes with estimated C content (using separate figures calculated below for array A and B), for each of the 0.15 to 1 m tall profile. 38% C of sediment dry weight is used for array A HMT, and 35% for array B (see below for calculation of this) (same figures as used in Figure 5.12)

Year	Integrated HMT A (g m <sup>-2</sup> )	Integrated HMT B (g m <sup>-2</sup> )	Array A Carbon content (g C m <sup>-2</sup> )	Array B Carbon content (g C m <sup>-2</sup> )	Mean <i>u</i> (m s <sup>-1</sup> )	Mean soil moisture (m <sup>3</sup> m <sup>-3</sup> )
<b>2013 (01/04-31/12)</b>	336.65	588.43	127.93	223.60	1.6	0.31
<b>2014</b>	230.23	564.78	87.49	214.62	1.92	0.27
<b>2015</b>	1283.33	774.53	487.67	294.32	2.13	0.29
<b>2016 (01/01-01/06)</b>	268.98	149.44	102.21	56.79	3.26	0.43

Despite the coincidence of several peak spring time *u* events and peak HMT no linear or non-linear regression was identified between these variables for the dataset, likely due to other limiting factors particularly SWC during winter months when *u* was consistently high. Similarly, no relationship was identified between variables such as, *u*\*, SWC and vegetation height, with HMT or HMFs at each height for the complete dataset. Multiple regressions of these influential variables also failed to identify any relationship with HMT and HMFs. It is possible that temporal coarseness of the wind eroded samples collected led to a masking of the driving factors, including management events which are likely contributors to fluxes but their contribution difficult to quantify within a month of data.

#### 5.2.4 Organic matter and carbon content

For several of the measurement periods the organic matter content was determined via loss on ignition. Carbon content was then estimated as 50% of the organic matter weight lost by ignition (Chambers et al., 2011). Samples collected in array A ranged in organic matter content from 63–83% while samples from array B ranged from 56–76% (Table 5.5; Figure 5.13).

Surveys (conducted by the author) of topsoil for each field reported an organic matter content of 72% (s.d.=2.89, n=15) for field A and 70% (s.d.=6.79, n=15) for field B

(dashed vertical lines Figure 5.13). While measurements for field A showed no trend and ranged from 67-76%, field B had a gradient of organic matter content that increased from 59% in the north-west corner of the field to 78% in the southeast corner of the field (range represented by shaded area in Figure 5.13). The soil surveyed within 100 m of sampling array B had an organic matter content of 67% which fitted with the average organic matter content in wind eroded samples (Figure 5.13).

The Student t-test was conducted to test for the significance of any differences between: i. all samples analysed at each measurement height, ii. all samples at all heights between the two arrays, and iii. the difference of the individual and mean of the wind eroded samples to the mean of the surveyed topsoil.

At heights of 1, 0.65 and 0.15 a significant difference ( $p < 0.05$ ) was identified in the mean organic matter content between samples collected at each location, but no significant difference at heights of 0.3 and 0.2 m (as is fairly evident in Figure 5.13), which likely reflects a difference in surface conditions (e.g. organic matter content of source field and vegetation type/heights) that led to a preference for transport and collection of lighter organic material particularly above 0.3 m in field A.

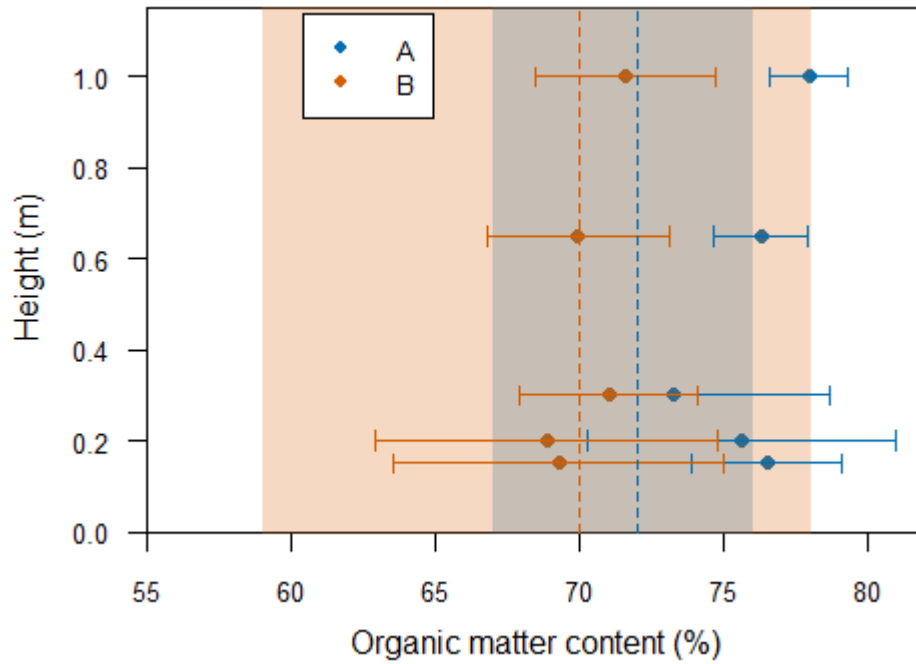


**Figure 5.13:** Average organic matter content of dried sediment samples collected in BSNE samplers for each collector height at array A and B with standard deviations as error bars,. Shaded areas represent the range of organic matter content from surface samples taken from across each field and dashed vertical lines are the mean of these for each field.

A significant difference was identified between all the values in collector A and those in collector B suggesting differing localised sources of material. Both the individual samples collected by the array in field B and the average values for each height in the array showed no significant difference ( $p < 0.05$ ) from the average organic matter content of the surveyed soil in field B (as suggested by Figure 5.13). However, this was not the case in field A where the array samples differed significantly ( $p < 0.05$ ) from the mean surveyed surface organic matter content. The difference in significance here suggests that sampling array A collected material with organic matter contents that were not within the average of the range of measured organic matter contents in field A, or the conditions in field A were such that the transport of the organic portion of the soil was greater than the mineral portion.

**Table 5.5:** Percentage organic matter content of wind-blown sediment samples that were collected at array A and B.

Sample collection period	Array A (Heights, m)					Array B (Heights, m)				
	1 m	0.65 m	0.3 m	0.2 m	0.15 m	1 m	0.65 m	0.3 m	0.2 m	0.15 m
12/04 – 11/05/2013	76.32	78.12	75.61	75.68	73.33	73.96	70.26	71.22	56.82	58.49
11/05 – 30/05/2013	77.19	74.32	76.47	66.67	78.95	72.73	70.27	72.09	NA	72.73
30/05 - 18/06/2013	NA	NA	NA	NA	NA	71.37	69.41	72.73	67.32	72.62
18/06 - 06/08/2013	80.00	75.00	62.50	83.33	80.00	NA	NA	NA	NA	NA
14/03 - 08/04/2014	NA	NA	NA	NA	NA	66.67	65.63	66.13	70.00	64.86
30/09 - 23/10/2014	NA	NA	NA	NA	NA	68.66	67.96	66.67	70.27	66.67
04/03 - 31/03/2015	NA	NA	75.34	75.00	74.11	NA	NA	73.45	73.63	73.23
31/03 - 23/04/2015	78.22	77.65	76.41	77.40	76.08	75.96	76.00	74.68	75.00	76.15
<b>Average</b>	<b>77.93</b>	<b>76.28</b>	<b>73.27</b>	<b>75.61</b>	<b>76.49</b>	<b>71.56</b>	<b>69.92</b>	<b>71.00</b>	<b>68.84</b>	<b>69.25</b>

The increase in the organic matter of samples collected by array B between the 4<sup>th</sup> March and 23<sup>rd</sup> April 2015 correspond well with the most pronounced period of HMT recorded by array A. Given that the presence of a barley crop in field B at this time is attributed above as the reason for reduced HMT, it is possible that a substantial portion for this period of HMF may originate from field A given the higher organic matter content of the soil in this field.

As there was no great variability in organic matter content with height within each individual array, an average of all the measurement heights for each array, 76% for A, and 70% for B, were used to calculate HMT of C (Table 5.4).

## 5.3 Discussion

### 5.3.1 HMF

The HMF of sediment flux has been identified as decreasing with height above the soil surface, but most noticeably above 0.3 m. This is a typical vertical distribution observed at other sites measuring mineral and peat soil flux (Panebianco et al., 2010, Warburton, 2003, Shao, 2005, Fryrear et al., 1991). The majority (~80%) of HMF was typically transported below 0.3 m which suggests that saltation of particles (which make up the bulk of the flux transport) is limited to this height (Funk and Reuter, 2006). Warburton (2003), measuring HMF at similar heights with BSNEs on an upland bog in the UK, found that the peat contribution to flux also reduced above a height of 0.3 m and that the sediment collected above 0.3 m was mostly mineral dust, as opposed to organic material. The C content of the HMFs measured in my study did not show a significant correlation with height of measurement between 0.15 to 1 m (Figure 5.13), suggesting no preference in peat transport over this height range.

No relationship was identified between HMT or HMFs with  $u$ ,  $u^*$  or SWC. This is understandable given the coarse temporal resolution of the sampling that inevitably included several different scale erosion events (Fryrear et al., 1991, Warburton, 2003). A further complication in my study was on-site activity of machinery, which was seen to trigger some increases in sediment flux, but without complete records of site activity the site management contribution to the total flux could not be separated from that caused by natural events.

The peak HMT measured at array B in 2013 reflects the importance of crop cover as opposed to bare soil during the spring at this site, despite the finding of Funk and Engel (2015) that <10% crop cover increased HMT. Similarly, the high HMT of array B during October 2014 highlights how important residual waste is in preventing sustained wind erosion. During this month the failed onion crop waste had been raked into piles on the soil surface and the field disked into a loose cover.

These findings suggest that, where possible, crop residues should be left on the field surface to reduce soil exposure to wind erosion.

### 5.3.2 HMT

Measurements of HMT are limited on peat soils, with the majority of sediment flux measurements being made in sandy dryland environments or over mineral soils (Harper et al., 2010, Dawson and Smith, 2007, Chappell and Warren, 2003, Warburton, 2003, Böhner et al., 2003, Pease et al., 2002). Most wind erosion studies utilise mobile wind tunnels, and those that measure natural events report just that, events, and not full annual cycles (Panebianco et al., 2010, Funk and Engel, 2015).

The results of this study demonstrate, as expected, that the greatest flux annually was measured during the spring months of March, April and May, with flux values ranging from 80 to 600 g m<sup>-2</sup> d<sup>-1</sup>. A large spring net flux was similarly measured by Warburton (2003) for an upland bog system in the UK who used similar sediment samplers to those in this study; measured HMT was not, however, of the same magnitude, being only 20 g m<sup>-2</sup> d<sup>-1</sup>. Warburton (2003) measured his largest HMT in association with high wind velocities during winter months, at 60 g m<sup>-2</sup> d<sup>-1</sup>.

Generally, the cultivated fen in this study experienced a similar range of winter flux values to the upland bog, being between 10 and 60 g m<sup>-2</sup> d<sup>-1</sup>. In-field management operations led to more readily transported material during certain months and hence a much greater flux than at the bog site which experienced no reported disturbances during the measurement period. Mean  $u^*$  for the complete dataset at both sites ranged between 0.25 and 0.4 m<sup>-2</sup> s<sup>-1</sup>. Warburton (2003) could not identify a simple correlation of  $u^*$  to HMF and attributed this to the low sampling resolution, a theory suggested by Fryrear et al. (1991). Similarly, I failed to identify a relationship to  $u^*$  due to other and greater influences on flux, e.g. management, vegetation cover and SWC (rather than just being due to poor sample resolution). Undoubtedly, however,  $u^*$  is a component in the complex interaction of drivers that contribute to the magnitude of HMT. Warburton (2003) found that the majority of dust flux was aggravated by rain-splash and therefore he noted that precipitation, high wind and frost were significant controlling factors on erosion.

While annual flux was calculated here as being between 2 and 13 t ha<sup>-1</sup> yr<sup>-1</sup> Warburton (2003) reported an annual flux sum of only 0.46 to 0.48 t ha<sup>-1</sup>. He highlighted that although this dry annual HMT is an order of magnitude less than that reported for sandy soils, the dry bulk density of peat is much lower than that of the sandy mineral soils of

the other studies and therefore will equate to a more similar volume loss of soil. Additionally, the C content of peat soil is also greater than that of mineral soils, resulting in a larger C flux. Therefore, despite measuring an order of magnitude less sediment flux than Chappell and Baldock (2016) estimated for a sandy agricultural soil in Australia, the scale of peat sediment flux from the East Anglian fen peats is comparable in terms of net C flux (Table 5.6).

**Table 5.6:** Literature summary of sediment yields from agricultural soils.

<b>Sediment yield (t ha<sup>-1</sup> yr<sup>-1</sup>)</b>	<b>Soil types, location and method</b>	<b>Source</b>
2.3 to 12.8 (flux)	Lowland peat soil, East Anglia, BSNE	<b>This study, 2017</b>
1.2 increased to 4.4 (net loss, much less C though 0.1 t C ha <sup>-1</sup> yr <sup>-1</sup> )	Sandy agricultural soil, SW Australia, Soil sampling of SOC and analysis for caesium-137 ( <sup>137</sup> Cs).	<b>Chappell and Baldock (2016)</b>
Mean 1.56 (maximum of 15.5)	Wind Erosion on European Light Soils (WEELS) model, Simulated 29 years of flux from Barnham site, UK.	<b>Böhner et al. (2003)</b>
-32.6 to 37.5 (flux) over 128 fields (0.6 net soil loss)	Lowland agricultural soil (peat included) mostly loamy sands. East Anglia, UK. <sup>137</sup> Cs mapping.	<b>Chappell and Warren (2003)</b>
0.46 – 0.48 (flux)	Upland blanket bog, Moor House, UK. Using BSNE, and flux gauges.	<b>Warburton (2003)</b>
20 to 44 t ha <sup>-1</sup> Single events, not annual	Fine sandy soil, Vale of York, UK, Wilson and Cooke samplers (similar to BSNE)	<b>Wilson and Cooke (1980)</b>

Using similar instrumentation to the BSNEs, Wilson and Cooke (1980) estimated a much greater sediment flux of 21 to 44 t ha<sup>-1</sup> for single flux events of fine sandy agricultural soil in the Vale of York. A more recent estimate by Chappell and Warren (2003) mapped the age of artificial nucleotide Caesium-137 (<sup>137</sup>Cs) to determine gains and losses of field soil over the last 50 years. Instead of monitoring wind erosion activity, they collected soils and measured the <sup>137</sup>Cs to estimate soil movement against an undisturbed reference. Their study was conducted in an agricultural area less than 50

km from the study site used in this work with a reported annual sediment flux of -32.6 to 37.5 t ha<sup>-1</sup> yr<sup>-1</sup>, but only a net loss of 0.6 t ha<sup>-1</sup> yr<sup>-1</sup>, much less than that reported here, perhaps due to the increased area that the study covers and not all sample sites being on peat soils. Böhner et al. (2003), for the same site at Barnham, UK, used the Wind Erosion on European Light Soils (WEELS) model based on soil susceptibility to wind erosion to estimate losses for 29 years and reported a mean annual loss of 1.56 t ha<sup>-1</sup>. Their results corroborate the increased flux expected in March, and found here, but additionally report high yields in September and November, with all three of these peak months experiencing >3 t ha<sup>-1</sup> loss. The estimation of net flux reported in my study for agricultural peat soils is much less than that reported for sandy agricultural soils, as expected given differences in bulk density.

### 5.3.3 Soil cover

The bulk of HMT measured in my study occurred during spring months when the soil had been ploughed in preparation for crop planting and prior to a developed crop soil cover. Wind-blown sediment samples were collected all year round at the two sites but little (none in some cases) was measured during periods when the crop cover was fully developed. During fallow periods the soil cover varied (Figure 5.3), ranging from weed growth, standing water and dry crusted peat, all of which were associated with limited soil erosion. A study by Campbell et al. (2002) at an abandoned milled peatland in Canada also reported that soil crusting led to the peat surface being resistant to  $u$  in excess of 12 m s<sup>-1</sup>. Maintaining a vegetation cover is suggested as the best preventative variable in reducing sediment flux, with a 40% soil cover thought to be effective enough to protect the underlying soil (Borrelli et al., 2014, Funk and Engel, 2015).

Peak  $u$  and  $u^*$  at the beginning of April 2015 combined with dry soil conditions and freshly ploughed soil led to the largest HMT of the complete measurement period for field A. During the same period field B was developing a barley crop and array B collected half as much soil in each of the samplers below 0.3 m compared to array A, reflecting a sizeable reduction in saltation due to the presence of the young crop. However, Funk and Engel (2015), for a mineral agricultural soil in Germany, reported a higher net flux from soil with a maize crop cover of <10% over that of bare soil. They investigated wind erosion using a portable wind tunnel to assess the impact of row crop (sugar beet and maize) orientation on restricting erosion, particularly during early crop growth. It was reported that a 45° or 90° orientation of the sugar beet to the prevailing

wind has a reductive effect on wind erosion, but not for maize. Maize, with a lower planting density and more streamlined shape, acts as less of a wind break and is less susceptible to damage unlike the sugar beet crop. Sugar beet is also grown on the peat soils studied here and also suffers from restricted yields due to damage by wind erosion in its early development (M. Hammond, Pers. comm.). Due to the sparse collection regime, it was not possible to assess the influence of different prevailing wind directions on soil flux from different crop types in this study.

It could be expected that the thinner more streamlined allium crops (leek and onion), which were both grown with a similarly streamlined spring barley cover crop, would reduce wind erosion less than the leafy, less streamlined, lettuce and celery crops. However, comparison of the soil flux data for the first few months after planting did not reveal this relationship. The lack of relationship may be due to: i. the long periods between data collection, ii. differences in other environmental conditions such as  $u^*$  and SWC in these months, iii. differences in planting densities of the crops, whereby the thinner crops allowed for closer planting (observations made on field visits gave an average of 29 leek plants  $m^{-2}$  to a figure of 14 plug plants  $m^{-2}$  – e.g. lettuce), iv. a combination of all of these factors.

#### 5.3.4 Deposition, where is the peat going?

As mentioned above, the majority (>80%) of HMT was measured below a height of 0.3 m and related to the saltation of peat particles. Given the sudden change in surface roughness and that the height of weeds surrounding the ditches for most of the year was greater than 0.3 m (Figure 5.4), thus providing effective in- and between-field wind breaks, the ditches and edge of the fields likely receive the majority of the aeolian flux as deposition. Peat in suspension may well be deposited on neighbouring fields, and the higher organic matter content in array B after the peak  $u$  conditions in April 2015 suggests that wind-borne material is capable of travelling across several fields during larger events. Wilson and Cooke (1980) similarly suggest that little sediment actually leaves agricultural fields, but rather is deposited at boundaries. Re-distribution of sediment to field boundaries has been noted by several studies utilising the  $^{137}\text{Cs}$  technique (Chappell and Baldock, 2016, Chappell and Warren, 2003). In their study of East Anglian agricultural soils, Chappell and Warren (2003) found that most of the soil eroded by the wind from high-loss fields accumulated in field boundaries. Observations during site visits identified that this was also likely the case for my study site: nettles

lining the ditches were observed to trap wind-blown peat on their spicules (Figure 5.14), although this deposition was not quantified.

Whilst the majority of the C in the transported sediment might not leave the site, Chappell and Baldock (2016) noted that once it had moved the likelihood of it being mineralised was greater. If peat is deposited into the ditch system it would be expected to be measured as a contribution to the ditch flux (i.e. as POC). Measurements of aquatic C fluxes at the field site were made in the ditches surrounding field A by Peacock et al. (2017) and are similarly reported by Evans (2017) for 2015. Their measurements showed an increase in DOC in March and April of 2015 that was attributed to stagnant conditions, but no increase in POC that could be attributable to aeolian deposition by the significant aeolian flux measured in this study for April of that year. This suggests that if wind eroded POC is being deposited in the ditch system that it is rapidly settling in the stagnant conditions at this time of year. POC deposited over ditches therefore is likely stored within the field network and contributes to the overall loss of C from the farm but on a much longer timescale.



**Figure 5.14:** Photos of nettles lining the ditches with trapped dust.

### 5.3.5 Footprint calculation and speculative field scale annual C loss

Without more instrumentation it was not possible to reasonably confine the footprint of the BSNEs to calculate an accurate estimate of the peat loss relative to the field source

area. Inclusion of multiple erosion events from multiple directions during each collection period and a lack of knowledge of particle size at the time of transport also made field scale estimation problematic.

The values presented here (Table 5.4) represent the minimum measured HMT for each array location. Therefore the minimum flux collected for each year at array A over the height range of 0.15 to 1 m was between 0.09 and 0.5 kg C m<sup>-2</sup> (Table 5.4) and at array B, over the same height range, was between 0.06 and 0.29 kg C m<sup>-2</sup>.

As array B represents a downwind equivalent of array A then, assuming the sediment transport is not at full capacity, it should measure a greater HMT. The results indicate, however, that array B did not collect a greatly increased sediment flux. This may be because:

1. The peat soil flux at array A is already at the carrying capacity of the wind.
2. The HMT contribution from field B is significantly less than field A.
3. A proportion (possibly all) of the HMT from field A is not measured by array B, due to deposition on field B (perhaps adding to the gradient in organic matter content that was observed across field B).
4. HMT from field A is deposited into the ditch and its marginal vegetation such that the HMT for each array is solely a measure of each individual field.

There is not enough evidence to firmly support any of the above options. A denser network of samplers and improved soil study would assist with this. Given the data provided above and observations during field visits I speculate that the answer lies between options 3 and 4, and that deposition of HMT from field A occurs into the ditch, on the ditch margin and field vegetation, and additionally on field B, which potentially aggravates soil erosion on field B but does not contribute to increased flux.

Despite the difficulty in defining the footprint, the organic matter contents given in Table 5.5 suggest that the majority of the collected sediment (when maximum  $u$  was below 10 m s<sup>-1</sup>) originated from the field that each collector was located within. However, the larger quantity of sediment routinely collected in the top sampler in array A compared to array B suggests that sediment contributions to this sampler could extend beyond the adjacent ditch and its vegetation to include the southern edge of field B.

## **5.4 Chapter Summary**

This research chapter has addressed research question 6 and quantified the flux of C being transported across, and potentially off, the surfaces of two adjacent fields of cultivated deep peat soil. The flux was measured using two arrays of passive wind samplers located on the north east boundaries of two fields under different crop management. These represent the first estimates of annual C flux from lowland cultivated fenland peat soils.

## **Chapter 6: Conclusions**

This final chapter brings together a summary of the findings from the three data chapters (3, 4 and 5) which address the research questions set out in chapter 1. The contribution and implications of the thesis findings to an improved understanding of the C cycle of lowland, agricultural peatlands and mitigation of C losses are discussed. Finally, limitations of the work are considered, leading into a discussion of the path that future research should take based on the thesis results.

## 6.1 Overview of chapter findings

**Chapter 3** set out to investigate the drivers of NEE for a drained and intensively managed lowland peat soil in the UK.

- Modelled TER based on Tsoil sensitivity explained 71% of the variability in observed nocturnal NEE during the fallow periods, while during cultivation only 43% was explained. Residuals of this relationship showed a significant positive correlation,  $r_s = 0.56$ ,  $n=169$ ,  $p < 0.001$ , to daytime NEE from the daytime values of the same 24 hr periods suggesting crop growth was leading to nocturnal autotrophic respiration and limiting the temperature response of nocturnal TER. This consequently meant that environmental influences on GPP led to a response in nocturnal TER during crop periods.
- A stomatal closure response was identified in daytime NEE as a response to high values of Tair, VPD and limited SWC. This was particularly noticeable in lettuce crops, and restricted the peak light use of these crops (Figure 3.12). The celery crop was not as clearly limited by high VPD and experienced the largest GPP and also, as a consequence, the largest autotrophic respiration contribution.
- The WTD/NEE relationship is not straightforward since it reflects both rainfall/evapotranspiration and agricultural water management. An investigation of the short-term response of NEE to WTD suggested a very strong negative correlation  $r_s = -0.87$ ,  $n = 9$ ,  $p < 0.001$  for a limited two week gradual rise in WTD from -0.9 to -0.6 m (Figure 3.9). But there was no evidence of this over longer time periods or during a managed lowering of the water table, with the latter likely due to sustained SWC during WTD lowering.

Additionally, the  $R_{10}$  calculated for each crop/fallow period showed a non-significant negative relationship with WTD (Figure 3.6a). This was mostly disrupted by crop periods, in particular the lettuce (2012) and leek crops which had the shallowest average WTD; the WTD during the 2012 lettuce crop was significantly shallower than during any other period (SWC) while the latter crop had a barley crop sprayed off during early development that led to above-ground decomposition and hence significant CO<sub>2</sub> loss despite a shallow WTD.

However, when comparing the NEE and WTD for the two lettuce crop periods, the 2012 crop had a 0.3 m shallower managed mean WTD and 0.25 m<sup>3</sup> m<sup>-3</sup> greater SWC compared to the 2014 lettuce crop which had a greater  $R_{10}$ ,

suggesting an overall reduction in CO<sub>2</sub> loss for the wetter 2012 crop. But this relationship is limited by insufficient data coverage.

- Decreasing SWC was also found to result in greater nocturnal NEE values particularly during the lettuce crop period of 2012. The data suggests an exponential relationship (Figure 3.8) between nocturnal TER and NEE although this relationship was only a weak explanation for the variability in TER and is unlikely to be true of much lower values of SWC where no TER would be expected.

**Chapter 4** reported the first multi-annual NEE of CO<sub>2</sub> for an intensively cultivated lowland agricultural soil, and provided an assessment of the reliability of the dataset through a review of the site EBC. Additionally, lateral C imports (C<sub>i</sub>) and exports (C<sub>e</sub>) associated with planting and harvesting of crops were quantified for their contribution to net C flux. The outcomes were:

- The quality of the dataset was assessed by calculating the EBC. This was calculated to be at the higher end of reported annual slope values of 0.87 to 0.89 for all available half-hourly values. This was improved to 0.91 to 0.96 by integration on a daily time frame but remained unclosed, with limitations of measurements suggested as a potential cause of this.
- With additional accounting for diurnal storage of energy there is still a 5-10% imbalance for separate crop and fallow periods and 6% over the complete dataset. This imbalance is likely a result of the placement of the instrumentation measuring available and stored energy. Nothing should be done to account for this. The measured fluxes were therefore deemed reliable within the context of other EC data produced within the EC measurement community.
- Plug crops, and in particular celery, had the greatest net daily uptake, with values comparable to those reported for spring barley grown on Finnish and German peat soils, but at the lower end of values reported for the bioenergy RCG crop also grown in Finland.
- Each plug crop followed a similar annual pattern of daily NEE, with variability in timings generally due to the program of agricultural management. The peak diurnal uptake demonstrated limitations due to R<sub>g</sub> and T<sub>air</sub> during peak months

for crop uptake. The longer leek crop period never established a strong series of net sink days, as the plug crops did.

- Crop waste left on the fields led to daily peaks in emission following harvest of the lettuce and celery crops, incorporation of this waste into the peat soil appeared to reduce daily CO<sub>2</sub> loss. The cooler climate following harvest of leek resulted in no peak in CO<sub>2</sub> loss due to decomposition of this residual waste.
- The two lettuce crop periods differed in average WTD by 0.3 m (mentioned above) with the shallower WTD measuring 20 g C-CO<sub>2</sub> m<sup>-2</sup> less net CO<sub>2</sub> loss. This reduction in net loss supports suggestions by field observations of Shurpali et al. (2009) and mesocosm measurements of Musarika et al. (2017) that shallower average WTD will result in reduced CO<sub>2</sub> loss from cultivated peat soils.
- The annual sums of NEE represent significant losses of 675.75 ± 101.45, 806.38 ± 88.75 and 797.18 ± 84.60 g C-CO<sub>2</sub> m<sup>-2</sup> yr<sup>-1</sup> (Figure 4.5 and Tables 4.3 and 4.4) for leek, lettuce and celery crops. A figure of 759.77 ± 91.6 g C-CO<sub>2</sub> m<sup>-2</sup> yr<sup>-1</sup> is therefore derived as an average of multi-annual NEE from these three years of measurements for a cultivated temperate deep peat soil in the UK. This value is similar to the IPCC (2014) emissions factor which was calculated as a mean of values for mostly cereal crops and some root vegetable crops grown on peat soils in both boreal and temperate climate zones, predominantly by implementing the flux chamber technique and making subsidence measurements. The findings are also similar to the value of 772 ± 63 g C-CO<sub>2</sub> m<sup>-2</sup> yr<sup>-1</sup> reported by Taft et al. (2017) at the same site for one year using the static chamber technique.
- The maximum annual loss of 806.38 ± 88.75 g C-CO<sub>2</sub> m<sup>-2</sup> was measured in 2014, which had the shortest crop period of the three full years. Despite the longer growing period and increased CO<sub>2</sub> sequestration of the celery crop in 2015, it was as large an annual net source of CO<sub>2</sub> as the lettuce crop at 797.18 ± 84.60 g C-CO<sub>2</sub> m<sup>-2</sup> yr<sup>-1</sup>. Whilst the 2013 leek crop was within the uncertainty range for the annual sum of NEE it was the weakest annual source of 675.75 ± 101.45 g C-CO<sub>2</sub> m<sup>-2</sup> which had the greater number of plants per square meter and greater biomass harvested.

- Lateral net flux was found to result in a net gain of C for lettuce cultivation. This was due to the peat based planting medium used for this plug crop and low yields. Celery, despite also being planted in a peat plug, had a greater  $C_e$  during harvest, while leek had minimal  $C_i$  but the greatest loss of C during harvest. Annual NECB therefore ranged from  $783.44 \pm 127.28$  to  $816.35 \pm 89.33$   $\text{g C m}^{-2} \text{ yr}^{-1}$ , only a roughly  $33$   $\text{g C m}^{-2}$  difference.
- The quantity of C removed as harvested lettuce, leek and celery was at the lower end of reported values for cereal or bioenergy crops and grasses grown on peat. A greater  $C_e$  was associated with the longer grown crops; this equated to a contribution of 4-16% to the annual C loss.

**Chapter 5** reported and analysed the first measurements of wind activated C flux of an intensively cultivated lowland peat soil to quantify the impact of ‘fen blow’ on the C balance of intensively managed peat soils.

- The majority of peat was transported below a height of 0.3 m in common with findings from other agricultural (non-peat) sites. The quantity of peat collected in upper samplers (0.65 and 1 m) increased during larger erosion events/periods. Measurements of HMF and HMT showed same annual patterns of loss as with previous research on an upland peat bog (Warburton, 2003) but with greater losses during spring months. The individual influence of management and environmental driving events could not be discerned due to the temporal resolution of the dataset. It is clear that the increase in erodibility as a result of management (e.g. ploughing) meant that erosivity factors ( $u$  and SWC) had a greater impact.
- Integrated measurements of HMF from the two fields quantified the flux past the measurement locations as reaching a maximum of  $0.6$   $\text{kg m}^{-2}$  over a 23 day period in spring of 2015, during which SWC was low,  $u$  was high, and management events (ploughing and planting) took place.
- The annual HMT sum integrated for measurements at a height of between 0.15 and 1 m above the soil surface ranged from 2.3 to  $12.8$   $\text{t ha}^{-1}$  which was much more than that reported for an upland peat bog (Warburton, 2003) but within the range of estimates reported for other (non-peat) agricultural soils (Böhner et al., 2003, Chappell and Warren, 2003).

- Analysis of C in these samples gave an indication of the origin of the flux as primarily being within each field of measurement, but primarily allowed for an estimated C flux of 90 to 490 g C m<sup>-2</sup> yr<sup>-1</sup>, 10-60% of the annual NEE.
- Greater transport of sediment in field A compared to field B during the peak transport period of April 2015 suggested that even the minimal crop cover of young barley seedlings was enough to reduce erodibility of field B and HMT.
- It was difficult to assess whether crop type had an effect on C loss due to the difference in erosivity factors each year, although literature suggests that more streamlined monocotyledonous crops would lead to greater exposure and erosional losses (Funk and Engel, 2015). Generally it is reported that broad-leaved crops with larger leaves would prevent flux but be damaged in the process resulting in diminished yields (Barring et al., 2003, M Hammond, Pers. Comm.).
- During fallow periods the soil cover varied (Figure 5.3), ranging from weed growth or standing water to dry crusted peat, all of which were associated with limited soil erosion.
- Although no depositional measurements were made, visual evidence suggests the weeds surrounding the field trap a large proportion of this horizontal flux. This in turn suggests that the majority of sediment is not leaving the field, but rather being redistributed, with potential knock on effects for ditch DOC.

## **6.2 Implications and mitigation**

### **6.2.1 Implications**

Cultivation of salad crops and vegetables on deep lowland peat soil in the UK is resulting in significant losses of C-CO<sub>2</sub> from the soil C store. The net balance of C loss is reduced by growing lettuce crops, but exacerbated following harvest of celery and leek crops. This net loss of C-CO<sub>2</sub> is generally greater than that of cereal crops and grasses grown on peat soils reported in the literature suggesting that intensive cultivation of salad crops and vegetables is one of the least C friendly land uses for peat soil.

It has also been demonstrated that the magnitude of annual flux varies with crop type and crop management activities. In particular, crop type, crop residues and time of harvest are important drivers of annual NEE at this site. Additionally, climate variables (e.g. T<sub>soil</sub>, WTD, SWC, VPD) have shown propensity to control CO<sub>2</sub> losses. Furthermore, preparation of the peat soil for cultivation is not only resulting in a C loss as particulate peat soil by wind erosion, but it also has the potential to damage crops; reducing yields in the process.

Soil temperature was identified as having a strong correlation with the magnitude of C-CO<sub>2</sub> loss from intensively managed lowland peat soil, particularly during fallow periods. The implication of this is that with global surface temperatures projected to continue to rise by 2 °C (from pre-industrial average) by the end of the century (IPCC, 2013b), C-CO<sub>2</sub> loss from this cultivated peat soil would also be expected to increase, especially during prolonged fallow periods.

Despite reductions in UK national emissions, the agricultural sector is reported to have failed to make progress. New targets are set out in UK Clean Growth Strategy (2017) but still need new policies to reduce agricultural emissions (Committee on Climate Change, 2018). The Department for Environment, Food and Rural Affairs (DEFRA) has begun a plan to develop a peatland strategy to assess current C and GHG budgets from peatland under agricultural use in an effort to establish emission factors and mitigation strategies for the intensive cultivation of the soils. The results from this thesis will make a contribution to this strategy.

NEE has been identified as the dominant contribution to NECB for managed peat soils whilst the contribution of crop harvest has been shown for many sites to be the second greatest contributor to net C loss from agricultural sites (Taft et al., 2017, Kutsch et al., 2010, Eickenscheidt et al., 2015, Evans, 2017, Lohila et al., 2004, Shurpali et al., 2009, Aubinet et al., 2009, Schmidt et al., 2012). The combination of the data presented in this thesis with other elements of NECB from a larger study (Evans, 2017) reports that cultivation of these deep peat soils results in the greatest average CO<sub>2</sub>e loss of 15 lowland peat soils in England and Wales covering a range of land use types (including: extraction, extensive/intensive grasslands, agriculture, and re-wetted bogs). It is estimated that the net annual loss of C (excluding by wind-erosion) will result in the total loss of peat from the study site within 500 years. However, estimates made by this author, for just oxidative loss, for a depth of peat between 1-2 m and a bulk density of 0.26 g cm<sup>-3</sup>, suggest a maximum estimate of 250 years for the field studied. The difference here likely reflects the higher value of soil bulk density (0.5 g cm<sup>-3</sup>) used by Evans (2017) which in itself may reflect a difference in field conditions at the time of each set of measurements. The figures found here are closer to those suggested by Taft et al. (2017) which gives a timeframe of 80 to 160 years. Regardless, the peat C store at this site is being depleted and will likely begin to be mixed with underlying clay soil within the next century unless current losses are mitigated.

### 6.2.2 Mitigation

Approaches to mitigation must balance the environmental benefits of peat soils with the economic costs to farmers and food security. Mitigation should therefore target reduction of the impact of current management practices.

There is the potential to use the findings of this thesis to guide future management practices in mitigating the rate of loss of C-rich farmland, and enhance the resilience of lowland peat soils to future climate forcing. These measures will thereby further the future of farming on organic soils by securing food production and reducing overall CO<sub>2</sub> emissions from the UK agricultural industry.

#### *Crop management and reducing fallow periods*

Managing crop cycles in a way that reduces the length of time that the field is under fallow is one potential mitigation option. This could include cultivating crops with a longer growing period and greater light response, growing two crops in one year, or

using cover crops during fallow periods. The longer growing period of the leek crop contributed to reduced CO<sub>2</sub> emission in 2013, while growing single lettuce crops should be avoided unless further fallow period mitigation strategies are implemented. Lohila et al. (2004) measured an increase in net uptake for a double harvest of grasses grown on a boreal peat soil. The additional impact on soil quality due to increased use of inorganic fertilisers and pesticides on the field would, however, need to be addressed.

Literature addressed in Chapter 4 suggests a reduced net CO<sub>2</sub> loss for cultivation of crops with longer growing seasons (cereal and bioenergy crops) on temperate and boreal peat soils (Karki et al., 2015, Kandel et al., 2013, Mander et al., 2012, Lohila et al., 2004, Kutsch et al., 2010, Beyer et al., 2015). It is acknowledged that prolonged crop periods lead to increased sequestration of CO<sub>2</sub> in NPP, which is then primarily exported from agricultural sites resulting in a greater contribution to net C<sub>e</sub> from the site, while the NEE still experiences a significant reduction in Rh.

Prolonged periods of crop cover would have the added benefit of reducing losses of peat by wind erosion.

#### *Incorporate crop waste*

Following harvest crop residue was incorporated into the topsoil. Following harvest of the lettuce and celery crops, peak daily CO<sub>2</sub> losses were measured due to the decomposing crop waste and declined following field disking activity. When the barley cover crop of 2013 was sprayed with selective herbicide, this residue could not be incorporated and resulted in the peak daily CO<sub>2</sub> flux for 2013. Incorporation of the residue will likely only extend the impact of the decomposition of this material.

#### *Reduce the waste of crops*

Given the quantity of crops that are rejected due to aesthetic reasons (i.e. that fail to reach the supermarket shelf), it is justifiable to suggest that improving public awareness of this issue and removing the aesthetic criteria from harvesting protocol would increase economic crop yield and reduce wastage. Crop lost due to damage by pests and wind erosion could then be addressed to further reduce this. This would have the dual benefit of increasing yields to address food security issues and reducing the land requirement for this intensive agricultural practice. The consequence could be that areas of farms would be set-aside more regularly and maintained for longer, or restored to grassland.

Reduced net CO<sub>2</sub> loss of set aside and re-wetted peat soil would then offset the increased C<sub>e</sub> as a result of higher yields.

#### *Raise the water table*

Raising the water table during both the crop and fallow periods has not been conclusively shown here to result in reduced CO<sub>2</sub> losses, despite the findings of mesocosm and restoration studies (Musarika et al., 2017, Lloyd, 2006). While in the short term a rising WTD resulted in a reduced loss of CO<sub>2</sub> (Figure 3.9 a; Table 3.3) longer averaged periods showed inconsistency which may reflect the complications of WTD management at the site as this was not always managed with a sole focus on the crop being grown on the field on which the fluxes were measured.

If water table was raised it would need to be managed at a level during crop periods that does not damage the crop roots or reduce yield, and allow access by agricultural machinery. Unpredictable weather makes maintaining a shallower water table problematic and costly if it goes wrong. Additionally, fields are never completely individual in that their ditch systems tend to be linked into smaller regions of the farm. These factors make it difficult to implement a shallower water table during crop periods. During the fallow periods this would be less of a problem, however concerns have been raised over the potential impact prolonged wetting of the peat over winter would have on the long term soil structure.

## **6.3 Limitations/future research direction**

### **6.3.1 EC methodology limitation**

It was shown in Chapter 3 that autotrophic respiration significantly impacted nocturnal TER during the crop season. It is suggested that the partitioning of fluxes into TER and GPP during these periods based on the temperature response is not appropriate. Other methodologies exist that partition by daytime NEE and light response (Lasslop et al., 2010). The daytime method would likely be wholly inappropriate for use during the fallow periods, but comparison of both methods alongside chamber measurements for the same period could reveal a hybrid partitioning tool involving both methodologies that would fit better to data from cropland.

Leaf Area Index (LAI) was not measured during this study, due to broken field equipment. LAI measurements would allow for improved understanding of the drivers of CO<sub>2</sub> flux and would improve partitioning of the flux. In this same vein, installing a phenology camera at the site would render similar information on crop growth. An additional method for calculating GPP could be the measurement of carbonyl sulphide (COS) as a proxy. COS is a trace atmospheric gas and occurs at about 500 ppt. Recent research has deployed quantum cascade laser absorption spectrometer technology in order to quantify COS uptake as it follows a similar pathway to CO<sub>2</sub> during photosynthesis and is thought to be uni-directional in its diffusion as no respiration response has been found (Gerdel et al., 2017).

The footprint of the measurements led to a removal of about half of the complete data period. Installation of EC instrumentation in a more central location of a larger field with a larger potential footprint would lead to a lower gap-filling requirement and less uncertainty in measurements.

Closure of the energy balance was additionally difficult due to the location of the instrumentation. Management activity altered the surface and upper soil profile of the field regularly. During each year the upper 0.5 m of peat, for the majority of the field surface, was disturbed by ploughing, planting, harvesting and disking activities. The impact of these activities, after the first ploughing in 2012, on soil conditions was not captured by the instrumentation. Soil instruments (heat flux plates, averaging thermocouples, time domain reflectometer) were installed in the upper profile of the freshly ploughed peat soil in 2012 and then left undisturbed for the entire measurement

period. It was decided that leaving the instrumentation under slightly compacted conditions was better than trying to replicate exactly the field conditions. The effect of this difference is therefore unknown. Future work should look to replicate the field management activities where the soil instruments are installed, to include ploughing, planting and harvesting activities. This will increase the labour required to observe this system, which detracts from the advantage of utilising the EC technique which allows for high resolution data with minimal maintenance. A small study would allow for characterisation of the impact this limitation of measurement location has on the data set, and may improve understanding of the drivers of CO<sub>2</sub> flux and the reliability of measurements by improving the EBC.

Additionally, it has recently been suggested by Kowalski (2018) that not all energy is captured by the measurement system. The specific energy used to evaporate water into the atmosphere is not all due to LE of vaporisation. Extra energy is expended to increase in volume during evaporation against atmospheric pressure. Calculating the contribution of this energy loss could account for an LE underestimation of 3 to 4 %.

Not all management practices were captured during the 3.5 years of measurements made here, so future work should aim to gain a record of fluxes for as many crop types typically grown at this farm; in particular, those with longer growing season (e.g. sugar beet, barley). Similarly, double cropping of some fields was observed at the farm, particularly of lettuce crops. The resultant reduction of fallow period and increased period of net CO<sub>2</sub> uptake would be expected to yield reduced NEE.

Additionally, on other areas of the farm, crops were fleeced during spring months to avoid frost damage. Given the quantity of fleecing evident on fields during these months the contribution it makes to NEE should be assessed for upscaling.

Raising the water table under crop and/or fallow periods has been suggested in the literature as a potential strategy for mitigation of CO<sub>2</sub> loss (Musarika et al., 2017, Lloyd, 2006, Evans, 2017), though it could not be identified as a clear control in the data analysed here. Implementation of raising the water table to investigate this further has been broached with farm managers by the author and colleagues, however deemed impractical at present given current lack of knowledge on the impact this will have on the soil profile over repeated crop cycles. Further research should be undertaken to understand the impact of the raising of water table fully across more crop types in

mesocosm studies and then potentially implemented at field scale. Alternatively, a parallel set of field observations of a field with similar properties growing the same crop under similar natural conditions, but different managed WTD would allow for an assessment of CO<sub>2</sub> losses.

### 6.3.2 Wind erosion

Due to limitations in available instrumentation, measurements in this study were made at single locations in two separate fields. This meant that it was only possible to speculate on the net C gain/loss of each field attributable to wind erosion due to the location of each array of samplers (on the downwind boundary of each field) and the lack of any vertical deposition measurements. Increased sampling locations would allow for a defensible estimate of C loss from the field, and therefore it is recommended that further research aims to make replicated measurements along up- and down-wind field boundaries (based on a predominant south westerly wind direction).

Additional measurements of deposition were attempted to attain an impression of how much deposition was happening within the fields using a makeshift marble dust collection sampler (MDCS). However these instruments never yielded any useful results<sup>i</sup>. Sow et al. (2006) tested several MDCO collectors and inverted frisbee collectors and found the deposition catching efficiency of these instruments was in the region of 20 to 40 %.

I would suggest that a controlled environment study using a wind tunnel would allow for improved understanding of wind-erosion of peat soil. Manipulating important parameters such as  $u$  and SWC would allow for not only an improved understanding of how well HMF is measured by the BSNE collectors, but in addition, would allow for quantification of flux per unit area, and furthermore give an impression of deposition. Wind tunnel experiments could then be used as a reference for interpreting field measurements.

The farm in this study has retained its network of hedges and relatively small fields; however this is atypical when compared to other farms in the region which have much larger fields and fewer hedgerows, which becomes apparent as you drive through the landscape. Hedgerow removal was encouraged since the end of the Second World War

---

<sup>i</sup> Largely due to the disappearance of marbles from the instruments, which are assumed to have been taken by birds.

until the implementation of The Hedgerows Regulation (1997). A continuation of this work is already being undertaken at a neighbouring farm, utilising more instrumentation arrays, combined with sonic anemometer arrays and soil moisture instrumentation and dust particle counters. The new site is more exposed with a greater fetch of 1 km, due to hedgerow removals in the 1980s and 90s (Rob Parker, Pers. comm.). This work is being undertaken as part of the Securing Ecosystem Function of Lowland Organic Soils (SEFLOS) project.

Additional work should be undertaken to understand the contribution of field cover in mitigating aeolian flux, to include crop type, barley stalks, residual crop waste left over winter, cover crops and weeds. More recently land operators at the site studied have discussed their interest in the use of soil binding agents to prevent this aeolian loss of soil (E. Garfield and R. Parker, Pers. comm.). Investigating these products under both field and controlled wind tunnel environments, would contribute greatly to mitigating losses.

Mitigating current erosion is paramount as it is expected that as SOC content of the peat soil continues to lower (from continued management) that continued wind erosion will lead to greater quantity of HMT as mineral soils are reported to be more readily transportable than organic material. This will not, however, necessarily result in an increase in C loss but it will cause increased subsidence.

### 6.3.3 General

This thesis reported annual CO<sub>2</sub> flux for calendar years from 1<sup>st</sup> January to 31<sup>st</sup> December. Whilst this was done with the best intent, it is recognised that a crop cycle has a longer impact on the ecosystem. Transference of mineralisation from one year to another has been identified as an issue in other literature for agricultural sites (e.g. Beyer et al., 2015, Anthoni et al., 2004). The impact of this ‘soil priming’ under rotational management is not easily discernible from one crop to another. The impact of this may be well measured by future mesocosm studies.

Finally, as mentioned above, a variety of other management strategies are employed on the 1,400 ha of Rosedene Farm that have yet to be quantified for their impact on NECB. Once further data has been collected on a more complete range of management regimes, upscaling spatially to a net NECB for the Farm and then the Fen region are the next logical steps. Upscaling to a farm scale would additionally benefit from a model

developed from farm records of SOC content, crops grown, and their productivity. Additionally, combined with the figures provided in Evans (2017) for a further range of land management types will allow for a well-developed understanding of lowland peat soils in England and Wales.

## 6.4 Final summary

The ambition of this thesis was to address the research questions brought forward in Chapter 1.4.1 which, along with the outcomes from this study, are presented here:

1. What are the key drivers of NEE at a lowland peat soil under intensively cultivated land use?
  - a. Tsoil was the key driver of CO<sub>2</sub> flux from this managed peat soil during fallow periods while GPP, limited by VPD, was a key driver of NEE during the crop periods.
  - b. Water table could not be clearly identified as a control on NEE.
2. What are the daily, seasonal (crop/fallow) and annual magnitudes of NEE from drained intensively cultivated lowland peat soil, under varying crop management?
  - a. Daily maximum CO<sub>2</sub> fluxes (emissions) were  $6.2 \pm 0.2$ ,  $7.82 \pm 0.3$ ,  $7.9 \pm 0.7$ ,  $13.33 \pm 0.4$  g C-CO<sub>2</sub> m<sup>-2</sup> d<sup>-1</sup> (for 2012-2015 respectively), and followed periods of increased abundance of labile material or aeration of the upper soil profile. Minimum CO<sub>2</sub> fluxes (uptake) were  $-4.9 \pm 0.3$ ,  $-3.7 \pm 0.4$ ,  $-6.3 \pm 0.4$ ,  $-4.2 \pm 0.5$  g C-CO<sub>2</sub> m<sup>-2</sup> d<sup>-1</sup> (for 2012-2015 respectively), and coincided with peak crop growth each year. Maximum and minimum daily fluxes clearly varied from year to year as a result of crop type and climatic factors.
  - b. Annual CO<sub>2</sub> flux was  $675.75 \pm 101.45$ ,  $806.38 \pm 88.75$  and  $797.18 \pm 84.6$  g C-CO<sub>2</sub> m<sup>-2</sup> yr<sup>-1</sup>, for 2013 – 2015 respectively, averaged to  $759.77 \pm 91.6$  g C-CO<sub>2</sub> m<sup>-2</sup> yr<sup>-1</sup> and demonstrating no significant difference as a result of crop type.
3. What contribution do planting and harvest of different crops have on the C balance of an intensively cultivated peat soil?
  - a. Lateral flux reduced C loss for the two lettuce crops due to the planting medium (imported peat) used, but contributed to as much as 16% of net C loss of the leek crop.
4. How much C is transported over intensively cultivated peatlands in East Anglia by aeolian action?

- a. Wind erosion led to an annual HMT of 90 to 490 g C m<sup>-2</sup> yr<sup>-1</sup>, but the destination of this flux is not defined, so it is unclear how much of this flux contributed to a loss of C.

Further NECB measurements related to other management strategies for the further variety crops grown on this soil should be made.

Implementation of mitigation strategies is necessary to reduce CO<sub>2</sub> loss from intensively cultivated land use, and measurements of their success/failure at reducing net CO<sub>2</sub> loss should be measured.

These findings have been shown to be essential for informing on the current state of C loss from intensively cultivated deep lowland peat soil in East Anglia, and provide a base of information on the C cost of growing key salad and vegetable crops on this potential C sink.

## Appendix

**Table A2.1:** Chronological table of known site management events including all fertiliser/pesticides taken from “Gatekeeper” farm records.

Date	Field event	Reason
<b>2012</b>		
22 <sup>nd</sup> June	Field ploughed to a depth of 0.2-0.3 m with additional 0.1 m sub-soiler tines	
26 <sup>th</sup> – 30 <sup>th</sup> June	Lettuce crop planted	
13 <sup>th</sup> July	Top irrigation, 25 mm	
12 <sup>th</sup> August	Harvest	
20 <sup>th</sup> August	Lettuce residuals turned into topsoil	
<b>2013</b>		
30 <sup>th</sup> June	Field ploughed to a depth of 0.2-0.3 m with additional 0.1 m sub-soiler tines	
5 <sup>th</sup> April	MOP and T.S.P. applied	Fertiliser
10 <sup>th</sup> – 12 <sup>th</sup> April	Leek crop planted with barley cover crop	
30 <sup>th</sup> April	Anthem, Cleancrop Amigo 2 and Master Gly 36 T applied	Pre EM residual and weed control
17 <sup>th</sup> May	Defy, Stomp Aqua and Cleancrop Amigo 2 applied	Weed control
1 <sup>st</sup> June	Herbicide applied Aramo and Manganese DF applied	Cover crop removal and fertiliser applied
8 <sup>th</sup> June	Afalon and Totril applied	Weed control
14 <sup>th</sup> June	Manganese DF and Bittersalrz applied	Fertilisers applied
21 <sup>st</sup> June	Totril and Starane 2 applied	Weed control
2 <sup>nd</sup> July	Dursban Wg, Manganese DF and Bittersaltz applied	Weed control
5 <sup>th</sup> July	Nitram applied	Fertiliser applied
6 <sup>th</sup> July	Teptra and Manganese DF applied	Grass weed control and fertiliser applied
15 <sup>th</sup> July	Totril, Starane 2 and Basagran SG applied	Weed control
17 <sup>th</sup> July	Dursban, Manganese DF and Bittersaltz applied	Thrip/cutworm
30 <sup>th</sup> July	Amistar Top, Hallmark With Zeon Technology, Manganese DF and Bittersaltz applied	Weeds
8 <sup>th</sup> August	Top irrigation, 25 mm	
12 <sup>th</sup> August	Amistar, Tracer, SP057, Manganese DF and Bittersaltz applied	Disease/Thrip
28 <sup>th</sup> August	Tracer, SP057, Manganese DF and Bittersaltz applied	Thrip control and fertiliser applied
12 <sup>th</sup> September	Top irrigation, 25 mm	
12 <sup>th</sup> September	Rudis, Manganese (N) and Bittersaltz applied Leek irrigated	Disease control and fertiliser
17 <sup>th</sup> – 22 <sup>nd</sup> October	Harvest	
<b>2014</b>		

<b>Date</b>	<b>Field event</b>	<b>Reason</b>
<b>22<sup>nd</sup> April</b>	Field ploughed to a depth of 0.2-0.3 m with additional 0.1 m sub-soiler tines	
<b>25<sup>th</sup> April</b>	6-6-12, Stomp Aqua, Wing-P and Dual Gold applied	Fertiliser and weed control
<b>29<sup>th</sup> April 2<sup>nd</sup> May</b>	Lettuce crop planted	
<b>1<sup>st</sup> May</b>	Invader, Plenum WG, Magnesium sulphate and Manganese sulphate applied	Weed/disease control and fertiliser
<b>1<sup>st</sup> May</b>	Top irrigation, 25 mm	
<b>7<sup>th</sup> May</b>	Top irrigation, 25 mm	
<b>12<sup>th</sup> June</b>	Revus, Gazelle, Magnesium sulphate, Manganese sulphate and Bandu (10994) applied	Disease control and fertiliser
<b>20<sup>th</sup> – 27<sup>th</sup> June</b>	Harvest	
<b>22<sup>nd</sup> - 23<sup>rd</sup> October</b>	Ditch weeds cleared, Hedges being trimmed	
<b>2015</b>		
<b>26<sup>th</sup> January</b>	T.S.P	Fertiliser applied
<b>3<sup>rd</sup> February</b>	Field ploughed to a depth of 0.2-0.3 m with additional 0.1 m sub-soiler tines	
<b>8<sup>th</sup> May</b>	6-6-12 and Cinder applied	Fertiliser and weed control
<b>12<sup>th</sup> May</b>	Celery crop planted	
<b>18<sup>th</sup> May</b>	Top irrigation, 25 mm	
<b>21<sup>st</sup> May</b>	Afalon and Stomp Aqua applied	Weed control
<b>28<sup>th</sup> May</b>	Afalon applied	Weed control
<b>1<sup>st</sup> June</b>	Manganese sulphate, Magnesium sulphate, Amistar, Plenum WG, Hallmark with Zeon technology applied	Fertiliser and disease control
<b>8<sup>th</sup> June</b>	Goltix Flowable and Defy applied	Weed control
<b>15<sup>th</sup> June</b>	Manganese sulphate, Magnesium sulphate, Plover, Aphox and Hallmark with Zeon Technology applied	Fertiliser and disease control
<b>20<sup>th</sup> June</b>	Goltix Flowable applied	Weed control
<b>30<sup>th</sup> June</b>	Manganese sulphate, Magnesium sulphate, Hallmark with Zeon Technology, Amistar and Plenum WG applied	Fertiliser and weed/disease control
<b>14<sup>th</sup> July</b>	Manganese sulphate, Magnesium sulphate, Tracer, Plenum WG and Switch applied	Fertiliser and disease control
<b>16<sup>th</sup> July</b>	Top irrigation, 25 mm	
<b>17<sup>th</sup> July</b>	Top irrigation, 25 mm	
<b>25<sup>th</sup> July</b>	Manganese sulphate, Magnesium sulphate, Aphox and Tracer applied	Fertiliser and disease control
<b>31<sup>st</sup> Jul - 11<sup>th</sup> August</b>	Harvest	

**Table A2.2:** Calibration coefficients for the Li7500 IRGA. Calibrations were undertaken at CEH Wallingford, using certified gas standards.

<b>Date calibrated</b>	<b>CO<sub>2</sub></b>		<b>H<sub>2</sub>O</b>	
	<b>Zero</b>	<b>Span</b>	<b>Zero</b>	<b>Span</b>
<b>01.06.2012</b>	0.9230	1.0046 (@607)	0.9050	1.0037 (@15 °C)
<b>17.12.2014</b>	0.9235	1.0300 (@400)	0.9146	1.0162 (@15.5 °C)
<b>06.01.2016</b>	0.9229	1.0262 (@400)	0.9145	0.9870 (@20.2 °C)
<b>11.01.2016</b>	0.9226	1.0288 (@400)	0.9179	1.0578 (@20.2 °C)

**Table A2.3:** Summary of number of half-hourly flux data values flagged by quality control.

	<b>2012</b>			<b>2013</b>			<b>2014</b>			<b>2015</b>		
	<b>NEE</b>	<b>H</b>	<b>LE</b>									
<b>NA's</b>	507	43	1182	1260	71	2594	2667	1248	3574	1767	514	2894
<b>Mauder and Foken = 2</b>	1049	566	940	1821	1251	1704	1630	1179	1427	1758	1361	1350
<b>De-Spiking</b>	115	271	529	2127	418	854	1843	442	860	2090	480	821
<b>Range limits</b>	19	2	9	84	2	29	92	6	36	70	8	13
<b>Footprint flags</b>	8147	8147	8147	6186	6186	6186	5206	5206	5206	5036	5036	5036
<b>Negative NEE at Night</b>	584	n/a	n/a	1134	n/a	n/a	907	n/a	n/a	913	n/a	n/a
<b>Visual inspection</b>	28	10	20	86	8	89	98	13	110	68	22	72
<b>u*</b>	130	248	147	445	767	424	486	836	489	333	645	422

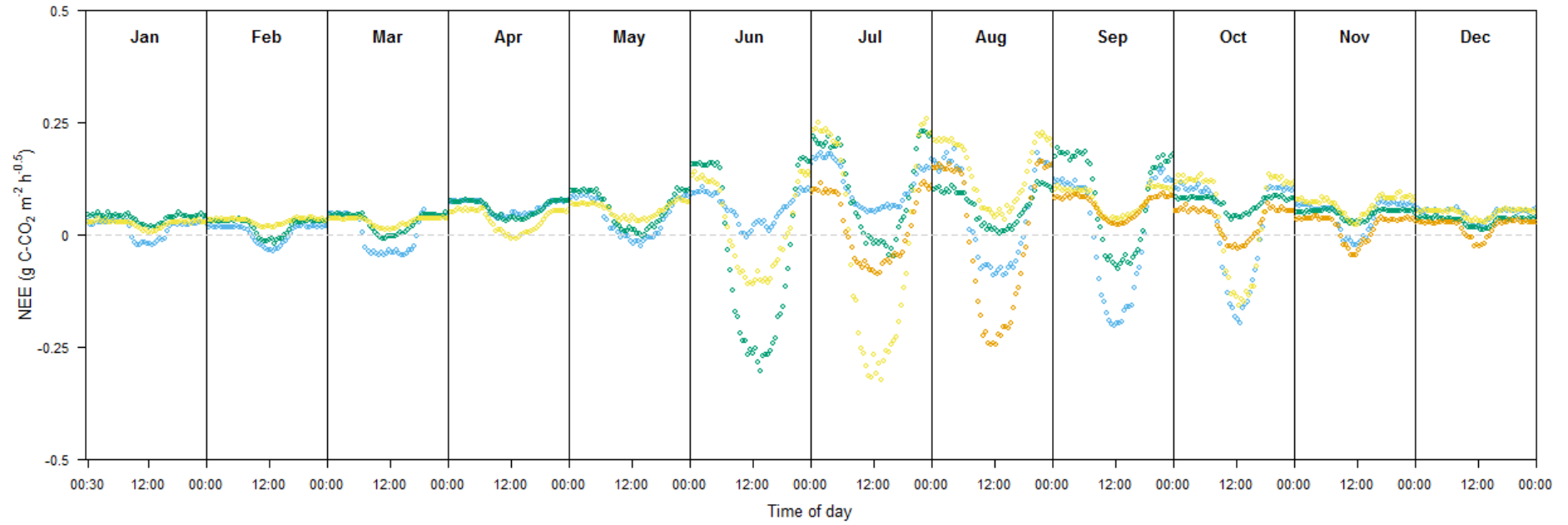


**Figure A4.1:** Monthly NEE for all years (22<sup>nd</sup> June 2012 – 31<sup>st</sup> December 2015). Orange for lettuce (2012), blue for leek (2013), green for lettuce (2014), and yellow for celery (2015).

## Bibliography

Anthoni, P. M., Freibauer, A., Kolle, O. & Schulze, E.-D. 2004. Winter wheat carbon exchange in Thuringia, Germany. *Agricultural and Forest Meteorology*, 121, 55-67.

Aubinet, M., Feigenwinter, C., Heinesch, B., Laffineur, Q., Papale, D., Reichstein, M., Rinne, J. & Van Gorsel, E. 2012a. Nighttime Flux Correction. In: Aubinet, M., Vesala, T. & Papale, D. (eds.) *Eddy Covariance: A Practical Guide to Measurement and Data Analysis*. Dordrecht: Springer Netherlands.

Aubinet, M., Grelle, A., Ibrom, A., Rannik, Ü., Moncrieff, J., Foken, T., Kowalski, A. S., Martin, P. H., Berbigier, P., Bernhofer, C., Clement, R., Elbers, J., Granier, A., Grünwald, T., Morgenstern, K., Pilegaard, K., Rebmann, C., Snijders, W., Valentini, R. & Vesala, T. 2000. Estimates of the annual net carbon and water exchange of forests: the EUROFLUX methodology. *Advances in Ecological Research*, 30, 113-175.

Aubinet, M., Moureaux, C., Bodson, B., Dufranne, D., Heinesch, B., Suleau, M., Vancutsem, F. & Vilret, A. 2009. Carbon sequestration by a crop over a 4-year sugar beet/winter wheat/seed potato/winter wheat rotation cycle. *Agricultural and Forest Meteorology*, 149, 407-418.

Aubinet, M., Vesala, T. & Papale, D. 2012b. *Eddy Covariance: A Practical Guide to Measurement and Data Analysis*, Dordrecht, Springer.

Baldocchi, D., Falge, E., Gu, L., Olson, R., Hollinger, D., Running, S., Anthoni, P., Bernhofer, C., Davis, K., Evans, R., Fuentes, J., Goldstein, A., Katul, G., Law, B., Lee, X., Malhi, Y., Meyers, T., Munger, W., Oechel, W., Paw, K. T., Pilegaard, K., Schmid, H. P., Valentini, R., Verma, S., Vesala, T., Wilson, K. & Wofsy, S. 2001. FLUXNET: A New Tool to Study the Temporal and Spatial Variability of Ecosystem-Scale Carbon Dioxide, Water Vapor, and Energy Flux Densities. *Bulletin of the American Meteorological Society*, 82, 2415-2434.

Baldocchi, D. D. 2003. Assessing the eddy covariance technique for evaluating carbon dioxide exchange rates of ecosystems: past, present and future. *Global Change Biology*, 9, 479-492.

Bärring, L., Jönsson, P., Mattsson, J. O. & Åhman, R. 2003. Wind erosion on arable land in Scania, Sweden and the relation to the wind climate—a review. *Catena*, 52, 173-190.

Batjes, N. H. 1996. Total carbon and nitrogen in the soils of the world. *European Journal of Soil Science*, 47, 151-163.

Beetz, S., Liebersbach, H., Glatzel, S., Jurasinski, G., Buczko, U. & Höper, H. 2012. *Effects of land use intensity on the full greenhouse gas balance in an Atlantic peat bog.*

Beyer, C. & Höper, H. 2015. Greenhouse gas exchange of rewetted bog peat extraction sites and a *Sphagnum* cultivation site in northwest Germany. *Biogeosciences*, 12, 2101-2117.

Beyer, C., Liebersbach, H. & Höper, H. 2015. Multiyear greenhouse gas flux measurements on a temperate fen soil used for cropland or grassland. *Journal of Plant Nutrition and Soil Science*, 178, 99-111.

Blonquist, J. M., Tanner, B. D. & Bugbee, B. 2009. Evaluation of measurement accuracy and comparison of two new and three traditional net radiometers. *Agricultural and Forest Meteorology*, 149, 1709-1721.

Böhner, J., Schäfer, W., Conrad, O., Gross, J. & Ringeler, A. 2003. The WEELS model: methods, results and limitations. *CATENA*, 52, 289-308.

Borrelli, P., Panagos, P., Ballabio, C., Lugato, E., Weynants, M. & Montanarella, L. 2014. Towards a pan-european assessment of land susceptibility to wind erosion. *Land Degradation & Development*.

Brooks, A. & Farquhar, G. D. 1985. Effect of temperature on the CO<sub>2</sub>/O<sub>2</sub> specificity of ribulose-1,5-bisphosphate carboxylase/oxygenase and the rate of respiration in the light. *Planta*, 165, 397-406.

Burba, G. 2013. *Eddy Covariance Method: for Scientific, Industrial, Agricultural and Regulatory Applications*, Lincoln, Nebraska, LI-COR Biosciences.

Businger, J. A. 1986. Evaluation of the Accuracy with Which Dry Deposition Can Be Measured with Current Micrometeorological Techniques. *Journal of Climate and Applied Meteorology*, 25, 1100-1124.

Byrne, K., Chojnicki, B., Christensen, T. R., Drösler, M., Freibauer, A., Friborg, T., Frolking, S., Lindroth, A., Mailhammer, J., Malmer, N., Selin, P. & Turunen, J. 2004. EU Peatlands: Current Carbon Stocks and Trace Gas Fluxes, Report 4/2004 to 'Concerted action: Synthesis of the European Greenhouse Gas Budget. Geosphere-Biosphere Centre, Univ. of Lund, Sweden.

Campbell, D. R., Lavoie, C. & Rochefort, L. 2002. Wind erosion and surface stability in abandoned milled peatlands. *Canadian Journal of Soil Science*, 82, 85-95.

Campbell Scientific 2016. Model HFP01 Soil Heat Flux Plate. *Instruction Manual*. Revision: 10/16 ed.: Campbell Scientific Inc.

Ceschia, E., Béziat, P., Dejoux, J. F., Aubinet, M., Bernhofer, C., Bodson, B., Buchmann, N., Carrara, A., Cellier, P., Di Tommasi, P., Elbers, J. A., Eugster, W., Grünwald, T., Jacobs, C. M. J., Jans, W. W. P., Jones, M., Kutsch, W., Lanigan, G., Magliulo, E., Marloie, O., Moors, E. J., Moureaux, C., Olioso, A., Osborne, B., Sanz, M. J., Saunders, M., Smith, P., Soegaard, H. & Wattenbach, M. 2010. Management effects on net ecosystem carbon and GHG budgets at European crop sites. *Agriculture, Ecosystems & Environment*, 139, 363-383.

Chambers, F. M., Beilman, D. W. & Yu, Z. 2011. Methods for determining peat humification and for quantifying peat bulk density, organic matter and carbon content for palaeostudies of climate and peatland carbon dynamics. *Mires and Peat*, 7.

Chappell, A. & Baldock, J. A. 2016. Wind erosion reduces soil organic carbon sequestration falsely indicating ineffective management practices. *Aeolian Research*, 22, 107-116.

Chappell, A. & Warren, A. 2003. Spatial scales of <sup>137</sup>Cs-derived soil flux by wind in a 25 km<sup>2</sup> arable area of eastern England. *Catena*, 52, 209-234.

Charman, D. 2002. *Peatlands and Environmental Change*, Chichester, Wiley.

Churkina, G. 2013. An Introduction to Carbon Cycle Science. In: Brown, D. G., Robinson, D. T., French, N. H. F. & Reed, B. C. (eds.) *Land Use and the Carbon Cycle: Advances in Integrated Science, Management, and Policy*. Cambridge: Cambridge University Press.

Ciais, P., Sabine, C., Bala, G., Bopp, L., Brovkin, V., Canadell, J., Chhabra, A., DeFries, R., Galloway, J., Heimann, M., Jones, C., Le Quéré, C., Myneni, R. B., Piao, S. & Thornton, P. 2013. Carbon and Other Biogeochemical Cycles. In: Stocker, T. F., Qin, D., Plattner, G.-K., Tignor, M., Allen, S. K., Boschung, J., Nauels, A., Xia, Y., Bex, V. & Midgley, P. M. (eds.) *Climate Change 2013: The Physical Science Basis. Contribution of Working Group I to the Fifth Assessment Report of the Intergovernmental Panel on Climate Change*. Cambridge, United Kingdom and New York, NY, USA: Cambridge University Press.

Clymo, R. S. 1965. Experiments on Breakdown of Sphagnum in Two Bogs. *Journal of Ecology*, 53, 747-758.

Clymo, R. S. 1984. The Limits to Peat Bog Growth. *Philosophical Transactions of the Royal Society of London. B, Biological Sciences*, 303, 605-654.

Clymo, R. S., Turunen, J. & Tolonen, K. 1998. Carbon Accumulation in Peatland. *Oikos*, 81, 368-388.

Committee on Climate Change 2016. UK climate action following the Paris Agreement  
Committee on Climate Change.

Committee on Climate Change 2017. Progress in preparing for climate change: 2017  
Report to Parliament.

Committee on Climate Change 2018. An independent assessment of the UK's Clean  
Growth Strategy – from ambition to action.

Couwenberg, J. 2011. Greenhouse gas emissions from managed peat soils: is the IPCC  
reporting guidance realistic? *Mires and Peat*, 8, 1-10.

Dargie, G. C., Lewis, S. L., Lawson, I. T., Mitchard, E. T. A., Page, S. E., Bocko, Y. E.  
& Ifo, S. A. 2017. Age, extent and carbon storage of the central Congo Basin peatland  
complex. *Nature*, 542, 86-90.

Dawson, J. J. C. & Smith, P. 2007. Carbon losses from soil and its consequences for  
land-use management. *Science of The Total Environment*, 382, 165-190.

Dawson, Q., Kechavarzi, C., Leeds-Harrison, P. B. & Burton, R. G. O. 2010.  
Subsidence and degradation of agricultural peatlands in the Fenlands of Norfolk, UK.  
*Geoderma*, 154, 181-187.

DEFRA 2017. Agriculture in the United Kingdom 2016. Department for Environment,  
Food and Rural Affairs; Department of Agriculture, Environment and Rural Affairs  
(Northern Ireland); Welsh Assembly Government; The Department for Rural Affairs  
and Heritage; The Scottish Government; Rural & Environment Science & Analytical  
Services.

Dengel, S., Levy, P. E., Grace, J., Jones, S. K. & Skiba, U. M. 2011. Methane emissions  
from sheep pasture, measured with an open-path eddy covariance system. *Global  
Change Biology*, 17, 3524-3533.

Denmead, O. T. 2008. Approaches to measuring fluxes of methane and nitrous oxide  
between landscapes and the atmosphere. *Plant and Soil*, 309, 5-24.

Dinsmore, K. J., Billett, M. F., Skiba, U. M., Rees, R. M., Drewer, J. & Helfter, C. 2010. Role of the aquatic pathway in the carbon and greenhouse gas budgets of a peatland catchment. *Global Change Biology*, 16, 2750-2762.

Drösler, M., Adelman, W., Augustin, J., Bergmann, L., Beyer, C., Chojniki, B., Förster, C., Freibauer, A., Giebels, M., Görlitz, S., Höper, H., Kantelhardt, J., Liebersbach, H., Hahn-Schöfl, M., Minke, M., Petschow, U., Pfadenhauer, J., Schaller, L., Schägner, J. P. & Wehrhahn, M. 2013. *Klimaschutz durch Moorschutz. Schlussbericht des BMBF-Vorhabens: Klimaschutz - Moornutzungsstrategien 2006-2010.*

Eickenscheidt, T., Heinichen, J. & Drösler, M. 2015. The greenhouse gas balance of a drained fen peatland is mainly controlled by land-use rather than soil organic carbon content. *Biogeosciences*, 12, 5161-5184.

Elsgaard, L., Görres, C.-M., Hoffmann, C. C., Blicher-Mathiesen, G., Schelde, K. & Petersen, S. O. 2012. Net ecosystem exchange of CO<sub>2</sub> and carbon balance for eight temperate organic soils under agricultural management. *Agriculture, Ecosystems & Environment*, 162, 52-67.

Evans, C., Allott, T., Billett, M., Burden, A., Chapman, P., Dinsmore, K., Evans, M., Freeman, C., Goulsbra, C., Holden, J., Jones, D., Jones, T., Moody, C., Palmer, S., Worrall, F. 2013. Greenhouse gas emissions associated with non gaseous losses of carbon from peatlands – Fate of particulate and dissolved carbon. *Final Report to the Department for Environment, Food and Rural Affairs, Project SP1205.* Centre for Ecology and Hydrology Bangor.

Evans, C., Morrison, R., Burden, A., Williamson, J., Baird, A., Brown, E., Callaghan, N., Chapman, P., Cumming, A., Dean, H., Dixon, S., Dooling, G., Evans, J., Gauci, V., Grayson, R., Haddaway, N., He, Y., Heppell, K., Holden, J., Hughes, S., Kaduk, J., Jones, D., Matthews, R., Menichino, N., Misselbrook, T., Page, S., Pan, G., Peacock, M., Rayment, M., Ridley, L., Robinson, I., Rylett, D., Scowen, M., Stanley, K., Worrall, F. 2017. Lowland peatland systems in England and Wales - evaluating greenhouse gas fluxes and carbon balances. *Final Report to Defra on Project SP1210.* Centre for Ecology and Hydrology, Bangor.

Evans, C. D., Chapman, P. J., Clark, J. M., Monteith, D. T. & Cresser, M. S. 2006. Alternative explanations for rising dissolved organic carbon export from organic soils. *Global Change Biology*, 12, 2044-2053.

Falge, E., Baldocchi, D., Olson, R., Anthoni, P., Aubinet, M., Bernhofer, C., Burba, G., Ceulemans, R., Clement, R., Dolman, H., Granier, A., Gross, P., Grunwald, T., Hollinger, D., Jensen, N. O., Katul, G., Keronen, P., Kowalski, A., Lai, C. T., Law, B. E., Meyers, T., Moncrieff, H., Moors, E., Munger, J. W., Pilegaard, K., Rannik, U., Rebmann, C., Suyker, A., Tenhunen, J., Tu, K., Verma, S., Vesala, T., Wilson, K. &

- Wofsy, S. 2001. Gap filling strategies for defensible annual sums of net ecosystem exchange. *Agricultural and Forest Meteorology*, 107, 43-69.
- Finkelstein, P. L. & Sims, P. F. 2001. Sampling error in eddy correlation flux measurements. *Journal of Geophysical Research: Atmospheres*, 106, 3503-3509.
- Foken, T. 2008. The Energy Balance Closure Problem: An Overview. *Ecological Applications*, 18, 1351-1367.
- Foken, T., Aubinet, M., Finnigan, J. J., Leclerc, M. Y., Mauder, M. & U, K. T. P. 2011. Results Of A Panel Discussion About The Energy Balance Closure Correction For Trace Gases. *Bulletin of the American Meteorological Society*, 92, ES13-ES18.
- Foken, T., Aubinet, M. & Leuning, R. 2012a. The Eddy Covariance Method. In: Aubinet, M., Vesala, T. & Papale, D. (eds.) *Eddy Covariance: A Practical Guide to Measurement and Data Analysis*. Dordrecht: Springer.
- Foken, T., Göockede, M., Mauder, M., Mahrt, L., Amiro, B. & Munger, W. 2005. Post-Field Data Quality Control. In: Lee, X., Massman, W. & Law, B. (eds.) *Handbook of Micrometeorology: A Guide for Surface Flux Measurement and Analysis*. Dordrecht: Springer Netherlands.
- Foken, T., Leuning, R., Oncley, S. R., Mauder, M. & Aubinet, M. 2012b. Corrections and Data Quality Control. In: Aubinet, M., Vesala, T. & Papale, D. (eds.) *Eddy Covariance: A Practical Guide to Measurement and Data Analysis*. Dordrecht: Springer Netherlands.
- Foken, T. & Wichura, B. 1996. Tools for quality assessment of surface-based flux measurements. *Agricultural and Forest Meteorology*, 78, 83-105.
- Foulds, S. A. & Warburton, J. 2007a. Significance of wind-driven rain (wind-splash) in the erosion of blanket peat. *Geomorphology*, 83, 183-192.
- Foulds, S. A. & Warburton, J. 2007b. Wind erosion of blanket peat during a short period of surface desiccation (North Pennines, Northern England). *Earth Surface Processes and Landforms*, 32, 481-488.
- Freeman, C., Ostle, N. & Kang, H. 2001. An enzymic "latch" on a global carbon store. *Nature*, 409, 149.

Freeman, C., Ostle, N. J., Fenner, N. & Kang, H. 2004. A regulatory role for phenol oxidase during decomposition in peatlands. *Soil Biology and Biochemistry*, 36, 1663-1667.

Frolking, S., Talbot, J., Jones, M. C., Treat, C. C., Kauffman, J. B., Tuittila, E.-S. & Roulet, N. 2011. Peatlands in the Earth's 21st century climate system. *Environmental Reviews*, 19, 371-396.

Fryrear, D. W. 1986. A field dust sampler. *Journal of Soil and Water Conservation*, 41, 117-120.

Fryrear, D. W., Stout, J. E., Hagen, L. J. & Vories, E. D. 1991. *Wind Erosion: Field Measurement And Analysis*.

Fuhrer, J. 2007. Sustainability of Crop Production Systems under Climate Change. *In: Newton, P. C. D., Carran, R. A., Edwards, G. R. & Niklaus, P. A. (eds.) Agrosystems in a Changing Climate*. Boca Raton: CRC Taylor & Francis Group.

Funk, R. & Engel, W. 2015. Investigations with a field wind tunnel to estimate the wind erosion risk of row crops. *Soil and Tillage Research*, 145, 224-232.

Funk, R. & Reuter, H. I. 2006. Wind Erosion. *In: J., B. & J., P. (eds.) Soil Erosion in Europe*. John Wiley & Sons.

G's Fresh. 2017. *Grower profiles: G S Shropshire & Sons Ltd* [Online]. Available: [https://www.gs-growers.com/growers\\_profiles/g-s-shropshire-sons-ltd/](https://www.gs-growers.com/growers_profiles/g-s-shropshire-sons-ltd/) [Accessed 20th April 2018].

Gerdel, K., Spielmann, F. M., Hammerle, A. & Wohlfahrt, G. 2017. Eddy covariance carbonyl sulfide flux measurements with a quantum cascade laser absorption spectrometer. *Atmos. Meas. Tech.*, 10, 3525-3537.

Gilmanov, T. G., Soussana, J. F., Aires, L., Allard, V., Ammann, C., Balzarolo, M., Barcza, Z., Bernhofer, C., Campbell, C. L., Cernusca, A., Cescatti, A., Clifton-Brown, J., Dirks, B. O. M., Dore, S., Eugster, W., Fuhrer, J., Gimeno, C., Gruenwald, T., Haszpra, L., Hensen, A., Ibrom, A., Jacobs, A. F. G., Jones, M. B., Lanigan, G., Laurila, T., Lohila, A., G.Manca, Marcolla, B., Nagy, Z., Pilegaard, K., Pinter, K., Pio, C., Raschi, A., Rogiers, N., Sanz, M. J., Stefani, P., Sutton, M., Tuba, Z., Valentini, R., Williams, M. L. & Wohlfahrt, G. 2007. Partitioning European grassland net ecosystem CO<sub>2</sub> exchange into gross primary productivity and ecosystem respiration using light response function analysis. *Agriculture, Ecosystems & Environment*, 121, 93-120.

- Goossens, D. & Buck, B. J. 2012. Can BSNE (Big Spring Number Eight) samplers be used to measure PM10, respirable dust, PM2.5 and PM1.0? *Aeolian Research*, 5, 43-49.
- Goossens, D., Offer, Z. & London, G. 2000. Wind tunnel and field calibration of five aeolian sand traps. *Geomorphology*, 35, 233-252.
- Goossens, D. & Offer, Z. Y. 2000. Wind tunnel and field calibration of six aeolian dust samplers. *Atmospheric Environment*, 34, 1043-1057.
- Gorham, E. 1991. Northern Peatlands: Role in the Carbon Cycle and Probable Responses to Climatic Warming. *Ecological Applications*, 1, 182-195.
- Grønlund, A., Hauge, A., Hovde, A. & Rasse, D. P. 2008. Carbon loss estimates from cultivated peat soils in Norway: a comparison of three methods. *Nutrient Cycling in Agroecosystems*, 81, 157-167.
- Grønlund, A., Sveistrup, T. E., Søvik, A. K., Rasse, D. P. & Kløve, B. 2006. Degradation of cultivated peat soils in northern Norway based on field scale CO<sub>2</sub>, N<sub>2</sub>O and CH<sub>4</sub> emission measurements. *Archives of Agronomy and Soil Science*, 52, 149-159.
- Hadley, P. & Causton, D. R. 1984. Changes in percentage organic carbon content during ontogeny. *Planta*, 160, 97-101.
- Harding, R. J. & Lloyd, C. R. 2008. Evaporation and energy balance of a wet grassland at Tadham Moor on the Somerset Levels. *Hydrological Processes*, 22, 2346-2357.
- Harper, R. J., Gilkes, R. J., Hill, M. J. & Carter, D. J. 2010. Wind erosion and soil carbon dynamics in south-western Australia. *Aeolian Research*, 1, 129-141.
- Hendricks Franssen, H. J., Stöckli, R., Lehner, I., Rotenberg, E. & Seneviratne, S. I. 2010. Energy balance closure of eddy-covariance data: A multisite analysis for European FLUXNET stations. *Agricultural and Forest Meteorology*, 150, 1553-1567.
- Hendriks, D. M. D., van Huissteden, J., Dolman, A. J. & van der Molen, M. K. 2007. The full greenhouse gas balance of an abandoned peat meadow. *Biogeosciences*, 4, 411-424.
- Holman, I. P., 2009, *An estimate of peat reserves and loss in the East Anglian Fens Commissioned by the RSPB*. Cranfield University. 'Available [Accessed January 2014].

Horst, T. W. 2000. On Frequency Response Corrections for Eddy Covariance Flux Measurements. *Boundary-Layer Meteorology*, 94, 517-520.

Hutchinson, J. N. 1980. The Record of Peat Wastage in the East Anglian Fenlands at Holme Post, 1848-1978 A.D. *Journal of Ecology*, 68, 229-249.

IMechE, 2013, *Global Food: Waste not, want not*. Institute of Mechanical Engineers. 'Available [Accessed February 2015].

Ingram, H. A. P. 1978. Soil layers in Mires: Function and Terminology. *Journal of Soil Science*, 29, 224-227.

IPCC 2006. *2006 IPCC Guidelines for National Greenhouse Gas Inventories*, Hayama, Japan, IGES, Japan.

IPCC 2013a. *Climate Change 2013: The Physical Science Basis. Contribution of Working Group I to the Fifth Assessment Report of the Intergovernmental Panel on Climate Change*, Cambridge, United Kingdom and New York, NY, USA, Cambridge University Press.

IPCC 2013b. Summary for Policymakers. In: Stocker, T. F., Qin, D., Plattner, G.-K., Tignor, M., Allen, S. K., Boschung, J., Nauels, A., Xia, Y., Bex, V. & Midgley, P. M. (eds.) *Climate Change 2013: The Physical Science Basis. Contribution of Working Group I to the Fifth Assessment Report of the Intergovernmental Panel on Climate Change*. Cambridge, United Kingdom and New York, NY, USA: Cambridge University Press.

IPCC 2014. *2013 Supplement to the 2006 IPCC Guidelines for National Greenhouse Gas Inventories: Wetlands*, IPCC, Switzerland.

Jia, J. X., Ma, Y. C. & Xiong, Z. Q. 2012. Net ecosystem carbon budget, net global warming potential and greenhouse gas intensity in intensive vegetable ecosystems in China. *Agriculture, Ecosystems & Environment*, 150, 27-37.

Joosten, H. & Clarke, D. 2002. *Wise Use of Mires and Peatlands: Background and Principles Including a Framework for Decision-making*, International Mire Conservation Group; International Peat Society.

Kaimal, J. C. & Finnigan, J. J. 1994. *Atmospheric Boundary Layer Flows: Their Structure and Measurement*, Oxford University Press.

- Kandel, T. P., Elsgaard, L. & Lærke, P. E. 2013. Measurement and modelling of CO<sub>2</sub> flux from a drained fen peatland cultivated with reed canary grass and spring barley. *GCB Bioenergy*, 5, 548-561.
- Karki, S., Elsgaard, L., Kandel, T. P. & Lærke, P. E. 2015. Full GHG balance of a drained fen peatland cropped to spring barley and reed canary grass using comparative assessment of CO<sub>2</sub> fluxes. *Environmental Monitoring and Assessment*, 187, 62.
- Kasimir-Klemedtsson, Å., Klemedtsson, L., Berglund, K., Martikainen, P., Silvola, J. & Oenema, O. 1997. Greenhouse gas emissions from farmed organic soils: a review. *Soil Use and Management*, 13, 245-250.
- Kirschbaum, M. U. F. 1995. The temperature dependence of soil organic matter decomposition, and the effect of global warming on soil organic C storage. *Soil Biology and Biochemistry*, 27, 753-760.
- Kirschbaum, M. U. F. 2000. Will changes in soil organic carbon act as a positive or negative feedback on global warming. *Biogeochemistry*, 48, 21-51.
- Koerber, G. R., Edwards-Jones, G., Hill, P. W., Canals, L. M. i., Nyeko, P., York, E. H. & Jones, D. L. 2009. Geographical variation in carbon dioxide fluxes from soils in agro-ecosystems and its implications for life-cycle assessment. *Journal of Applied Ecology*, 46, 306-314.
- Kormann, R. & Meixner, F. X. 2001. An Analytical Footprint Model For Non-Neutral Stratification. *Boundary-Layer Meteorology*, 99, 207-224.
- Kowalski, A. S. 2018. Technical note: rectifying systematic underestimation of the specific energy required to evaporate water into the atmosphere. *Hydrol. Earth Syst. Sci. Discuss.*, 2018, 1-4.
- Kunwor, S., Starr, G., Loescher, H. W. & Staudhammer, C. L. 2017. Preserving the variance in imputed eddy-covariance measurements: Alternative methods for defensible gap filling. *Agricultural and Forest Meteorology*, 232, 635-649.
- Kutsch, W. L., Aubinet, M., Buchmann, N., Smith, P., Osborne, B., Eugster, W., Wattenbach, M., Schrumpf, M., Schulze, E. D., Tomelleri, E., Ceschia, E., Bernhofer, C., Béziat, P., Carrara, A., Di Tommasi, P., Grünwald, T., Jones, M., Magliulo, V., Marloie, O., Moureaux, C., Olioso, A., Sanz, M. J., Saunders, M., Sjøgaard, H. & Ziegler, W. 2010. The net biome production of full crop rotations in Europe. *Agriculture, Ecosystems & Environment*, 139, 336-345.

- Lafleur, P. M., Moore, T. R., Roulet, N. T. & Frolking, S. 2005. Ecosystem Respiration in a Cool Temperate Bog Depends on Peat Temperature But Not Water Table. *Ecosystems*, 8, 619-629.
- Lasslop, G., Reichstein, M., Papale, D., Richardson, A. D., Arneeth, A., Barr, A., Stoy, P. & Wohlfahrt, G. 2010. Separation of net ecosystem exchange into assimilation and respiration using a light response curve approach: critical issues and global evaluation. *Global Change Biology*, 16, 187-208.
- Leclerc, M. Y. & Thurtell, G. W. 1990. Footprint prediction of scalar fluxes using a Markovian analysis. *Boundary-Layer Meteorology*, 52, 247-258.
- Leiber-Sauheitl, K., Fuß, R., Voigt, C. & Freibauer, A. 2014. High CO<sub>2</sub> fluxes from grassland on histic Gleysol along soil carbon and drainage gradients. *Biogeosciences*, 11, 749-761.
- Leifeld, J., Müller, M. & Fuhrer, J. 2011. Peatland subsidence and carbon loss from drained temperate fens. *Soil Use and Management*, 27, 170-176.
- Leuning, R. 2005. Measurements of Trace Gas Fluxes in the Atmosphere Using Eddy Covariance: WPL Corrections Revisited. In: Lee, X., Massman, W. & Law, B. (eds.) *Handbook of Micrometeorology: A Guide for Surface Flux Measurement and Analysis*. Dordrecht: Springer Netherlands.
- Leuning, R., van Gorsel, E., Massman, W. & R. Isaac, P. 2012. *Reflections on the surface energy imbalance problem*.
- Li, S., Lobb, D. A., Kachanoski, R. G. & McConkey, B. G. 2011. Comparing the use of the traditional and repeated-sampling-approach of the <sup>137</sup>Cs technique in soil erosion estimation. *Geoderma*, 160, 324-335.
- Lloyd, C. R. 2006. Annual carbon balance of a managed wetland meadow in the Somerset Levels, UK. *Agricultural and Forest Meteorology*, 138, 168-179.
- Lloyd, J. & Taylor, J. A. 1994. On the Temperature Dependence of Soil Respiration. *Functional Ecology*, 8, 315-323.
- Lohila, A., Aurela, M., Tuovinen, J.-P. & Laurila, T. 2004. Annual CO<sub>2</sub> exchange of a peat field growing spring barley or perennial forage grass. *Journal of Geophysical Research: Atmospheres*, 109, n/a-n/a.

Luyssaert, S., Reichstein, M., Schulze, E. D., Janssens, I. A., Law, B. E., Papale, D., Dragoni, D., Goulden, M. L., Granier, A., Kutsch, W. L., Linder, S., Matteucci, G., Moors, E., Munger, J. W., Pilegaard, K., Saunders, M. & Falge, E. M. 2009. Toward a consistency cross-check of eddy covariance flux-based and biometric estimates of ecosystem carbon balance. *Global Biogeochemical Cycles*, 23, n/a-n/a.

Malhi, Y., McNaughton, K. & Von Randow, C. 2005. Low Frequency Atmospheric Transport and Surface Flux Measurements. In: Lee, X., Massman, W. & Law, B. (eds.) *Handbook of Micrometeorology: A Guide for Surface Flux Measurement and Analysis*. Dordrecht: Springer Netherlands.

Maljanen, M., Sigurdsson, B. D., Guðmundsson, J., Óskarsson, H., Huttunen, J. T. & Martikainen, P. J. 2010. Greenhouse gas balances of managed peatlands in the Nordic countries – present knowledge and gaps. *Biogeosciences*, 7, 2711-2738.

Mander, Ü., Järveoja, J., Maddison, M., Soosaar, K., Aavola, R., Ostonen, I. & Salm, J.-O. 2012. Reed canary grass cultivation mitigates greenhouse gas emissions from abandoned peat extraction areas. *GCB Bioenergy*, 4, 462-474.

Mander, Ü., Uuemaa, E., Kull, A., Kanal, A., Maddison, M., Soosaar, K., Salm, J.-O., Lesta, M., Hansen, R., Kuller, R., Harding, A. & Augustin, J. 2010. Assessment of methane and nitrous oxide fluxes in rural landscapes. *Landscape and Urban Planning*, 98, 172-181.

Mauder, M. & Foken, T. 2004. *Documentation and Instruction Manual of the Eddy Covariance Software Package TK2*, Univ., Abt. Mikrometeorologie.

Mendez, M. J., Funk, R. & Buschiazzi, D. E. 2011. Field wind erosion measurements with Big Spring Number Eight (BSNE) and Modified Wilson and Cook (MWAC) samplers. *Geomorphology*, 129, 43-48.

Milne, R. & Brown, T. A. 1997. Carbon in the Vegetation and Soils of Great Britain. *Journal of Environmental Management*, 49, 413-433.

Mitsch, W., Bernal, B., Nahlik, A., Mander, Ü., Zhang, L., Anderson, C., Jørgensen, S. & Brix, H. 2013. Wetlands, carbon, and climate change. *Landscape Ecology*, 28, 583-597.

Moffat, A. M., Papale, D., Reichstein, M., Hollinger, D. Y., Richardson, A. D., Barr, A. G., Beckstein, C., Braswell, B. H., Churkina, G., Desai, A. R., Falge, E., Gove, J. H., Heimann, M., Hui, D., Jarvis, A. J., Kattge, J., Noormets, A. & Stauch, V. J. 2007. Comprehensive comparison of gap-filling techniques for eddy covariance net carbon fluxes. *Agricultural and Forest Meteorology*, 147, 209-232.

Moncrieff, J., Clement, R., Finnigan, J. & Meyers, T. 2005. Averaging, Detrending, and Filtering of Eddy Covariance Time Series. *In*: Lee, X., Massman, W. & Law, B. (eds.) *Handbook of Micrometeorology*. Springer Netherlands.

Moncrieff, J. B., Massheder, J. M., De Bruin, H., Elbers, J., Friborg, T., Heusinkveld, B., Kabat, P., Scott, S., Soegaard, H. & Verhoef, A. 1997. A system to measure surface fluxes of momentum, sensible heat, water vapour and carbon dioxide. *Journal of Hydrology*, 188-189, 589-611.

Moore, S., Evans, C. D., Page, S. E., Garnett, M. H., Jones, T. G., Freeman, C., Hooijer, A., Wiltshire, A. J., Limin, S. H. & Gauci, V. 2013. Deep instability of deforested tropical peatlands revealed by fluvial organic carbon fluxes. *Nature*, 493, 660-663.

Moore, T. & Knowles, R. 1989. *The Influence of Water Table Levels on Methane and Carbon Dioxide Emissions From Peatland Soils*.

Morelle, R. 2014. *Colossal peat bog discovered in Congo* [Online]. BBC News. Available: <http://www.bbc.co.uk/news/science-environment-27492949> [Accessed 27th May 2014].

Morrison, R., Cumming, A. M. J., Taft, H. E., Kaduk, J., Page, S. E., Jones, D. L., Harding, R. J. & Balzter, H. 2013. Carbon dioxide fluxes at an intensively cultivated temperate lowland peatland in the East Anglian Fens, UK. *Biogeosciences Discuss.*, 10, 4193-4223.

Musarika, S., Atherton, C. E., Gomersall, T., Wells, M. J., Kaduk, J., Cumming, A. M. J., Page, S. E., Oechel, W. C. & Zona, D. 2017. Effect of water table management and elevated CO<sub>2</sub> on radish productivity and on CH<sub>4</sub> and CO<sub>2</sub> fluxes from peatlands converted to agriculture. *Science of The Total Environment*, 584, 665-672.

Namikas, S. L. 2003. Field measurement and numerical modelling of aeolian mass flux distributions on a sandy beach. *Sedimentology*, 50, 303-326.

Natural England 2009. *Agricultural Land Classification: protecting the best and most versatile agricultural land (TIN049)*, Crewe, Natural England.

Natural England 2010. *England's Peatlands: Carbon Storage and Greenhouse Gases*, Peterborough, Natural England.

Natural England 2015. *National Character Area Profile: 46. The Fens*, Peterborough, Natural England.

Neftel, A., Spirig, C. & Ammann, C. 2008. Application and test of a simple tool for operational footprint evaluations. *Environmental Pollution*, 152, 644-652.

Newton, P. C. D., Carran, R. A., Edwards, G. R. & Niklaus, P. A. 2007. Introduction. *In: Newton, P. C. D., Carran, R. A., Edwards, G. R. & Niklaus, P. A. (eds.) Agrosystems in a Changing Climate*. Boca Raton: CRC Taylor & Francis Group.

Nieveen, J. P., Campbell, D. I., Schipper, L. A. & Blair, I. J. 2005. Carbon exchange of grazed pasture on a drained peat soil. *Global Change Biology*, 11, 607-618.

Nilsson, M., Sagerfors, J., Buffam, I., Laudon, H., Eriksson, T., Grelle, A., Klemmedsson, L., Weslien, P. & Lindroth, A. 2008. Contemporary carbon accumulation in a boreal oligotrophic minerogenic mire – a significant sink after accounting for all C-fluxes. *Global Change Biology*, 14, 2317-2332.

Oechel, W. C., Cowles, S., Grulke, N., Hastings, S. J., Lawrence, B., Prudhomme, T., Riechers, G., Strain, B., Tissue, D. & Vourlitis, G. 1994. Transient nature of CO<sub>2</sub> fertilization in Arctic tundra. *Nature*, 371, 500-503.

Oechel, W. C., Vourlitis, G. L., Hastings, S. J., Ault, R. P. & Bryant, P. 1998. The effects of water table manipulation and elevated temperature on the net CO<sub>2</sub> flux of wet sedge tundra ecosystems. *Global Change Biology*, 4, 77-90.

Office for National Statistics, 2017, *Population estimates*. Office for National Statistics, UK. Available at: <https://www.ons.gov.uk/peoplepopulationandcommunity/populationandmigration/populationestimates> [Accessed 18th April 2018].

Oke, T. 1978. *Boundary layer climates*, New York, John Wiley and Sons.

Oleszczuk, R., Regina, K., Szajdak, L., Höper, H. & Maryganova, V. 2008. Chapter 3: Impacts of agricultural utilization of peat soils on the greenhouse gas balance. *In: Strack, M. E. (ed.) Peatlands and Climate Change*. Saarijärven Offset Oy, Saarijärvi, Finland: International Peat Society.

Oncley, S. P., Foken, T., Vogt, R., Kohsiek, W., DeBruin, H. A. R., Bernhofer, C., Christen, A., Gorsel, E. v., Grantz, D., Feigenwinter, C., Lehner, I., Liebenthal, C., Liu, H., Mauder, M., Pitacco, A., Ribeiro, L. & Weidinger, T. 2007. The Energy Balance Experiment EBEX-2000. Part I: overview and energy balance. *Boundary-Layer Meteorology*, 123, 1-28.

Ostle, N. J., Levy, P. E., Evans, C. D. & Smith, P. 2009. UK land use and soil carbon sequestration. *Land Use Policy*, 26, S274-S283.

Page, S. E., Morrison, D. R., Malins, C., Hooijer, A., Rieley, J. O. & Jauhiainen, J. 2011a. Review of peat surface greenhouse gas emissions from oil plantations in Southeast Asia. *White Paper*, 15.

Page, S. E., Rieley, J. O. & Banks, C. J. 2011b. Global and regional importance of the tropical peatland carbon pool. *Global Change Biology*, 17, 798-818.

Panbianco, J. E., Buschiazzo, D. E. & Zobeck, T. M. 2010. Comparison of different mass transport calculation methods for wind erosion quantification purposes. *Earth Surface Processes and Landforms*, 35, 1548-1555.

Papale, D. 2012. Data Gap Filling. In: Aubinet M., Vesala T. & D., P. (eds.) *Eddy Covariance*. Dordrecht: Springer Atmospheric Sciences.

Papale, D., Reichstein, M., Aubinet, M., Canfora, E., Bernhofer, C., Kutsch, W., Longdoz, B., Rambal, S., Valentini, R., Vesala, T. & Yakir, D. 2006. Towards a standardized processing of Net Ecosystem Exchange measured with eddy covariance technique: algorithms and uncertainty estimation. *Biogeosciences*, 3, 571-583.

Parmentier, F. J. W., van der Molen, M. K., de Jeu, R. A. M., Hendriks, D. M. D. & Dolman, A. J. 2009. CO<sub>2</sub> fluxes and evaporation on a peatland in the Netherlands appear not affected by water table fluctuations. *Agricultural and Forest Meteorology*, 149, 1201-1208.

Peacock, M., Ridley, L. M., Evans, C. D. & Gauci, V. 2017. Management effects on greenhouse gas dynamics in fen ditches. *Science of The Total Environment*, 578, 601-612.

Pease, P., Gares, P. & Lecce, S. 2002. Eolian Dust Erosion from an Agricultural Field on the North Carolina Coastal Plain. *Physical Geography*, 23, 381-400.

Petersen, S. O., Hoffmann, C. C., Schäfer, C. M., Blicher-Mathiesen, G., Elsgaard, L., Kristensen, K., Larsen, S. E., Torp, S. B. & Greve, M. H. 2012. Annual emissions of CH<sub>4</sub> and N<sub>2</sub>O, and ecosystem respiration, from eight organic soils in Western Denmark managed by agriculture. *Biogeosciences*, 9, 403-422.

Pinsonneault, A. J., Moore, T. R. & Roulet, N. T. 2016. Temperature the dominant control on the enzyme-latch across a range of temperate peatland types. *Soil Biology and Biochemistry*, 97, 121-130.

Pollard, E. & Millar, A. 1968. Wind erosion in the East Anglian Fens. *Weather*, 23, 415-417.

Post, W. M., Peng, T.-H., Emanuel, W. R., King, A. W., Dale, V. H. & DeAngelis, D. L. 1990. The Global Carbon Cycle. *American Scientist*, 78, 310-326.

Poyda, A., Reinsch, T., Kluß, C., Loges, R. & Taube, F. 2016. Greenhouse gas emissions from fen soils used for forage production in northern Germany. *Biogeosciences*, 13, 5221-5244.

Rebmann, C., Kolle, O., Heinesch, B., Queck, R., Ibrom, A. & Aubinet, M. 2012. Data Acquisition and Flux Calculations. In: Aubinet, M., Vesala, T. & Papale, D. (eds.) *Eddy Covariance: A Practical Guide to Measurement and Data Analysis*. Dordrecht: Springer Netherlands.

Red Tractor, 2010, *Crop-specific Protocol Leeks*. Assured Food Standards. 'Available at:

[http://www.assuredproduce.co.uk/eblock/services/resources.ashx/000/528/912/leeks\\_2010\\_final.pdf](http://www.assuredproduce.co.uk/eblock/services/resources.ashx/000/528/912/leeks_2010_final.pdf) [Accessed 22nd March 2018].

Reeburgh, W. S. 1997. Figures Summarizing the Global Cycles of Biogeochemically Important Elements. *Bulletin of the Ecological Society of America*, 78, 260-267.

Reichstein, M., Falge, E., Baldocchi, D., Papale, D., Aubinet, M., Berbigier, P., Bernhofer, C., Buchmann, N., Gilmanov, T., Granier, A., Grünwald, T., Havránková, K., Ilvesniemi, H., Janous, D., Knohl, A., Laurila, T., Lohila, A., Loustau, D., Matteucci, G., Meyers, T., Miglietta, F., Ourcival, J.-M., Pumpanen, J., Rambal, S., Rotenberg, E., Sanz, M., Tenhunen, J., Seufert, G., Vaccari, F., Vesala, T., Yakir, D. & Valentini, R. 2005. On the separation of net ecosystem exchange into assimilation and ecosystem respiration: review and improved algorithm. *Global Change Biology*, 11, 1424-1439.

Renou-Wilson, F., Barry, C., Müller, C. & Wilson, D. 2014. The impacts of drainage, nutrient status and management practice on the full carbon balance of grasslands on organic soils in a maritime temperate zone. *Biogeosciences*, 11, 4361-4379.

Reynolds, O. 1895. On the Dynamical Theory of Incompressible Viscous Fluids and the Determination of the Criterion. *Philosophical Transactions of the Royal Society A: Mathematical, Physical and Engineering Sciences*, 186, 123-164.

Richardson, A. D., Aubinet, M., Barr, A. G., Hollinger, D. Y., Ibrom, A., Lasslop, G. & Reichstein, M. 2012. Uncertainty Quantification. In: Aubinet, M., Vesala, T. & Papale,

D. (eds.) *Eddy Covariance: A Practical Guide to Measurement and Data Analysis*. Dordrecht: Springer Netherlands.

Rieley, J. O., Wüst, R. A. J., Jauhiainen, J., Page, S. E., Wösten, H., Hooijer, A., Siegert, F., Limin, S. H., Vasander, H. & Stahlhut, M. 2008. Chapter 6. Tropical Peatlands: Carbon stores, carbon gas emissions and contribution to climate change processes. *In*: Strack, M. (ed.) *Peatlands and Climate Change*. Saarijärven Offset Oy, Saarijärvi, Finland: International Peat Society.

Rogiers, N., Eugster, W., Furger, M. & Siegwolf, R. 2005. Effect of land management on ecosystem carbon fluxes at a subalpine grassland site in the Swiss Alps. *Theoretical and Applied Climatology*, 80, 187-203.

Roulet, N. T., Ash, R. & Moore, T. R. 1992. Low boreal wetlands as a source of atmospheric methane. *Journal of Geophysical Research: Atmospheres*, 97, 3739-3749.

Rydin, H. & Jeglum, J. K. 2013. *The Biology of Peatlands*, Oxford, Oxford University Press.

Sachs, L. 2004. *Angewandte Statistik*, Berlin, Springer-Verlag Berlin Heidelberg.

Schlesinger, W. H. & Andrews, J. A. 2000. Soil respiration and the global carbon cycle. *Biogeochemistry*, 48, 7-20.

Schmidt, M., Reichenau, T. G., Fiener, P. & Schneider, K. 2012. The carbon budget of a winter wheat field: An eddy covariance analysis of seasonal and inter-annual variability. *Agricultural and Forest Meteorology*, 165, 114-126.

Schrier-Uijl, A. P., Kroon, P. S., Hendriks, D. M. D., Hensen, A., Van Huissteden, J., Berendse, F. & Veenendaal, E. M. 2014. Agricultural peatlands: towards a greenhouse gas sink &ndash; a synthesis of a Dutch landscape study. *Biogeosciences*, 11, 4559-4576.

Shao, Y. 2005. A Similarity Theory for Saltation and Application to Aeolian Mass Flux. *Boundary-Layer Meteorology*, 115, 319-338.

Shao, Y., Mctainsh, G., Leys, J. & Raupach, M. 1993. Efficiencies of sediment samplers for wind erosion measurement. *Soil Research*, 31, 519-532.

Sharratt, B., Feng, G. & Wendling, L. 2007. Loss of soil and PM10 from agricultural fields associated with high winds on the Columbia Plateau. *Earth Surface Processes and Landforms*, 32, 621-630.

Shurpali, N. J., HyvÖNen, N. P., Huttunen, J. T., Clement, R. J., Reichstein, M., NykÄNen, H., Biasi, C. & Martikainen, P. J. 2009. Cultivation of a perennial grass for bioenergy on a boreal organic soil – carbon sink or source? *GCB Bioenergy*, 1, 35-50.

Shurpali, N. J., Strandman, H., KilpelÄinen, A., Huttunen, J., HyvÖNen, N., Biasi, C., KellomÄki, S. & Martikainen, P. J. 2010. Atmospheric impact of bioenergy based on perennial crop (reed canary grass, *Phalaris arundinaceae*, L.) cultivation on a drained boreal organic soil. *GCB Bioenergy*, 2, 130-138.

Silvola, J., Alm, J., Ahlholm, U., NykÄnen, H. & Martikainen, P. J. 1996. The contribution of plant roots to CO<sub>2</sub> fluxes from organic soils. *Biology and Fertility of Soils*, 23, 126-131.

Smith, P., Smith, J., Flynn, H., Killham, K., Rangel-Castro, I., Foereid, B., Aitkenhead, M., Chapman, S., Towers, W., Bell, J., Lumsdon, D., Milne, R., Thomson, A., Simmons, I., Skiba, U., Reynolds, B., D. Evans, C., Frogbrook, Z., Bradley, I. & Falloon, P. 2007. *ECOSSE: Estimating Carbon in Organic Soils - Sequestration and Emissions: Final Report*.

Sow, M., Goossens, D. & Rajot, J. L. 2006. Calibration of the MDCO dust collector and of four versions of the inverted frisbee dust deposition sampler. *Geomorphology*, 82, 360-375.

Strack, M., Waddington, J. M. & Tuittila, E. S. 2004. Effect of water table drawdown on northern peatland methane dynamics: Implications for climate change. *Global Biogeochemical Cycles*, 18.

Strack, M., Waddington, J. M., Turetsky, M., Roulet, N. T. & Byrne, K. A. 2008. Chapter 2. Northern Peatlands, Greenhouse Gas Exchange and Climate Change. *In*: Strack, M. (ed.) *Peatlands and Climate Change*. Saarijärven Offset Oy, Saarijärvi, Finland: International Peat Society.

Strack, M. e. 2008. *Peatlands and Climate Change*, Saarijärven Offset Oy, Saarijärvi, Finland, International Peat Society.

Taft, H. E., Cross, P. A., Edwards-Jones, G., Moorhouse, E. R. & Jones, D. L. 2017. Greenhouse gas emissions from intensively managed peat soils in an arable production system. *Agriculture, Ecosystems & Environment*, 237, 162-172.

Tarnocai, C., Canadell, J. G., Schuur, E. A. G., Kuhry, P., Mazhitova, G. & Zimov, S. 2009. Soil organic carbon pools in the northern circumpolar permafrost region. *Global Biogeochemical Cycles*, 23.

Taylor, J. R. 1997. *Introduction To Error Analysis: The Study of Uncertainties in Physical Measurements*, University Science Books.

Terry, N. & Mortimer, D. C. 1972. Estimation of the rates of mass carbon transfer by leaves of sugar beet. *Canadian Journal of Botany*, 50, 1049-1054.

Tiemeyer, B., Albiac Borraz, E., Augustin, J., Bechtold, M., Beetz, S., Beyer, C., Drösler, M., Ebli, M., Eickenscheidt, T., Fiedler, S., Förster, C., Freibauer, A., Giebels, M., Glatzel, S., Heinichen, J., Hoffmann, M., Höper, H., Jurasinski, G., Leiber-Sauheitl, K., Peichl-Brak, M., Roßkopf, N., Sommer, M. & Zeitz, J. 2016. High emissions of greenhouse gases from grasslands on peat and other organic soils. *Global Change Biology*, 22, 4134-4149.

UK Met Office. 2010. *Climate monitoring of the land and atmosphere* [Online]. Met Office Website. Available: <https://www.metoffice.gov.uk/research/climate/climate-monitoring/land-and-atmosphere> [Accessed 16th April 2014].

UK Met Office. 2015. *Growing season length - Annual average: 1981-2010* [Online]. Met Office Website. Available: <https://www.metoffice.gov.uk/public/weather/climate/u1214qgj0> [Accessed 10th April 2018].

Van Oost, K., Quine, T. A., Govers, G., De Gryze, S., Six, J., Harden, J. W., Ritchie, J. C., McCarty, G. W., Heckrath, G., Kosmas, C., Giraldez, J. V., da Silva, J. R. & Merckx, R. 2007. The impact of agricultural soil erosion on the global carbon cycle. *Science*, 318, 626-9.

Vickers, D. & Mahrt, L. 1997. Quality Control and Flux Sampling Problems for Tower and Aircraft Data. *Journal of Atmospheric and Oceanic Technology*, 14, 512-526.

Warburton, J. 2003. Wind-splash erosion of bare peat on UK upland moorlands. *Catena*, 52, 191-207.

Webb, E. K., Pearman, G. I. & Leuning, R. 1980. Correction of flux measurements for density effects due to heat and water vapour transfer. *Quarterly Journal of the Royal Meteorological Society*, 106, 85-100.

Webb, N. P., Strong, C. L., Chappell, A., Marx, S. K. & McTainsh, G. H. 2013. Soil organic carbon enrichment of dust emissions: magnitude, mechanisms and its implications for the carbon cycle. *Earth Surface Processes and Landforms*, 38, 1662-1671.

Wilczak, J., Oncley, S. & Stage, S. 2001. Sonic Anemometer Tilt Correction Algorithms. *Boundary-Layer Meteorology*, 99, 127-150.

Wilson, K., Goldstein, A., Falge, E., Aubinet, M., Baldocchi, D., Berbigier, P., Bernhofer, C., Ceulemans, R., Dolman, H., Field, C., Grelle, A., Ibrom, A., Law, B. E., Kowalski, A., Meyers, T., Moncrieff, J., Monson, R., Oechel, W., Tenhunen, J., Valentini, R. & Verma, S. 2002. Energy balance closure at FLUXNET sites. *Agricultural and Forest Meteorology*, 113, 223-243.

Wilson, S. J. & Cooke, R. U. 1980. Wind erosion. In: Kirkby, M. J. & Morgan, R. P. C. (eds.) *Soil erosion*. Chichester: John Wiley & Sons, Ltd.

Wohlfahrt, G., Bahn, M., Haslwanter, A., Newesely, C. & Cernusca, A. 2005. Estimation of daytime ecosystem respiration to determine gross primary production of a mountain meadow. *Agricultural and Forest Meteorology*, 130, 13-25.

Wohlfahrt, G. & Galvagno, M. 2017. Revisiting the choice of the driving temperature for eddy covariance CO<sub>2</sub> flux partitioning. *Agricultural and Forest Meteorology*, 237-238, 135-142.

Worrall, F. & Burt, T. 2004. Time series analysis of long-term river dissolved organic carbon records. *Hydrological Processes*, 18, 893-911.

Worrall, F., Burt, T. & Adamson, J. 2004. Can climate change explain increases in DOC flux from upland peat catchments? *Science of The Total Environment*, 326, 95-112.

Worrall, F., Chapman, P., Holden, J., Evans, C., Artz, R., Smith, P. & Grayson, R. 2011. A review of current evidence on carbon fluxes and greenhouse gas emissions from UK peatland. *JNCC Report, No. 442*.

Zicheng, Y., Loisel, J., Brosseau, D., P., Beilman, D., W., & Hunt, S., J., 2010. Global peatland dynamics since the Last Glacial Maximum. *Geophysical Research Letters*, 37.

Zobeck, T. M., Sterk, G., Funk, R., Rajot, J. L., Stout, J. E. & Van Pelt, R. S. 2003. Measurement and data analysis methods for field-scale wind erosion studies and model validation. *Earth Surface Processes and Landforms*, 28, 1163-1188.